Replication fork collapse and recombination-dependent replication restart at replication fork barriers

DEPARTMENT OF BIOCHEMISTRY
UNIVERSITY OF OXFORD

A DPhil thesis presented to the Faculty of Medical Sciences Division,
University of Oxford for the degree of Doctor of Philosophy in Biochemistry

SANJEETA TAMANG
St Hilda's College
Department of Biochemistry
University of Oxford

Acknowledgments

I owe my deepest gratitude to my supervisor Professor Matthew C. Whitby. Without his continuous optimism, enthusiasm, encouragement and support, this work would not have been possible. It has been wonderful to be a part of this research group and I have been able to gain knowledge and acquire skills that will help me step into a bright future ahead.

I would like to thank my fellow members at the Whitby Lab, specifically, Nadiya Ishnazarova, Dr. Fikret Osman, Dr. Carl Morrow, Manisha Jalan, Dr Anastasiya Kishkevich for their assistance and encouragement. I want to especially thank my secondary supervisor Dr Judith Oehler for her valuable guidance and support.

I am grateful to the Government of India for supporting my doctoral degree and giving me this wonderful opportunity. I would also like to thank my family members, my teachers and my friends for their support and encouragement.

Finally, I would like to thank my parents, for their love and support and for the effort they put into giving me a wonderful life. I try to do my best to make them happy and proud.

Declaration

I hereby declare that this report entitled “Replication fork collapse and recombination-dependent replication restart at replication fork barriers” has been originally carried out by me under the supervision of Professor Matthew C. Whitby, Faculty Scientist, Department of Biochemistry, University of Oxford. This work has not formed the basis for award of any degree or diploma previously, except for the data presented in Figure 6.1 from Nguyen 2014, DPhil thesis). The particulars given in the report are true to the best of my knowledge.

Sanjeeta Tamang
St Hilda’s College
Department of Biochemistry
University of Oxford

Date: 18/02/2019

Abstract

In order for the genome of any organism to be successfully replicated its replication machinery has to overcome barriers in the template DNA. These so-called replication fork barriers (RFBs) can sometimes cause the replication fork to collapse. Replication fork collapse is a poorly understood process that is thought to involve either replisome remodelling and/or disassembly paving the way for homologous recombination (HR) proteins to act and restart replication, by a process known as recombination dependent replication restart (RDR), which is essential for completing DNA synthesis. In this thesis I present my work identifying factors that are instrumental in the replication restart process, with a particular focus on those factors that are needed to aid the transition from collapsed fork to one that is receptive to HR proteins. I have used the *RTS1* site-specific RFB in fission yeast for this study as it acts as a potent polar RFB that triggers fork collapse and recombination protein recruitment. By screening candidate factors, I identified the PCNA unloader Elg1 as being strongly required for *RTS1*-induced recombination. By genetic experiments and live cell imaging, I show that unloading of PCNA by Elg1 promotes RDR by allowing efficient recruitment of Rad52 to the blocked replication fork and by limiting the anti-recombinogenic activity of Fbh1. I also provide evidence that Ctf18 acts in opposition to Elg1 to limit *RTS1*-induced recombination. Finally, I investigate the importance of Rad51, the central HR protein, and its mediators (Rad55-Rad57, Swi5-Sfr1, and Rdl1-Rlp1-Sws1) in RDR. By genetic analysis of *RTS1*-induced recombination, I discover that neither Rad51 nor its aforementioned mediators are essential for RDR. These findings indicate the existence of a robust Rad51-independent pathway of RDR in fission yeast.

Table of Contents

Abbreviations

AO	*RTS1* active orientation
ATP	adenosine triphosphate
ATPase	adenosine triphosphatase
BIR	break-induced replication
bp	base pair
CFP	cyan fluorescent protein
Chr	Chromosome
CIN	chromosome instability
CMG	Cdc45/Mcm2-7/GINS
CPT	camptothecin
D-loop	displacement loop
DDR	DNA damage response
DDT	DNA damage tolerance pathway
dHJ	double Holliday junction
DMSO	dimethylsulfoxide
DNA	deoxyribonucleic acid
dNTP	deoxyribonucleotide triphosphate
DSBR	double-strand break

EDTA	ethylenediaminetetraacetic acid
EMMG	Edinburgh minimal media glutamate
FACT	facilitates chromatin transcription
5-FOA	5-Fluoroorotic Acid
FPC	fork protection complex
GCRs	gross chromosomal rearrangements
HJ	Holliday junction
HORReR	homologous recombination-restarted replication
HR	homologous recombination
HU	hydroxyurea
ICL	inter-strand crosslink
IDCL	interdomain connector loop
IFSA	inter-fork strand annealing
IO	*RTS1* inactive orientation
IR	ionizing radiation
iRNA	initiator RNA
Kb	kilobases
LA	low adenine
LB	Luria-Bertani
LD	linear dichroism

LOH	loss of heterozygosity
MCM	minichromosome maintenance
ME	malt extract
MEA	malt extract agar
MiDAS	mitotic DNA synthesis
MIR	multi-invasion recombination
MMBIR	microhomology-mediated BIR
MMR	mismatch repair
MMS	methyl methanesulfonate
MRN	Mre11-Rad50-Nbs1 complex
MRX	Mre11-Rad50-Xrs2 complex
NA	numeric aperture
NER	nucleotide excision repair
NHEJ	non-homologous end-joining
NLS	nuclear localization signal
Nmt	no message in thiamine
OB	oligonucleotide/oligosaccharide binding
ORC	origin recognition complex
ORF	open reading frame
PCNA	proliferating cell nuclear antigen

PCR	polymerase chain reaction
PIP	PCNA-interacting peptide
PMSF	phenylmethylsulphonylfluoride
Pol	DNA Polymerase
PRR	post-replicative repair
pre-RC	prereplication complex
PTMs	post-translational modifications
Pu-Seq	polymerase usage sequencing
rDNA	ribosomal DNA
RDR	recombination-dependent replicationrestart
RF	replication fork
RFB	replication fork barrier
RFC	replication factor C
RLC	RFC-like complex
RPA	replication protein A
RPC	replisome progression complex
rpm	revolutions per minute
RTS1	replication termination sequence 1
SDSA	synthesis-dependent strand annealing
SIM	SUMO-interacting motif

SSA	single-strand annealing
SSC	saline-sodium citrate
ssDNA	single-stranded DNA
SUMO	small ubiquitin-like modifier
TE	Tris-buffered EDTA
TLS	translesion synthesis
tRNA	transfer ribonucleic acid
UBD	ubiquitin-binding domain
UBM	ubiquitin-binding motif
UBZ	ubiquitin-binding zinc finger
UFB	ultra-fine bridge
UV	ultra violet
WRN	Werner syndrome helicase/exonuclease
YE	yeast extract
YES	yeast extract with supplements
YFP	yellow fluorescent protein
1D	one dimensional
2D	two dimensional

1 Introduction

1.1 Eukaryotic DNA Replication

DNA replication is a fundamental process in living organisms. Accurate and timely duplication of the genome is essential for maintenance of its integrity and proper transmission to the next generation. Defects in DNA replication comprise one of the hallmarks of cancer as it leads to chromosomal instability and genomic rearrangements (Hanahan and Weinberg 2011; Burrell et al. 2013). In eukaryotes, replisomes are assembled at multiple origins which fire stochastically with different segments of the chromosome being replicated in a temporal order due to their varying initiation efficiencies (Rhind and Gilbert 2013). Post firing, a pair of bidirectional replication forks (RFs) move in opposite directions away from their origin, replicating DNA until they each encounter an opposing RF from a neighbouring origin, leading to fork merging and termination of replication (Edenberg and Huberman 1975).

The replisome is a large multi-component protein machine, which is specifically assembled at the origin site and is responsible for catalysing DNA synthesis. It is composed of many dedicated proteins with functions in supporting replication by DNA polymerases. In the following sections I discuss the major components of the eukaryotic core replisome.

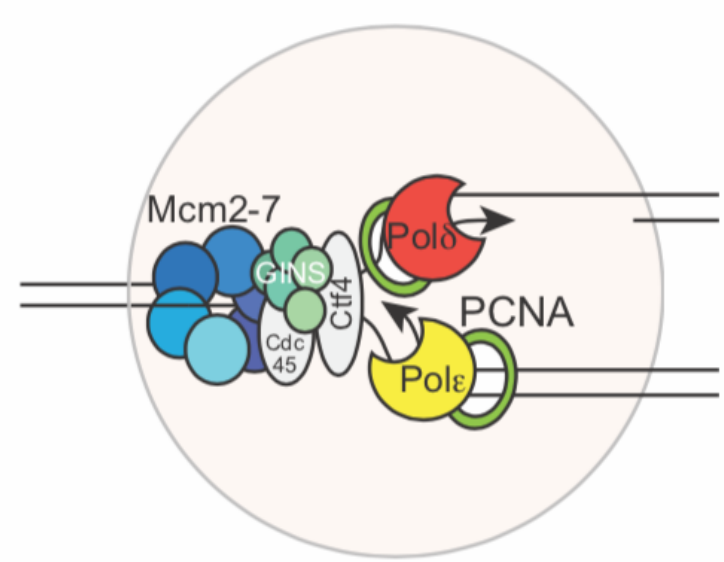

Figure1.1 Eukaryotic replisome
A representation of the eukaryotic replisome showing some of the core components

1.1.1 CMG (cdc45-MCM-GINS) DNA Helicase

The CMG helicase is an 11-subunit complex that encircles the DNA to unwind the replication fork (Moyer et al. 2006; Gambus et al. 2006). The hexameric core of CMG is the minichromosomal maintenance (Mcm2-7) complex of AAA^{+} motor proteins (Bochman et al., 2008a,b). There are five additional accessory factors, Cdc45 and the four-subunit GINS complex (Psf1, 2, 3 and Sld5 in fission yeast) that do not have ATPase sites but are significantly required for efficient activity of the complex (Ilves et al., 2010; Kang et al., 2012). The Cdc45/GINS accessory factors are proposed to bring about allosteric changes in the Mcm2-7 subunits, bringing them into the proper conformation for helicase activity (Ilves et al. 2010; Moyer et al. 2006). The accessory factors might also be necessary for opening up the Mcm2-7 ring during origin assembly (Samel et al. 2014). A recent study indicates that Cdc45 serves as a shield to guard against occasional slippage of the leading strand from the core helicase that periodically re-opens during helicase action (Petojevic et al. 2015).

The CMG helicase travels along the DNA in a 3'–5' direction, placing it on the leading strand of a replication fork (Enemark and Joshua-Tor 2006; Bell and Botchan 2013). It is thought to operate by the steric exclusion model of DNA unwinding, whereby it encircles one DNA strand and translocates along it, excluding the other strand and thus acting as a wedge to melt the duplex (Enemark and Joshua-Tor 2006; Lyubimov et al. 2011; Patel and Donmez 2006). High resolution structures of the CMG complex, with and without DNA, have been obtained recently by EM single-particle 3D reconstruction techniques from studies on *Drosophila* and budding yeast (Abid Ali et al. 2016; Yuan et al. 2016). They reveal the existence of this complex in two different conformers - a compact and a relaxed form. They also indicate that the CMG complex translocates along the DNA by passing the DNA from the C-terminal ATPase tier to the N-terminal tier of the MCM motor ring, while changing from compact to relaxed form (Abid Ali et al. 2016; Yuan et al. 2016). In fact, two conformers of CMG indicate a maximum distance change between the N- and C-tiers of 20 angstroms, suggesting that CMG may inchworm along DNA during ATP hydrolysis (Yuan et al. 2016).

Formation of the CMG helicase at eukaryotic DNA replication origins is distributed into two distinct stages of the cell cycle. In G1 phase, the Mcm2-7 hexamer is loaded onto the DNA by the action of the origin recognition complex (ORC), Cdt1 and Cdc6 (Cdc18 in fission yeast) in an ATP dependent reaction (Remus et al. 2009; Evrin et al. 2009; Yardimci et al. 2010; Botchan and Berger 2010). The 6-protein ORC recognises and binds the origin sites throughout the cell cycle, in a sequence specific manner in budding yeast but with little or no sequence specifity in fission yeast and metazoans (Mojardin et al. 2013; Hoffman et al. 2015). ORC recruits the Cdc6 protein to facilitate Mcm2-7 loading, Cdt1 forms a complex with Mcm2-7 and inturn recruits it

to the ORC-Cdc6-DNA complex via an interaction with Orc1, forming a prereplication complex (pre-RC) (Chen et al. 2007). This step is also known as origin licensing. ATP hydrolysis promotes loading of the Mcm2-7 ring around the DNA but can also promote its release if components required for correct licensing are not present or if ORC has been inactivated by phosphorylation by cyclin-dependent kinases (Frigola et al. 2013). Concomitant with entry into S phase, Cdc45 and the GINS tetramer associate with Mcm2–7 to form the CMG helicase (Gambus et al. 2006; Moyer et al. 2006; Remus and Diffley 2009). Now activated, the CMG likely acts as the front end of the replisome progression complex (RPC) along the leading strand to provide single-stranded DNA (ssDNA) for DNA polymerases (Ilves et al. 2010; Pacek et al. 2006). The entire process of initiation and formation of replication forks has recently been reconstituted using 16 purified replication factors from budding yeast (Yeeles et al. 2015).

1.1.2 DNA polymerases

At the eukaryotic RF, coordinated actions of three distinct B family DNA polymerases (polymerase α, ε and δ) contribute to canonical DNA replication. The basic function of DNA polymerases is to synthesize a DNA strand complementary to the original template strand. However, DNA polymerization-independent functions of Pol ε have been widely reported. Studies in budding and fission yeast show that Pol ε is required for stable CMG formation (Sengupta et al. 2013, Handa et al. 2012) and studies in fission yeast and mice show that Pol ε is needed for activation of origins and initiation of DNA replication (Handa et al. 2012, Bellelli et al. 2018).

Both the leading and lagging strand DNA syntheses are initiated by the Pol α-RNA primase complex. This complex contains two catalytic activities, the RNA primase activity in the smallest p48 subunit (Pri1) and the polymerase activity in the

largest p180 subunit (Pol1), plus two additional regulatory subunits. It synthesizes primers that consists of a short, ~10 nucleotide, RNA stretch followed by 10 to 20 DNA bases (Fisher 1979; Nethanel et al. 1992). Thus, pol α primes the synthesis of the leading strand and each Okazaki fragment on the lagging strand. Polymerase ε (Pol ε) synthesizes the ongoing leading strand while polymerase δ (Pol δ) synthesizes the lagging strand by generating the Okazaki fragments (Pursell et al. 2007; McElhinny et al. 2008). These assignments are suggested by genetic (Miyabe et al. 2011; Clausen et al. 2015; Kunkel and Burgers 2008; Pursell et al. 2007; McElhinny et al. 2008), biochemical (Georgescu et al. 2015; J. Sun et al. 2015; Georgescu et al. 2014; Langston et al. 2014) and strand specific polymerase-DNA crosslinking studies (Yu et al. 2014). However, there are some uncertainties about these assignments and further work is needed for clarification (Johnson et al. 2015; Stillman 2015).

Pol ε and Pol δ are composed of multiple subunits; their largest subunit is the DNA polymerase (Burgers 2009). Interestingly, the Pol2 subunit of Pol ε consists of two polymerase sequences linked head-to-tail; the amino-terminal half encodes the active polymerase that also has 3′-exonucleolytic activity, while the carboxy-half encodes an inactive polymerase required for replisome assembly and checkpoint activation (Lou et al. 2008; Tahirov et al. 2009, Sengupta et al. 2013). Crystal structures of the active polymerase region of Pol2 and Pol δ revealed that they have the shape of a right hand, such as observed for all other DNA polymerases (Shechter et al. 2000; Kelman et al. 1999). The architecture of the whole eukaryotic core replisome has been determined by single particle electron microscopy, which also suggested a path for threading the leading ssDNA through the CMG complex and Pol ε (Sun et al. 2015). Pol ε is a high-fidelity polymerase with high nucleotide selectivity.

Unlike Pol α, both Pol ε and Pol δ possess 3'–5' exonuclease activity but Pol ε does not perform efficient strand displacement synthesis like Pol δ (Ganai et al. 2016; Flood et al. 2015). DNA polymerase 3'–5' exonuclease activity is a major determinant of replication fidelity and Pol δ exonuclease proofreading plays important role in maturation of Okazaki fragments and also mismatch repair (MMR) (Jin et al. 2001, 2003). Primers synthesized by Pol α are extended by Pol δ on each Okazaki fragment. When Pol δ reaches the 5′-end of the preceding Okazaki fragment, it initiates strand displacement synthesis. This generates a single stranded iRNA/DNA flap of varying lengths, which must be cleaved, and the nick between the two Okazaki fragments must be sealed by DNA ligase 1. Okazaki fragment maturation and can be handled in two ways: one mechanism is designed to process short flaps, while the other deals with long flaps (Balakrishnan and Bambara 2013; Stodola and Burgers 2016). In the primary mechanism, Pol δ is able to displace up to 2 to 3 nucleotides of DNA or RNA ahead of its polymerization, generating a short flap recognised by flap endonuclease 1 (FEN1) which can remove nucleotides from the flap, about one nucleotide at a time. The RNA primer is completely removed leaving a DNA nick. It is proposed to be achieved by iterative Pol δ strand displacement and FEN1 cleavage, a process termed nick translation (Stodola and Burgers 2016).

In the event of deregulated Fen1/Pol δ activity, long 5' flap is generated and bound by replication protein (RPA). Biochemical studies show that Pif1 helicase accelerates flap displacement and promotes the formation of long flaps which are processed by the two-nuclease pathway discussed below (Pike et al. 2009). The RPA bound long flap is resistant to FEN1 cleavage and is processed by Dna2, an essential multifunctional nuclease/helicase, which displaces RPA and cleaves the flap to make

it shorter. The remaining flaps of 0-5 nt needs precise cutting by FEN1 (Kang et al. 2010). It has been recently postulated that missed cleavage opportunity by FEN1 leads to Okazaki fragment processing through the two-nuclease pathway (Zaher et al. 2018). FEN1 binds and bends a short flap and cleaves it efficiently in the first encounter. FEN1 binds and bends a long flap with similar efficiency but it misses cleaving it because, with RPA bound to the flap, FEN1-DNA complex cannot achieve a stable, catalytically active conformation for cleaving (Zaher et al. 2018). During Okazaki fragment maturation, after degradation of primer RNA, DNA ligation occurs close to the RNA-DNA junction, however some amount of Pol α –synthesized DNA with low fidelity still remains (Reijns et al. 2015; McElhinny et al. 2010).

1.1.3 Proliferating cell nuclear antigen (PCNA)

DNA polymerases have a semi closed 'hand' structure, which allows the polymerase to load onto the template DNA and begin translocating, incorporating dNTPs forming nascent DNA (Federley and Romano 2010). However, it needs a sliding clamp to strengthen this interaction. PCNA serves as a DNA sliding clamp for the replicative DNA polymerase and increases its processivity. This places PCNA at the heart of the eukaryotic chromosomal DNA replisome. PCNA is a homo-trimeric ring that encircles dsDNA and slides along it (De March and De Biasio 2017; Federley and Romano 2010). PCNA recognizes the DNA structure through a set of basic residues in the ring channel, which strategically form a right-hand spiral that matches the pitch of B-DNA and establishes polar interactions with consecutive DNA backbone phosphates of one DNA strand (De March et al. 2017). This enables PCNA to orient perfectly on the DNA, which is necessary for its proper functioning. The PCNA ring interacts with DNA polymerases through amino acid polarity on its front face and tethers them securely to

the DNA and enhances polymerase processivity up to 100-fold (Chilkova et al. 2007). Pol ε has intrinsically higher processivity than Pol δ which is increased even further (~6-fold) by PCNA. The very low intrinsic processivity of Pol δ is vastly enhanced (~100-fold) by PCNA bringing it to a comparable level with Pol ε (Chilkova et al. 2007). PCNA interacts with DNA Pol δ, FEN1 and LIG1 (DNA ligase 1) to synthesize, process and join Okazaki fragments, during lagging strand synthesis (Boehm et al. 2016).

PCNA also acts as a platform that mediates the recruitment of many factors involved in DNA replication, DNA repair, chromatin remodelling and other DNA-related activities that are important for cell viability, cell division, and genomic stability (Moldovan et al. 2007; Cox 1997; De March et al. 2017). PCNA recruits important factors needed for translesion synthesis (Vaisman and Woodgate 2017; Zhao and Washington 2017), replication traverse of DNA interstrand crosslinks (ICL) (Rohleder et al. 2016; Porro et al. 2017), promoting ICL repair (Yang et al. 2010), fork reversal during RF restart (Vujanovic et al. 2017; Ciccia et al. 2012), base excision repair (BER) (Fromme and Verdine 2004), nucleotide excision repair (NER) (Choe and Moldovan 2017) and mismatch repair (Boehm et al. 2016). PCNA interacts with various proteins via its PCNA-protein interaction interface at the front face of PCNA. This interface is comprised of the interdomain connector loop (IDCL), which connects the two similar domains of PCNA monomer. Many of the PCNA-interacting proteins bind to IDCL via a PCNA-interacting peptide (PIP) or motif defined by a consensus sequence (Warbrick et al. 1995; Warbrick et al. 1997; Warbrick 2000). The sequence variations of PIP-boxes modify their PCNA binding strength (Kaufmann et al. 2017; Hishiki et al. 2009). However, regulation of strength of PCNA binding is critical for normal cellular functions as prolonged binding of factors can have deleterious consequences (Mattock et al.

2001; Fridman et al. 2010). Ubiquitin-binding domains (UBD), ubiquitin-binding motifs (UBM), ubiquitin-binding zinc fingers (UBZ) and SUMO-interacting motifs (SIM) are additional modules that promote binding of proteins to ubiquitinated or SUMOylated PCNA (Vaisman and Woodgate 2017; Guo et al. 2008; Plosky et al. 2006; Bienko 2005; Armstrong et al. 2012).

Post-translational modifications (PTMs) of both PCNA and its binding partners mediate the cycling of various proteins at PCNA during the dynamic process of DNA replication and repair. Mass spectrometry analyses revealed that of 16 lysines in PCNA, 13 can be ubiquitinated, of which eight can be SUMOylated or acetylated, four can be NEDDylated, and three can be ISGylated (Kim et al. 2011; Elia et al. 2015; Lumpkin et al. 2017; Coleman et al. 2017; Park et al. 2014). Upon DNA damage, PCNA can be mono-ubiquitinated at the highly conserved lysine residue 164 by the E2 ubiquitin-conjugating enzymes Rad6 and E3 ubiquitin ligase Rad18 (Hoege et al. 2002; Davies et al. 2008) This modification of PCNA activates the DNA Damage Tolerance pathway (DDT, also known as post-replication repair or PRR). Mono-ubiquitination of PCNA enhances the binding of specialised DNA translesion synthesis (TLS) polymerases, enabling lesion bypass (Parker et al. 2007; Haracska et al. 2004). Alternatively, PCNA can undergo further ubiquitination on the same lysine residue to form poly-ubiquitin chains. Polyubiquitination of PCNA requires Ubc13-Mms2 (an E2 heterodimer) and Rad5 (an E3 ubiquitin ligase) and facilitates an error-free repair whose precise nature is still unclear (Hoege et al. 2002; Branzei et al. 2008; Chiu et al. 2006; Branzei et al. 2004). Interestingly, the same residue of PCNA (lysine 164) can also be SUMOylated in budding yeast, and SUMOylated PCNA exists in vertebrates (Leach and Michael 2005; Ulrich et al. 2005). This modification takes place

during S-phase or after high doses of DNA damage and requires the SUMO-specific E2 Ubc9 and the E3 SUMO ligase Siz1 (Hoege et al. 2002). During S-phase, this suppresses homologous recombination (HR) by recruitment of the PCNA-interacting protein PARI in mammalian cells (Moldovan et al. 2012) and Srs2 in yeast (Pfander et al. 2005; Papouli et al. 2005). An additional residue, lysine 127, can also be SUMOylated, but not ubiquitinated. In contrast to mutations in lysine 164, those in lysine 127 do not lead to DNA damage sensitive phenotypes (Hoege et al. 2002). This modification is thought to suppress ubiquitination of PCNA, therefore inhibiting TLS and other DNA repair pathways, which are potentially harmful to the cell because they can introduce mutations and genome rearrangements (Pfander et al. 2005; Papouli et al. 2005; Parnas et al. 2010).

1.1.4 The Ctf4 trimer hub

With recent findings from studies in budding yeast, Ctf4 is emerging as a hub that links factors with diverse functions to the eukaryotic replisome (Villa et al. 2016; Simon et al. 2014). These studies revealed that Ctf4 is a homotrimer that can bind Pol1 (of Pol α) on the lagging strand and Sld5 (of GINS) on the leading strand, thereby linking the two machineries (Villa et al. 2016; Simon et al. 2014). Ctf4 is part of the replisome progression complex (RPC) that includes factors like the essential initiation and elongation factor, Cdc45, the checkpoint mediator Mrc1, the Tof1–Csm3 complex that allows replication forks to pause at protein-DNA barriers and the histone chaperone FACT (facilitates chromatin transcription) (Gambus et al. 2006). Mass spectrometry analysis of CMG pulldowns has revealed that CMG associates with Pol α and many of these RPC proteins (Gambus et al. 2006). Thus, other factors could also contribute to coordinating the leading and lagging strands, such as the Tof1-Csm3-Mrc1

replication pausing complex that associates with many factors in the replisome (Calzada et al. 2005). Ctf4 was also reported to interact with other replication proteins, such as Dna2 and the sister chromatid cohesion protein Chl1 (Villa et al. 2016). AND-1, the human Ctf4 homolog also interacts with Pol α (Kilkenny et al. 2017) and shows additional interactions with Pol δ (Bermudez et al. 2010). Surprisingly, cells deleted for *CTF4*, or the fission yeast homolog *mcl1,* are viable, although they do exhibit genome stability defects (Williams and Mcintosh 2002; Fumasoni et al. 2015; Hanna et al. 2001). The Ctf4 homotrimer could bind to other proteins that are yet to be identified and, in this regard, it is interesting to note that Ctf4 binds a short peptide sequence, like the PIP of PCNA, which has been termed "Ctf4-interacting-peptide" or CIP-box. This suggests that Ctf4 might act as a centre like PCNA, trafficking many proteins and recruiting them dynamically to the replication fork (Villa et al. 2016; Simon et al. 2014).

1.2 Replication stress

The significance of studying the problems that arise during DNA replication is underlined by the fact that they can lead to many deleterious genome rearrangements such as duplications, deletions and inversions, which are associated with cancer and other disease states (Aguilera and García-Muse 2013; Arlt et al. 2012; Macheret and Halazonetis 2018). Further, oncogenes are known to interfere with the process of replication resulting in replication stress, which causes genomic instabilities that are associated with cancer (Karakaidos et al. 2005; Miron et al. 2015; Hills and Diffley 2014). This phenomenon is known as oncogene induced replicative stress, whereby initial activation of oncogenes wrecks the balance of replication. It can cause: excessive firing of origins, such as origins within highly transcribed genes that are normally suppressed by transcription; deregulation of replication initiation; increased

interference between transcription and replication; perturbed fork progression; impaired fork initiation; depletion of deoxyribonucleotide pools; and increased chromosomal instability at fragile sites due to an inability to activate additional origins (Macheret and Halazonetis 2018; Jones et al. 2013; Ozeri-Galai et al. 2011; Mannava et al. 2013; Ekholm-Reed et al. 2004). Replication stress has also been linked to structural and numerical chromosomal instability (CIN) that drives metastasis (Burrell et al. 2013; Bakhoum et al. 2018). Whilst replication stress can drive cancer cell development, even these cancerous cells need to rely on various pathways that enable them to complete DNA replication (under conditions where it is perturbed) for survival. Thus, the pathways that allow cancer cells to survive replication stress are important targets of anti-cancer therapies.

Under normal physiological conditions, the completion of DNA replication is impeded by a host of different obstacles such as DNA lesions, DNA secondary structures, tRNA genes, G-quadruplex (G4) DNA, Ty elements, transcription machinery and various DNA binding proteins (Admire et al. 2006; Lemoine et al. 2005; Azvolinsky et al. 2009; Deshpande and Newlon 1996; Tuduri et al. 2009; Dalgaard et al. 2011; Aguilera and García-Muse 2013). Replication through chromosomal regions containing high densities of these factors is especially reliant on mechanisms that promote RF stability and progression (Greenfeder and Newlon 1992; Cha and Kleckner 2002). Also, late replicated regions of the chromosome, which are poor in origin density, pose a problem as they risk entering into mitosis with unresolved replication intermediates. They form recurrent DNA breaks that can be visualized on metaphase chromosomes as breaks and gaps and are known as fragile sites (Chan et al. 2009; Ying et al. 2013). The un-replicated region forms an ultra-fine bridge (UFB)

during mitosis, resulting into chromosome breakage and aneuploidy (Zhang et al. 2013; Lukas et al. 2011; Moreno et al. 2016). Depending on the nature of the impedance, RFs can undergo broadly three types of events. The most common one is fork pausing where the RF is transiently stalled by weaker barriers like tRNA genes and various other protein-DNA interactions (Deshpande and Newlon 1996; Greenfeder and Newlon 1992; Makovets et al. 2004; Miller et al. 2006; Wang et al. 2001). Under these circumstances the integrity of the fork is maintained, often with the help of the Fork Protection Complex (FPC) and checkpoint kinases, until the barrier is removed, and replication is resumed. Polymerase ε serves as a centre for S-phase checkpoint signalling at stalled replication forkslinking the DNA replication machinery to the S-phase checkpoint (Navas et al. 1995; Puddu et al. 2011). In other cases, the RF is arrested by a barrier like the polar fork barrier in the non-transcribed spacers of rDNA, yet the replisome is stable and there is no fork collapse or induction of recombination (Mizuno et al. 2013). Fork termination is mediated by the arrival of the converging fork. Alternatively, at some strong replication fork barriers (RFBs) the RF may collapse through a poorly understood process, thought to involve either replisome remodeling and/or disassembly paving the way for HR proteins to act and restart replication (Ahn et al. 2005; Lambert and Carr 2005; Lambert et al. 2010). The S-phase checkpoint response, previously implicated in preserving the stability of the replisome at defective RFs (Cobb et al. 2003; Cobb et al. 2005; Lucca et al. 2004; Naylor et al. 2009; Raveendranathan et al. 2006), seems to be blind to certain types of blocked and collapsed RFs (Lambert et al. 2005; De Piccoli et al. 2012; Mohebi et al. 2015). RF collapse leads to the induction of homologous recombination (HR), which, in addition to promoting the repair of DNA double strand breaks (DSBs), can

act to restart replication. Various aspects of this process are discussed in the next section.

1.3 Homologous recombination

1.3.1 Pathways of DSB repair by HR and the key roles that Rad51 and Rad52 play

HR is an evolutionarily conserved DNA repair pathway involved in the repair of several types of DNA lesions, including DSBs and ssDNA gaps. The process of HR is well characterised in the context of DSB repair by genetic, biochemical and molecular studies (Mimitou and Symington 2009). The basic principle of HR involves the invasion of a homologous DNA duplex on the sister chromatid or homologous chromosome, which is used as a template for genetic information needed to repair the DSB (Figure1.2). In eukaryotes, during the initial steps of DSB repair, the broken DNA is processed by exonucleases generating a 3' ssDNA tail that is instantly coated by RPA (West 2003). In yeast, Rad52 then mediates the nucleation of Rad51 by displacing RPA from the ssDNA, forming a Rad51 nucleoprotein filament with the help of other mediator proteins. The Rad51 nucleofilament is capable of invading into a homologous DNA duplex, to pair with its complementary DNA strand (strand invasion), and in so-doing form a displacement loop (D-loop) structure. DNA synthesis is then primed from the 3' end of the invading strand so that any genetic information that was lost at the DSB site can be recovered. Following this, the ssDNA tail on the other end of the DSB can anneal to the displaced strand of the D-loop (second end capture) to form a double Holliday junction (dHJ), which is then resolved. Alternatively, the invaded strand is displaced from the template to allow it to anneal to its complementary strand on the other side of the DSB. This is known as synthesis dependent strand annealing (SDSA)

(Allers and Lichten 2001; Resnick 1976) (Figure1.2). SDSA is important for avoiding crossovers because the D-loop is disrupted before it forms a more complex recombinogenic structure that has the potential to be resolved as a crossover. Different pathways of resolution of the heteroduplex structure following strand invasion and initiation of DNA synthesis are discussed in more detail in section 1.3.3.

Rad52, the principal mediator of Rad51 in yeasts (*Schizosaccharomyces pombe, Saccharomyces cerevisiae*) which facilitates the loading of Rad51, can promote HR in a Rad51-independent pathway through single strand annealing (SSA) (Figure1.2). SSA is the pairing of two complementary, RPA coated, ssDNA stretches. It can repair DSBs that occur between a direct repeat of homologous sequences (Zhao et al. 2015). Strand resection generates 3' overhangs, revealing complementary sequences, and the complementary ssDNA ends coated with RPA anneal through the aid of Rad52's strand annealing activity and RPA is released (Sugiyama et al. 1998; Petukhova et al. 1999; Davis and Symington 2001). The nonhomologous DNA forms 3' flaps that are cleaved by the NER proteins Rad1 and Rad10 in *S. cerevisiae* (Rad16 and Swi10 in *S. pombe*) (Petukhova et al. 1999; Davis and Symington 2001). SSA is a mutagenic process as it causes the deletion of one of the two repeats and the nonhomologous sequence between them. Rad52-mediated strand annealing is strongly inhibited by the formation of a Rad51 filament (Wu et al. 2008).

In both budding and fission yeast, Rad52 is essential for all recombination events whether Rad51-dependent or -independent (Doe et al. 2004; Krogh and Symington 2004). Its importance for DNA repair is highlighted by the extreme hypersensitivity of a *rad52*Δ mutant in budding yeast to DNA damaging agents like ionizing radiation (IR) that cause DSBs (Symington 2002; Malkova et al. 1996).

However, in higher eukaryotes, BRCA2 (breast cancer type 2 susceptibility protein) is postulated to be the major loader of Rad51 onto DNA. Unlike Rad52, BRCA2 cannot mediate SSA or RPA displacement. RPA displacement is mediated by DSS1, a BRCA2 interacting factor (Zhao et al. 2015) and SSA is performed by a structural homolog of Rad52 (Bhargava et al. 2016). Although RAD52 cannot fully substitute for BRCA2, inactivation of RAD52 in BRCA2-deficient cells is synthetically lethal (Feng et al. 2011). Interestingly human RAD52 also plays a role in tolerating replication stress, which is independent of RAD51 (Sotiriou et al. 2016; Bhowmick et al. 2016).

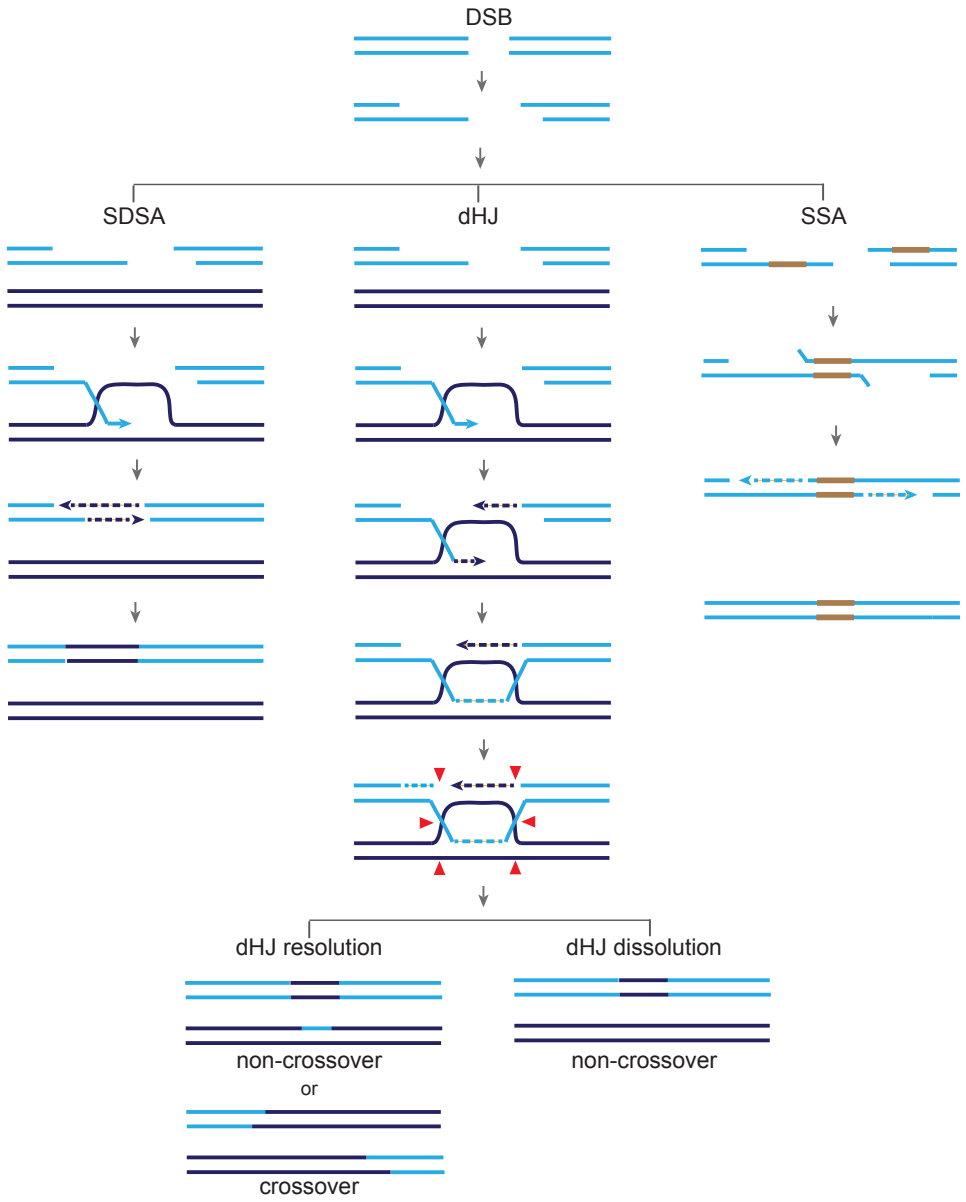

Figure1.2 Different pathways of DSB repair by HR

A DSB can be repaired by 3 different pathways of HR following on from 5'-3' resection: (i) SDSA involves invasion of a 3' ssDNA end into a homologous template forming a D-loop. DNA synthesis is primed by the invading strand and the newly synthesized strand is displaced from its template and annealed to the second end of the break, which initiates a second round of in-fill DNA synthesis. (ii) In the dHJ pathway, following strand invasion and DNA synthesis, second-end capture by the invading strand by annealing to the displaced strand forms a dHJ. Resolution of dHJ (vertical or horizontal, red arrows) produces noncrossover or crossover outcomes, dissolution of dHJ produces noncrossover outcomes. (iii) SSA involves 5'-3' resection to expose flanking homologous sequences which are annealed to each other. The nonhomologous 3' flaps are trimmed off and the 3' ends are used as primers to fill in the gaps (Figure adapted from Kramara et al. 2018).

1.3.2 Rad51 and Rad51 mediator complexes

Rad51 is the RecA homolog in eukaryotes that performs the central reaction of HR by forming a dynamic active nucleoprotein filament capable of searching for sequence homology and catalysing DNA strand exchange in an ATP-dependent manner (Brouwer et al. 2018; Xu et al. 2017). Deletion of Rad51 is not lethal in budding yeast or fission yeast, but is lethal in higher eukaryotes such as mice and chicken DT40 cells, which may suggest that it is more critically required for preserving larger genomes (Vainio and Imhof 1995; Lim and Hasty 1996; Tsuzuki et al. 1996). It facilitates efficient strand exchange by polymerizing onto DNA in a right-handed helical filament and then stretching the DNA to 18.6 basepairs per turn from 12.5 basepairs per turn increasing the accessibility of the basepairs within the filament (Chen et al. 2008; Klapstein et al. 2004; Nishinaka et al. 1998; Ogawa et al. 1993). Efficient homology search for the 3' ssDNA end is one of its most essential functions. According to single-molecule analyses of RecA filaments, Rad51 may accomplish this through both an 'intersegmental contact sampling model' i.e. simultaneous sampling of multiple disconnected dsDNA segments (Forget and Kowalczykowski 2012) and a 'sliding model' with the filament diffusing along dsDNA at a rate of 7700 basepairs^2/sec sampling several hundred base pairs before dissociating (Ragunathan et al. 2012).

Rad51 requires a number of other mediators that promote the formation and stability of its nucleoprotein filament, which is necessary for the strand invasion step *in vivo*. In most cases their exact roles remain to be defined. However, each mediator complex is considered to facilitate Rad51 assembly via a different mechanism, and with recent developments we are approaching an understanding of what distinguishes their functions. In the following sections I discuss three mediator complexes that play

significant roles during HR in *S. pombe*. However, bioinformatic, genetic and biochemical analyses suggest that these complexes are highly conserved and have non-overlapping roles in regulating HR.

1.3.2.1 Rad55-Rad57

Rad55 and Rad57 share sequence similarity with Rad51 (e.g. 38% for Rad55 and 49% for Rad57 in *S. cerevisiae*) and, therefore, are considered to be Rad51 paralogs (Tsutsui et al. 2000; Khasanov et al. 1999; Lovett 1994; Kans and Mortimer 1991). Although they share the core ATPase domain with Rad51, they are not able to form nucleoproteinfilaments or perform a homology search or strand invasion reaction (Symington 2002; Sung 1997; Thacker 2005). In mammals, the Rad51 paralogs are RAD51B, RAD51C, RAD51D, XRCC2, and XRCC (Liu et al. 1998; Cartwright et al. 1998a; Albala et al. 1997; Pittman et al. 1998; Dosanjh et al. 1998; Cartwright et al. 1998b). In response to DNA damage and replication barriers, Rad55 is phosphorylated by the effector kinase Rad53 on multiple residues, which has been proposed to positively regulate HR (Bashkirov et al. 2000; Herzberg et al. 2006; Janke et al. 2010). The Rad55-Rad57 heterodimer is able to overcome RPA inhibition of Rad51-mediated strand exchange *in vitro* like Rad52 (Sung 1997), but unlike Rad52, neither Rad55 nor Rad57 interact with RPA (Bashkirov et al. 2000; Herzberg et al. 2006; Janke et al. 2010). A role in promoting Rad51 activity is also indicated by the finding that the DNA damage sensitivity of *rad55*Δ and *rad57*Δ mutants is suppressed by overexpression of Rad51 (Hays et al. 1995; Johnson and Symington 1995). However, Rad51 is able to form IR-induced foci without Rad55-Rad57 *in vivo* suggesting that their critical role is not to mediate nucleation of Rad51 onto DNA in the presence of RPA (Lisby et al. 2004). Instead, the finding that a Rad51 mutant with

higher ssDNA binding affinity bypasses the need for Rad55 and Rad57 (but not RPA, Rad52, or Rad54) for strand exchange, suggests that Rad55-Rad57 is needed for Rad51 filament stabilization (Fortin and Symington 2002).

Rad55-Rad57 stabilizes the Rad51 presynaptic filament by balancing the anti-recombinase activity of the Srs2 helicase (Liu et al. 2011). Srs2 causes Rad51 to dissociate from DNA by triggering ATP hydrolysis within the Rad51 filament (Antony et al. 2009) and once a Rad51 molecule is displaced from DNA, Srs2 translocates along the ssDNA to displace the next Rad51 subunit in the filament (Krejci et al. 2003; Qiu et al. 2013; Veaute et al. 2003). A recent single molecule imaging study showed that $Rad51^{I345T}$, containing a suppressor mutation that partially bypasses the requirement for Rad55-Rad57 (Fortin and Symington 2002), is removed more slowly by Srs2 from ssDNA, compared to wild-type Rad51 (Kaniecki et al. 2017).

1.3.2.2 Swi5-Sfr1

The Swi5-Sfr1 complex activates Rad51-mediated strand exchange. It was reported to function in parallel with Rad55-Rad57 as a Rad51 mediator (Akamatsu et al. 2003; Akamatsu et al. 2007). Swi5-Srf1 cannot remove RPA but can promote strand exchange by the presynaptic Rad51 filament. It was reported to stabilize Rad51-ssDNA in a ATP dependent manner which was important for activation of Rad51 for strand exchange (Haruta et al. 2006; Kurokawa et al. 2008). Biochemical analyses using mouse proteins showed that SWI5-SFR1 helps maintain the catalytically active ATP-bound state of the RAD51 presynaptic filament by enhancing ADP release from the filament (Su et al. 2014). Further studies showed that SFR1 interacts with the oligomeric, but not the monomeric, form of RAD51 and the C-terminus of SWI5 is

important for SWI5–SFR1 and RAD51 complex formation (Su et al. 2016). *In vitro* studies by flow linear dichroism (LD) spectroscopy using *S. pombe* Swi5-Sfr1 and Rad51 showed that Swi5-Sfr1 stimulates Rad51-promoted strand exchange by causing more perpendicular organisation of the DNA bases in the presynaptic filament facilitating base pairing with an incoming dsDNA (Fornander et al. 2014). A synaptic role for Swi5–Sfr1 in Rad51-driven strand exchange is also supported by recent molecular kinetic studies of DNA strand exchange involving these proteins (Ito et al. 2018).

1.3.2.3 Rdl1-Rlp1-Sws1

Rdl1-Rlp1-Sws1 is the functional equivalent of the budding yeast Shu complex consisting of Shu1-Shu2-Psy3-Csm2, and the mammalian enzymes XRCC2- SWS1-RAD51D-SWSAP1 (Martin et al. 2006; Martino and Bernstein 2016). The single mutants of Rdl1-Rlp1-Sws1 show milder sensitivity to hydroxyurea (HU), camptothecin (CPT), methyl methanesulphonate (MMS), UV, and IR compared to Rad55-Rad57 and Swi5-Sfr1 mutants (Khasanov et al. 2004; Martín et al. 2006). However, yeast two-hybrid analysis shows that Rlp1 and Rad57 interact and *rlp1*Δ is epistatic to *rad55*Δ for MMS and IR sensitivity, indicating that the Rdl1-Rlp1-Sws1 complex works with Rad55-Rad57 (Khasanov et al. 2004). Csm2, a member of the budding yeast Shu complex, has been shown to interact with Rad55 independently of Rad51 in yeast two-hybrid assays (Godin et al. 2013; Xu et al. 2013) and to promote Rad55 foci induced by IR and Rad51- dependent direct repeat recombination (Godin et al. 2013).

Interestingly, yeast two-hybrid screens showed that Shu1 physically interacts with Srs2 (Martín et al. 2006), and deletion of the budding yeast Shu1 leads to

increased Srs2 recruitment to both spontaneous foci and that induced by a DSB, correlating with a decrease in Rad51 foci (Bernstein et al. 2011). Thus, the Shu complex is an important negative regulator of the recruitment of Srs2. Recently, using a fully reconstituted system, it was demonstrated that the Shu complex, Rad55-Rad57 and Rad52 act as a functional ensemble to promote nucleation of Rad51 on RPA coated ssDNA (Gaines et al. 2015).

1.3.3 Post synaptic resolution of recombination intermediates

1.3.3.1 D-loop disruption

Following strand invasion and D-loop formation, the subsequent steps to resolve the heteroduplex structure vary depending on the particular HR pathway used (Figure1.2). One option is D-loop disruption, displacing the invading strand from the template. Helicases like Fml1/Mph1/FANCM, Srs2, and the RecQ-type helicases Rqh1/Sgs1/BLM/WRN/RECQ1/R (in budding and fission yeasts and mammals) have all been shown to be capable of catalyzing D-loop unwinding *in vitro* (Chu and Hickson 2009; Bachrati et al. 2006; Bernstein et al. 2010; Dupaigne et al. 2008; Prakash et al. 2009; Sharma et al. 2005; Sun et al. 2008) and thus, may play a role in promoting SDSA. Srs2 can additionally promote SDSA by disrupting the Rad51 nucleofilament to prevent engagement or invasion of the second end with the invaded strand (Dupaigne et al. 2008). Increased cross over events during DSB repair in yeast cells are associated with deletions of Fbh1, Fml1/Mph1, Rqh1/Sgs1 and Srs2, which is also consistent with one or more of these helicases playing a role in promoting SDSA (Ira et al. 2003; Morishita et al. 2005; Robert et al. 2006; Sun et al. 2008; Prakash et al. 2009; Bzymek et al. 2010; Lorenz et al. 2012). The importance of these helicases is emphasized in humans by their association with autosomal recessive genomic

instability diseases like Fanconi anemia and Bloom's, Werner's, and Rothmund-Thomson Syndrome (Ellis et al. 1995; Yu et al. 2016; Gray et al. 1997; Kitao et al. 1999; Kennedy and Andrea 2005).

1.3.3.2 Resolution of Double Holliday junctions

HJs are resolved by DNA structure-specific nucleases (so-called HJ resolvases) that cut two non-crossed strands or two crossed strands of the HJs. In the case of dHJs, if these cuts are done in the same strands at both junctions, noncrossover products are produced; however, if they are introduced into opposite strands then the products of the reaction are crossovers. GEN1 in mammals (with functional similarity to Yen1 in budding yeast and RuvC in bacteria) is a monomeric 5'-flap endonuclease that can dimerize on HJs to make symmetrical nicks on non-crossing strands thereby resolving the junction (Rass et al. 2010). Due to the absence of a GEN1 ortholog in fission yeast, the endonuclease Mus81-Eme1 (Mus81-Mms4 in budding yeast and MUS81-EME1 in mammals) may perform this function. Mus81-Eme1 plays a major role in cleaving recombination intermediates during meiosis to form crossovers (Osman et al. 2003; Smith et al. 2003). However, studies show that Mus81-Eme1 does not preferentially cleave four-way HJs, but prefers nicked HJs and D-loops (Osman and Whitby 2007; Pfander and Matos 2017). Another structure- specific endonuclease identified in yeast and humans, Slx1-Slx4, has been shown to have Y-junction, 5' flap, and HJ endonuclease activity that resides within Slx1 (Fricke and Brill 2003; Andersen et al. 2009; Fekairi et al. 2009; Muñoz et al. 2009; Saito et al. 2009; Svendsen et al. 2009). Interestingly, there is evidence that shows that HJ resolvases, such as Mus81-Mms4 and Yen1, are cell cycle regulated and not activated until G2/M phase, which suggests that the endonucleolytic processing of HJs, which risks generating crossovers, may

be used only as a last resort in mitotic cells to ensure that sister chromatids can segregate during anaphase (Matos et al. 2011; Pfander and Matos 2017). Alternative non-nucleolytic methods of processing HJs, such as dHJ dissolution (see below), which do not form crossovers, act earlier in the cell cycle (Wechsler et al. 2011; Sarbajna and West 2014). However, even though HJ resolution may only be a backup, it seems to be one that is frequently required, as depletion/loss of GEN1 and MUS81 in human cells causes cell cycle delay and considerable cell death associated with unresolved recombination intermediates that manifest as ultrafine DNA bridges during anaphase (Chan et al. 2018; Chan and West 2018).

1.3.3.3 Dissolution of double Holliday junctions

The dissolution of dHJs creates noncrossover products with the cooperative action of an HJ branch migration enzyme (Rqh1 in fission yeast and its counterparts, Sgs1 in budding yeast and BLM in mammals) and a topoisomerase III. The convergent branch migration of the two HJs leads to a hemicatenane intermediate, which can be decatenated by topoisomerase III (Hiasa and Marians 1994; L. Wu and Hickson 2003) (Figure1.2). The branch migrating helicase works in complex with the OB (oligonucleotide/oligosaccharide binding) fold containing accessory factor Rmi1 to dissolve dHJ intermediates (Wu and Hickson 2003; Mankouri and Hickson 2007). This complex, together with the type IA topoisomerase (Top3/TopoIIIα) forms a “dissolvasome” (Manthei and Keck 2013; Hickson 2014). The importance of dHJ dissolution is shown by the high levels of inter-sister chromatid exchange in BLM-deficient patients (Wu and Hickson 2003) and by the high levels of crossover recombinants generated during mitotic DSB repair in budding and fission yeast (Ira et al 2003; Sun et al 2008).

1.4 Repairing DSBs by break-induced DNA replication

Break-induced replication (BIR) is a pathway that specializes in the repair of one-ended double-strand DNA breaks (DSBs) (Figure1.3). Most HR repair pathways involve both ends of the DSB with invasion of homologous DNA by one end of the break followed by DNA synthesis and ligation of the two ends. BIR is a specialized mechanism of HR involving a single end of the DSB, which may occur when the other end of the break fails to engage with a homologous sequence, or when the two ends of the break find homologous template independently of each other, possibly at different ectopic sites (Sakofsky and Malkova 2017). Another scenario for BIR can arise at eroded telomeres that exposes a single DNA end or in situations when replication through a DNA lesion causes fork collapse and creation of one ended breaks (Sakofsky and Malkova 2017; Llorente et al. 2008; Anand et al. 2013).

Eukaryotic BIR has been studied extensively in budding yeast using several different approaches of controlled induction of DSBs. The approaches included transformation of yeast cells with linearised DNA fragments for initiating BIR at a homologous site (Morrow et al. 1997); or using the HO site-specific endonuclease to induce a chromosomal DSB such that only one end of the break can find homology in the genome (Bosco and Haber 1998; Malkova et al. 1996; Morrow et al. 1997). Some studies were done using yeast cells lacking telomerase, which maintain their telomeres via a BIR based pathway called alternative lengthening of telomeres (ALT) (Le et al. 1999; Lydeard et al. 2007). A recent approach involves introducing a site specific nick which gets converted into a one-ended break during replication (Cortes-Ledesma & Aguilera, 2006; Katz, Gimble, & Storici, 2014; Mayle et al., 2015; Nielsen et al., 2009). New experimental systems have now been developed in higher

eukaryotes for studying BIR in *Xenopus laevis* egg extracts (Hashimoto & Costanzo 2011) and mammalian cell lines (Costantino et al. 2014; Chandramouly et al. 2013; Cho et al. 2014; Bhowmick et al. 2016).

Similar to other HR-mediated DSB repair pathways, BIR initiates with 5'-3' resection of the DSB end which generates a 3' ssDNA tail (Chung et al. 2010). In *S. cerevisiae*, the initial resection is catalysed by the Mre11–Rad50–Xrs2 (MRX) complex (Mre11, Rad50, Nbs1 (MRN) in *S. pombe* and mammals) and Sae2 (Ctp1 in *S. pombe* and CtIP in mammals), which is followed by longer range resection catalysed either by Exonuclease 1 (Exo1) or Sgs1 in conjunction with Dna2 (Symington 2016). The subsequent interaction between the homologous template and ssDNA needs Rad52 but in yeast can proceed via a Rad51-dependent or Rad51-independent pathway (Davis & Symington, 2004; Malkova et al., 2005; Malkova et al., 1996). The main pathway for BIR in yeast is Rad51-dependent, which is more efficient and requires significantly more DNA sequence homology to proceed than the Rad51-independent pathway (Lydeard et al. 2007). As might be expected, the Rad51-dependent pathway requires the proteins that promote Rad51 nucleofilament formation and stability (i.e. Rad52, Rad54, Rad55 and Rad57), however, interestingly, it has a greater dependence on the Shu complex proteins than other Rad51-mediated DSB repair pathways (Signon et al. 2001; Anand, Lovett, and Haber 2013; Lydeard et al. 2010). The Rad51-independent pathway is mediated by Rad52 and also needs Rad59, Rdh54 and the Swi2/Snf2 chromatin remodeler complex (Malkova et al. 1996; Signon et al. 2001). Rad59 is a homologue of Rad52 that is suggested to play an important role in stabilizing the initial encounter between the DSB end and the donor sequence (Sugawara et al. 2000). Rad51-independent BIR is a less efficient process considered

to proceed by SSA between short stretches of homology (homeology) and is suppressed by Rad51 filament formation (Downing et al. 2008). Interestingly it has been suggested that Rad51-independent BIR may be akin to microhomology-mediated BIR (MMBIR) which is thought to be responsible for generating some of the complex genomic rearrangements detected in patients with various neurological diseases (Carvalho and Lupski 2016; Hastings et al. 2009).

The initiation of BIR can take several hours but varies for different experimental systems. This delay is proposed to result from the recombination execution checkpoint (REC), activated in response to the absence of the second end to participate in the HR. Two helicases, Sgs1 and Mph1, are considered to be involved by promoting multiple rounds of dissociation and reinvasion of the broken DNA end into its template (Jain et al. 2009; Jain et al. 2016). The most peculiar feature of Rad51-dependent BIR is its mode of DNA synthesis, which is carried out via a migrating D-loop (or bubble) driven by branch migration of its four-way DNA junction that displaces the newly synthesized strand. The synthesis is asynchronous with the leading strand primed at the 3' end extending while the D-loop migrates (Saini et al. 2013; Wilson et al. 2013). The lagging strand utilizes the leading strand as the template, therefore resulting in conservative inheritance of nascent DNA (Saini et al. 2013; Maradeo and Skibbens 2010; Donnianni and Symington 2013). The mode of synthesis of the lagging strand is not known; it could either be discontinuous, forming Okazaki fragments, or be continuous beginning from the terminal end of the leading strand. Stretches of DNA extending upto 100 kb have been detected representing BIR (Saini et al. 2013).

All three replicative polymerases, Pol α, Pol ε and Pol δ, participate in BIR DNA synthesis, though their exact roles and distribution of labour remains unclear. Yet there

is evidence suggesting that Pol δ is the main polymerase performing leading-strand synthesis (Lydeard et al. 2007; Deem et al. 2008; Smith et al. 2009). A specific feature of BIR is its need for Pol32, a subunit of Pol δ, which is not essential for S-phase DNA synthesis. It is possibly responsible for strand displacement during bubble migration (Lydeard et al. 2007). Studies show that the Pol α primase complex participates in both lagging and leading-strand synthesis, although its role in the context of leading strand synthesis is still unclear (Lydeard et al. 2007; Lydeard et al. 2010). Temperature sensitive mutants of Pol α (*po1-17*) and primase (*pri2-1*) were unable to complete HO-endonucleae induced BIR (Lydeard et al. 2007). Data also suggest that Pol ε is not needed for initiating DNA synthesis but promotes DNA synthesis post BIR establishment (Lydeard et al. 2007).

The identity of the main helicase that drives BIR progression is not clear. An initial study on HO endonuclease induced BIR in yeast proposed that Mcm2-7 is the main replicative helicase in BIR. The system comprises of a galactose-inducible HO endonuclease cut site integrated into the *CAN1* gene on a template chromosome deleting the 3' end portion of the gene. The DSB shares homology, only on the centromere-proximal side, with a segment of the *CAN1* gene that is inserted on a donor chromosome. Repair of the break by BIR DNA synthesis results in a nonreciprocal translocation that restores an intact *CAN1* gene, while the entire donor chromosome arm is duplicated and sequences distal to the original HO cut site are lost. The initiation of new DNA synthesis was detected by PCR and BIR was defective at the restrictive temperature of 37°C in the temperature sensitive *mcm4-td* degron strain (Lydeard et al. 2010). However, another study using a budding yeast strain disomic for chromosome 3 to assay allelic interhomolog BIR found that *mcm4-td*

has only mild BIR deficiency at restrictive temperature (Wilson et al. 2013). This strain has a galactose-inducible HO endonuclease cut site integrated at the *MAT*a locus of one copy of Chromosome 3 which is truncated distal to the DSB site for efficient BIR. The second copy of the chromosome contained an uncleavable *MATα*-inc allele and serves as a template for DSB repair (Wilson et al. 2013). Cells lacking Pif1 or its helicase activity were found to be deficient in allelic interhomolog BIR. By monitoring the association of RPA with the template chromosome by ChIP and quantitative PCR, extensive ssDNA generated during BIR was observed, that was Pif1 dependent. It was proposed that Pif1 can support long range BIR in the absence of Mcm2-7 (Wilson et al. 2013). Although the specific role of Pif1 is unknown, it has been postulated that it either works ahead of the replication bubble to unwind the DNA duplex or behind the bubble to extract the nascent leading strand from the replication machinery (Saini et al. 2013; Wilson et al. 2013). Srs2 is also considered to have a role in BIR, preventing the formation of toxic intermediates that would otherwise form upon invasion of the newly synthesized leading strand into the template duplex DNA (Elango et al. 2017).

PCNA plays an important role in BIR and both sumoylation and ubiquitination of PCNA at K164 are involved. This implies that these modifications either occur sequentially or on different monomers (Lydeard et al. 2010). Two specific alleles of PCNA, namely *pol30-89* and *pol30-92* were identified capable of affecting BIR efficiency without affecting gene conversions. PCNA being a homotrimer, one subunit that is *pol30-89* or *pol30-92* can possibly affect BIR without affecting replication (Lydeard et al. 2010). Another important factor for BIR is RPA, which protects large stretches of ssDNA created in the case of extensive resection and during leading strand synthesis. Hypomorphic alleles of *RFA1*, the gene encoding the large RPA sub-

unit, that only mildly affected normal DNA synthesis, resulted in a dramatic defect in BIR (Ruff et al. 2016). BIR was assayed in a system consisting of a recipient 3' truncated *lys2* gene with a galactose inducible HO endonuclease cut site on one chromosome and a donor 5' truncated *lys2* gene on a different chromosome. The donor shares homology only on the right side of DSB resulting into reconstitution of the *LYS2* gene by BIR. The *rfa1-D228Y and rfa1-S373P* mutants exhibited BIR frequency 20 to 50-fold lower than that of the wild-type. BIR frequency was also verified by physically measuring the product formation by PCR. The BIR defect was proposed to be mainly associated with the instability of the 3' invading end, which is degraded by the Sgs1/Dna2 complex, in the absence of adequate protection by RPA. RPA could be important in protecting long-lived ssDNA intermediates during BIR such as the displaced strand of the D-loop (Wold 1997; Ruff et al. 2016).

DNA synthesis associated with BIR is considerably more error-prone than normal S-phase DNA replication, yielding increased rates of both frameshift mutations and chromosomal rearrangements (Deem et al. 2008; Ruff et al. 2016; Deem et al. 2011; Sakofsky et al. 2015; Sakofsky et al. 2014; Smith et al. 2007; Anand et al. 2014; Jain et al. 2009; Smith et al. 2009; Vasan et al. 2014). The majority of frameshift mutations have been attributed to a reduced fidelity of Pol δ that may be related to frequent dissociation of Pol δ from the template DNA during bubble migration. Frequent dissociation of the invading 3' end during BIR may occur due to the action of helicases like Mph1 and Sgs1, which also cause delay in BIR initiation (Sakofsky and Malkova 2017; Smith et al. 2007; Jain et al. 2009). In addition, the rapid dissociation of nascent DNA from the template during bubble migration may prevent correction by MMR (Deem et al. 2011). The asynchrony between leading and lagging strand

synthesis also results in increased levels of base substitutions, as it creates long stretches of ssDNA on which excision DNA repair pathways cannot operate (Sakofsky et al. 2014). These lesions may be later bypassed by the incorporation of erroneous bases in the opposite strand by TLS polymerases. It is thought that the formation of clustered mutations in cancer genomes by apolipoprotein B mRNA editing enzymes catalytic polypeptide-like enzyme (APOBEC) may involve damaged ssDNA that accumulates during BIR (Chan & Gordenin, 2015; Roberts & Gordenin, 2014). BIR can also give rise to chromosomal rearrangements both through frequent template switching and through the premature resolution of BIR intermediates that can result in half-crossovers that resemble chromosome fusions reported in human cancer cells (Smith et al. 2009; Deem et al. 2008).

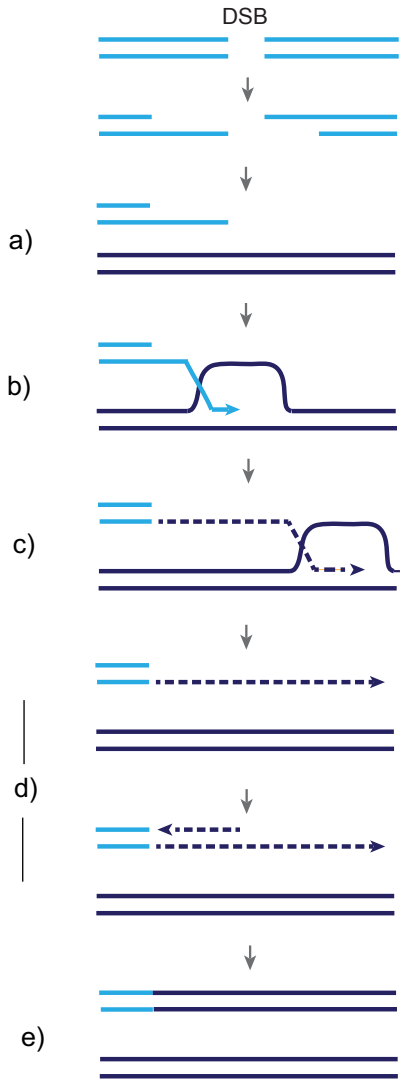

Figure1.3 Model of DSB repair by BIR
a) During BIR, a single end of the DSB is available for strand invasion, 5'-3' resection generates a 3' ssDNA end. b) 3' ssDNA end invades a homologous DNA molecule to form a D-loop. c) DNA synthesis carried out via a migrating D-loop driven by branch migration of an unresolved HJ, displacing the newly synthesized strand. d) Asynchronous DNA synthesis, with newly synthesized leading strand persisting as a long tract and delayed lagging strand synthesis that uses leading strand as the template. e) Completion of BIR with conservative inheritance of newly synthesized DNA.

1.4.1 BIR in replication fork restart

BIR has been implicated in the restart of collapsed RFs in bacteriophage T4, as well as in bacteria (Michel and Sandler 2017; Mosig 1998; Mueser et al. 2010). In *Escherichia coli*, where replication is initiated from a single replication origin and terminates at a single locus, BIR is the primary pathway to ensure completion of replication following fork collapse. It involves cleaving of the dysfunctional fork, if not already broken, and resection of the broken end to generate a ssDNA tail that is coated with RecA. The RecA filament invades the template duplex and and primes DNA synthesis. The structure is then processed by nucleases and the replicative helicase is reloaded yielding a canonical RF (Anand et al. 2013; Malkova and Ira 2013; Sakofsky et al. 2012). However, eukaryotic cells are less dependent on BIR for the recovery of broken RFs because the majority of dysfunctional forks are likely to be rescued by a converging fork derived from a nearby origin of replication. Hence, shorter tracts of mutagenic BIR synthesis are observed in S-phase compared to G2 as discussed below (Mayle et al. 2015).

BIR is also able to restart broken RFs in eukaryotes as shown by studies in both *S. cerevisiae* and *Xenopus laevis* egg extracts (Hashimoto and Costanzo 2011; Mayle et al. 2015). In *S. cerevisiae*, a site-specific single-strand DNA break was used to induce replication fork breakage, which was successfully repaired by BIR initiated during S-phase (Mayle et al. 2015). The nature of this BIR was similar to that studied in G2, in that it was associated with increased mutagenesis and template switching, and was dependent on Pol32 and Pif1 (Mayle et al. 2015). However, unlike non-S-phase associated BIR, only few kilobases of BIR synthesis and associated mutagenesis and template switching were detected. This was attributed to fork

convergence with the oncoming RF and cleavage of BIR intermediates by Mus81. Long-tract BIR DNA synthesis was induced only when the replication collapse occurred in a *mus81*Δ mutant in regions of the genome devoid of replication origins (Mayle et al. 2015).

BIR events have been shown to be triggered under unusual conditions, such as post-RF collapse at fragile sites under conditions of reduced levels of Pol α in budding yeast (Lemoine et al. 2005) and in regions with hairpin-capped DSBs that promote RF collapse (Narayanan et al. 2006). BIR is also triggered by oncogene induced replication stress in cancer cells (Sotiriou et al. 2016; Costantino et al. 2014). These events depend on Rad52 and need POLD3, a mammalian homolog of Pol32. It was recently reported that replication stress induced by p53-independent expression of p21 in cancer cells, promotes Rad51-independent, but Rad52-dependent events, which could be due to BIR (Galanos et al. 2016). There is also an interesting report on BIR leading to large scale expansions of $(CAG)_n$•$(CTG)_n$ trinucleotide repeats, which are similar to those responsible for a number of neuromuscular and neurodegenerative disorders (Kim et al. 2017).

1.5 Recombination-dependent replication restart without a DSB

RF collapse does not always result from (or lead to) breakage of the DNA. It can sometimes just involve the dissociation of replisome components (Cortez 2015). A model system for studying the consequences of RF collapse without DNA breakage has been developed in *S. pombe* using the site-specific protein-DNA polar RFB Replication termination sequence 1 (*RTS1*) (Lambert et al. 2010; Miyabe et al. 2015; Mizuno et al. 2013; Nguyen et al. 2015; Ahn et al. 2005). RF blockage at *RTS1* leads to fork collapse followed by the recruitment of HR proteins within approximately 10

minutes, which then act to restart replication, which is then driven by Pol δ-mediated synthesis of both leading and lagging strands (Miyabe et al. 2015; Nguyen et al. 2015; Lambert et al. 2010; Mohebi et al. 2015). This type of recombination-dependent replication (RDR) has been termed homologous recombination-restarted replication (HoRReR) (Miyabe et al. 2015) however, I will refer to it simply as RDR henceforth. Like BIR, RDR induced by *RTS1* depends on Rad51 and Rad52, which can inadvertently recombine ectopic homologous sequences during the restart process generating a variety of genome rearrangements and alterations (Ahn, Osman, and Whitby 2005; Lambert et al. 2005; Lambert et al. 2010; Mizuno et al. 2009; Morrow et al. 2017; Nguyen et al. 2015). Also similar to BIR, RDR induced by *RTS1* is very mutagenic and liable to template switching (Iraqui et al. 2012; Mizuno et al. 2013; Nguyen et al. 2015) However, unlike BIR, RDR is semi-conservative (Miyabe et al. 2015).

A favoured model for RDR induced by *RTS1* is depicted in Figure1.4. In this model the collapsed fork is regressed (or reversed) into a so-called “chicken foot” structure that resembles an HJ (Sun et al. 2008; Ait Saada et al. 2018). Fork regression involves the unwinding of the two nascent strands from their templates followed by their annealing to each other such that they form a DSB end (Higgins et al., 1976; Postow et al., 2001; Sogo et al., 2002). Fml1, Rqh1, Fbh1 and Rad54, have been shown to promote fork regression *in vitro* and hence could promote RDR at *RTS1* (Atkinson and McGlynn 2009; Sun et al. 2008; Whitby 2010; Zheng et al. 2011; Ralf et al. 2006; Gari et al. 2008; Fugger et al. 2015; Bugreev et al. 2011). However, from this list of proteins, only Fml1 and Rad54 appear to promote *RTS1*-induced recombination, whereas Fbh1, Rqh1 and Srs2 have been shown to limit it (Ahn et al.

2005; Lorenz et al. 2009). Interestingly, replication restart is reported to be reduced in a *srs2*Δ mutant (Lambert et al. 2010; Inagawa et al. 2009). The DSB end generated by fork regression is resected to form a 3' ssDNA tail onto which Rad51 loads. The process of resection was recently shown to involve two steps, an initial short-range resection mediated by the MRN complex and Ctp1, followed by a long-range resection that is mediated by Exo1 (Tsang et al. 2014; Teixeira-Silva et al. 2017). The initial DNA resection at the collapsed fork is governed by the binding of the Non-Homologous End Joining (NHEJ) protein Ku, which seems to prevent extensive degradation of the DNA. Loss of Rad51 or Rad52 has also been reported to prevent fork restart due to extensive resection at the collapsed fork by Exo1 (Ait Saada et al. 2017). Once loaded, the Rad51 nucleofilament conducts a homology search and strand invasion to form a D-loop. It is thought that this D-loop acts as a platform for the reassembly of replisome components and that replication may then proceed in a fashion similar to BIR (i.e. as a migrating D-loop) (Nguyen et al 2015). It has also been suggested that the semi-conservative mode of DNA synthesis stems from the branch migration of the four-way junction following behind the D-loop (Nguyen et al 2015).

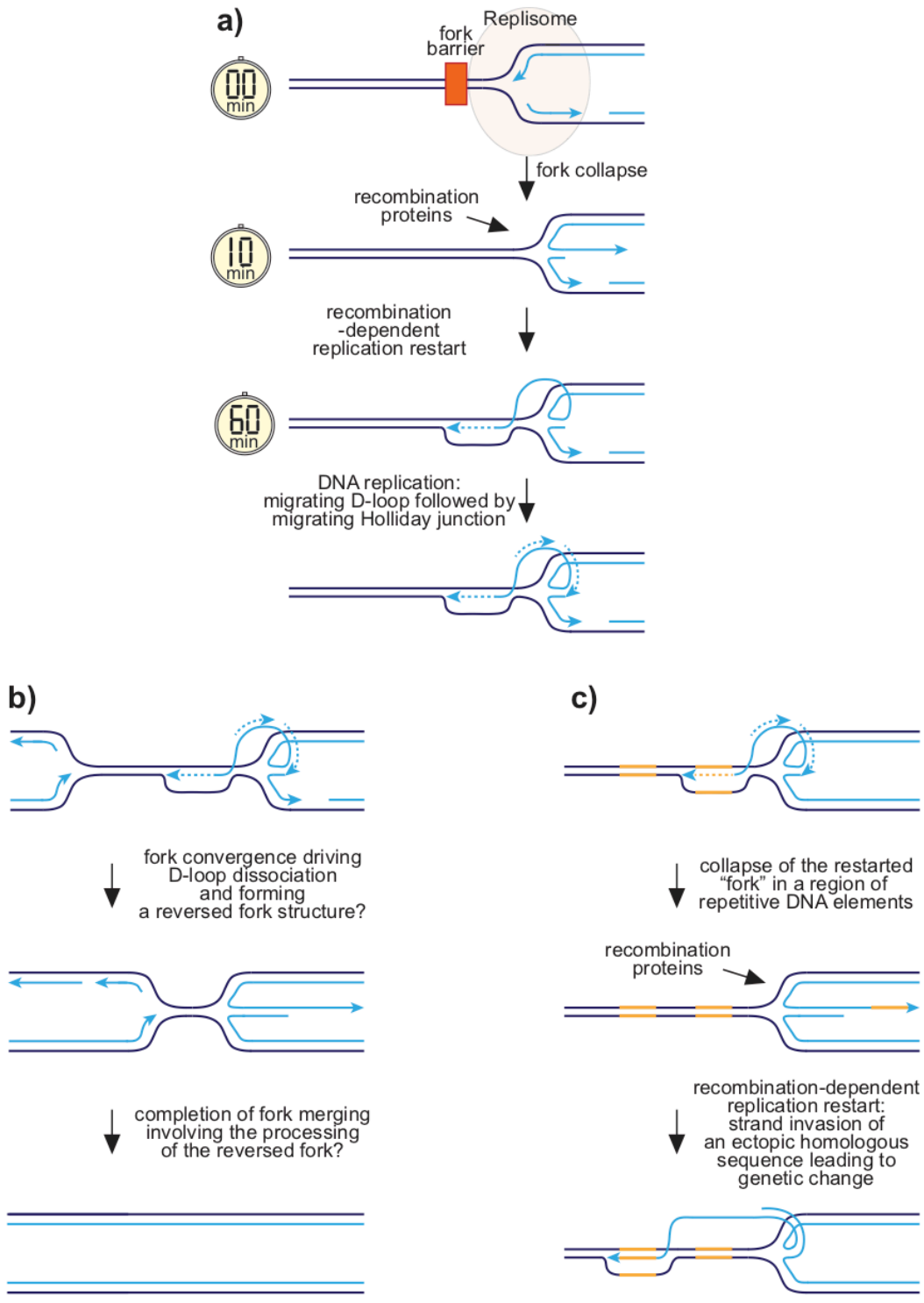

Figure1.4 Hypothetical model for RFB-induced RDR
a) RF blockage at *RTS1* leads to fork collapse and RDR initiates within 10 minutes and gives rise to a restarted fork within 60 mins. Parental DNA strands are shown in dark blue and nascent strands in light blue. b) Model to show how a canonical and restarted fork might merge. c) Model to show how RDR might give rise to genetic change. The two yellow patches represent a direct repeat of homologous sequences. Figure adapted from Nguyen et al. 2015.

1.6 Aims of study

RDR is important for ensuring completion of replication by restarting collapsed RFs, although this comes at the cost of increased genomic instability. Fork restart could be more crucial in regions where replication is unidirectional, such as the rDNA locus, in regions of low origin density, such as some human fragile sites, and under situations where both converging forks are impeded (Lambert and Carr 2013; Murray and Carr 2008; Lambert et al. 2010). During replication fork collapse, the protein components of the fork are thought to partially or completely dissociate from the DNA (Cortez 2015). In *E. coli*, fork collapse entails replisome disassembly, and restart of a collapsed fork involves HR and the PriA helicase that catalyses the assembly of a new replisome de novo on joint-molecule structures (Heller and Marians 2006; Michel et al. 2007). In eukaryotes, it remains to be understood clearly if fork collapse involves unloading of the replisome and whether origin-independent loading of the replisome occurs during RDR. The primary aim of my study was to investigate whether fork collapse is an "active" process that involves unloading of specific components of the replisome. To this end, I investigated whether specific factors are needed to dismantle the replisome in order for RDR to occur at *RTS1*. These investigations comprise the first and major part of my work (Chapters 3, 4 and 5).

Similar to BIR, Rad51 and Rad52 promote replication restart at *RTS1.* The reengagement of the nascent strands with the parental DNA duplex, mediated by Rad51 seems to be vital for the process of RDR. Rad51 activity in general requires various mediators that facilitate formation and functional activation of Rad51 nucleofilament. Understanding more about the role of Rad51 and its mediators in fork

restart from *RTS1,* in order to advance our knowledge on the mechanism of fork restart and the nature of the restarted fork, comprises the latter part of my work (Chapter 6).

2 Materials and methods

2.1 *Escherichia coli* media

E. coli was grown at 37°C in Luria-Bertani (LB) (10g Tryptone, 5 g yeast extract, 5 g NaCl per litre) broth or on LB-agar (15 g/l agar), supplemented with antibiotics where appropriate (Sambrook and Russell 2001). Antibiotics were filtered (0.2µm Millipore syringe filters) and stored as 1000X stocks at 4°C (Sambrook and Russell 2001) and mixed into the media (under 50°C), just before use. Antibiotics were used at recommended concentrations (ampicillin: 50 µg/ml; kanamycin: 50 µg/ml; chloramphenicol: 20 µg/ml) (Sambrook and Russell 2001).

2.1.1 *Schizosaccharomyces pombe* media

Yeast extract (YE) (30 g D-Glucose and 5 g Yeast Extract in 1litre water) and YE containing all supplements (YES) (225 mg/l uracil, leucine, lysine, histidine, and adenine each) were used as complete media. Edinburgh Minimal Medium with 3.7 mg/ml L-glutamic acid monosodium salt (EMMG) (20 ml 50x salts, 1 ml 1000x vitamins, 0.1 ml 10000x minerals, 30 g D-Glucose, 3.7 g sodium glutamate, 2.2 g anhydrous Na_2HPO4, 3 g potassium hydrogen phthalate in 1 litre water) was used as minimal media and supplemented with amino acids as appropriate (Sabatinos and Forsburg 2010). The 1000X vitamins stock contains 0.1% pantothenic acid, 1% nicotinic acid, 1% myo-inositol and 0.001% biotin. The 10,000X minerals stock contains 1% citric acid, 0.04% cupper sulphate, 0.1% potassium iodide, 0.16% molybdic acid, 0.2% ferric chloride, 0.4% zinc sulphate heptahydrate, 0.4% manganese (II) sulphate and 0.5% boric acid. When needed, 18 g/l Difco™ agar was added to the media. *S. pombe* were grown at 30°C unless otherwise stated.

Strains that are auxotrophic for one or more of the following: adenine, arginine, histidine, leucine, and/or uracil, were supplied with the respective supplements at 0.25 mg/ml for growth on minimal media. To differentiate between *ade*$^{+}$ and *ade*$^{-}$ colonies, cells were plated onto low adenine (LA) medium containing 0.01 mg/ml adenine, which allows *ade*$^{+}$ colonies to appear white and *ade*$^{-}$ colonies red. The red colour is due to the accumulation of a precursor in the adenine biosynthesis pathway, P-ribosylaminoimidazole, that oxidizes to a red pigment (Schär and Kohli 1994). *Ade*$^{+}$ recombinants were selected on YE supplemented with 0.2 mg/ml guanine dissolved in 1 M NaOH to prevent uptake of residual adenine (Osman and Whitby 2009)

For selection of strains carrying antibiotic resistance, media was supplemented with the recommended concentrations of geneticin (G418; 100mg/l), nourseothricin (clonNat; 100 mg/l) or hygromycin B (200 mg/l). To repress expression from the *nmt* promoter, 20 nM – 4 μM thiamine was added to the minimal media as indicated. To test for 5-Fluoroorotic Acid (5-FOA) resistance, cells were plated onto YES medium (30 g D-Glucose, 5 g Yeast Extract, 20 g agar, 200 mg leucine, lysine, histidine, adenine and 50 mg uracil in 1 litre water) containing 1g/l 5-FOA (5-Fluoroorotic Acid Monohydrate, Formedium Ltd.)(Petersen and Russell 2016). 5-FOA was dissolved in water and mixed 1:1 with 55°C 2XYES for pouring the plates. Malt extract (ME) media [30 g malt extract, 20 g agar in 1litre water (pH>5.5)] was used for mating strains, which was carried out at 25°C.

2.2 *S pombe* strain construction

2.2.1 Transformation

To integrate linear DNA constructs into the *S. pombe* genome, *S. pombe* cells were transformed by an established lithium acetate transformation protocol (Okazaki et al. 1990). Cells were washed three times in sterile Milli-Q water and resuspended 1:1 in 0.1 mM lithium acetate (pH 7.5) with 1x TE (pH 7.5). 10 µg of linear DNA for integration and 20 µg of carrier DNA (sonicated salmon sperm DNA, to protect the DNA from degradation by nucleases) were mixed with 100 µl of cells and incubated at room temperature for 10 minutes. 260 µl 0.1 mM lithium acetate, 1x TE and 40% PEG were added to the mixture at 30°C for 60 – 90 minutes. Finally, cells were heat shocked with 43 µl DMSO at 42°C for 5 minutes, washed and resuspended in Milli-Q water. The cells were handled gently at all stages, avoiding the use of vortex mixer for resuspending them. The transformed cells were plated in 1:1, 1:10 and 1:100 dilutions, either directly onto selective media (for nourseothricin selection and/or auxotrophic markers) or plated onto complete media without antibiotics and incubated at 30°C for 48 hours before replica plating the transformants onto selective media (for geneticin and hygromycin B). Colonies were screened for correct integration of the DNA construct by colony polymerase chain reaction (PCR) (described in Section 2.2.3)

2.2.2 Genetic crosses

Cells with opposite mating types (h^+/h^-) were mixed and grown on Malt Extract Agar (MEA) at 25°C for 3 days. Spores were released by overnight digestion with glusulase (PerkinElmer) at 30°C. Successful mating was determined microscopically by observing the formation of asci. Cells were then washed in sterile Milli-Q water and

plated on YES agar or directly onto the appropriate selective medium. Progeny were screened for the appropriate genetic markers and genotoxin sensitivities.

2.2.3 Colony PCR

Colony PCRs were performed to confirm accurate integration of linear DNA fragments into the *S. pombe* genome. Chromosomal DNA was released from yeast cells by boiling a yeast colony in 5 μl ddH_2O at 100°C for 5 minutes. This was followed by amplification of specific DNA fragments, that would result from correct integration of the DNA construct by *Taq* DNA polymerase (New England BioLabs) using at least one primer that anneals to a unique chromosomal sequence that flanks the targeted site. Where appropriate, PCR products were sequenced to confirm the presence of point mutations. Independent transformants were subsequently tested for growth and genotoxin sensitivity to determine the reproducibility of the phenotype.

2.3 Molecular and cell biology techniques

2.3.1 *E. coli* transformation

Competent *E. coli* DH5α or Mach1 cells were transformed with a minimum of 100 ng plasmid DNA using the standard 42°C heat shock treatment for bacterial transformation (Sambrook and Russell 2001). Cells were plated on LB agar medium with 50 μg/ml ampicillin and grown at 37°C overnight. For mini- and medium-scale plasmid preps, the QIAScreen Miniprep protocol and QIAprep Spin Midiprep Kits (Qiagen, Hilden, Germany) were used, respectively, following instructions from the manufacturer.

2.3.2 Cloning and subcloning DNA fragments

For plasmid construction, the appropriate DNA fragment was excised or PCR-amplified with Phusion High-Fidelity DNA Polymerase (Thermo Scientific, Loughborough, UK) or KAPA HiFi DNA Polymerase (KAPA Biosystems, Wilmington, MA) from the relevant plasmid construct and isolated from 0.8% agarose gels using a QIAquick Gel Extraction Kit (Qiagen). Fragments were ligated with T4 DNA ligase (New England Biolabs) at room temperature for a minimum of 2 hours or at 4°C overnight. Correctly constructed plasmid isolates were verified by restriction digest and sequencing. The plasmids used in this study are listed in Table 5.

2.3.3 Site directed mutagenesis

Site directed mutagenesis of the desired plasmid was done with the Q5 Site-Directed Mutagenesis Kit (New England BioLabs) as per manufacturer's instructions, using standard primers as it does not require phosphorylated or purified oligos. The plasmid was transformed into high-efficiency NEB 5α competent *E. coli* cells provided with the kit, following the manufacturer's instructions.

2.3.4 *S. pombe* genomic DNA extraction

Small-scale preparations for PCR or southern blot analyses were made from 10ml overnight *S. pombe* cultures. Harvested cells were spheroplasted by incubating in 1ml of citrate phosphate buffer (40mM EDTA, 50mM Na_2HPO_4, 55mM citric acid and 1.2M sorbitol) containing 2.5 mg of Zymolyase 20T (MP Biomedical) for 1 hour at 37°C. The efficiency of spheroplasting was assessed by microscopic examination of cells mounted in 2% SDS. Spheroplasts lyse in SDS solution and cells that are sufficiently spheroplasted will no longer refract light. Spheroplasts were resuspended in 550µl TE

[10mM Tris-HCl (pH 8.0), 1mM EDTA (pH 8.0)] with 1% SDS and incubated at 65°C for 1 hour. 175µl of 5M potassium acetate was then added and the sample was centrifuged at 13000 RPM for 15 minutes at 4°C. 450µl of the supernatant was retained and the DNA was precipitated by adding 200µl of 5M ammonium-acetate and 1ml isopropanol. After pelleting the DNA by centrifugation at 13000 RPM for 30 minutes at 4°C, the DNA was resuspended in 90 µl 1XTE [10mM Tris-HCl (pH 8.0), 1mM EDTA (pH 8.0)] containing 1µg/µl RNase A and incubated at 37°C for 1 hour. The DNA precipitation step was repeated, and the DNA was washed with 70% ice-cold ethanol. The DNA was resuspended in 1XTE and stored at -20°C.

2.3.5 Genomic DNA extraction embedded in agarose plugs

To isolate intact chromosomal DNA for running 1D and 2D gels, 500 ml asynchronous cultures of *S. pombe* cells were grown overnight at 30°C to a concentration of 1 X 10^7 cells/ml. Cells were then killed by the addition of 0.1% sodium azide (Sigma- Aldrich) and washed with sterile Milli-Q water. The cells were stored at -80°C at this point. Subsequently, the cells were spheroplasted in an equal volume of CPES buffer (40 mM EDTA, 120 mM Na_2HPO_4, 40 mM citric acid, 1.2 M sorbitol, 5 mM DTT) containing 10mg/ml *Trichoderma harzianum* lysing enzymes (L-1412, Sigm- Aldrich) and 0.625mg/ml *Arthrobacter luteus* lyticase (L-4025, Sigma-Aldrich) for 1 hour at 37°C. The spheroplasted cells were embedded in 1.2% agarose plugs as described by Hyppa and Smith (2009) using Bio-Rad Low Melt Agarose (Bio-Rad). To degrade the proteins, the plugs were incubated for two days in 3ml NDS buffer [495 mM EDTA, 10 mM Tris-HCl (pH 7.5), 1% N-lauroylsarcosine] containing 1 mg/ml Proteinase K at 50°C. To inactivate residual Proteinase K activity, the plugs were incubated in 10 ml 1XTE with 0.5 mM PMSF on a rocking platform for 1 hour at room temperature. They

were then subsequently washed three times in 15 ml 1X TE for 1 hour each on a rocking platform before being stored in 1X TE at 4°C.

2.3.6 Two-dimensional (2D) gel electrophoresis – for analysing replication intermediates

The method of DNA preparation and the neutral-neutral 2D gel electrophoresis has been previously established (Brewer and Fangman 1988). Following genomic DNA extraction in agarose plugs (as described in Section 2.3.5), plugs containing equivalent of 1.5 to 2 X 10^9 cells were washed three times with copious amounts of sterile Milli-Q water to get rid of the 1X TE buffer used for storage. Next, the plugs were washed three times with 1X CutSmart Buffer (New England Biolabs), melted at 65°C for 10-15 minutes and then incubated with 10 µl of β-agarase I (New England Biolabs) for 2 hours at 42°C for complete digestion of the agarose. The genomic DNA was then incubated with 10 µl (200 units) of *SacI* and 10 µl of RNaseA (10mg/ml) overnight at 37°C. The next day, the incubation mixture was supplemented with 2.5 µl (50 units) of *SacI* and further incubated overnight at 37°C. The following day, the reaction was then centrifuged at 4000 RPM for 15 minutes at room temperature to get rid of the agarose. The supernatant containing the digested genomic DNA was stripped of residual proteins by passing it through one round of phenol: chloroform: isoamyl alcohol (25:24:1) extraction. The DNA was then precipitated by the addition of one volume of isopropanol and 1/10^{th} volume of 3M sodium-acetate overnight at -20°C. After pelleting the DNA by centrifugation at 13000 RPM for 30 minutes at 4°C, the DNA was washed twice with 70% ice- cold ethanol and resuspended in 40µl of 1X TE.

The digested DNA was loaded onto a 0.4% agarose gel and run in the first dimension, in 1X TBE without ethidium bromide to ensure uninterrupted migration. The first dimension was run for ~48 hours at 25 V at room temperature where DNA fragments were separated on the basis of their size. The gel was stained with 0.3 µg/ml ethidium bromide for 1 hour to visualize the DNA. The slice containing the DNA fragments of interest was excised and DNA from this slice was then run in the second dimension in a 1.2% agarose gel in 1X TBE with 0.3 µg/ml ethidium bromide under continuous buffer (1X TBE with 0.3 µg/ml ethidium bromide) recirculation at 4°C to separate the intermediates on the basis of their shape. The second dimension was run for ~18 hours at 120 V, until the dye front had migrated at least 8 cm. This was followed by Southern blotting (as described below).

2.3.7 Southern blotting

Before blotting, gels were gently shaken at room temperature in 0.25 M HCl for 15 to 20 minutes to depurinate the DNA and then in transfer buffer (0.5 M NaOH, 1.5 M NaCl) for 10 minutes. DNA was transferred from the gels onto positively-charged nylon membranes (Hybond^{TM}-XL, GE Healthcare) by capillary transfer (Sambrook and Russell, 2001). After dismantling the blot, membranes were briefly washed with 2x saline sodium citrate (SSC) (0.03 M sodium citrate, 0.3 M NaCl buffer, pH 7-8) and stored at -20°C. Pre-hybridization was done at 55°C for 60 minutes in modified Church and Gilbert Buffer (0.5 M Phosphate buffer (pH 7.2), 7% SDS, 10 mM EDTA) (Church and Gilbert 1984). Hybridization was performed at 55°C overnight as described in Sambrook & Russell (2001) in a Grant Boekel hybridization oven (HIR10M). Bands of interest were detected by radiolabeling the appropriate probe with [α-^{32}P] dCTP (PerkinElmer) using an Amersham^{TM} Rediprime II Random Prime Labeling System kit

following the manufacturer's instructions. Probe A is an *EcoNI-XbaI* restriction fragment from pFOX2 (Ahn et al. 2005). Probe D is a DNA fragment amplified from genomic DNA by PCR using primers oMW706 and oMW707 (Ahn et al. 2005). Probe E is an *BlpI-NdeI* restriction fragment from pFOX2 (Osman et al. 2016). Following one wash with 1X SSC and 0.1% SDS and another wash with 0.5X SSC and 0.1% SDS, both at 55°C for 20 minutes, probed membranes were exposed to phosphor-screens for up to one week, which were then scanned using a Fuji FLA-3000 phosphorimager (FujiFilm) and analysed using Image Gauge software (FujiFilm).

2.3.8 Microscopy

For time-lapse imaging experiments, cells were grown overnight in 30°C EMMG lacking histidine. 1 μM thiamine was also included in the media unless stated otherwise. Cells were mounted with soybean lectin (200 μl 1X solution of soyabean lectin, Sigma-Aldrich) in a glass bottom culture dish (MatTek Corp., Ashland, MA) and observed in the appropriate medium in a thermally insulated temperature-controlled chamber at 30°C. For snapshot imaging, cells were spun down and mounted as a smear on a glass slide (Jaytec, MCG 01012) with cover slips (VWR, 631-0124). Live cells were imaged on an inverted Olympus IX71 microscope controlled by a DV Elite Core using DeltaVision softWoRx 5.5.0 software using either CFP/YFP/mCherry filter (Applied Precision Inc., Issaquah, WA). Images were taken with an Evolve^{TM} 512 EMCCD camera (Photometrics, Tucson, AZ) using an oil-immersion Olympus 100X UPlanSApo objective with a numeric aperture (NA) of 1.40. A stack of 16 focal planes at a step-size of 0.3 μm was taken every 5 minutes for 4 hours. Brightfield images of cells, LacI- tdKatushka2, eCFP-PCNA and Rad51-CFP were imaged with a 100 ms exposure time and 10% neutral density filter. Rad52-YFP was imaged with a 100 ms

exposure time and 5% neutral density filter. CFP-YFP-mCherry filter set was used for the imaging. Excitation middle wavelength/bandpass values for CFP, YFP and mCherry are 438/24, 513/17 and 575/25 respectively. Emission middle wavelength/bandpass values for CFP, YFP and mCherry are 475/24, 548/22 and 625/45 respectively.

2.4 Genetic assays

2.4.1 Genotoxin sensitivity assay

Exponentially growing cells from liquid culture were harvested, washed and resuspended in sterile Milli-Q water to an initial concentration of 1 X 10^7 cells/ml. Subsequent 10-fold dilutions were performed from 1 X 10^6 to 1 X 10^4 cells/ml. Aliquots (10µl) of the cell suspensions were spotted onto YES plates containing appropriate concentrations of chemical genotoxins (made from stock solutions of 10% MMS, 2M HU and 15mM CPT in water and stored at -20°C) or onto YES plates that were then irradiated with various doses of UV light using a Stratalinker (Stratagene). Plates were typically incubated at 30°C for up to 3-4 days, with growth being recorded daily by taking photographs of the plate. The spot assays reveal relative differences in survival and growth following a single (acute) exposure to UV or prolonged (chronic) exposure to MMS, HU and CPT, which generate DNA lesions that can variously cause replication fork stalling, blockage and breakage.

2.4.2 Direct repeat recombination assay

The mitotic direct-repeat recombination assay was performed according to the previously established protocol (Osman and Whitby, 2009). The cells were initially grown on YES or appropriately supplemented EMMG plates, with 1 µM thiamine (for imaging strains), for 5 to 6 days at 30°C. 10-20 single colonies from these were then

resuspended in sterile Milli-Q water. Approximately 10^4-10^6 cells were plated onto YE plates lacking adenine to score for *ade*$^+$ recombinants and 10^2-10^3 cells were plated onto non-selective plates of YE to assess cell viability. The frequency of the recombinants was calculated by counting the colonies on Protos automated colony counter (Synbiosis), after growth for 4 to 6 days at 30°C. Plates with *ade*$^+$ recombinants were then replica- plated onto minimal media lacking both histidine and adenine to estimate the proportion of gene conversions. For strains with the direct-repeat reporter 12.4 kb away from the endogenous *ade6* locus and *RTS1* and the reporter at a sub-telomeric site on chromosome 1, YE plates lacking adenine were incubated for 8 to 10 days at 30°C to ensure that *ade*$^+$ colonies had sufficient time to grow. The number of colonies analysed for each strain in the assay has been listed in Table 1, 2, 3 (see Appendix) and it involves a single assay or upto 8 repeats for a strain.

2.4.3 5-FOA resistance assay

The cells were initially grown on YES plates for 5 to 6 days at 30°C. 10-20 single colonies from these were then resuspended in sterile Milli-Q water. Approximately 10^6-10^7 cells were plated onto YES plates containing 5-FOA and 10^2-10^3 cells were plated onto non-selective plates of YE to assess cell viability. The frequency of the 5-FOA resistant colonies was calculated by counting the colonies after growth for 4 to 6 days at 30°C.

2.5 Analysis

2.5.1 Image processing and analysis

For time-lapse imaging experiments, raw images collected on the Delta Vision Elite Core were subsequently de-noised with Priism (Agard and Sedat Labs, UCSF) with the dimensionality set to “3D: xyz” for three iterations (Kervrann and Boulanger, 2006). De-noised images were then deconvolved with softWoRx 5.5.0 software with the “additive” method for 12 cycles (Applied Precision). Co-localization analysis of foci was done as previously established (Nguyen et al. 2015) with softWoRx 5.5.0 software. Foci were scored manually and separately for each of the fluorescent channels. Foci were distinguished from background as having at least three to five times higher intensity and having a minimum volume of 2X2 pixels. Perfect co-localisation was manually assessed and scored as foci in separate channels overlapping in xyz by a minimum of 2 pixels. Fluoresecent signals were quantified using Volocity (Improvision, Coventry, England) or Imaris (Bitplane, South Windsor, CT). Snapshot images were analysed as raw images manually for determination of foci and localisation, using Fiji (Image J) an open source Java image processing program (Schindelin et al. 2012). Intensity analysis of the foci was also done using Fiji. The foci and nuclei were detected separately using standard settings (‘Shanbag’ for foci and ‘Huang’ for nuclei) for thresholding and particle analysis. The selections were then superimposed on the raw image and integrated densities were measured, after subtracting the background.

2.5.2 Statistics

All statistical tests were performed using GraphPad Prism version 7.0 for Macintosh (GraphPad Software, La Jolla California, USA). Data were tested for normal distribution by the Shapiro-Wilk normality test. In accordance with the distribution of

data, means were compared by the appropriate independent-sample two-tailed T-test. Where normality of distribution of data could not be determined due to low sample size ($n<30$), means were compared by using the Mann-Whitney test. *P* values under 0.05 (5% significance interval) were considered significant and under 0.01 (1% significance interval) were highly significant.

3 Investigating whether unloading of replisome components is important for recombination dependent replication restart

3.1 Introduction

At some strong RFBs, the RF may collapse rendering the fork unable to resume replication even if the barrier is removed. In such cases, replication can be completed by the oncoming fork converging with the collapsed fork. However, if the oncoming fork also collapses, or is too distant from the collapsed fork to reach it in a timely manner, then the collapsed fork may be restarted by HR proteins in a process termed recombination-dependent replication (RDR). (Lambert et al. 2010; Miyabe et al. 2015; Mizuno et al. 2013; Nguyen et al. 2015). Fork collapse is a poorly understood process, thought to involve either replisome remodeling and/or disassembly paving the way for HR proteins to act and restart replication (Ahn et al. 2005; Lambert and Carr 2005; Lambert et al. 2010).

To study the process of fork collapse and RDR, the Whitby lab uses a programmed polar RFB called *RTS1*, the normal role of which is to promote mating type switching in *S. pombe* (Dalgaard and Klar 2001). The *RTS1* element is contained within a ~800 bp *EcoRI* fragment and is comprised of three full length and one truncated repeat of a ~ 60bp sequence motif (Codlin and Dalgaard 2003). Barrier activity also depends on several trans-acting factors including the FPC proteins Swi1 and Swi3, the myb domain-containing protein Rtf1 and the PCNA interacting protein Rtf2 (Noguchi et al. 2004; Ahn et al. 2005; Dalgaard and Klar 2000; Eydmann et al. 2008). *RTS1* is normally located on the centromere proximal side of the mating type switching locus *mat1*, allowing only unidirectional replication of this locus for strand-specific imprinting, which is necessary for mating type switching (Dalgaard and Klar 2001). However, *RTS1* acts as a potent polar RFB wherever it is positioned, and recent studies have shown that RF blockage at *RTS1* positioned at the *ade6* locus on

chromosome 3 triggers recombination protein recruitment within minutes, seemingly as a default response, and recombination dependent replication restart occurs within 10-60 minutes (Nguyen et al. 2015). This led to the hypothesis that *RTS1* actively promotes RF collapse. *RTS1* thus serves as an ideal model for studying RF collapse and RDR. By determining the mechanism of RF collapse at *RTS1* we may therefore understand the early stages of RDR (i.e. the "handover" from replisome to recombinosome).

In this Chapter, I describe my attempts to investigate whether fork collapse is an "active" process, which requires specific factors to dismantle the replisome in order for RDR to occur. Specifically, I focus on the dismantling of the replisome's two major ring structures, the MCM helicase and PCNA, which presumably need to be actively unloaded as they are topologically linked to DNA.

PCNA is a homotrimeric ring loaded onto DNA by the RFC clamp loader (Yao et al. 2006; Zhang et al. 1999). It tethers the polymerases to the template DNA acting as a sliding clamp, enhancing their processivity. It also acts as a platform to recruit other replication proteins (Moldovan et al. 2007; Cox 1997; Zhang et al. 1999; Warbrick et al. 1997; Eisenberg et al. 1997; Fotedar et al. 1996; Levin et al. 1997). Unloading of PCNA from DNA is performed by a variant of the RFC clamp loader, which contains the Elg1 protein in place of Rfc1 (Ben-Aroya et al. 2003). In budding yeast, Elg1 has been shown to unload both sumoylated and unmodified PCNA from the chromatin (Kubota et al. 2013; Kubota et al. 2013; C. Yu et al. 2014a; Parnas et al. 2010). However, it is not known whether Elg1 is needed for RDR.

As discussed in Chapter 1, the MCM2-7 helicase is the main replicative helicase in eukaryotes responsible for unwinding the two parental DNA strands at the

replication fork (Bochman and Schwacha 2008; Bochman et al. 2008). It forms a complex together with the GINS proteins and Cdc45, which is termed the CMG helicase (Ilves et al. 2010; Kang et al. 2012; Moyer et al. 2006; Gambus et al. 2006). Unloading CMG during the termination of DNA replication depends on the Cdc48 segregase (Maric et al. 2014; Moreno et al. 2014; Fullbright et al. 2016; Semlow et al. 2016). In budding yeast, Cdc48 is targeted to CMG by the F-box protein Dia2, which forms a Skp1-Cul1-F-box (SCF) E3 ubiquitin ligase complex that ubiquitylates the Mcm7 subunit of CMG (Maculins et al. 2015; Maric et al. 2014). The equivalent E3 ligase in metazoans is CUL-2^{LRR-1} (Sonneville et al. 2017). The Ufd1-Npl4 complex binds to the ubiquitylated CMG and recruits Cdc48, which extracts CMG from the DNA (Maric et al. 2017). The orthologue of Dia2 in fission yeast is Pof3 and the SCF^{Pof3} ubiquitin ligase is known to be involved in targeting several replisome components for degradation by the proteasome (Roseaulin et al. 2013). However, it is not known whether Pof3 is needed for RDR.

3.2 Results

3.2.1 Experimental system

To investigate whether Elg1 and/or Pof3 might be needed for RDR, I used an *RTS1*-based direct repeat recombination reporter (Ahn et al. 2005; Osman and Whitby 2009). This consists of two *ade6*$^-$ heteroalleles with an intervening *his3*$^+$ gene inserted at the *ade6* locus on Chromosome 3. Recombination between the two different loss-of-function *ade6*$^-$ alleles (*ade6-L469* and *ade6-M375*) restores the wild-type *ade6*$^+$ gene. Hence, the frequency at which Ade$^+$ cells are generated reflects the prevalence of recombination at this site. There are two classes of recombinants, gene conversions (Ade$^+$ His$^+$), in which both the repeats and their intervening sequence are maintained

and deletions (Ade^+ His^-), in which one repeat and the intervening DNA are lost through either reciprocal crossing-over, or by non-reciprocal events such as single-strand annealing (Figure 3.1a). A hypothetical model for induction of these gene conversions and deletions by *RTS1* at the *ade6* locus of Chromosome 3 has been discussed in detail before (Lorenz et al. 2009). Since only Ade^+ recombinants are scored, this assay only measures ectopic recombination that restores a functional *ade6*$^+$ allele, and not other forms of recombination, which would be genetically silent. Nevertheless, it provides a robust readout of a subclass of recombination events from which the overall recombination activity at the site can be inferred (Osman and Whitby 2009). At the *ade6* locus, replication is essentially unidirectional (in the telomere to centromere direction) due to the relative positioning of replication origins flanking it (Figure 3.1a) (Ahn et al. 2005). Accordingly, one orientation of *RTS1* – known as the active orientation (*RTS1-AO*) – will block replication forks, while the other orientation of *RTS1* – known as the inactive orientation (*RTS1-IO*) – will not block replication forks coming from the telomere proximal side.

3.2.2 Elg1 promotes *RTS1* induced recombination

To investigate whether Elg1 is needed for the recombination that is induced by RF blockage at *RTS1,* I made use of the *RTS1*-based direct repeat recombination reporter. As shown in previous works, *RTS1-AO* strongly induces both gene conversions and deletions, whereas *RTS1-IO* exhibits spontaneous levels of recombination (i.e. the same as when *RTS1* is absent) (Ahn et al. 2005; Lorenz et al. 2009; Nguyen et al. 2015). To determine whether Elg1 is needed for *RTS1-AO*-induced levels of recombination I crossed an *elg1*Δ mutant into both *RTS1-IO* and -*AO* strains and measured the effect on Ade^+ frequency. In the *RTS1-IO* strain small

increases in the frequency of both gene conversions (1.6-fold, p<0.0001) and deletions (1.2-fold, p<0.0001) were observed (Figure 3.1b). In contrast, the normally high levels of recombinants in the *RTS1-AO* strain were dramatically reduced, with 20-fold reduction in gene conversions (p<0.0001) and 3.8-fold reduction in deletions (p<0.0001) (Figure 3.1b; note the difference in y-axes for *RTS1-IO* and *AO* strains). I also observed that this reduction in *RTS1-AO* recombination in *elg1*Δ mutant is not associated with reduction in the barrier intensity (Section 4.2.1). Given that *elg1*Δ does not reduce the level of spontaneous recombination, we can conclude that it is not required for HR *per se*. Indeed, the modest increase in spontaneous recombination observed in the *RTS1-IO* strain is consistent with previous observations in budding yeast, that *elg1*Δ mutants exhibit a hyper-recombination phenotype (Alvaro et al. 2007; Ben-Aroya et al. 2003). The reduction in *RTS1-AO* recombination is therefore especially telling and suggests that PCNA unloading is critical for efficient RDR.

3.2.3 Pof3 promotes *RTS1* induced recombination

To investigate whether Pof3 is required for the recombination that is induced by *RTS1-AO*, I crossed a *pof3*Δ mutant into both *RTS1-IO* and -*AO* strains and once again measured the effect on recombinant frequency (Figure 3.1b). In the *RTS1-IO* strain, small increases in the frequency of both gene conversions (1.7-fold, p<0.0001) and deletions (1.7-fold, p<0.0001) were observed. Similar to *elg1*Δ, the frequency of *RTS1-AO*-induced Ade$^+$ recombinants were reduced in a *pof3*Δ mutant. However, unlike with *elg1*Δ, the reduction in recombinants was relatively modest and specific to gene conversions (2.3-fold reduction) (Figure 3.1b). Whilst the reduction in gene conversions in a *pof3*Δ mutant is significant (p<0.0001), I decided to focus my further investigations on Elg1 as it appeared to be more important for the recombination

induced by *RTS1*. I did not test *elg1*Δ *pof3*Δ double mutant as *pof3*Δ is a sick strain showing low viability.

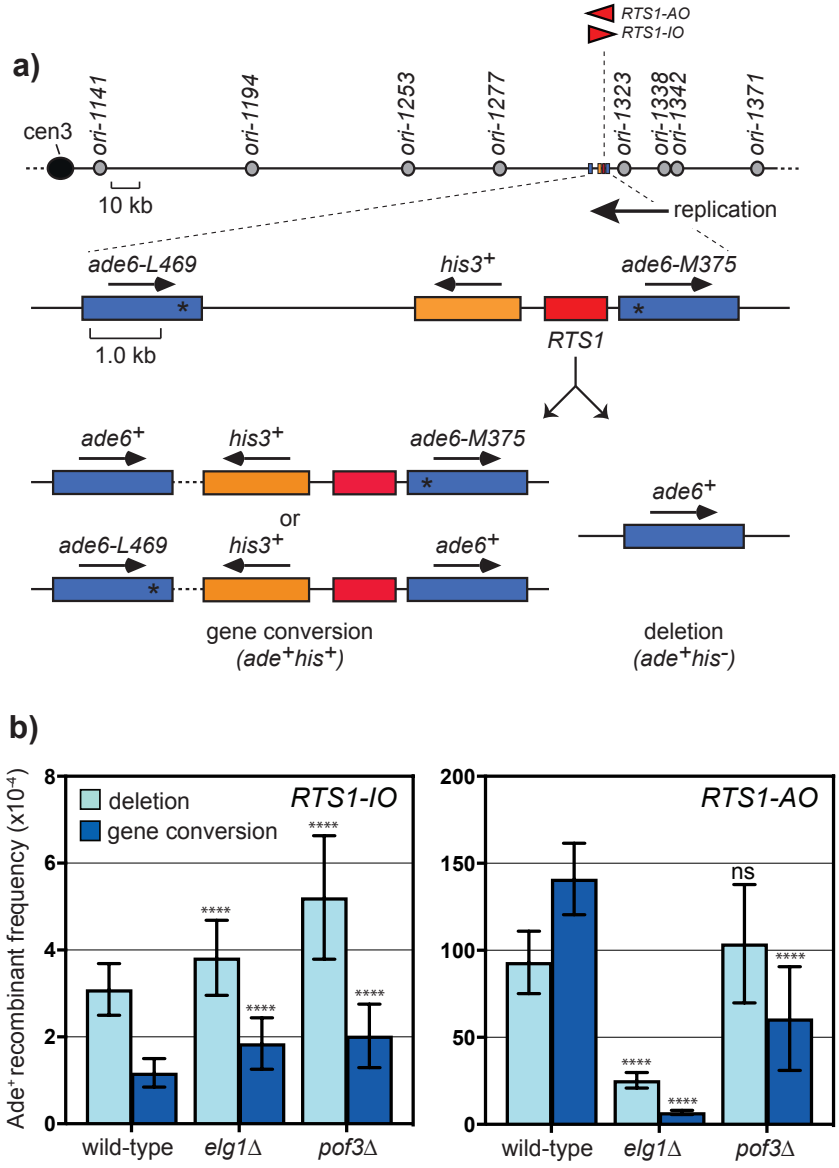

Figure 3.1 Both Elg1 and Pof3 promote RTS1-induced direct repeat recombination
a) Schematic showing the location of the *ade6*- intra-chromosomal recombination reporter and *RTS1* in relation to nearby replication origins (grey circles) at the endogenous *ade6* locus on chromosome 3. The reporter is comprised of a direct repeat of *ade6*– heteroalleles with intervening his3+ gene, asterisks indicate the position of point mutations in *ade6*-L469 and *ade6*-M375. *RTS1* is placed between the repeats in either orientation. Based on its polarity, the first orientation blocks RFs travelling from the centromere proximal direction, whereas the second orientation blocks centromere distal RFs. Due to the positioning of replication origins, replication proceeds across the barrier towards the centromere. This makes the second orientation of *RTS1* the fork blocking or "active orientation" (AO), and the first orientation the "inactive orientation" (IO). (b) Bar charts showing the effect of *elg1*Δ and *pof3*Δ on the frequency and type of Ade+ recombinants in *RTS1-IO* and *RTS1-AO* strains. In order of presentation the strains are MCW4712, MCW7706, MCW7710, MCW4713, MCW7708, MCW7712. Error bars represent standard deviation. Significant changes compared to the wild-type strain are indicated. P-values were calculated using the Shapiro-Wilk normality test (ns p>0.05, *p<0.05, **p<0.01, ***p<0.001, ****p<0.0001). Ade+ recombinant frequency with statistical analysis is also shown in Table 1.

3.2.4 Effect of *elg1Δ* on direct repeat recombination at a site where replication fork restart at *RTS1* is limited

To investigate whether Elg1 promotes *RTS1*-induced recombination at other genomic sites, I made use of strains in which the direct repeat recombination reporter, with and without *RTS1*, was inserted at a sub-telomeric region on the left arm of Chromosome 1 (Figure 3.2a). At this site the reporter is positioned in the midst of a cluster of replication origins. The origins between *ori-51* to *ori-79*, on the telomere proximal side of the reporter, have a total origin efficiency of ~95%, whereas those between *ori-85* to *ori-113* on the centromere proximal side have a combined firing efficiency of ~132%. This means that there is a high probability of one of these origins on both sides of *RTS1* firing in the same S phase. If this happens then fork convergence at *RTS1* will occur within 10 minutes of the first fork arriving at the barrier assuming a fork velocity of 3 kb/min and the two origins fire at the same time. This would mean that there would be insufficient time for RDR to be initiated and give rise to an Ade^+ recombinant as it takes approximately 10 minutes for Rad52 to load at the barrier following replication fork blockage (Nguyen et al. 2015). Consistent with this prediction, and previous data from the lab, I found lower levels of *RTS1*-induced recombination at this site compared to when the reporter is at the *ade6* locus on chromosome 3 (Neo 2015, DPhil thesis) (Fig. 3.2b). Moreover, the increases in gene conversions (~6-fold, $p<0.0001$) and deletions (~13-fold, $p<0.0001$) when *RTS1* is present compared to when it is absent are similar irrespective of the orientation of the RFB. This finding indicates that there is no strong directional bias for replication across this sub-telomeric site – a conclusion that is supported by 2D gel analysis of replication intermediates at the RFB (Neo 2015, DPhil thesis).

Intriguingly, *elg1*Δ exhibits a marked increase in spontaneous recombination frequencies at the sub-telomeric site compared to the wild-type strain without *RTS1* with 70-fold increase in deletions ($p<0.0001$) and 1.8-fold increase in gene conversions ($p=0.004$) (Figure 3.2b). Moreover, the inclusion of *RTS1*, in either orientation, had little effect on the frequency of recombination in an *elg1*Δ mutant (Figure 3.2b). These data indicate that Elg1 is needed to suppress recombination at this sub-telomeric site and is also needed to promote *RTS1*-induced recombination.

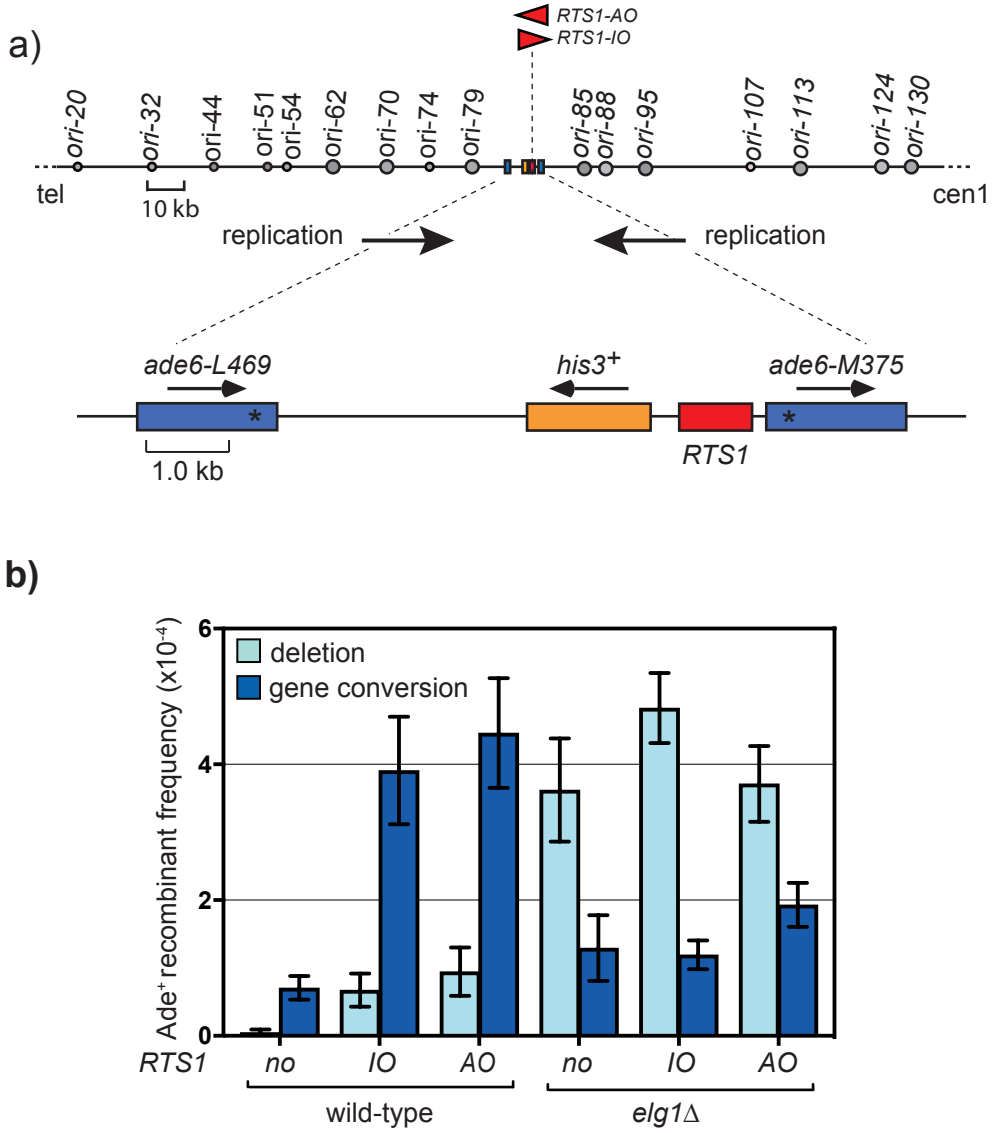

Figure 3.2 Effect of *elg1Δ* on direct repeat recombination with *RTS1* at a sub-telomeric site on chromosome 1, where it induces relatively little recombination

a) Schematic showing the location of the direct repeat recombination reporter with *RTS1*, positioned in the midst of a cluster of replication origins at a sub-telomeric site on chromosome 1. Confirmed and likely origins are represented by bigger circles and dubious origins are represented by smaller circles. At this site, replication across the direct repeat recombination reporter occurs with equal frequency from both directions. (b) Bar chart showing the frequency of Ade$^+$ recombinants in no *RTS1, RTS1-IO* and *RTS1-AO* strains in wild-type and *elg1Δ* background. In order of presentation, the strains are MCW6472, MCW6557, MCW6474, MCW8204, MCW8206 and MCW8208. Error bars represent standard deviation. Ade$^+$ recombinant frequency with statistical analysis is also shown in Table 1.

3.2.5 The effect of *elg1*Δ on direct repeat recombination at an RFB where RF is only paused and there is no fork collapse or induction of recombination

Ter2 is a programmed polar RFB present in the rDNA of *S. pombe*. Similar to *RTS1,* it depends on a myb domain-containing protein (Reb1) and Swi1-Swi3 for its barrier activity (Biswas and Bastia 2008); however, unlike *RTS1*, RF blockage at *ter2* does not induce recombination even when three tandem copies of it are introduced into the genome as demonstrated by previous work in our laboratory (unpublished). It appears that RFs blocked at *ter2x3* do not collapse and therefore are maintained in a stably stalled state until they either overcome the barrier and resume DNA replication or merge with the oncoming RF (Mizuno et al. 2013; Sánchez-Gorostiaga et al. 2004; Krings and Bastia 2004).

To investigate whether the *elg1*Δ mutant has any effect on direct repeat recombination when *ter2* is positioned between the repeats, I crossed it into strains harbouring a tandem repeat of three *ter2*s *(ter2*x3*)*, inserted between the *ade6*$^{-}$ repeats on chromosome 3 (Figure 3.3a). Strains were constructed with each orientation of *ter2*x3 – termed O1 (blocking forks coming from the centromeric side of the reporter) and O2 (blocking forks coming from the telomeric side of the reporter). Consistent with previous data from the lab, *ter2*x3 in either orientation (O1 or O2) had little or no effect on the frequency of spontaneous recombination in a wild-type strain (Figure 3.3b and data not shown). In an *elg1*Δ mutant, there was a slight increase in recombinants with *ter2*X3 O1 (1.3-fold increase in deletions ($p<0.001$) and 1.9-fold increase in gene conversions ($p<0.001$)). However, with *ter2*X3 O2 (the orientation which blocks replication forks at the *ade6* locus) there was a more dramatic increase in gene

conversions (4.7-fold; p<0.001) (Figure 3.3b). These data indicate that Elg1 is needed to prevent recombination following RF blockage at *ter2*x3.

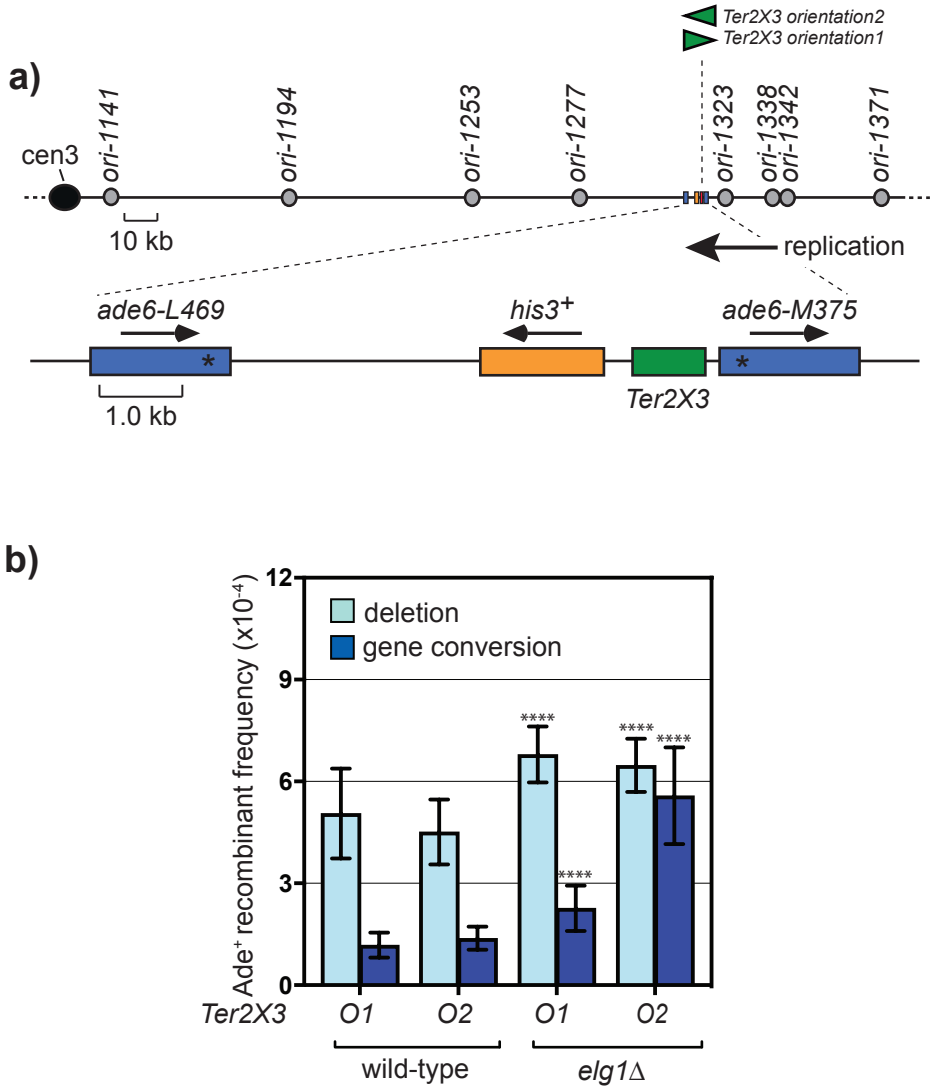

Figure 3.3 *Ter2X3* at the *ade6* locus of Chromosome 3 and the effect of *elg1*Δ
a) Schematic showing the relative position of the *ade6*- intra-chromosomal recombination substrate flanking the *his3*+ gene and tandem repeat of three *ter2s (ter2x3)* forming a polar RFB, in relation to nearby replication origins on chromosome 3. *Ter2X3* is placed between the repeats in either orientation, the permissive (O1) and the obstructive (O2) orientation, with respect to the direction of replication. Unlike *RTS1,* RF blockage at *ter2X3* does not induce increased recombination. (b) Bar charts showing the effect of *elg1*Δ on the frequency and type of Ade+ recombinants in *ter2X3 O1* and *O2* strains. In order of presentation, the strains are MCW7045, MCW7046, MCW8130 and MCW8132. Error bars represent standard deviation. P-values were calculated using the Shapiro-Wilk normality test (ns p>0.05, *p<0.05, **p<0.01, ***p<0.001, ****p<0.0001). Ade+ recombinant frequency with statistical analysis is also shown in Table 2.

3.2.6 Prolonged persistence of PCNA foci in cells lacking Elg1

It has been shown in budding yeast and humans that loss/mutation of Elg1 (termed ATAD5 in humans) is associated with an excessive accumulation of PCNA on the DNA (Kubota et al. 2013; Parnas et al. 2010; Lee et al. 2013). Therefore, the effect of *elg1*Δ on *RTS1*-induced recombination is most probably explained by the need for Elg1 to remove PCNA from the blocked RF. To investigate this possibility, I first wanted to confirm that loss of *elg1* resulted in a similar accumulation of PCNA on DNA in fission yeast as observed in budding yeast and humans. To do this I used time lapse microscopy to analyse PCNA throughout the cell cycle, visualizing it with an ECFP tag in asynchronously growing cultures of wild-type and *elg1*Δ mutant strains. PCNA is a central and essential factor for DNA replication and repair (Pascal et al. 2004; Hoege et al. 2002; Unk et al. 2006; Gary et al. 1997; Cox 2015; Maga and Hübscher 2003; Garg and Burgers 2005; Arias and Walter 2006; Barbour and Xiao 2003; Moldovan et al. 2006), despite lacking any enzymatic activity of its own, as it is a moving platform for numerous factors that act concomitantly with the RF. Thus, in order to avoid causing any major detrimental effect on protein function, I visualised PCNA by introducing an ECFP tagged copy of the *pcn1* gene at a secondary genomic site (*ura4* locus) whilst keeping the endogenous *pcn1* locus intact. In this configuration cells exhibit normal growth and genotoxin sensitivity (Meister et al. 2007).

In wild-type yeast cells, PCNA foci form successive distinguishable patterns during S phase that can be classified into various stages as reported previously (Figure 3.4a, c) (Meister et al. 2007). In stage a, bright patches appear on the extranucleolar region without filling it entirely. In stage b, the bright patches extend and fill the entire extranucleolar space. Stage c shows bright spots at the edge of the

nucleolus and smaller spots in the rest of the nucleus. Finally, in stage d, only a few bright spots located at the edges of the nucleolus are observed, that gradually diminish. These foci are S-phase specific and were shown to correspond to replication factories as there was a charactersitc change observed in the pattern of foci in S-phase checkpoint mutants like *chk1*Δ, *cds1*Δ and *rad3*Δ (Meister et al. 2007). Stages a - d were also observed in the *elg1*Δ mutant, albeit stages b and d were on average longer in duration (Figure 3.4 a and d). Indeed, even though PCNA foci appeared with the same timing post anaphase in both wild-type and *elg1*Δ mutant, they persisted by an extra ~30 minutes in the *elg1*Δ mutant compared to the wild-type (Figure 3.4b). Moreover, the *elg1*Δ mutant exhibits an additional stage of ECFP-PCNA fluorescence between stages c and d (termed c*), where the gradually fading spots in stage c become unusually bright blobs prior to the appearance of more discrete foci that are typical of stage d (Figure 3.4a, d). Altogether these data indicate that loss of *elg1* causes PCNA to remain associated with chromatin longer during the cell cycle, similar to what has been observed in other organisms (Kubota et al. 2013; Parnas et al. 2010; Lee et al. 2013).

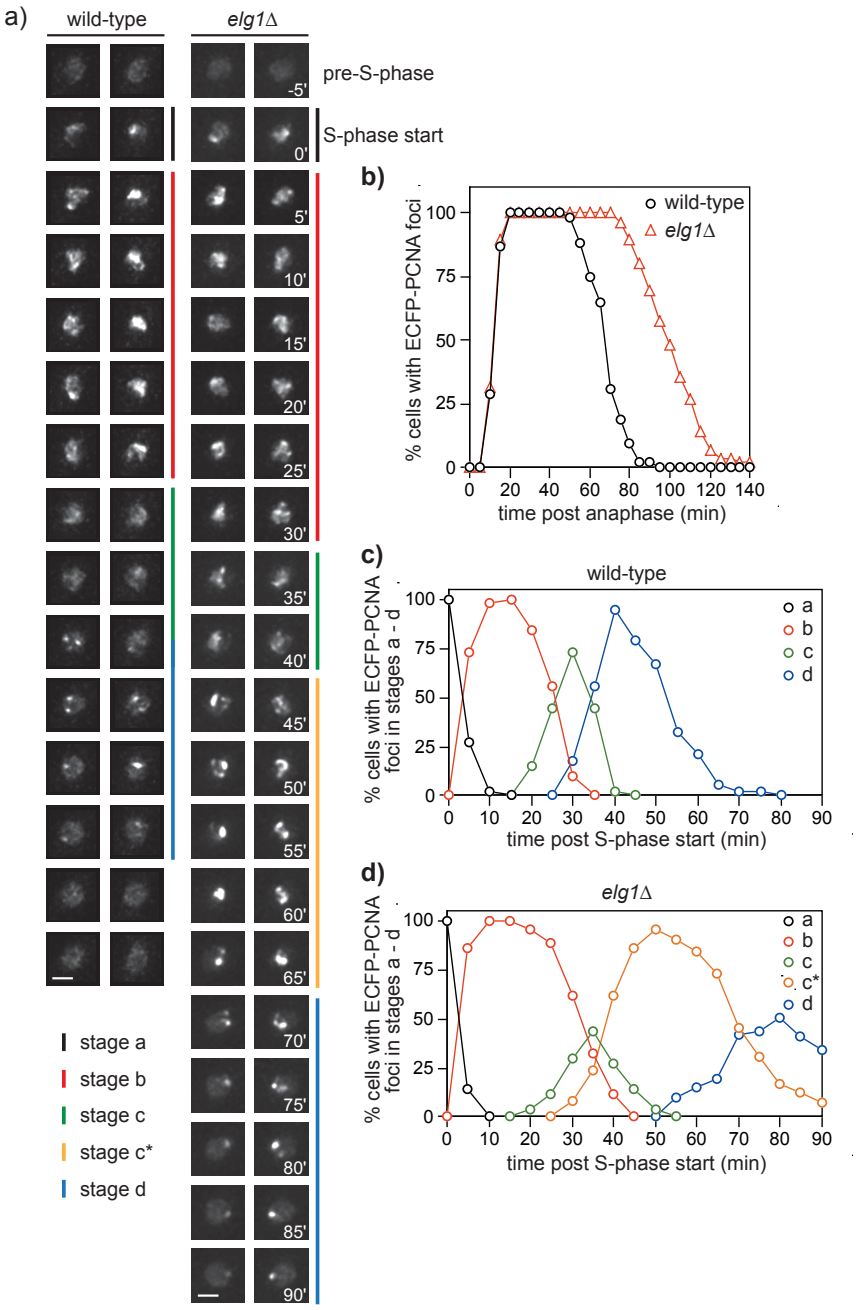

Figure 3.4 Prolonged persistence of PCNA foci in cells lacking Elg1
a) Images from time-lapse microscopy showing ECFP-PCNA nuclear fluorescence that form successive distinguishable patterns represented as different stages, shown to illustrate the difference between wild-type and *elg1*Δ cells. Images from four different time-lapse series are shown (two for wild-type and two for *elg1*Δ). Scale bar = 2μm. b) Line graph of the percentage of cells with ECFP-PCNA foci in the cell cycle following anaphase at five-minute intervals, showing longer persistence of ECFP-PCNA foci in *elg1*Δ cells compared to wild-type. c) Line graph of the percentage of cells with ECFP-PCNA foci belonging to four different stages (stages a, b, c and d), in the cell cycle following S-phase at five-minute intervals, in wild-type cells. d) Line graph of the percentage of cells with ECFP-PCNA foci belonging to five different stages (stages a, b, c, c* and d) in the cell cycle following S-phase at five-minute intervals, in *elg1*Δ cells. The wild-type strain is MCW7065 (n=52) and the *elg1*Δ strain is MCW7965 (n=85). The data are from a single experiment.

3.2.7 A disassembly-prone PCNA mutant suppresses the need for Elg1 to promote recombination at a collapsed replication fork

There are clear connections between various phenotypes of *elg1*Δ and its PCNA unloading role, but Elg1 is also known to have other PCNA-independent functions and to interact with proteins that belong to the SUMO pathway (Parnas et al. 2011; Parnas et al. 2010; Davidson and Brown 2008). It was therefore possible that Elg1's role in promoting *RTS1*-induced recombination was not linked to its role in unloading PCNA from DNA. To investigate whether a deficiency in PCNA unloading was the root cause of *elg1*Δ's hypo-recombination at the *ade6* locus *RTS1-AO*, I set out to test whether mutations in PCNA could suppress this phenotype. A previous study in budding yeast had shown that mutations at the subunit interfaces of the PCNA homotrimer (*C81R, E143K* and *D150E*) made PCNA prone to disassembly from DNA (Johnson et al. 2016). Moreover, these mutations were found to suppress an *elg1*Δ mutant's elevated rate of sister chromatid recombination, increased telomere length and, in the case of the *E143K* and *D150E* mutations, also its hypersensitivity to the alkylating agent methyl methanesulfonate (MMS) (Johnson et al 2016). Residues C81, E143 and D150 are all conserved between budding yeast, fission yeast and humans (Figure 3.5a, b) and, therefore, I attempted to introduce the same *C81R, E143K* and *D150E* mutations into *S. pombe* PCNA. However, I was only successful in making a PCNA^{D150E} strain due to time constrains. Nevertheless, I proceeded to test whether the *D150E* mutation suppressed the hypo-recombination phenotype of a *elg1*Δ mutant (Figure 3.5c). In strains with *RTS1-IO*, the *D150E* mutant exhibited hyper-levels of spontaneous recombination that were similar in both *elg1+* (~6-fold increase in deletions, $p<0.001$; ~8-fold increase in conversions, $p<0.001$) and *elg1*Δ (~5-fold increase in deletions, $p<0.001$; ~6-fold increase in conversions, $p<0.001$) backgrounds. Importantly, while

RTS1-induced *(RTS1-AO)* recombination in *elg1+* did not change significantly in the *D150E* mutant with ~1.2-fold increase in deletions (p=0.160) and ~1.3-fold increase in conversions (p=0.079). It suppressed the hypo-levels of *RTS1*-induced recombination in an *elg1*Δ mutant (Figure 3.5c). This observation indicates that PCNA accumulation on DNA at the barrier is associated with the reduction in *RTS1*-induced recombination in an *elg1*Δ mutant. Presumably by making PCNA prone to disassembly, the requirement for Elg1 to promote recombination at the RFB is removed.

In addition to testing the recombination phenotype of a *D150E* mutant, I also examined its genotoxin sensitivity in both wild-type and *elg1*Δ mutant backgrounds comparing it back to the parental wild-type and *elg1*Δ strains (Figure 3.6). Consistent with previous findings in budding yeast (Johnson et al. 2016), the $PCNA^{D150E}$ mutant is hypersensitive to the alkylating agent MMS and epistatic with *elg1*Δ. However, unlike in budding yeast, the $PCNA^{D150E}$ mutant is more sensitive to MMS than an *elg1*Δ mutant and, therefore, I observed no suppression of *elg1*Δ MMS hypersensitivity by the $PCNA^{D150E}$ mutant. These data are consistent with the idea that Elg1 promotes MMS resistance by unloading PCNA from DNA. They also suggest that PCNA stability on the DNA is important for resistance to MMS. Whilst the *elg1*Δ mutant is sensitive to MMS, it is insensitive to ultraviolet light (UV), the topoisomerase I poison CPT and the DNA replication inhibitor HU (Kim et al. 2005; Bellaoui et al. 2003, Ben-Aroya et al. 2003). These data indicate that Elg1 is not generally required for DNA damage repair. Importantly MMS sensitivity has previously been linked to Elg1's PCNA unloading role (Johnson et al. 2016), and consistent with this I Intriguingly the *elg1*Δ mutant exhibited slightly better resistance to HU and CPT than the wild-type strain. It was previously reported in budding yeast that mutation of *ELG1* confers resistance to inhibition of

DNA replication by HU due to expansion of intracellular dNTP pools during G1. It was proposed that upregulation of RNR activity, by the DNA damage responding to the accumulation of spontaneous DNA damage, leads to the increase in intracellular dNTP concentration (Davidson et al. 2012). The basis for the enhanced CPT resistance of a *elg1*Δ mutant is less clear. CPT-induced DSBs (formed when a RF runs into a CPT stabilized Top1 cleavage complex) and fork collapse are largely repaired by recombination (Saleh-Gohari et al. 2005). Perhaps CPT resistance of a *elg1*Δ mutant is due to a general augmentation of homologous recombination as suggested by the hyper-recombination phenotype of a *elg1*Δ mutant, previously reported in budding yeast (Alvaro et al. 2007; Ben-Aroya et al. 2003) and also found be conserved in fission yeast under two conditions (Figure 3.2b, 3.3b). Alternatively loss of Elg1 might in some way lead to less replication fork runoff at Top1 cleavage complexes. Further studies will be needed to investigate the basis of *elg1*Δ CPT resistance.

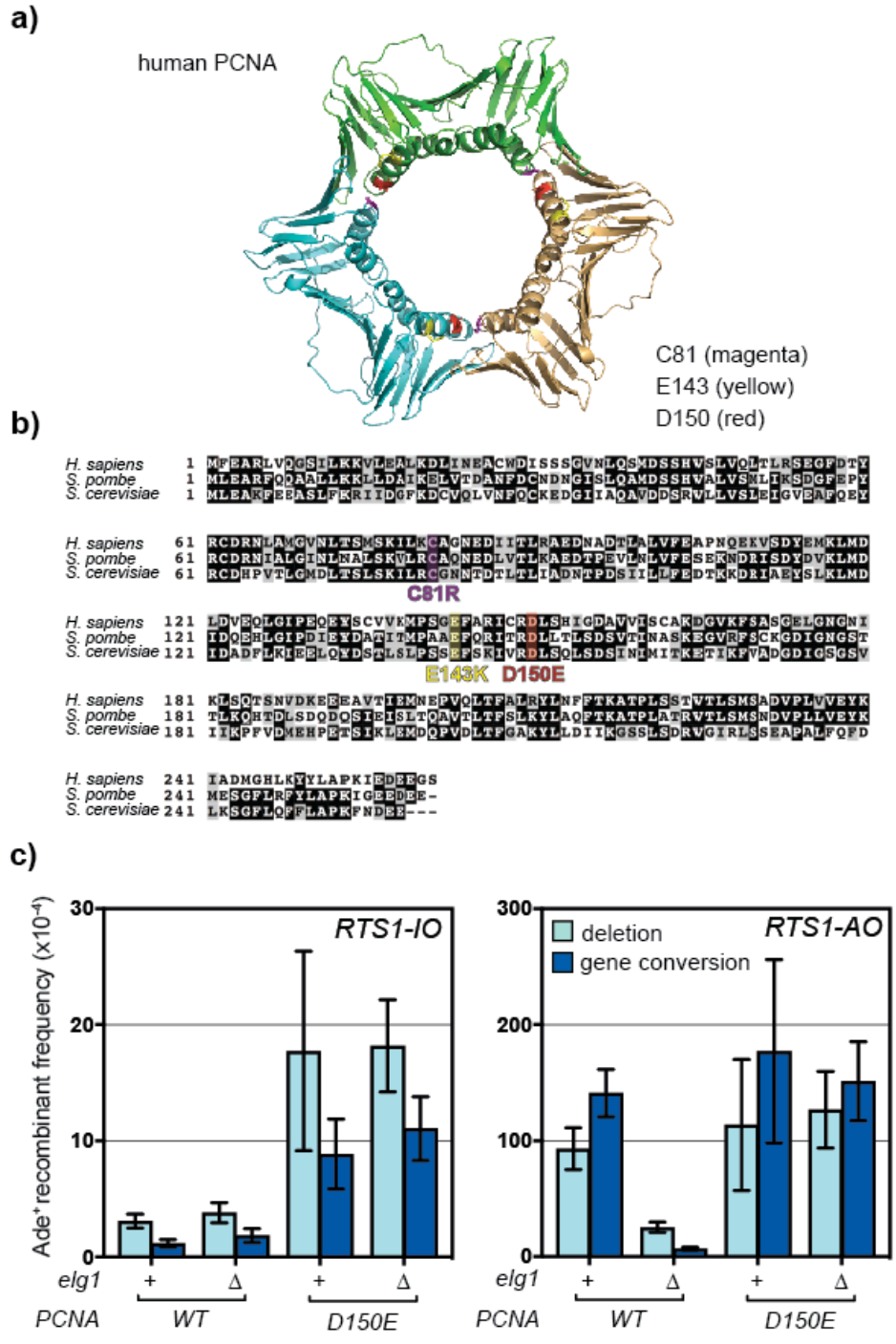

Figure 3.5 A disassembly prone mutant supresses the need for Elg1 to promote *RTS1*-induced recombination

a) 3-D ribbon model of a human PCNA trimer showing the positions of the three mutated residues C81 (magenta), E143 (yellow) and D150 (red) important for the trimer formation. b) Alignment of the residues of PCNA monomer showing conservation of the residues important for trimer formation (C81, E143 and D150) in humans, *S. pombe* and *S. cerevisiae*. c) Bar charts showing the effect of D150E point mutation on the frequency and type of Ade$^+$ recombinants in *elg1*$^+$ and *elg1*Δ strains in *RTS1-IO* and *RTS1-AO* background. *RTS1* is placed between the *ade6*$^-$ repeats in either orientation at the endogenous *ade6* locus on chromosome 3. In order of presentation, the strains are MCW4712, MCW7706, MCW9183, MCW9187, MCW4713, MCW7708, MCW9185 and MCW9189. Error bars represent standard deviation. Ade$^+$ recombinant frequency with statistical analysis is also shown in Table 1.

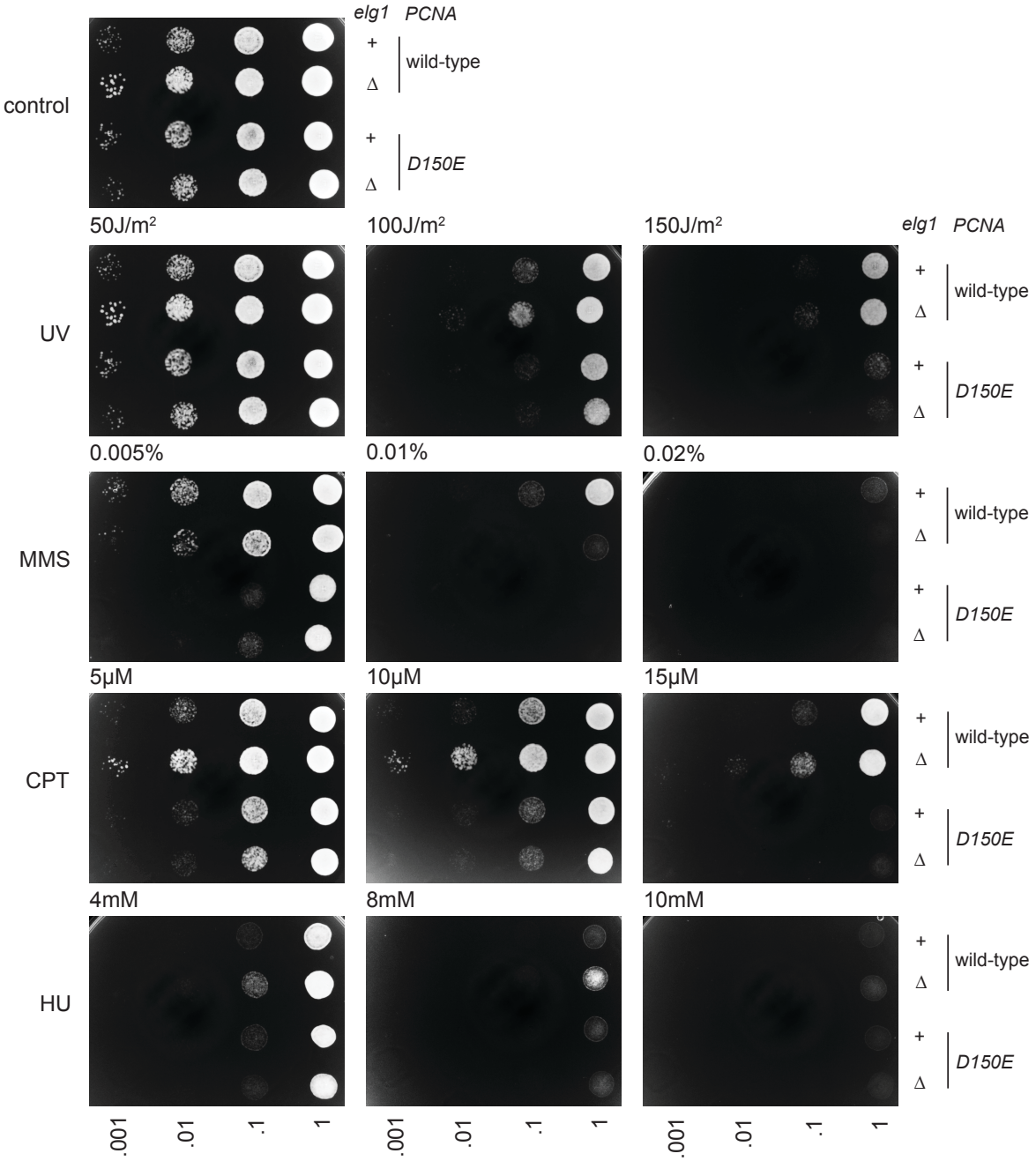

Figure 3.6 Deletion of *elg1* does not increase the sensitivity of disassembly-prone PCNA mutant (D150E) to MMS

Spot assays comparing the sensitivities of *elg1*$^{+}$ or *elg1*Δ strains with wild-type PCNA or disassembly-prone PCNA mutant (D150E) to different genotoxins. In order of presentation (from top to bottom in each panel), the strains are MCW4713, MCW7708, MCW9195 and MCW9199. Strains were grown on complete media for 3 days at 30ºC before being photographed.

3.2.8 Ways in which PCNA interacting factors may supress *RTS1*-induced recombination

The prolonged presence of PCNA at the RFB in an *elg1*Δ mutant could be affecting the frequency of inter-repeat recombination either directly or indirectly through its interacting partners. PCNA acts as a hub for the recruitment of many different proteins that might be responsible for reducing recombination (Figure 3.7). Some candidate PCNA interacting factors, which are implicated in *RTS1*-induced recombination, were screened by testing if the loss of these factors can supress the *elg1*Δ phenotype.

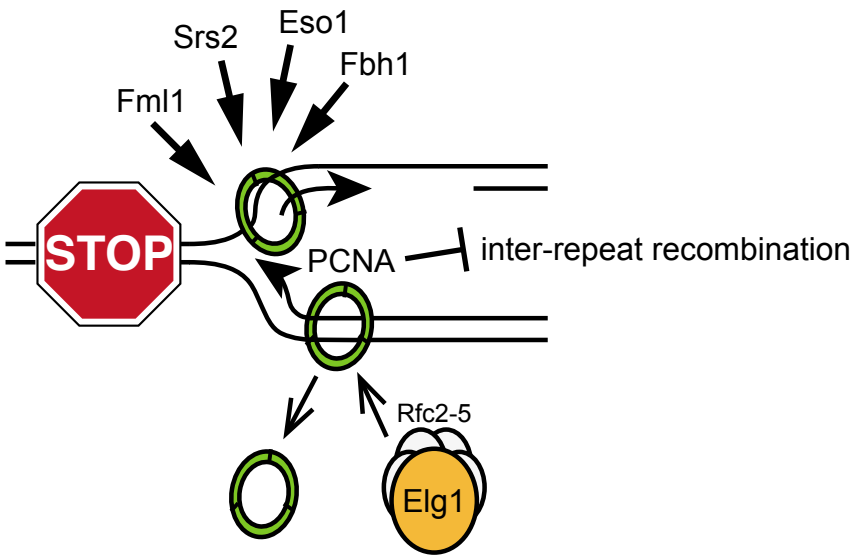

Figure 3.7: PCNA acts as a interaction platform which may recruit crucial regulators of HR to the replication fork
Retention of PCNA on the DNA in the absence of Elg1, may lead to increased recruitment of various factors implicated in the supression of HR, which might be responsible for the reduction of direct repeat recombination at the *RTS1* barrier.

3.2.8.1 Fml1

Fml1, the first candidate, is a member of a conserved family of DNA helicases, which includes human FANCM and budding yeast Mph1, that have been implicated in processing stalled RFs and D-loops. Both FANCM and its archaeal homolog Hef have been shown to interact with PCNA via a conserved PIP-box (Rohleder et al. 2016). Moreover, it has been reported that FANCM/Fml1/Mph1's binding partners Mhf1-Mhf2 physically interact with Elg1 in budding yeast (Singh et al. 2013). In *S. pombe*, Fml1 plays a significant role in *RTS1*-induced recombination by promoting gene conversions and limiting deletions (Nandi and Whitby 2012; Morrow et al. 2017). It is thought to promote gene conversions by catalyzing fork reversal - a step necessary for the generation of a 3' ssDNA tail onto which Rad51 loads and then uses to catalyze strand invasion. The mechanism by which it curbs deletions is currently unclear but it could do it by modulating fork regression or unwinding inter-fork strand annealing intermediates before they are processed into deletion products (Sun et al. 2008).

To see if Fml1 is responsible for the hypo-recombination of an *elg1*Δ mutant, I constructed an *elg1*Δ *fml1*Δ double mutant and determined its phenotype for *RTS1-AO*-induced recombination (Figure 3.8). As expected, the *fml1*Δ single mutant exhibited increased deletions (~1.6-fold increase, $p<0.05$) and reduced gene conversions (~7.9-fold decrease, $p<0.0001$) compared to wild-type. However, there was no supression of *elg1*Δ hypo-recombination in the double mutant; rather, there was an additive decrease in gene conversions and a ~3-fold decrease in deletions ($p<0.01$) compared to a *fml1*Δ single mutant, which is similar to the fold reduction between wild-type and the *elg1*Δ single mutant (Figure 3.8). These data suggest that Fml1 is unlikely to be the factor responsible for the hypo-recombination phenotype of

an *elg1*Δ mutant. Indeed, it would seem that Fml1 and Elg1 promote gene conversions by independent mechanisms and that Fml1 can supress deletions regardless of whether or not Elg1 is present.

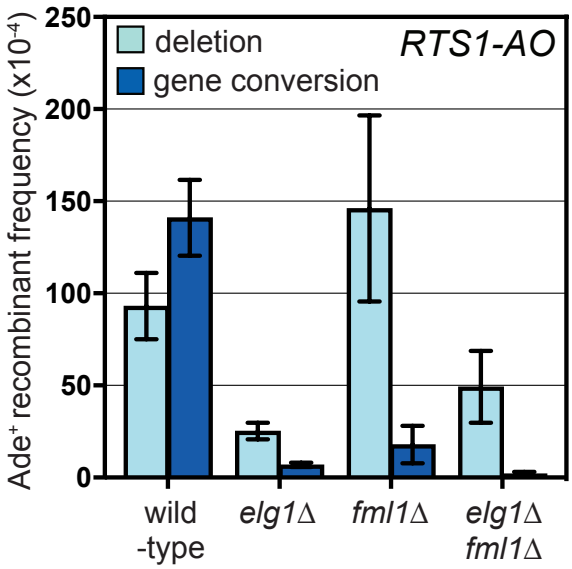

Figure 3.8 Hypo-recombination of *elg1*Δ at *RTS1-AO* is not supressed by deleting *fml1*
Bar chart showing the frequency of deletion- and conversion- type Ade$^+$ recombinants in wild-type, *elg1*Δ, *fml1*Δ and *elg1*Δ *fml1*Δ strains, with *RTS1-AO*. *RTS1* is placed between the *ade6*$^-$ repeats at the endogenous *ade6* locus on chromosome 3. In order of presentation, the strains are MCW4713, MCW7708, MCW4752 and MCW8431. Error bars represent standard deviation. Ade$^+$ recombinant frequency with statistical analysis is also shown in Table 1.

3.2.8.2 Srs2

In budding yeast, SUMOylated PCNA recruits the UvrD family helicase Srs2 in S phase in order to prevent unwanted recombination events (Pfander et al. 2005; Papouli et al. 2005; Urulangodi et al. 2015). Moreover, it was shown that Srs2 accumulated, along with SUMOylated PCNA, in the chromatin fraction in the absence of Elg1 (Parnas et al. 2010). As Srs2 is an anti-recombinase that disrupts the Rad51 presynaptic filament (Veaute et al. 2003; Lessard and Sauvageau 2003), retention of PCNA at the *RTS1* barrier in an *elg1*Δ mutant might lead to excessive recruitment of Srs2, thus reducing recombination. However, it should be noted that there is no evidence that PCNA is SUMOylated in *S. pombe* (Watts 2006; Frampton et al. 2006).

To see if Srs2 is responsible for the hypo-recombination of an *elg1*Δ mutant I constructed an *elg1*Δ *srs2*Δ double mutant and determined its recombination phenotype (Figure 3.9). As expected, the level of spontaneous recombination (*RTS1-IO*) is significantly higher than wild-type in a *srs2*Δ single mutant with ~3-fold ($p<0.0001$) increase in deletions and ~10.4-fold ($p<0.0001$) increase in gene conversions. The *elg1*Δ *srs2*Δ double mutant exhibits a similar increase in deletions (~3.5-fold, $p<0.0001$) to the *srs2*Δ single mutant, and additive increase in gene conversions (~14.6-fold, $p<0.0001$). The level of *RTS1*-induced recombination (*RTS1-AO*) also increased dramatically in a *srs2*Δ mutant as reported previously (Lorenz et al. 2009), with ~4.8-fold increase in deletions ($p<0.0001$) and ~7.7-fold increase in gene conversions ($p<0.0001$) (Figure 3.9). However, unlike with *RTS1-IO*, the hyper-recombination in a *srs2*Δ mutant with *RTS1-AO* is reduced 7.8-fold (~4-fold reduction in deletions, $p<0.0001$; ~13-fold reduction in gene conversions, $p<0.0001$) when *elg1* is deleted (Figure 3.9). Importantly, this fold reduction is similar to that seen between

wild-type and *elg1*Δ single mutant, except that the reduction in conversions is lower here. If Elg1's role in *RTS1*-induced recombination was simply to exclude Srs2, then *srs2*Δ should supress the hypo-recombination of an *elg1*Δ (i.e. the *elg1*Δ *srs2*Δ double mutant would exhibit similar hyper-recombination as a *srs2*Δ single mutant). However, this is patently not the case and, therefore, I can conclude that Elg1's role in promoting recombination at *RTS1* is independent of any role it might play in excluding Srs2 via removal of PCNA from the DNA.

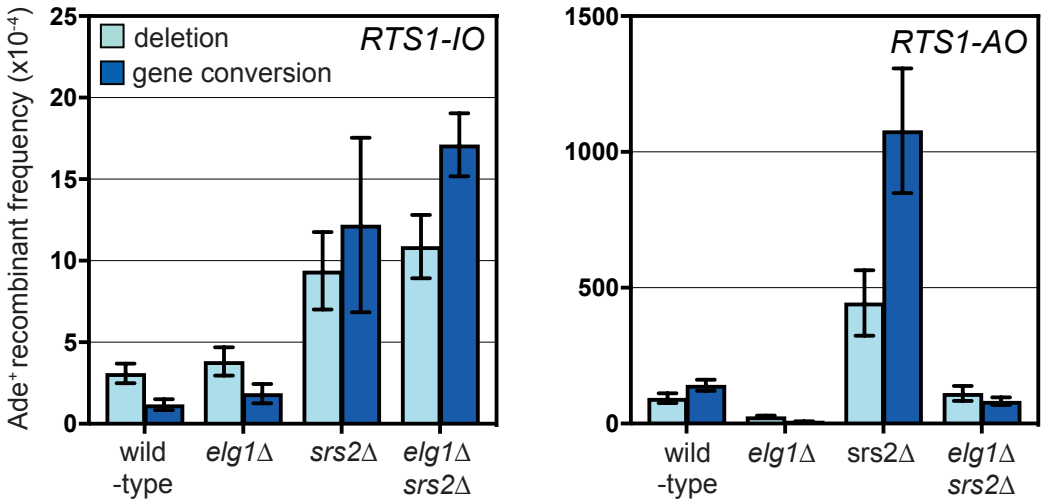

Figure 3.9 Hypo-recombination of *elg1*Δ at *RTS1-AO* is not supressed by deleting *srs2*
Bar charts showing the frequency of deletion- and conversion- type Ade+ recombinants in wild-type, *elg1*Δ, *srs2*Δ and *elg1*Δ *srs2*Δ strains, with either *RTS1-IO* or *RTS1-AO* (note the major difference in y-axes between the two plots). *RTS1* is placed between the *ade6*- repeats in either orientation at the endogenous *ade6* locus on chromosome 3. In order of presentation, the strains are MCW4712, MCW7706, FO1748, MCW8328, MCW4713, MCW7708, FO1750 and MCW8330. Error bars represent standard deviation. Ade+ recombinant frequency with statistical analysis is also shown in Table 1.

3.2.8.3 Wpl1

Cohesin, a ring-like protein complex composed of the four subunits Smc1, Smc3, Scc1, and Scc3, holds sister chromatids together from S phase until the chromatids separate at anaphase and ensures the orderly segregation of sister chromatids (Haering et al. 2004; Nasmyth and Haering 2005). Eco1 (termed Eso1 in *S. pombe*) is an essential factor for cohesion establishment in yeast during S phase (Tóth et al. 1999). It is an acetyltransferase that acetylates Smc3 which is thought to block the anti-cohesion activity of the Wpl1-Pds5 heterodimer (Guacci et al. 2015). Eco1 binds directly to PCNA via its PIP box, and this interaction is essential for normal loading of Eco1 on chromatin and establishment of cohesion in S phase (Moldovan et al. 2006). It is therefore not surprising that Elg1 acts as an anti-establishment activity for sister chromatid cohesion in budding yeast, as Elg1 removes PCNA so Eco1 cannot be recruited (Tong and Skibbens 2015; Maradeo and Skibbens 2010). If the same is true in *S. pombe*, then the hypo-recombination phenotype of an *elg1*Δ mutant could be explained by increased Eso1 recruitment to the blocked replication fork via PCNA, which might result in enhanced cohesin establishment that might restrict inter-repeat recombination (Cortes-Ledesma and Aguilera 2006).

Based on genetic studies in budding yeast, Elg1 seems to participate in a single pathway of cohesion anti-establishment, together with Wpl1 and Pds5 (Guacci et al. 2015). Therefore, I reasoned that if Elg1's role in promoting *RTS1-AO*-induced inter-repeat recombination was due to it functioning in the Wpl1/Pds5 cohesion anti-establishment pathway, then deletion of *wpl1* should exhibit a similar hypo-recombination phenotype and be epistatic with *elg1*Δ. To test this hypothesis, I constructed and assayed recombination reporter strains with *wpl1*Δ and *elg1*Δ *wpl1*Δ

mutations (Figure 3.10). The level of spontaneous recombination (*RTS1-IO*) in both in both *wpl1*Δ single and *elg1*Δ*wpl1*Δ double mutant was similar to wild-type. Importantly, there was also no major change in *RTS1*-induced (*RTS1-AO*) recombination in a *wpl1*Δ single mutant, and it did not affect the reduced recombination of *elg1*Δ, except for a ~2-fold increase ($p<0.01$) in gene conversions (Figure 3.10). Therefore, it seems that cohesion establishment is not responsible for the reduction in inter-repeat recombination at *RTS1* in an *elg1*Δ mutant.

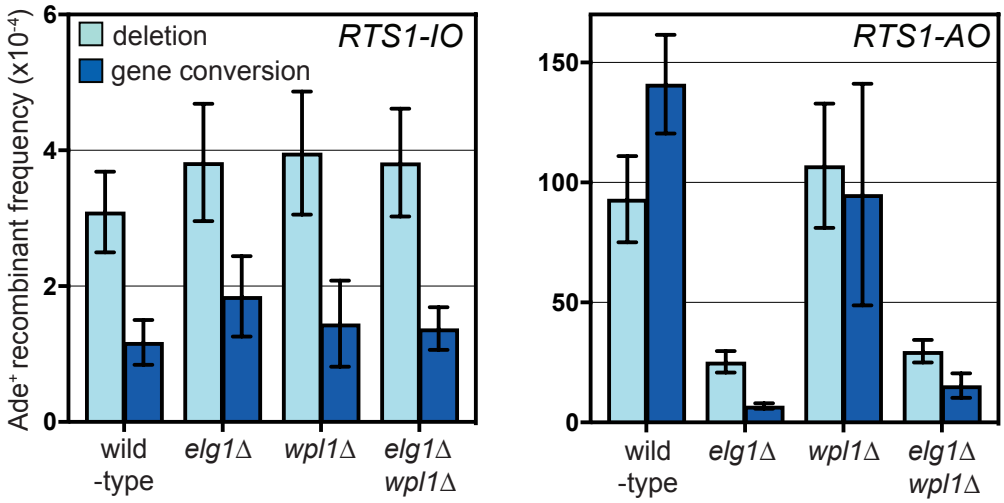

Figure 3.10 Deleting *wpl1* does not affect the hypo-recombination of *elg1*Δ at *RTS1-AO*
Bar charts showing the frequency of deletion- and conversion- type Ade$^+$ recombinants in wild-type, *elg1*Δ, *wpl1*Δ and *elg1*Δ *wpl1*Δ strains, with either *RTS1-IO* or *RTS1-AO*. *RTS1* is placed between the *ade6*$^-$ repeats in either orientation at the endogenous *ade6* locus on chromosome 3. In order of presentation, the strains are MCW4712, MCW7706, MCW8919, MCW8995, MCW4713, MCW7708, MCW8920 and MCW8998. Error bars represent standard deviation. Ade$^+$ recombinant frequency with statistical analysis is also shown in Table 1.

3.2.8.4 Fbh1

The DNA helicase Fbh1, which is another member of the UvrD family of proteins, is a known regulator of Rad51-mediated recombination, especially at sites of replication fork stalling and collapse (Chiolo et al. 2007; Fugger et al. 2009; Lorenz et al. 2009; Marini and Krejci 2010; Morishita et al. 2005; Osman et al. 2005; Simandlova et al. 2013; Tsutsui et al. 2014). Indeed a previous study from our lab showed that Fbh1 strongly limits inter-repeat recombination at the *RTS1* RFB (Lorenz et al. 2009). Intriguingly, it has been reported that PCNA recruits FBH1 to sites of DNA replication and DNA damage in human cells via novel PCNA interacting motifs in FBH1 (Bacquin et al. 2013). Even though these PCNA interacting motifs do not appear to be conserved in *S. pombe* Fbh1, I decided to test whether the hypo-recombination phenotype of an *elg1*Δ mutant was due to excessive Fbh1 activity.

If the reduction in *RTS1*-induced recombination in *elg1*Δ is caused by the increased recruitment of Fbh1 to the barrier by PCNA, then deleting *fbh1* should supress its hypo-recombination. Indeed, a comparison of an *elg1*Δ single mutant and an *elg1*Δ *fbh1*Δ double mutant for *RTS1-AO*-induced recombination shows that the hypo-recombination of *elg1*Δ is mostly supressed in the double mutant, which exhibits a frequency of Ade^+ recombinants that is similar to that of a *fbh1*Δ single mutant (Figure 3.11). Indeed, the double mutant shows no significant change in deletions ($p=0.54$), although it does show a 1.6-fold decrease in conversions ($p<0.001$) which indicates that Elg1 may promote the formation of some gene conversions by a mechanism that is independent of its control over Fbh1. Overall these data indicate that Fbh1 is mostly responsible for the reduction in *RTS1-AO*-induced recombination when Elg1 is absent.

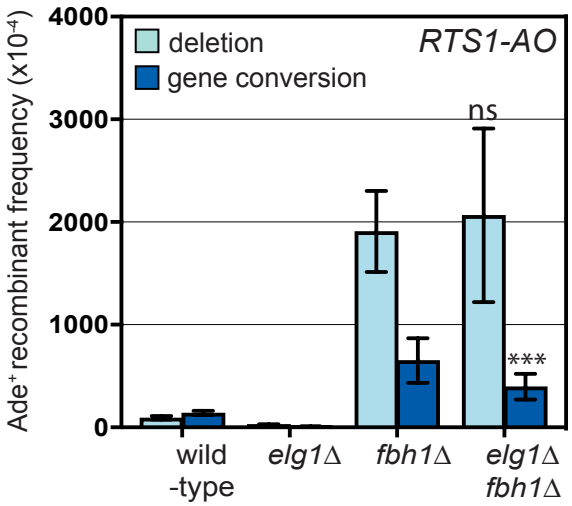

Figure 3.11 Hypo-recombination of *elg1*Δ at *RTS1-AO* is supressed by deleting *fbh1*
Bar chart showing the frequency of deletion- and conversion- type Ade$^+$ recombinants in wild-type, *elg1*Δ, *fbh1*Δ and *elg1*Δ*fbh1*Δ strains, with *RTS1-AO*. *RTS1* is placed between the *ade6*$^-$ repeats at the endogenous *ade6* locus on chromosome 3. In order of presentation, the strains are MCW4713, MCW7708, FO1816 and MCW8946. Error bars represent standard deviation. Significant changes compared to the *fbh1*Δ strain indicated. P-values were calculated using the Shapiro-Wilk normality test (ns p>0.05, *p<0.05, **p<0.01, ***p<0.001, ****p<0.0001). Ade$^+$ recombinant frequency with statistical analysis is also shown in Table 1.

3.3 Discussion

It is estimated that more than 100 different proteins are associated with the eukaryotic RF, forming a large multi-component protein machine termed the replisome. I wanted to investigate, (when the fork encounters a barrier and collapses), whether active disassembly of the replisome is needed for RDR to occur especially the ring structures like MCM and PCNA that encircle the DNA and act as platforms for various replication proteins.

In this chapter, I focused on studying whether Elg1, a major unloader of PCNA, is needed for RDR. I found that Elg1 is essential for recombination induced by *RTS1* at the *ade6* locus on Chromosome 3 (Figure 3.1b). My finding that PCNA persists on the DNA much later in the cell cycle in an *elg1*Δ mutant, and that a disassembly prone

PCNA mutant suppresses *elg1*Δ hypo-recombination (Figure 3.5), provides strong evidence that Elg1 promotes recombination at *RTS1-AO* by unloading PCNA from the blocked fork. This finding can be further verified by checking the recruitment of recombination proteins at *RTS1* in *elg1*Δ, $PCNA^{D150E}$ and *elg1*Δ $PCNA^{D150E}$ cells by fluorescence microscopy.

My finding that Elg1 is not normally required for limiting spontaneous direct repeat recombination at the *ade6* locus and promotes recombination at *RTS1-AO* contrasts with a previous report that Elg1 is needed to suppress recombination in budding yeast (Ben-Aroya et al. 2003), where strains lacking Elg1 show increased recombination between homologous and nonhomologous chromosomes, sister chromatids and direct repeats. However, I did find two conditions where Elg1 was needed to suppress recombination: at a sub-telomeric site on Chromosome 1 (Figure 3.2b); and at *ade6* when *ter2x3* was inserted in the orientation that blocks RFs at this site (Figure 3.3b). Moreover, Elg1 has been shown to be required to promote HR in response to MMS or phleomycin treatment in budding yeast (Ogiwara et al. 2007). Therefore, it seems that Elg1 is capable of promoting and constraining recombination in both yeasts.

What determines whether Elg1 promotes or constrains recombination remains an open question. However, one key factor may be whether the RF simply stalls or collapses. At *RTS1,* forks appear to collapse as a default response, suggesting that this programmed RFB has evolved to trigger replisome disassembly. However, at *ter2X3* the RF stalls but does not collapse. Therefore, it may be that Elg1 promotes recombination when forks collapse but constrains it when they stall. It is also possible that the two states are distinguished by post-translational modification (PTMs) of

PCNA. PCNA is known to undergo multiple different PTMs in response to RF perturbation (Davies et al. 2008; Hoege et al. 2002; Branzei et al. 2004; Branzei et al. 2008; Chiu et al. 2006). The best characterised of these are monoubiquitination, polyubquitination and SUMOylation of K164, which act to recruit TLS polymerases, promote template switching and inhibit HR by recruiting Srs2/PARI, respectively (Pfander et al. 2005; Papouli et al. 2005; Moldovan et al. 2012). However, 13 of 16 lysine residues in human PCNA have been reported to be ubquitinated and some of these can also be acetylated or be modified by ubiquitin-like proteins (McIntyre and Woodgate 2015). Therefore, there is plenty of scope for how PCNA may be able to direct how Elg1 interacts with it and the rest of the replisome. However, it is unclear how exactly Elg1 may protect sites of fork stalling from becoming recombinogenic. It may be through its role in PCNA unloading (Parnas et al. 2010; Kubota et al. 2013; Piazza and Heyer 2018) or via a role that is independent of its interaction with PCNA (Parnas et al. 2011; Parnas et al. 2010; Davidson and Brown 2008). PCNA retention on chromatin in the absence of Elg1 activity may cause genome instability through altered recruitment of PCNA-interacting factors. However, recent reports from a study, where effects of overexpressing PCNA in *elg1+* and *elg1*Δ were examined, indicate that PCNA accumulation on DNA can result in genome instability simply by interfering with chromosome transactions (Johnson et al. 2016). Interestingly, human Elg1 (ATAD5) has been shown to be involved in deubiquitinating PCNA by recruiting the USP1 deubiquitinase to ubiquitinated PCNA (Papouli et al. 2005). In theory this could free up lysines that could then be modified by other types of PTMs, which could direct an anti-recombinogenic response. For example, SUMOylation that is known to recruit

Srs2 in yeast (Pfander et al. 2005; Papouli et al. 2005) and PARI in humans (Moldovan et al. 2012).

Further investigation on reduced *RTS1*-induced recombination in *elg1*Δ was done by exploring the factors that might be recruited by PCNA accumulated at the barrier in the absence of Elg1. PCNA acts as a hub for the recruitment of many different proteins that might be responsible for reducing the recombination, and I investigated if deletion of these factors suppresses the hypo recombination of an *elg1*Δ mutant. Among the factors I investigated (Srs2, Fml1, Eso1 and Fbh1), I found that deletion of *fbh1* suppressed the hypo-recombination of *elg1*Δ and that recombination was increased to the level of a *fbh1*Δ mutant. Therefore, it can be postulated that, when Elg1 is not present, Fbh1 is important for regulating the recombination at *RTS1*, and that the majority of the direct repeat recombination promoted by Elg1 at *RTS1* is supressed by Fbh1 (Figure 3.12). Fbh1 probably suppresses the recombination by its known function of acting as a Rad51 disruptase (Lorenz et al. 2009). However, the question remains whether more Fbh1 at the RFB can be expected to result in a reduction in RTS1-induced recombination. The possibility is supported by an earlier report that overexpression of *fbh1* reduces RFB-induced recombination, and the number of Rad51 nuclear foci induced by replicative stress (Lorenz et al. 2009). Yet, it remains to be determined whether increased retention of PCNA at the barrier leads to greater Fbh1 recruitment at the barrier. We know that PCNA recruits FBH1 to sites of DNA replication and DNA damage in human cells (Bacquin et al. 2013) - but the PCNA interacting motifs in human FBH1 do not appear to be conserved in fission yeast Fbh1. It is also likely that Fbh1 is recruited through its interaction with other proteins that interact with PCNA, like Pfh1 (McDonald et al. 2016). It needs to be

determined in the future whether PCNA directly recruits Fbh1 to *RTS1*, by employing methods like chromatin immunoprecipitation (ChIP) or co-immunoprecipitation (co-IP). Importantly, it is also unclear whether increased Fbh1 activity at the RFB blocks efficient replication restart or simply inhibits ectopic recombination.

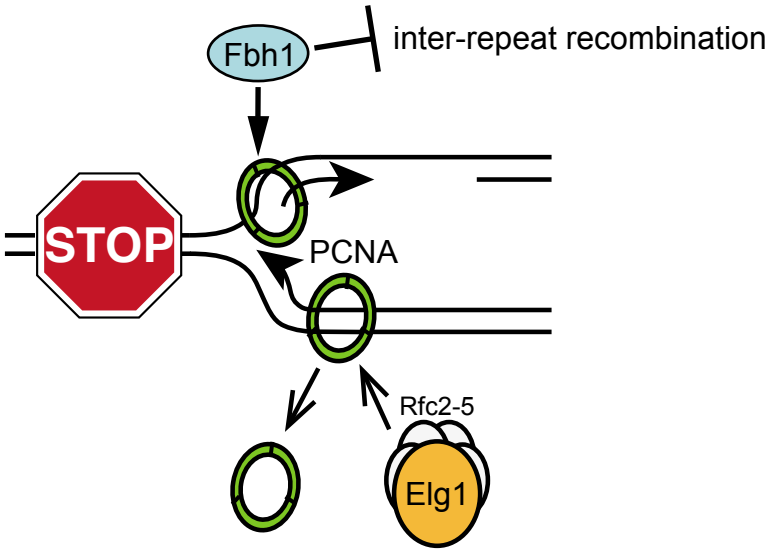

Figure 3.12 Model for how Elg1 promotes direct repeat recombination at *RTS1*
The anti-recombinase Fbh1 is recruited to the RFB by PCNA. Elg1 unloads PCNA from the DNA and thereby limits the recruitment of Fbh1.

4 Investigating what loss of direct repeat recombination in the absence of Elg1 means in terms of recruitment of recombination proteins and fork restart at *RTS1*

4.1 Introduction

The results presented in Chapter 3 show that Elg1 plays a role in promoting ectopic recombination that is associated with the replication restart process at *RTS1*. It most likely does this by unloading PCNA from the site of replication fork blockage/collapse, which in turn limits the recruitment/activity of Fbh1. However, it is unclear whether increased Fbh1 activity at the RFB only limits ectopic recombination or whether it is also a barrier to efficient replication restart. It is also unclear whether increased retention of PCNA at the barrier leads to greater Fbh1 recruitment or facilitates its activity by some other means. For example, it is possible that deficient PCNA unloading might interfere with the recruitment of recombination proteins that precede Rad51 (e.g., Rad52), which could have a knock-on effect for the recruitment of Rad51. Indeed, if retention of PCNA impeded efficient recruitment of Rad52 this might make a fledgling Rad51 nucleofilament more susceptible to disruption by Fbh1 (Osman et al. 2005). In this model, the failure to unload PCNA does not result in more Fbh1 being recruited; rather it blocks efficient recruitment of one of its key antagonists.

A useful tool to assess whether the reduction in recombination in the absence of Elg1 correlates with a reduction in replication restart at the barrier would be native 2D gel electrophoresis. By the use of this technique, replication intermediates at and surrounding *RTS1-AO* can be analysed making a comparison between the pattern of intermediates in wild-type and *elg1*Δ strains.

RDR can also be indirectly estimated using genetic reporters that measure the heightened genomic rearrangements at sites downstream of *RTS1-AO,* that are indicators of restarted fork progression (Nguyen et al. 2015). Although RDR is essential for genome stability as it ensures timely completion of replication by rescuing

collapsed RFs (Lambert et al. 2005; Lambert et al. 2010), the forks restarted by HR are error-prone and thus can cause mutations as well as non-allelic HR that leads to chromosome rearrangements (Mizuno et al. 2013; Iraqui et al. 2012). Forks restarted at *RTS1* can cause genomic rearrangements through the process of template switching, which occurs as the fork progresses away from the site of its initiation (Nguyen et al. 2015). The main constraint over the genomic region in which such template switching can occur is the oncoming replication fork that merges with the restarted fork (Nguyen et al. 2015; Mayle et al. 2015). Under conditions where arrival of the oncoming replication fork is delayed, heightened template switching has been measured up to 75 kb downstream of *RTS1-AO* (Nguyen et al. 2015; Jalan et al. unpublished data). I investigated the effect of *elg1*Δ on direct repeat recombination and mutagenesis induced by the restarted fork at a site downstream of *RTS1*, in an attempt to get an indirect estimate of the relative number of restarted forks reaching the site.

The *RTS1*-based direct repeat recombination reporter only provides a measure of ectopic recombination that gives rise to an Ade^+ recombinant. The vast majority of recombination induced at *RTS1* will actually be genetically silent, thus the reporter only provides a readout of a subclass of recombination events from which the overall recombination activity at the site can be inferred (Osman and Whitby 2009). Moreover, the reporter does not capture the variation in recombination activity between cells as it is an ensemble method. To more directly assess recombination activity at the *RTS1* barrier, our lab developed live cell imaging methodologies that enable monitoring the recruitment of recombination proteins to the RFB in individual cells and in real time (Nguyen et al. 2015).

In this chapter, I make use of the aforementioned experimental tools to investigate whether Elg1 is needed for efficient replication restart by facilitating the recruitment of recombination proteins to the *RTS1* barrier. I also assess whether it specifically affects the recruitment/retention of Rad51 without affecting Rad52 recruitment, as might be expected with a localised increase in Fbh1 concentration (Lorenz et al. 2009).

4.2 Results

4.2.1 2D gel analysis reveals no major difference in the profile of replication intermediates at and around *RTS1* in an *elg1*Δ mutant

Having discovered that *elg1* is required for wild-type levels of *RTS1-AO*-induced recombination, it was important to ascertain whether the *RTS1* barrier remains fully functional without this gene, and to assess whether the reduction in recombination correlates with a reduction in replication restart and increase in replication termination at the barrier. To do this, I used native 2D gel electrophoresis analysis of replication intermediates at and surrounding *RTS1-AO* in the *EcoNI* restriction fragment that encompasses the *RTS1* site (Figure 4.1a).

2D gel analysis reveals no major difference in the profile of replication intermediates at and around *RTS1* between wild-type and *elg1*Δ strains (Figure 4.1b, c). Similar levels of RF blockage signal confirm that *RTS1-AO* still strongly blocks the passage of RFs in an *elg1*Δ mutant, and that the reduction in recombination is not due to a reduction in barrier strength. The accumulation of double Y-shaped DNA molecules, which result from merging of an oncoming fork with a fork held at the barrier, and large Y-shaped molecules, that represent forks that have restarted and

progressed beyond the barrier, are both similar in the two strains (Figure 4.1c). In contrast to the significant reduction in direct repeat recombination in *elg1*Δ mutant from the wild-type, there does not appear to be any significant difference in fork restart and replication past the barrier, comparing wild-type and *elg1*Δ strains, as judged by 2D gel analysis.

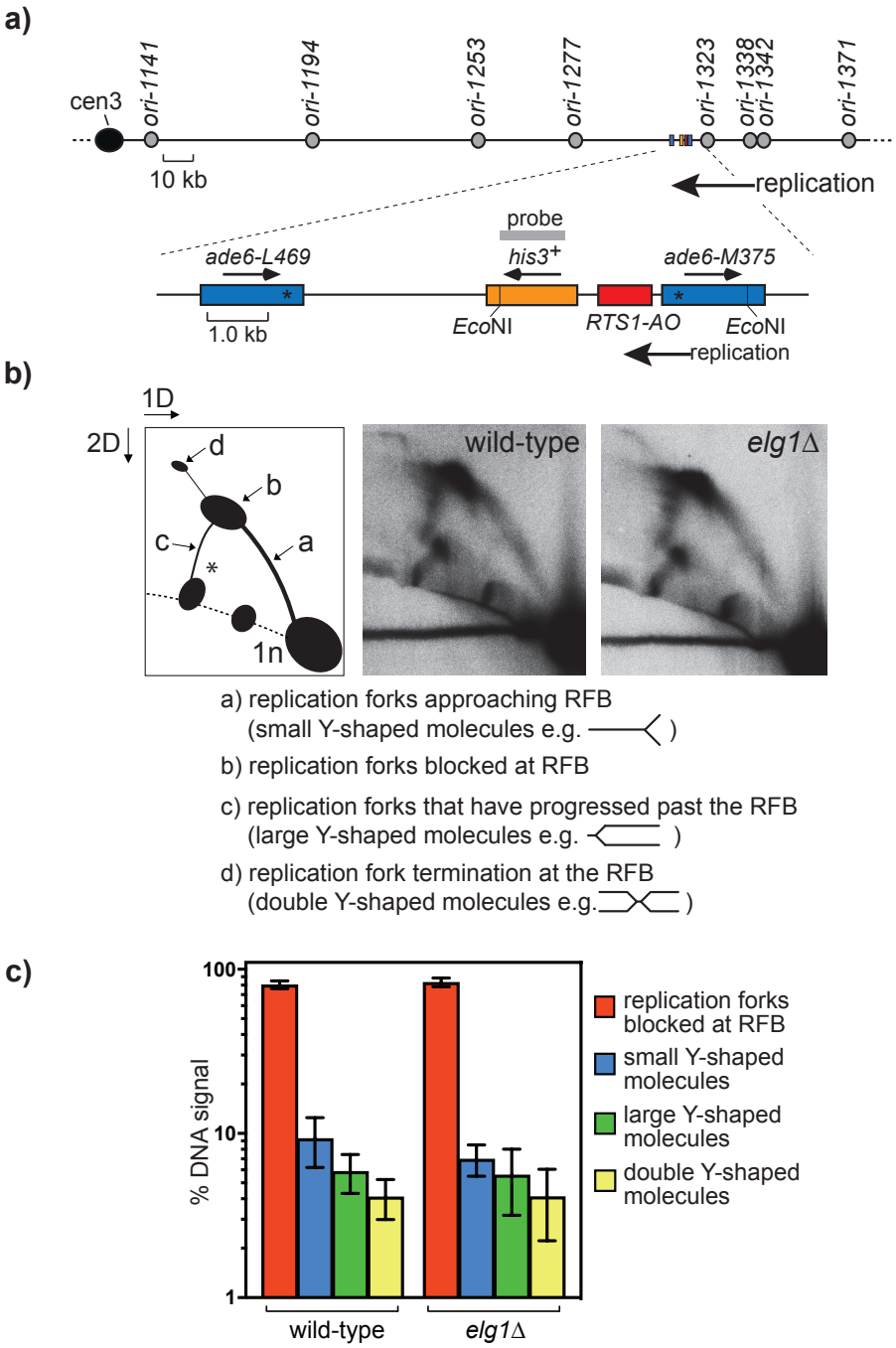

Figure 4.1 2D gel analysis of replication intermediates at and around RTS1 shows no major difference between wild-type and elg1Δ

a) Schematic showing the relative position of RTS1 on chromosome 3 and the fragment used for 2D gel analysis showing the position of the probe. b) 2D gel analysis of replication intermediates within the EcoNI fragment. The panel on the left is a guide for interpreting the 2D gels ('∗' indicates a signal seen as an artefact in these experiments). c) Quantification of the 2D gels displayed as bar charts. The DNA was extracted from asynchronously growing cultures of the strains MCW 4713 (wild-type) and MCW 7708 (elg1Δ). Error bars represent standard deviation.

4.2.2 Effect of *elg1*Δ on direct repeat recombination and mutagenesis downstream of *RTS1*

Forks restarted from *RTS1* remain prone to template switching as they progress from the RFB (Iraqui et al. 2012; Nguyen et al. 2015). To measure this template switching, I used an *ade6*$^{-}$ direct repeat reporter (reporter system 1) inserted 12.4 kb downstream of *RTS1* and the frequency of Ade^{+} recombinants can be determined (Figure 4.2a and b) (Nguyen et al 2015). In the wild-type strain with *RTS1-IO*, the recombinant frequency is similar to a strain with no *RTS1* (Nguyen et al 2015; unpublished data), whereas with *RTS1-AO* it increases by ~29-fold with an Ade^{+} recombinant frequency of approximately 69 in every 10,000 viable cells (Figure 4.2a). The majority (~93%) of these recombinants are deletions (see Table1 in appendix).

The direct repeat recombination, downstream of *RTS1-AO*, is limited by the oncoming fork, which can converge with the restarted fork before it reaches the downstream site (Nguyen et al. 2015). This is evident from the fact that, when the strongest origin in this chromosomal region (*oriIII-1253*) is deleted, the frequency of recombinants increases by ~10-fold in a strain with *RTS1-AO* (Figure 4.2b). Thus, heightened recombination at sites downstream of *RTS1-AO* is an indirect indicator of restarted fork progression/RDR efficiency.

Work by a previous student in the lab (Manisha Jalan) had shown that an *elg1*Δ mutant, with reporter system 1 positioned 12.4 kb downstream of *RTS1-AO*, exhibited ~8-fold reduction in gene conversions and ~6-fold reduction in deletions compared to wild-type (Fig. 4.2b). Deletion of *oriIII-1253*, resulted in ~8-fold increase in gene conversions and ~7-fold increase in deletions in the *elg1*Δ mutant compared to ~24-fold increase in gene conversions and ~11-fold increase in deletions in the equivalent

wild-type strain (Figure 4.2b). These data indicated that Elg1 promotes template switching associated with a restarted fork. However, it remained unclear whether Elg1 was affecting the restart/progression of the fork or the template switch process itself. The observation that providing more time for restart, by deleting *oriIII-1253,* did not reduce the difference in recombinant frequencies between wild-type and *elg1*Δ, suggested that Elg1 might directly affect template switching by modulating the association of PCNA with the restarted fork.

In addition to increased levels of template switching, restarted forks are highly error-prone, causing small deletions and duplications by replication slippage between tandem sequences with shared micro-homology (Mizuno et al. 2013; Iraqui et al. 2012). Thus, another way of indirectly estimating RDR is to measure the mutagenesis induced by the restarted fork downstream of *RTS1*. Recently, a system was developed in our lab by which ectopic recombination and mutagenesis could be monitored at neighbouring genomic sites simultaneously, by placing a *ura4*$^{+}$ gene immediately adjacent to the ade*6*$^{-}$ direct repeat reporter 12.4 kb downstream of *RTS1* (reporter system 2, Figure 4.2a). The *ura4*$^{+}$ gene is used in this system as an additional reporter to score genetic instability by measuring the frequency of cell resistance to 5-FOA resulting from loss of *ura4*+ function. I confirmed that an *elg1*Δ mutant exhibits a similarly low level of Ade^{+} recombinants with this reporter system as it does with reporter system 1 (Figure 4.2b). Deleting *oriIII-1253*, also resulted in similar fold increases in gene conversions and deletions (Figure 4.2b). To maximise the number of restarted forks reaching the *ura4*+ reporter, I used strains with the *oriIII-1253* deletion to assess the frequency of 5-FOA resistance as measured by a plating assay (Figure 4.2c). In a wild-type background, the presence of *RTS1-AO* causes a ~50-fold

increase in the frequency of FOA resistant colonies compared to an equivalent strain with *RTS1-IO* (Figure 4.2c). In an *elg1*Δ mutant the *RTS1-A*O-induced frequency of FOA resistant colonies was reduced ~9-fold ($p<0.001$) compared to wild-type (Figure 4.2c). If we assume that Elg1 is not required for directly promoting replication slippage events, then these data suggest that replication restart and/or progression of the restarted fork is less efficient in an *elg1*Δ mutant. However, in Chapter 6 I will discuss how the majority of FOA resistant colonies appear to stem from a multi-invasion recombination event rather than from replication slippage and, therefore, do not provide information on RDR.

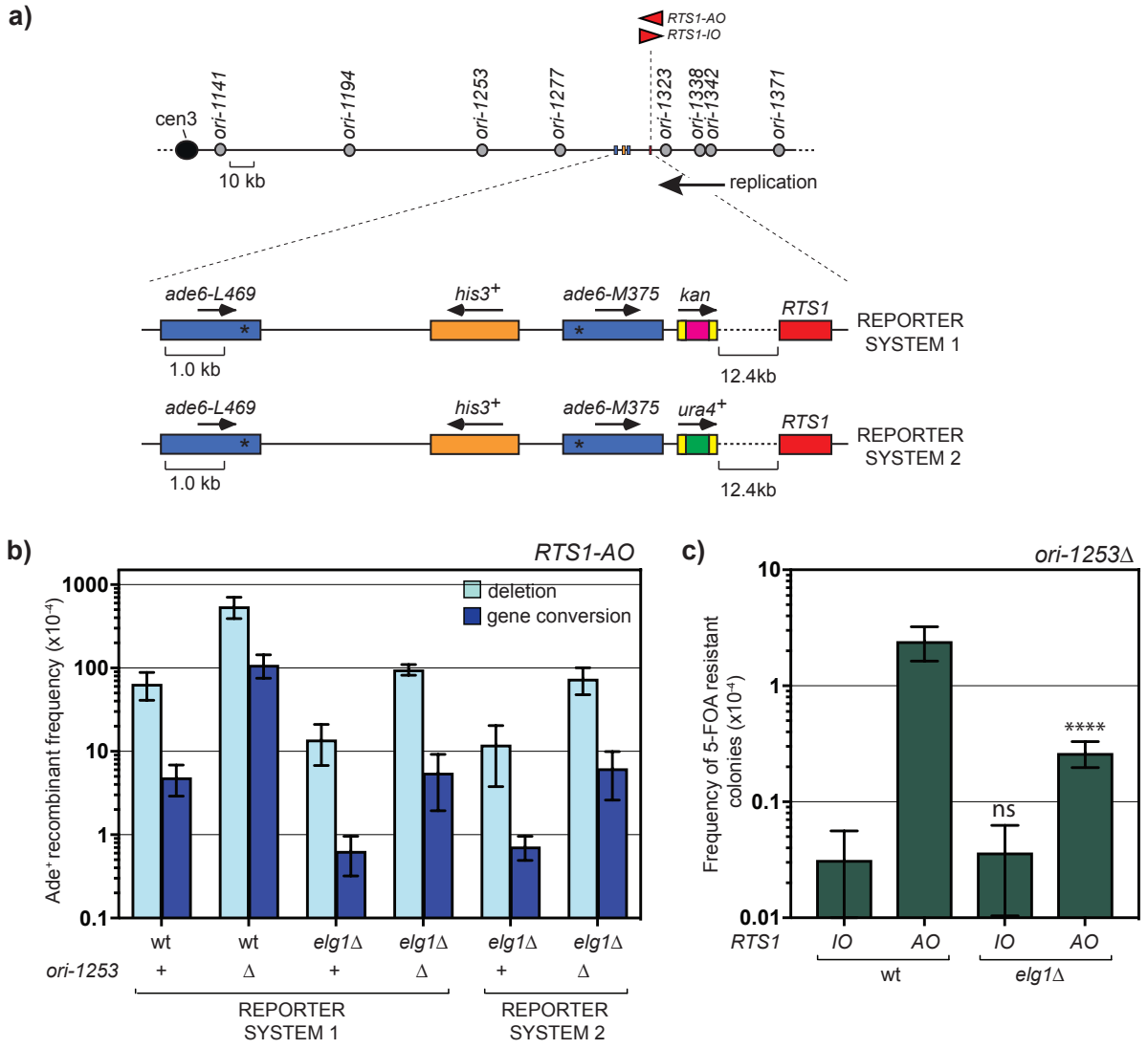

Figure 4.2 Direct repeat recombination and mutagenesis downstream of *RTS1* is reduced in an *elg1*Δ mutant

a) Schematic showing the location of *RTS1* and *ade6*- recombination reporter with and without *ura4*+ reporter in relation to nearby replication origins (grey circles) at the endogenous *ade6* locus on chromosome 3. Direction of replication indicates the direction of the recombination dependent restarted fork through *ade6*- direct repeat reporter. b) Bar charts showing the frequency and type of Ade+ recombinants in MCW7259, MCW7295, MCW8191, MCW8290, MCW8992, MCW8990. c) Bar charts showing the frequency of 5-FOA resistance in MCW8700, mcw8888, MCW8988, MCW 8990. Error bars represent standard deviation. Significant changes compared to the wild-type strain are indicated. P-values were calculated using the Shapiro-Wilk normality test (ns $p>0.05$, * $p<0.05$, ** $p<0.01$, *** $p<0.001$, **** $p<0.0001$). Ade+ recombinant frequency with statistical analysis is shown in Table 1.

4.2.3 Recruitment of Rad52 at the *RTS1* barrier is less efficient in an *elg1*Δ mutant

Increased Fbh1 activity at the RFB would be expected to lead to a reduction in the amount of Rad51 that accumulates at the site without affecting levels of Rad52 (Lorenz et al. 2009). To investigate this, I decided to directly assess the effect of *elg1*Δ on recombination protein recruitment at *RTS1*. For this, I used a system in which the position of the *RTS1* barrier is marked by an adjacent array of *lacO* sequences, which is visualised through the association of LacI repressor to the far-red fluorescent protein tdKatushka2 (Figure 4.3a). Being aware that *lacO*-LacI interaction can act as an RFB, imaging parameters were adjusted, for the amount of LacI, such that the *lacO* is detectable through the long hours of imaging but is insufficient to block RFs as judged by 2D gel analysis and *ade6*$^{-}$ recombination. Thus, LacI-tdKatushka2 expression levels driven by the *nmt41* promoter is repressed by 1 µM thiamine to get the balance right (Nguyen et al. 2015). The recruitment and retention of a recombination protein at *RTS1* can be followed by tagging the recombination protein with a different colour fluorescent protein and scoring whether it forms foci that co-localise with *lacO*-LacI foci (Nguyen et al. 2015). In the case of Rad52, yellow fluorescent protein (YFP) was fused to its C-terminus. Rad52-YFP was expressed from its endogenous promoter, the locus is fully functional and the protein forms foci that co-localise with *RTS1* (Meister et al. 2003; Nguyen et al. 2015) (Figure 4.3b).

I analysed the presence of Rad52 foci and their co-localization with *lacO*-LacI foci in asynchronous cultures of wild-type and *elg1*Δ strains, containing either *RTS1-IO* or *RTS1-AO*, by snapshot imaging. For each strain, a total of >500 cells with a detectable *lacO*-LacI focus were analysed for the presence and localisation of Rad52

foci from three independent cultures. Cells were also staged, based on their length and number of *lacO*-LacI foci, into two groups: 1) M phase to early G2 phase cells (46% of the population in wild type *RTS1-IO*, 48% in wild type *RTS1-AO*, 52% in *elg1*Δ *RTS1-IO* and 54% in *elg1*Δ *RTS1-AO*); 2) late G2-phase cells (54% of the population in wild type *RTS1-IO*, 52% in wild type *RTS1-AO*, 48% in *elg1*Δ *RTS1-IO* and 46% in *elg1*Δ *RTS1-AO*).

In the wild-type strain containing *RTS1-IO*, about 14% of cells in the M phase to early G2 phase group exhibit Rad52 foci that do not co-localize with a *lacO*-LacI focus (Figure 4.3c). This value is consistent with a previous report for late-S or early G2 cells and probably reflects the repair of spontaneous DNA damage that occurs or is exacerbated during DNA replication (e.g., single-stranded gaps and broken replication forks) (Meister et al. 2003). A similar percentage of late G2 phase cells also exhibit Rad52 foci, which likewise show little or no co-localization with *lacO*-LacI. As expected, the percentage of Rad52 foci in the wild-type strain with *RTS1-AO* increases by almost 3-fold in the M phase to early G2 phase group of cells. Most of these extra foci co-localize with a *lacO*-LacI focus, indicating Rad52 recruitment to replication forks blocked/collapsed at *RTS1*. The percentage of these co-localizing foci is reduced by >4-fold in late G2 phase cells suggesting that, in the majority of cells, the problems associated with replication fork collapse at *RTS1* are resolved prior to mitosis. Overall, this pattern of Rad52 foci is similar in an *elg1*Δ mutant (Figure 4.3c). Indeed, loss of Elg1 does not seem to result in an increase in the percentage of cells with spontaneous Rad52 foci, as reported in budding yeast (Alvaro et al. 2007). However, there does seem to be a slight but significant (~1.7-fold, p=0.01) reduction in Rad52 foci co-localizing with the barrier in the M phase to early G2 phase group of cells, albeit

the overall percentage of cells with Rad52 foci in the presence of *RTS1-AO* is similar to wild-type (Figure 4.3c). Altogether these data suggest that loss of Elg1 may impair the recruitment/retention of Rad52 at *RTS1*.

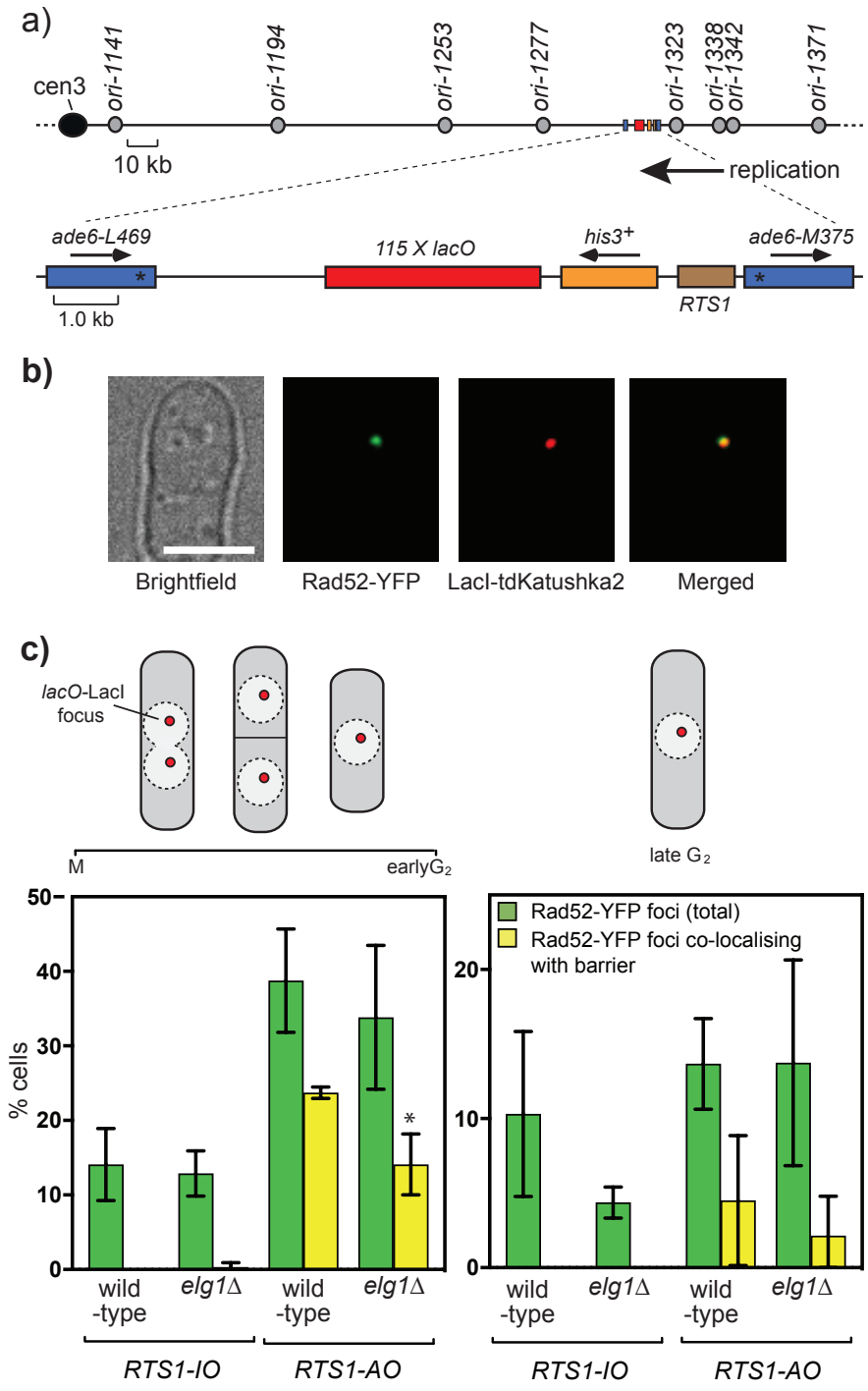

Figure 4.3 Effect of *elg1*Δ on the presence of Rad52-YFP foci and their co-localization with the *RTS1* barrier
a) Schematic showing the modification of the direct repeat recombination reporter for live-cell imaging. b) Example of a cell with a Rad52-YFP focus co-localizing with a *lacO*-LacI-tdKatushka2 focus. The scale bar represents 5μm. The strain shown is MCW 7065. c) Bar chart showing the percentage of cells with total Rad52-YFP foci and Rad52-YFP foci co-localizing with *lacO*-LacI-tdKatushka2 focus for wild-type and *elg1*Δ strains with *RTS1-IO* and *RTS1-AO*. The population was divided to two groups (M-earlyG_2 and late G_2) on the basis of cell length and morphology. The strains are MCW6712 (n=523), MCW7969 (n=550), MCW7065 (n=671), MCW7965 (n=671). Error bars represent standard deviation. Significant change compared to the wild-type strain is indicated. P-values were calculated using the Mann-Whitney test (ns $p>0.05$, *$p<0.05$).

4.2.4 Recruitment of Rad51 at the *RTS1* barrier is also reduced in an *elg1*Δ mutant

If Fbh1 is responsible for the reduction in *RTS1-AO*-induced direct repeat recombination in an *elg1*Δ mutant, as my data in Chapter 3 suggest, then Rad51 recruitment/retention at the RFB should be lower in an *elg1*Δ mutant than in wild-type cells. To investigate this, I used wild-type and *elg1*Δ strains containing *RTS1-AO* marked by an adjacent array of *lacO* sequences, LacI-tdKatushka2, Rad52-YFP and Rad51 tagged at its N-terminus with cyan fluorescent protein (CFP) (Figure 4.4). As CFP-Rad51 is not fully functional, untagged Rad51 was expressed in the same cells from an integrated construct at the *ura4* locus (Nguyen et al. 2015). A total of ~400 *lacI*-LacO focus-positive cells from four independent cultures were analysed for both wild-type and *elg1*Δ strains (Figure 4.5). The overall percentage of cells with Rad52 foci is 30% and 28% for wild-type and *elg1*Δ respectively, which is within the range of the values observed in the previous experiment (bearing in mind that in this experiment all cells are considered together regardless of their cell cycle stage) (Figure 4.5a). Approximately half (55%) of the Rad52 foci co-localize with a *lacO*-LacI focus in the wild-type, whereas this reduces to only 28% in the *elg1*Δ mutant (Figure 4.5a and c). Approximately 22% of both wild-type and *elg1*Δ cells exhibit Rad51 foci, of which the majority (90% and 80%, respectively) co-localize with Rad52. Importantly, whereas ~44% of Rad51 foci co-localize with a *lacO*-LacI focus in the wild-type, only ~10% do so in an *elg1*Δ mutant, which is markedly less than the percentage of Rad52 foci that co-localize with *lacO*-LacI (Figure 4.5a and c). Of the Rad52 foci co-localizing at the barrier, 62% co-localize with Rad51 in wild-type, which is reduced to 30% in *elg1*Δ cells (Figure 4.5b). Altogether these data indicate that the recruitment and/or retention

of both Rad51 and Rad52 is less in an *elg1*Δ mutant than in wild-type. However, the reduction appears to be greater for Rad51 than for Rad52

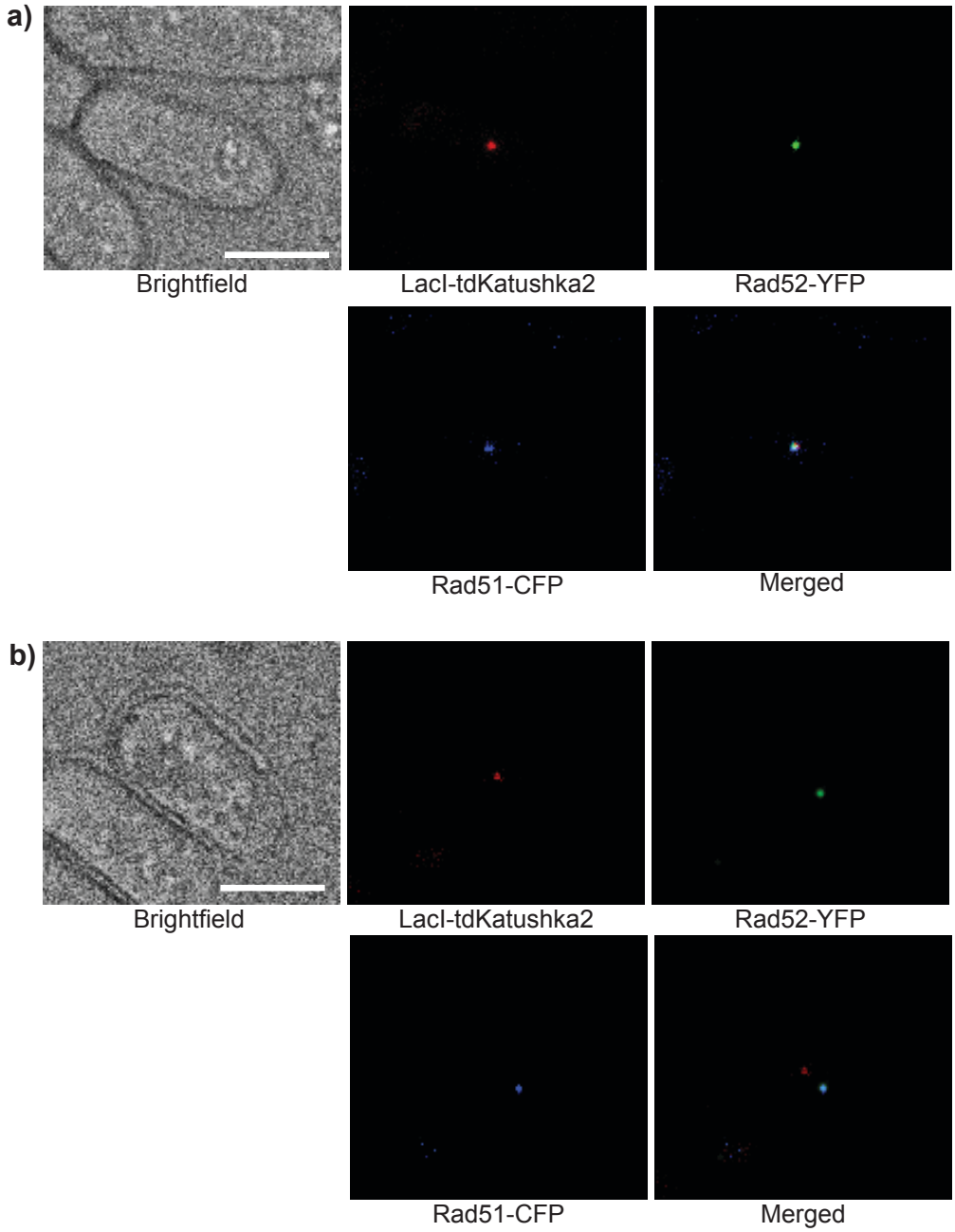

Figure 4.4 Examples of images used for the analysis of Rad52-YFP and Rad51-CFP foci co-localization with *RTS1*-AO
a) An example of a cell with Rad52-YFP, Rad51-CFP and *lacO*-LacI-tdKatushka2 foci co-localising. b) An example of a cell with Rad52-YFP and Rad51-CFP foci co-localising but not with *lacO*-LacI-tdKatushka2 foci. The scale bar represents 5μm. The strain shown is MCW7638. These images are representative of those used for the analysis shown in Figure 4.5.

a)

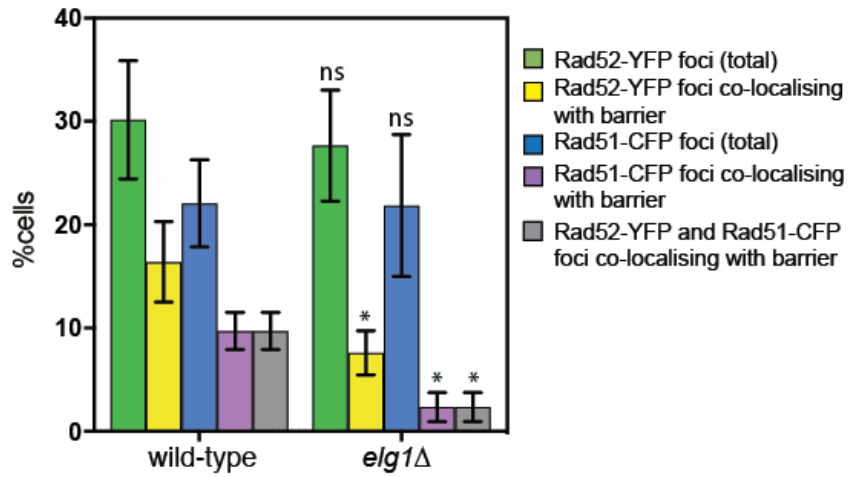

b)

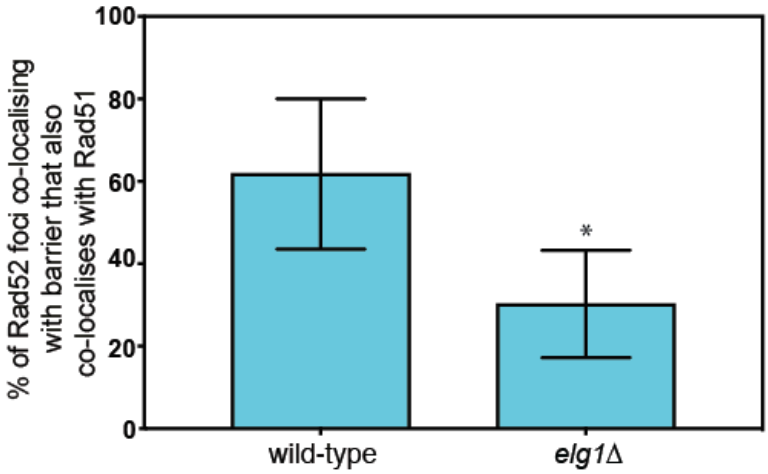

c)

	Number of cells analysed	% cells with a Rad52 focus	% cells with a Rad51 focus	% Rad52 foci that co-localize with Rad51	% Rad51 foci that co-localize with Rad52	% Rad52 foci that co-localize with *lacO*-LacI	% Rad51 foci that co-localize with *lacO*-LacI	% Rad52 foci that co-localize with Rad51 at *lacO*-LacI	% Rad51 foci that co-localize with Rad52 at *lacO*-LacI
wild-type *RTS1-AO*	404	30.2	22.1	66.7	90.2	54.9	44.3	35.6	44.3
*elg1*Δ *RTS1-AO*	394	27.7	21.9	60.1	79.6	28	10.5	8.36	10.5

Figure 4.5 Effect of *elg1*Δcauses reduced recruitment/retention of Rad51 foci at the *RTS1* barrier
a) Bar chart showing: the percentage of cells with Rad52-YFP and Rad51-CFP foci; percentage of cells with Rad52-YFP and Rad51-CFP foci co-localizing with a *lacO*-LacI-tdKatushka2 focus; and percentage of cells with all three foci co-localizing. b) Bar graph showing the percentage of Rad52-YFP foci colocalizing with *lacO*-LacI-tdKatushka2 that also have co-localizing Rad51-CFP. c) Table showing the profile of co-localizations of Rad52-YFP, Rad51-CFP and *lacO*-LacI-tdKatushka2. The wild-type strain is MCW7638 (n=404) and the *elg1*Δ strain is MCW8921 (n=394), both strains contain *RTS1-AO*. Error bars represent standard deviation. Significant changes compared to the wild-type strain are indicated. P-values were calculated using the Mann-Whitney test (ns $p>0.05$, *$p<0.05$).

4.2.5 Studying the effect of *elg1*Δ on the recruitment of recombination proteins at *RTS1* in real time

Time lapse imaging can provide a clear picture of the spatiotemporal dynamics of recombination and replication protein association with *RTS1*. Thus, I decided to complement the snapshot analysis with time-lapse microscopy to monitor recombination protein recruitment to the RFB in individual cells and in real time. In these experiments I monitored Rad52-YFP foci alongside eCFP-PCNA fluorescence signal to track the timing and progression of S phase in cells where the *RTS1* barrier was again marked by an adjacent array of *lacO* sequences visualised through the binding of LacI-tdKatushka2. Cells were monitored from the start of S phase up to 90 minutes, following and recording Rad52-YFP foci in individual cells at five-minute intervals (Figure 4.6a and b). Unfortunately, time-lapse experiments with CFP-Rad51 foci proved unsuccessful due the tendency of these foci to photo bleach much quicker than Rad52-YFP foci (data not shown).

Time-lapse imaging of wild-type and *elg1*Δ cells reveals a consistent pattern of PCNA focus appearance 10-15 minutes post anaphase marking the start of S phase (PCNA focus merely used as a marker here, is later assessed comparing the two strains: Figure 4.10). As expected, relatively few Rad52 foci co-localize with a *lacO*-LacI focus in either wild-type or *elg1*Δ cells containing *RTS1-IO*, and where there is co-localization might have occurred by chance (Figure 4.6b). In the wild-type strain with *RTS1-AO*, Rad52 foci that co-localise with the barrier start to appear about 10 minutes after the start of S phase with the peak number of cells with such foci occurring a further 30 minutes later (Figure 4.6c, Figure 4.8a). Out of the 52 cells that were analysed, 49 (94%) exhibited a Rad52 focus that co-localized with the RFB in at least one time point during the 90-minute period following the start of S-phase. In the *elg1*Δ

mutant containing *RTS1-AO*, Rad52 foci that co-localized with *lacO*-LacI started to appear 15 minutes after the start of S phase (Figure 4.6a and c). Indeed, overall there was an average delay in the appearance of Rad52 foci at the barrier of ~10 minutes compared to wild-type (Figure 4.6c). However, even though these co-localizing foci tended to appear later in an *elg1*Δ mutant, they disappeared at a similar time to that observed in the wild-type (Figure 4.6c). This suggests that the delay in Rad52 recruitment is not a consequence of a general reduction in replication fork velocity, as this would result in a later time for both fork blockage and fork convergence at *RTS1*. A total of 85 *elg1*Δ cells were analysed. In addition to the apparent later time of Rad52 recruitment to the barrier, overall slightly fewer cells exhibited Rad 52 focus that co-localises with the barrier in *elg1*Δ mutant compared to the wild type (82% versus 94%), whilst the experiment was done only once. Altogether these data indicate that Elg1 is needed for the timely recruitment of Rad52 to replication forks blocked/collapsed at the *RTS1* barrier.

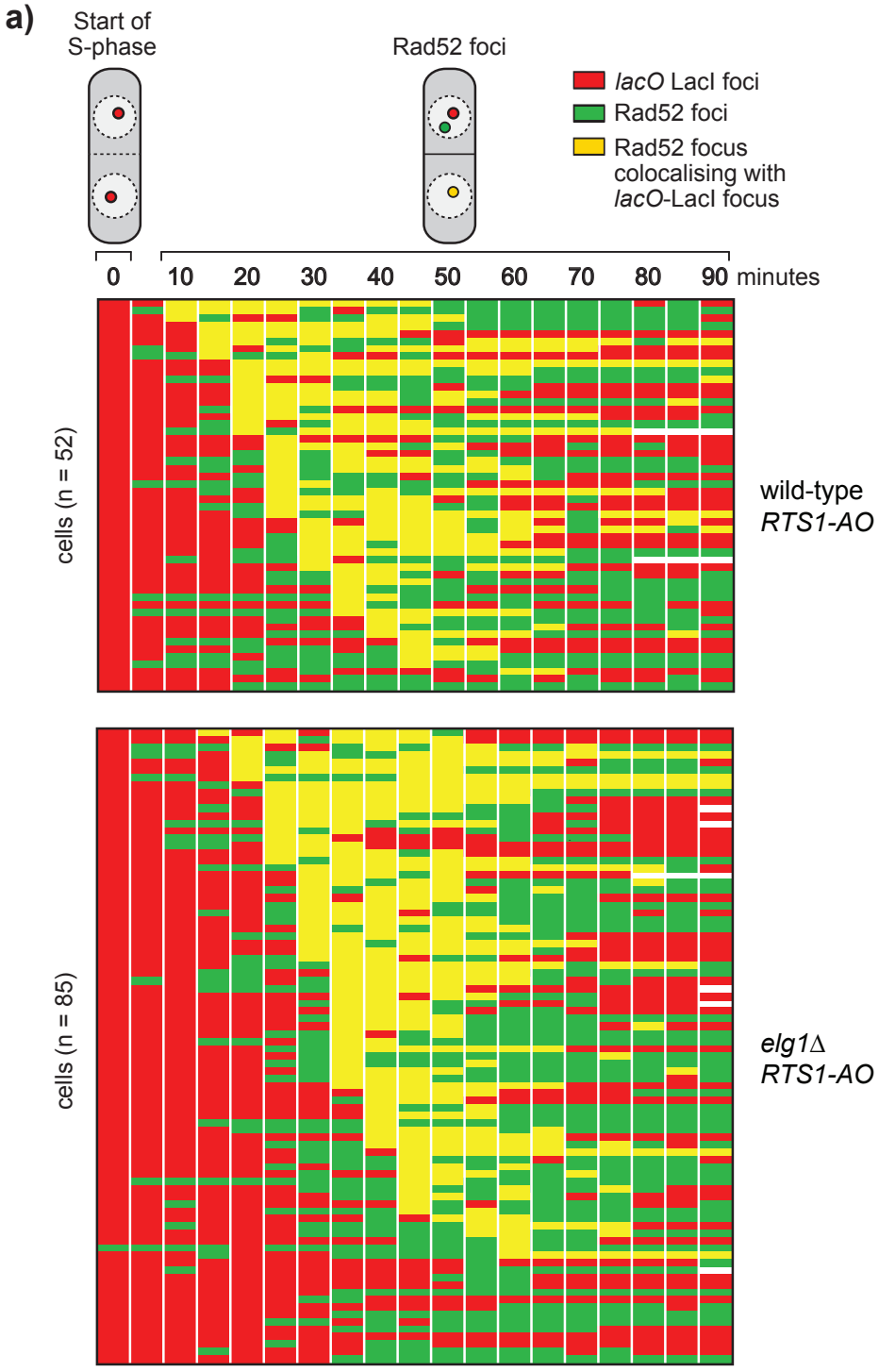
a)
Start of S-phase
Rad52 foci
lacO LacI foci
Rad52 foci
Rad52 focus colocalising with lacO-LacI focus
0
10
20
30
40
50
60
70
80
90
minutes
cells (n = 52)
wild-type RTS1-AO
cells (n = 85)
elg1Δ RTS1-AO

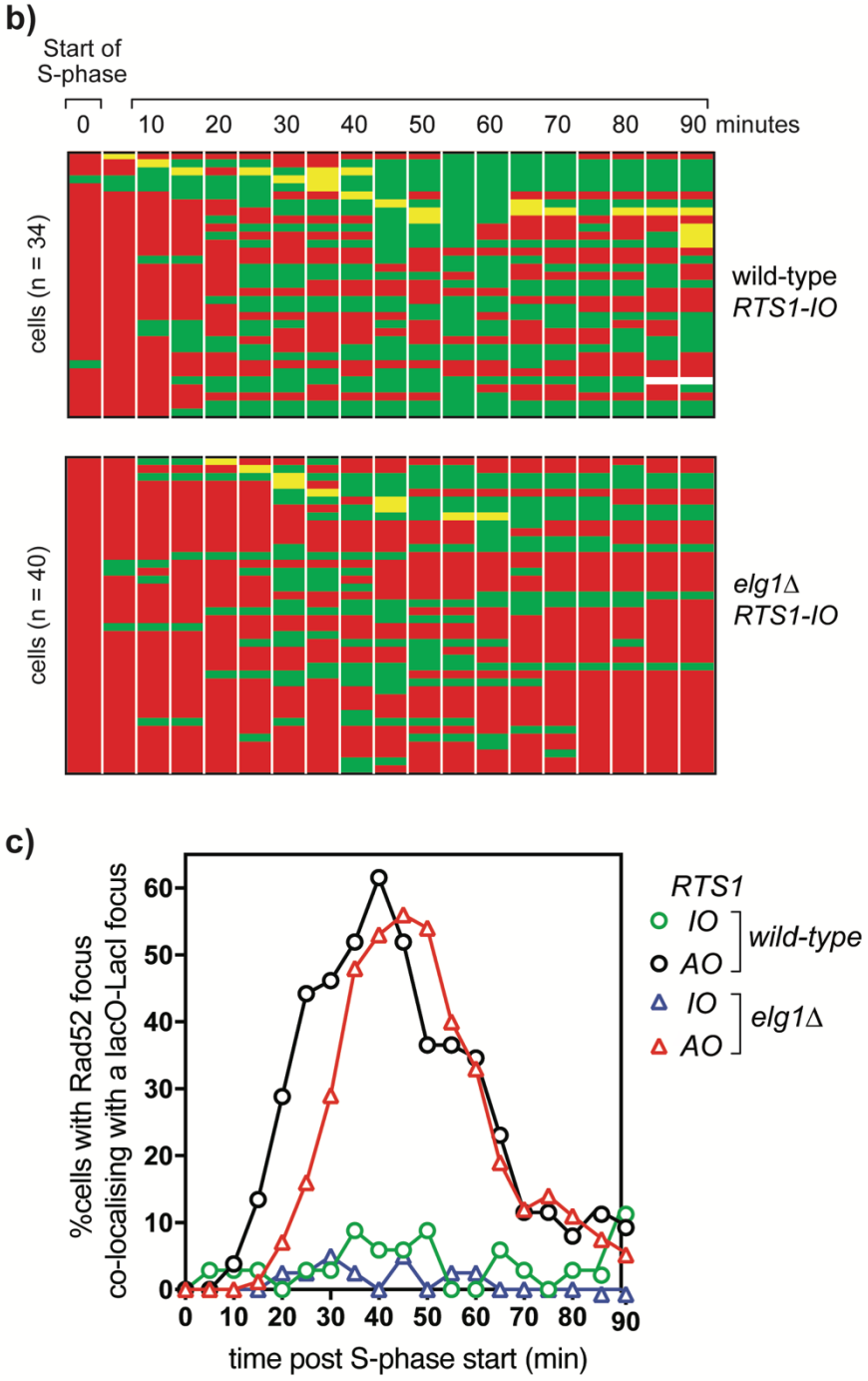

Figure 4.6 Tracking Rad52-YFP focus co-localization at *RTS1* by time-lapse microscopy in wild-type and *elg1*Δ cells

a) Analysis of time-lapse movies of *RTS1-AO* wild-type and *elg1*Δ strain for the presence of a Rad52 focus and whether it co-localizes with the *lacO*-LacI-tdKatushka2 focus. The top panel is a schematic of *S. pombe* cells at the start of S-phase and during the 90-minute time course. b) Analysis of time-lapse movies of *RTS1-IO* wild-type and *elg1*Δ strain. The presence of a Rad52 focus and whether it co-localizes with the *lacO*-LacI-tdKatushka2 focus is recorded every 5 minutes for 90 minutes post S-phase start in each cell. Nuclear *lacO*-LacI foci are in red, Rad52 foci are in green and co-localizing foci are in yellow. c) Line graph of the percentage of cells with a Rad52-YFP focus that co-localizes with the *lacO*-LacI focus in the 90 minutes post S-phase start. The *RTS1-AO* wild-type strain is MCW7065 (n=52), the *RST1-AO elg1*Δ strain is MCW7965 (n=85), the *RTS1-IO* wild-type strain is MCW6712 (n=34) and the *RST1-IO elg1*Δ strain is MCW7969 (n=40).

As mentioned in Chapter 3, eCFP tagged PCNA is not fully functional and, therefore, “normal” PCNA activity is achieved in these cells through the expression of untagged PCNA from its endogenous locus, with eCFP-PCNA expressed from a construct inserted at the *ura4* locus (Meister et al. 2007). However, even though cells that co-express tagged and untagged PCNA appear to grow normally and exhibit wild-type levels of genotoxin sensitivity (Meister et al. 2007) it remained possible that tagged PCNA might have some impact on Elg1’s unloading role. For example, CFP-PCNA may be more easily unloaded from DNA in the absence of Elg1 than its untagged form. To investigate whether the presence of eCFP-PCNA influences the recruitment/retention of Rad52 foci at the *RTS1-AO* barrier, I performed further time-lapse experiments in strains without the *eCFP-pcn1* construct (Figure 4.7). Similar to cells with eCFP-PCNA, *elg1*Δ resulted in a delay of ~10 minutes in the appearance of Rad52 foci co-localizing with *lacO*-LacI (Figure 4.8a). Importantly, non-co-localizing foci appeared with similar timing in both wild-type and mutant showing that Elg1 is not generally required for efficient Rad52 focus formation (Figure 4.8b). Overall 75% of wild-type cells exhibited a Rad52 focus that co-localized with *lacO*-LacI during at least one time point during the 90-min period post anaphase. This reduces to 51% in the *elg1*Δ mutant, which is a greater reduction than seen in the strains with eCFP-PCNA, even when accounting for the fact that the percentage of cells with Rad52-*lacO*-LacI co-localizing foci is also reduced in the wild-type strain. Overall these data provide further evidence that Elg1 is needed for the efficient recruitment of Rad52 at the *RTS1* barrier.

I also investigated whether deleting *elg1* affected the number of Rad52 molecules that were recruited to the RFB. To do this I analysed the intensity of Rad52

foci that co-localized with *lacO*-LacI, and those that did not, in both wild-type and *elg1*Δ cells (Figure 4.9). Focus intensity was assessed in two consecutive time points in cells from the aforementioned time-lapse experiment by measuring the percentage fluorescence intensity with respect to total nuclear fluorescence. By this analysis, I did not detect any significant change in the intensity of co-localizing or non-co-localizing Rad52 foci in the *elg1*Δ mutant.

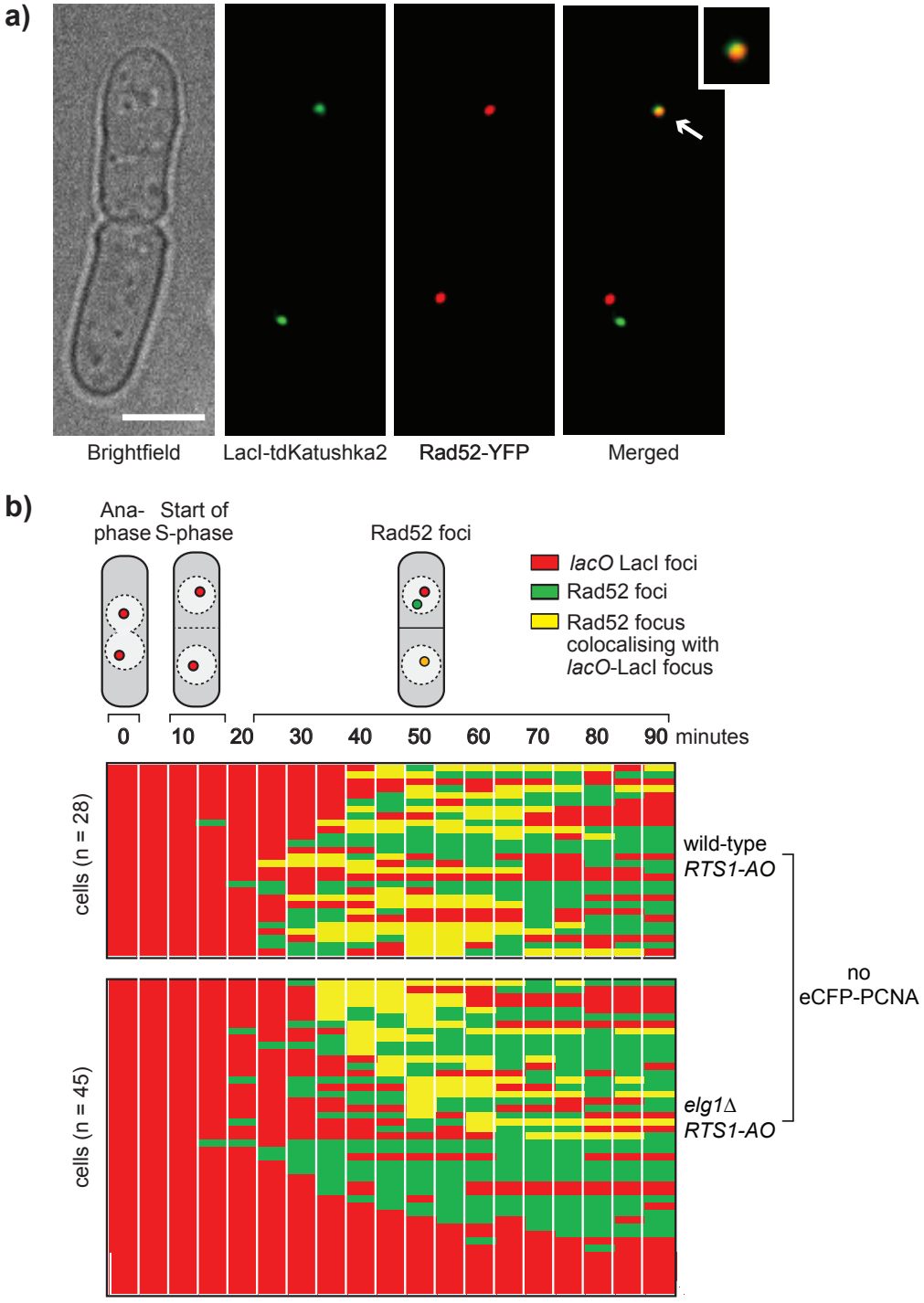

Figure 4.7 Tracking Rad52-YFP focus co-localization at *RTS1* by time-lapse microscopy in wild-type and *elg1*Δ cells without eCFP-PCNA

a) An example of a cell with a Rad52-YFP focus co-localizing with a *lacO*-LacI-tdKatushka2 focus. The scale bar represents 5 µm. The strain shown is MCW 6556. b) Analysis of time-lapse movies of *RTS1-AO* wild-type and *elg1*Δ strain. The presence of a Rad52 focus and whether it co-localizes with the *lacO*-LacI-tdKatushka2 focus is recorded every 5 minutes for 90 minutes post anaphase in each cell. The top panel is a schematic of *S. pombe* cells at various stages post-anaphase with nuclear *lacO*-LacI foci in red, Rad52 foci in green, co-localizing foci in yellow. The *RTS1-AO* wild-type strain is MCW6556 (n=28) and the *RST1-AO elg1*Δ strain is MCW8486 (n=45), these strains do not have eCFP tagged PCNA.

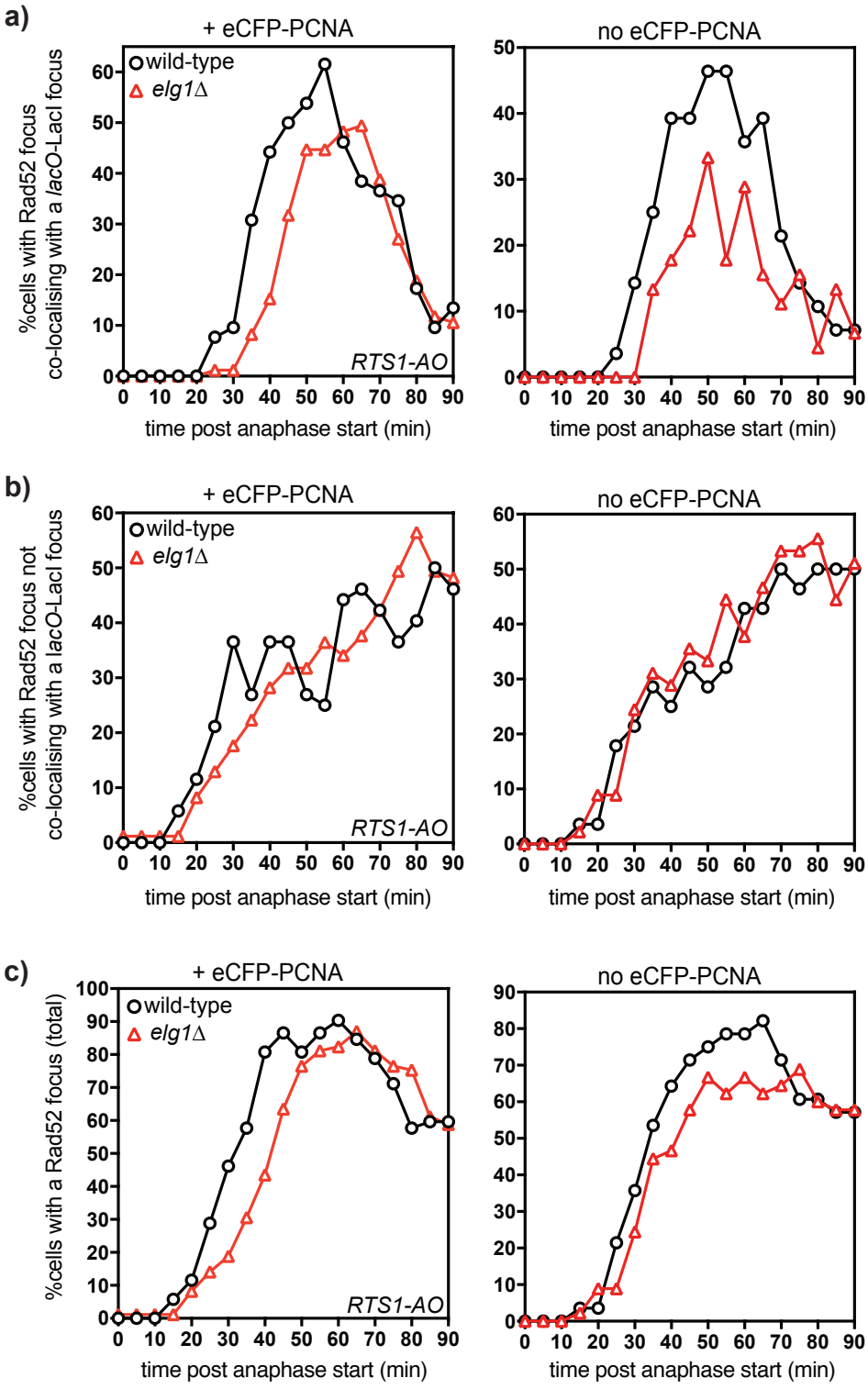

Figure 4.8 Effect of *elg1*Δ on the temporal kinetics of Rad52-YFP foci localization to *RTS1* in strains with and without eCFP tag on PCNA

Line graphs of the percentage of cells with a) Rad52-YFP focus that co-localizes with the *lacO*-LacI focus, b) Rad52-YFP focus not co-localizing with the *lacO*-LacI focus and c) Rad52-YFP focus, during the first 90 minutes following anaphase at five-minute intervals. The wild-type and *elg1*Δ strains with eCFP-PCNA are MCW7065 (n=52) and MCW7965 (n=85) respectively; the wild-type and *elg1*Δ strains without eCFP-PCNA are MCW6556 (n=28) and MCW8486 (n=45) respectively. All the strains contain *RTS1-AO*.

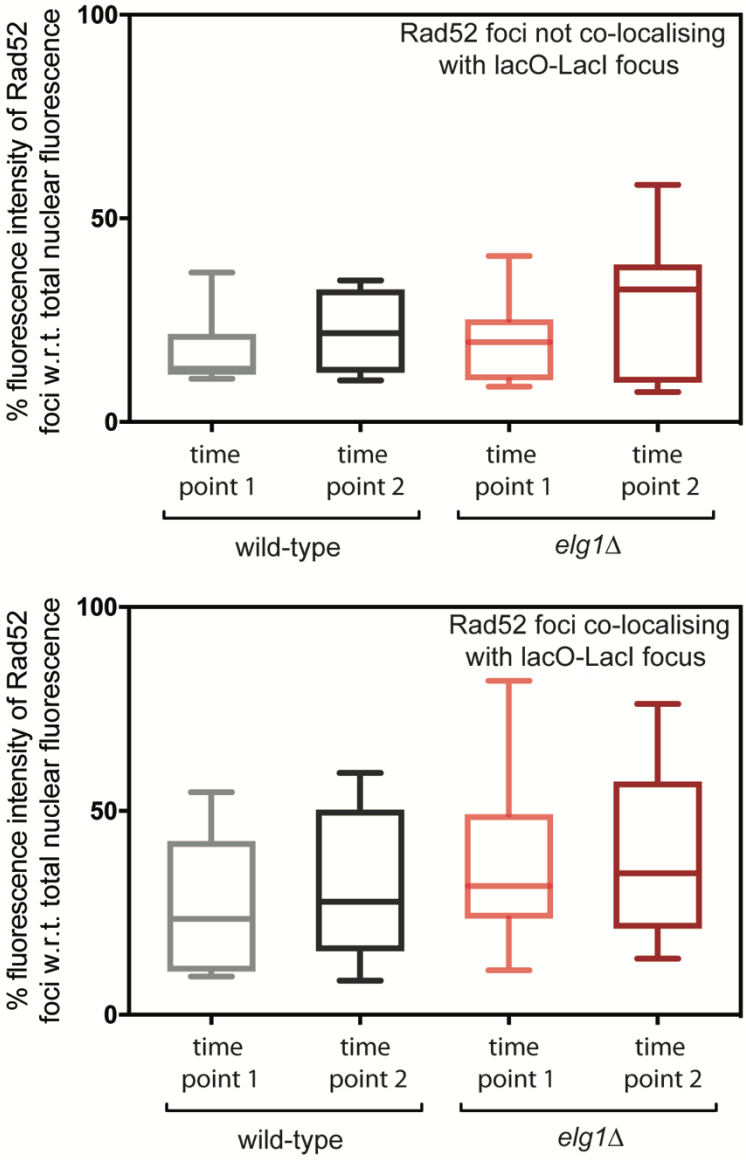

Figure 4.9 Loss of Elg1 does not lead to a reduction in Rad52 focus intensity
Box plots showing % fluorescence intensity of Rad52 foci with respect to total nuclear fluorescence of two consecutive time points of wild-type and elg1Δ strains. The comparison between the two strains was done for both Rad52 foci that co-localize with lacO-LacI foci and those that do not co-localize. The wild-type strain is MCW6556 (n=10+10) and the elg1Δ strain is MCW8486 (n=10+10), both the strains contain *RTS1-AO*. Error bars represent standard deviation.

4.2.6 Investigating whether persistence of PCNA at the barrier in *elg1*Δ is hindering efficient recruitment of Rad52

I showed in the previous chapter (Section 3.2.4) that PCNA persists on chromatin late into the cell cycle when Elg1 is absent. The effect on *RTS1*-induced recombination is most likely explained by the need for Elg1 to remove PCNA from the blocked RF. I wanted to determine whether the persistence of PCNA at *RTS1* is directly affecting the co-localizing of Rad52-YFP foci during time-lapse imaging of strains with *RTS1-AO*. Using strains in which both Rad52 and PCNA are tagged (i.e. Rad52-YFP and eCFP-Pcn1), I monitored the relative localization of the two proteins at the *RTS1-AO* barrier (again marked by an adjacent array of *lacO* sequences that was visualised by expression of LacI-tdKatushka2) in wild-type and *elg1*Δ strains by time-lapse microscopy (Figure 4.10 and 4.11b). In this way, I wanted to determine whether there was a mutual exclusivity between PCNA and Rad52 foci and whether this differed in the presence and absence of Elg1.

As reported in Chapter 3, eCFP-Pcn1 does not form discrete foci under my imaging conditions. Nevertheless, I was able to determine when eCFP fluorescence co-localized with the *lacO*-LacI focus that marks the position of the *RTS1-AO* barrier (Figure 4.11a and 4.12a). In the wild-type cells, eCFP-Pcn1 fluorescence started appearing at *RTS1* (i.e. co-localizing with *lacO*-LacI from the start of S phase (10 minutes after anaphase), reaching a maximum number of cells (~79%) with co-localizing fluorescence 10 minutes later. By 60 minutes post-anaphase the percentage of cells with PCNA drops to 15% and after 80 minutes no cells exhibited PCNA fluorescence at the barrier above pre-S phase levels (Figure 4.12a). A similar temporal pattern of PCNA appearance and co-localization with *RTS1-AO* is seen in *elg1*Δ cells,

however, unlike wild-type, ~11% of the cells still retain co-localizing PCNA foci even after 90 minutes post-anaphase (Figure 4.12a). There is a marked reduction in the percentage of cells with PCNA and Rad52 foci co-localizing at the barrier in an *elg1*Δ mutant compared to the wild-type cells (Figure 4.12b). Next it was also important to check if this reduction in the PCNA and Rad52 foci co-localizing at the barrier in an *elg1*Δ mutant, is not solely due to reduced Rad52 foci co-localizing at the barrier as shown in Figure 4.12c. Through this analysis, I found that among the Rad52 foci co-localizing at the barrier (Figure 4.12c), the percentage of foci that co-localise with PCNA was clearly reduced (Figure 4.12d). This implies that PCNA and Rad52 tend to be mutually exclusive. It is to be noted that Figure 4.12d shows an abrupt rise in the percentage of Rad52 foci co-localizing with PCNA at the barrier, in *elg1*Δ cells at 90 minutes. This might have occured due to chance co-localization of a Rad52 foci at the barrier with PCNA in a few cells (in two out of the four cells with Rad52 foci at the barrier, Figure 4.11b) due to longer persistance of PCNA in *elg1*Δ cells. Altogether, the data suggest that in the absence of Elg1, PCNA accumulated at the barrier either a) recruits factors that inhibit Rad52 or b) inhibits processing of the RF to recruit Rad52.

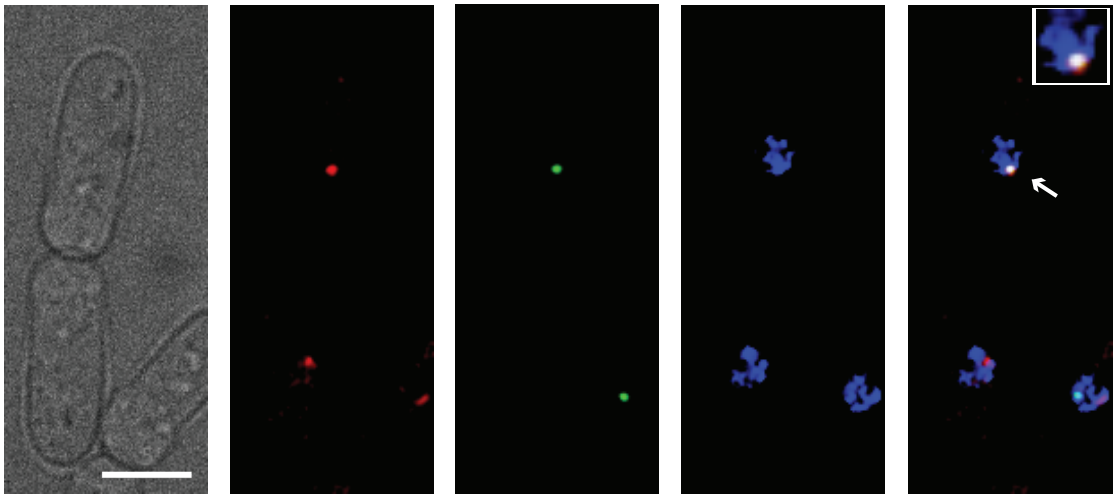

Figure 4.10 An example of images used for the analysis of Rad52-YFP and eCFP-PCNA foci co-localizing with *RTS1-AO.*
An example of a cell with eCFP-PCNA, Rad52-YFP and *lacO*-LacI-tdKatushka2 foci co-localizing. The scale bar represents 5 μm. The strain shown is MCW7065. These images are representative of those used for the analysis shown in Figure 4.11 and 4.12.

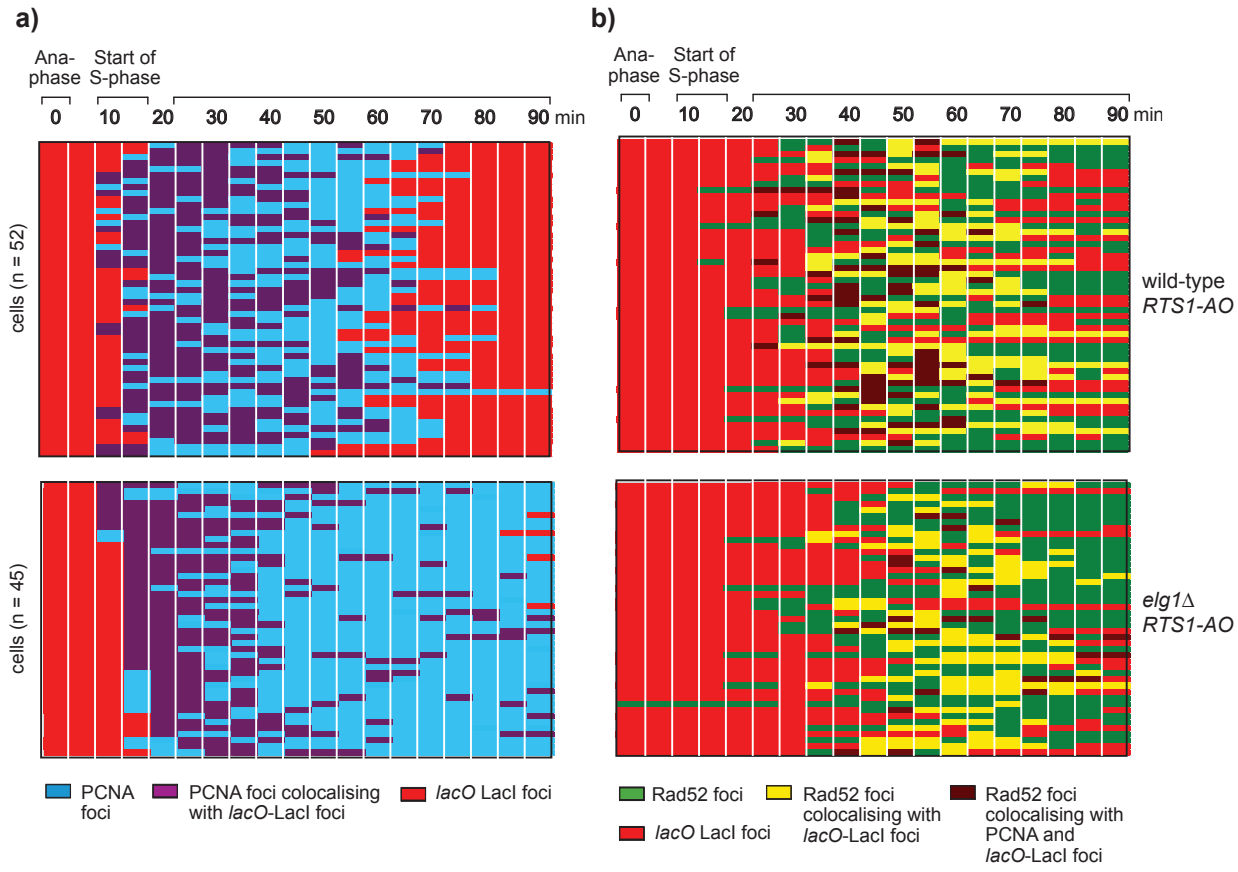

Figure 4.11 Persistence of PCNA at *RTS1* in *elg1*Δ mutant hinders recruitment of Rad52
a) Analysis of time-lapse movies of *RTS1-AO* wild-type and *elg1*Δ strain. The presence of a PCNA focus and whether it co-localizes with the *lacO*-LacI-tdKatushka2 focus is recorded every 5 minutes for 90 minutes post anaphase in each cell. Nuclear *lacO*-LacI foci are shown in red, PCNA foci in blue and PCNA foci co-localizing with *lacO*-LacI foci in purple. b) Analysis of time-lapse movies of *RTS1-AO* wild-type and *elg1*Δ strain. The presence of a Rad52 focus and whether it co-localizes with the *lacO*-LacI-tdKatushka2 and PCNA focus is recorded every 5 minutes for 90 minutes post anaphase in each cell. The nuclear *lacO*-LacI foci are shown in red, Rad52 foci in green, Rad 52 foci co-localizing with *lacO*-LacI foci foci in yellow and Rad 52 foci co-localizing with both PCNA and *lacO*-LacI foci foci are shown in brown. The *RTS1-AO* wild-type strain is MCW 7065 (n=52) and the *RST1-AO* *elg1*Δ strain is MCW7965 (n=45).

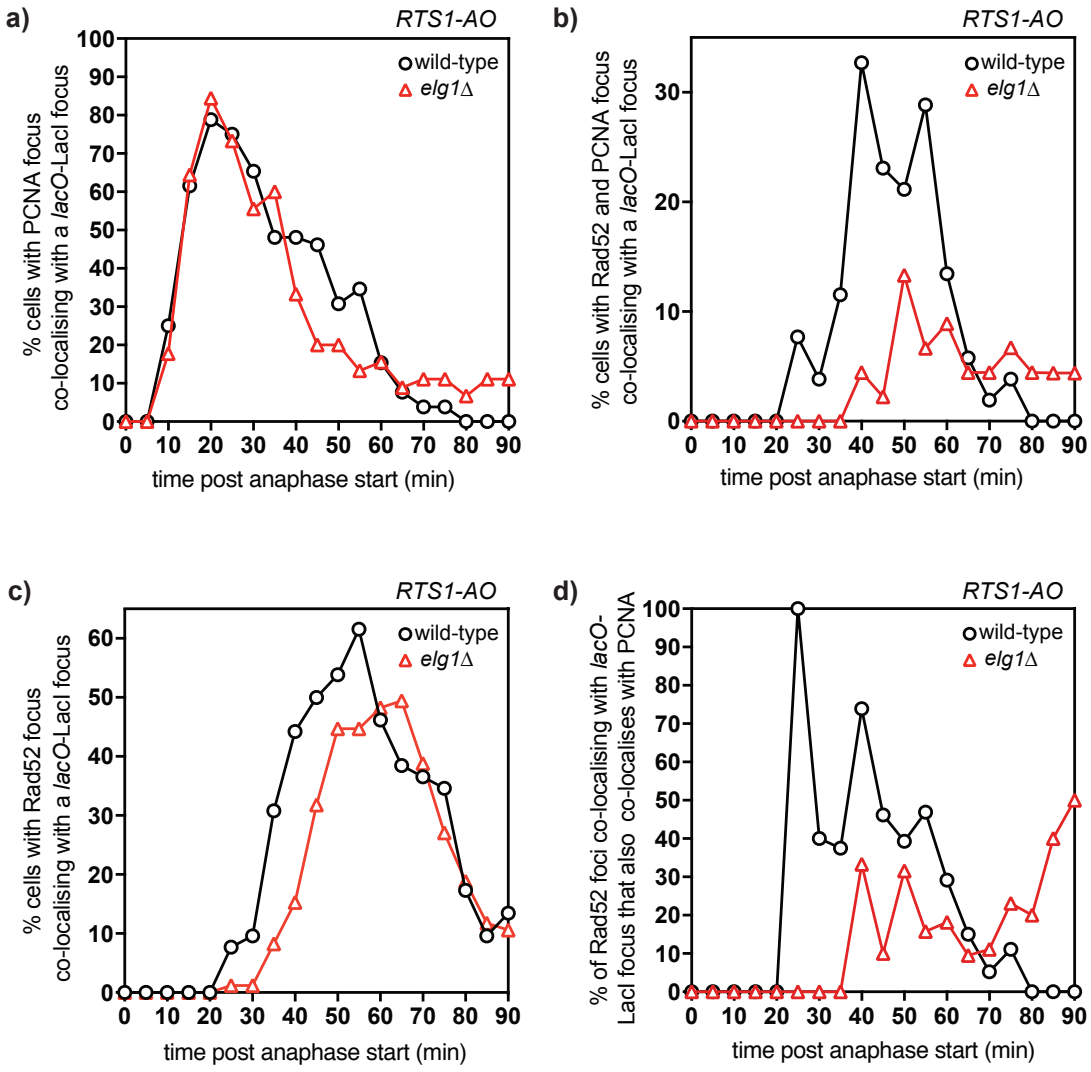

Figure 4.12 Persistence of PCNA at *RTS1* in *elg1*Δ mutant hinders recruitment of Rad52
Line graph of the percentage of cells with a) eCFP-PCNA focus co-localizing with the *lacO*-LacI focus, b) eCFP-PCNA and Rad52-YFP foci co-localizing with the *lacO*-LacI focus, c) Rad52-YFP foci co-localizing with the *lacO*-LacI focus, during the first 90 minutes following anaphase at five-minute intervals. d) Percentage Rad52-YFP foci co-localizing with the *lacO*-LacI focus that also co-localises with eCFP-PCNA during the first 90 minutes following anaphase at five-minute intervals. The wild-type strain is MCW7065 (n=52) and the *elg1*Δ strain is MCW7965 (n=45), both the strains contain *RTS1-AO*.

4.2.7 Loss of Elg1 affects Rad51-dependent as well as Rad51-independent recombination

As already discussed, one way in which Elg1 may promote *RTS1*-induced recombination is by limiting the recruitment of Fbh1 to the barrier by PCNA. Fbh1 controls recombination by acting as a Rad51 disruptase and is not thought to displace Rad52. Indeed, it has been shown that *fbh1* overexpression, whilst strongly reducing DNA damage-induced Rad51 foci, has no effect on Rad52 foci (Lorenz et al. 2009). However, my finding that Rad52 recruitment to the *RTS1* barrier is impaired in an *elg1*Δ mutant indicates that Elg1's pro-recombinogenic activity may not simply work through limiting Fbh1 recruitment. Indeed, impaired Rad52 recruitment would be expected to affect both Rad51-dependent and Rad51-independent recombination.

In addition to promoting the formation of Rad51 nucleofilaments (C. A. Morrow et al. 2017b; Anand et al. 2013), Rad52 can also promote recombination independently of Rad51 by catalysing SSA between homologous DNA strands coated in RPA (Shinohara et al. 1998; Sugiyama et al. 1998; Mortensen et al. 1996; Reddy et al. 1997). This activity of Rad52 promotes the repair of DSBs by SSA and may also promote a Rad51-independent mode of replication restart (Morrow et al. 2017; Anand et al. 2013). Recently, it was shown by our lab that Rad52 promotes Inter-Fork Strand Annealing (IFSA), a mechanism by which non-canonical fork convergence in fission yeast is prone to trigger deletions between repetitive DNA sequences (Morrow et al. 2017). It was found that increasing the distance between the *ade6*$^{-}$ direct repeats of standard recombination reporter by adding DNA spacers on the centromere-proximal side of *RTS1-AO* (Figure 4.13a), resulted in a dramatic increase in inter-repeat

recombination, rising by as much as ~5.4-fold with a 5 kb spacer. Almost 90% of these recombinants were Rad51-independent deletions, which depended on Rad52 (Morrow et al. 2017) (Figure 4.13b). To investigate whether Elg1 is needed for this "spacer-dependent" recombination, I crossed *elg1*Δ into the strains harbouring the recombination reporter with the 5kb spacer and determined its effect on the frequency of Ade$^+$ recombinants (Figure 4.13b). In a *rad51*$^+$ background, *elg1*Δ eradicates most of the "spacer-dependent" recombination, with ~9-fold reduction in deletions and ~26-fold reduction in conversions, however the frequency of deletions is still ~3-fold greater than in the equivalent strain without the 5 kb spacer (compare data in Figure 4.13b and Figure 3.1b). Intriguingly, in a *rad51*Δ background, loss of *elg1* causes a ~2-fold reduction in deletions ($p<0.0001$) compared to a *rad51*Δ single mutant (Figure 4.13b). These data show that Elg1 promotes both Rad51-dependent and Rad51-independent recombination, albeit it appears to be more strongly required for promoting Rad51-dependent recombination. These data also suggest that Rad51 drives most of the spacer-dependent recombination in wild-type cells, and its presence in an *elg1*Δ mutant blocks the formation of deletions by Rad52.

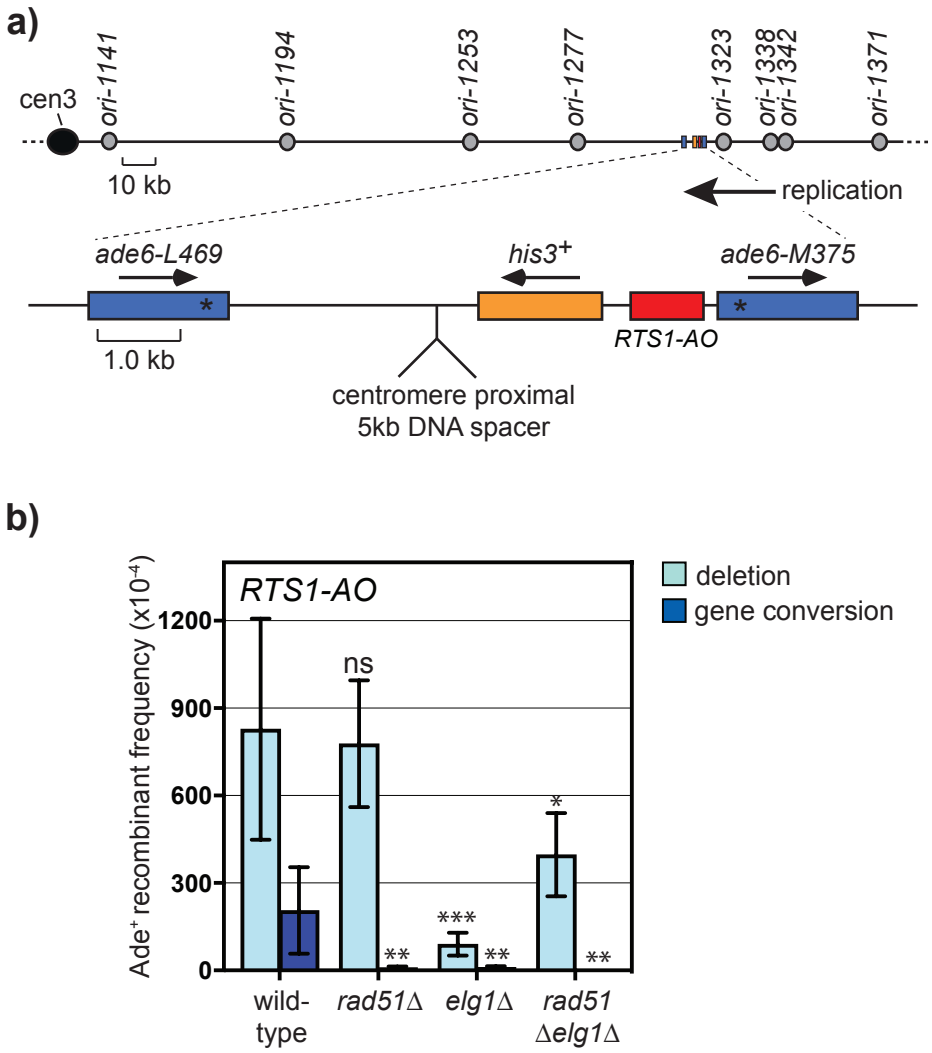

Figure 4.13 Loss of Elg1 also affects Rad51-independent recombination
a) Schematic showing the location of *RTS1* and *ade6*- recombination reporter with site of spacer insertion, in relation to nearby replication origins (grey circles) at the endogenous *ade6* locus on chromosome 3. Replication across the *ade6* locus occurs in the telomere to centromere direction as indicated by the arrow. b) Bar charts showing the frequency and type of Ade+ recombinants in MCW8023, MCW8136, MCW8941, MCW8943. Error bars represent standard deviation. Significant fold changes compared to the wild-type strain are indicated. P-values were calculated using the Shapiro-Wilk normality test (ns p>0.05, *p<0.05, **p<0.01, ***p<0.001, ****p<0.0001). Ade+ recombinant frequency with statistical analysis is also shown in Table 1.

4.3 Discussion

In this chapter, I wanted to establish if the reduction in *RTS1*-induced ectopic recombination in an *elg1*Δ mutant reflects a reduction in the recruitment of recombination proteins to the RFB and a deficiency in the restart of replication. 2D gel analysis did not show any reduction in replication restart at *RTS1* in an *elg1*Δ mutant, whereas analysis of template switching as assayed by direct repeat recombination reporter downstream of the RFB suggested that it might be impaired. However, neither of these experimental approaches provides a definitive measure of replication restart efficiency. The 2D gel analysis only measures forks that have progressed up to 2 kb downstream of the RFB and would give a skewed indication of restart efficiency if the restarted forks moved with a different velocity in the mutant and wild-type cells. The genetic reporter downstream of *RTS1* provides at best only an indirect measure of restart efficiency, with a reduction in template switching potentially resulting from a defect in the template switch process and/or in the progression of the restarted fork rather than from a defect in restart itself.

Recognising the deficiencies in the approaches that I had used, I set about trying to establish a more direct method of assessing restart efficiency. The first method I investigated was Polymerase Usage Sequencing (Pu-Seq) (Miyabe et al. 2015). In this method one can determine the relative usage of each template DNA strand by the two replicative polymerases (Pol ε and Pol δ) genome-wide via a next generation sequencing approach (Keszthelyi et al. 2015). In this way replication origins and termination zones can be mapped and origin-firing efficiencies estimated (Keszthelyi et al. 2015). Importantly for my intended use of this technique, restarted replication, unlike canonical replication, is driven solely by Pol δ synthesizing both the

leading and lagging strands (Miyabe et al. 2015). This means that in principle one can assess restart efficiency at *RTS1* by determining how much of the DNA replicated downstream of it comes solely from Pol δ. The Pu-Seq technique utilizes strains with mutations in either Pol ε (*cdc20-M630F*) or Pol δ (*cdc6-L591G*) that mis-incorporate ribonucleotides at elevated frequencies (Keszthelyi et al. 2015). These strains also contain a deletion of the *rnh201* gene that encodes the catalytic subunit of RNase H2, which usually removes mis-incorporated ribonucleotides (Keszthelyi et al. 2015). In these strains, ribonucleotides accumulate in the DNA strands that are used most commonly by the mutant polymerase and this can be quantified by either next generation sequencing or by assessing the amount of fragmentation of each DNA strand on an alkaline agarose gel (Miyabe et al. 2015). I successfully introduced *RTS1-IO/AO* into the Pu-seq strain backgrounds and had begun to optimise the analysis by alkaline agarose gel electrophoresis and southern blotting (using strand-specific DNA probes). However, I decided to abandon this approach when I was unable to introduce *elg1*Δ into the *cdc6-L591G* (Pol δ) Pu-seq strain background. Interestingly, it has been reported that *elg1*Δ has a strong negative genetic interaction with *cdc2-2* (a mutation in catalytic subunit of Pol δ affecting Pol δ function) in budding yeast (Dubarry et al. 2015). Since Pol δ is associated with the synthesis of the lagging strand, this loss of fitness could be associated with the importance of Elg1 in removing PCNA during the synthesis of each Okazaki fragment.

The second method I started to investigate for analysing restart efficiency was DNA fibre analysis (Kaykov and Nurse 2015; Patel et al. 2006). To this end, I made wild-type and *elg1*Δ strains containing *RTS1-IO/AO* that express *hENT1* (human equilibrated nucleoside transporter 1) along with herpes simplex virus thymidine

kinase that can incorporate exogenous thymidine analogs (Sivakumar et al. 2004). However, I was unable to progress this work beyond the strain constructions as I ran out of time.

By snap shot and time-lapse microscopy, I was able to determine that Elg1 is required for the efficient recruitment of both Rad51 and Rad52 to the *RTS1* barrier (Figure 4.3c, 4.5). This correlates with the reduction in both Rad51-dependent and Rad51-independent direct repeat recombination in an *elg1*Δ mutant (Figure 4.13b) and implies that replication restart is likely to be delayed and/or impaired. The finding that *elg1*Δ affects the recruitment of Rad52 opens up the possibility that Elg1 counters Fbh1 not by limiting its recruitment to the RFB (as discussed in Chapter 3), but by ensuring that its key antagonist (Rad52) is efficiently recruited. To distinguish between these two possibilities, it will be important to establish whether Fbh1 recruitment/retention at *RTS1* is affected in an *elg1*Δ mutant.

Exactly how Elg1 promotes Rad52 recruitment to the RFB is unclear. Based on my time-lapse microscopy experiments, it appears that the persistence of PCNA at *RTS1* is related to inhibition of recruitment of Rad52 (Figure 4.11). In most of the *elg1*Δ mutant cells, co-localization of Rad52 at the barrier is greatly reduced when PCNA is also present at the barrier. Potentially, the retention of PCNA at *RTS1* physically impedes the recruitment of Rad52 or prevents the processing of the fork into a substrate that Rad52 can bind to. In future experiments it will be important to try and distinguish between these possibilities by assessing the recruitment of proteins that precede Rad52 at the RFB (e.g., RPA) and by analysing how efficiently DNA is resected by measuring the amount of ssDNA (Teixeira-Silva et al. 2017; Ait Saada et al. 2017). However, it is also possible that PCNA indirectly inhibits Rad52 recruitment

by recruiting a protein(s) that antagonises Rad52. This is unlikely to be Fbh1 since, as discussed above, overexpression of *fbh1* does not inhibit the formation of DNA damage-induced Rad52 foci (Lorenz et al. 2009). However, it would be prudent to test whether Rad52 recruitment at *RTS1* is similarly unaffected by *fbh1* overexpression. Other factors that might inhibit Rad52 include Fml1 and Srs2, which both seemed to have a role in supressing deletions to some extent in the absence of Elg1 (see sections 3.2.6.1 and 3.2.6.2). The *RTS1-AO* induced deletions that are reduced 3.7-fold in the *elg1*Δ mutant is increased 1.9-fold in *elg1*Δ *fml1*Δ double mutant and 4.4-fold in *elg1*Δ *srs2*Δ double mutant. Fml1 is known to limit spacer dependent deletions mediated by IFSA although it has little effect on the frequency of deletions when there is no DNA spacer between the *ade6*$^{-}$ repeats (C. A. Morrow et al. 2017b). Srs2 was recently shown to be capable of displacing Rad52 from RPA-coated ssDNA in single molecule experiments (De Tullio et al. 2017). Also, it was recently reported that Srs2 directly interacts with Rad52 in budding yeast and that Rad52 inhibits the disruption of Rad51 by Srs2 during DSB break repair, by competitively binding to Srs2 (Cam et al. 2018). It would be important to ascertain if Elg1, either independently or through its effect on PCNA accumulation, influences the recruitment of these factors to the *RTS1* barrier.

5 Studying the role of Ctf18, as an alternative PCNA unloader/loader, in RDR at *RTS1*

5.1 Introduction

When PCNA was initially identified as an important factor for DNA replication in *in vitro* reconstitution experiments, it was only thought to have a role in conferring high processivity to DNA polymerases (Melendy and Stillman 1991). We now know that it is a homotrimeric ring that encircles DNA to act as a polymerase clamp as well as a sliding platform for the recruitment of multiple factors required for DNA replication, DNA repair, cell cycle regulation and chromatin assembly (Cox 1997; Zhang et al. 1999; Warbrick et al. 1997; Eisenberg et al. 1997; Fotedar et al. 1996; Levin et al. 1997; Moldovan et al. 2007; Gazy and Kupiec 2012; Moldovan et al. 2006; Maga 2003). PCNA not only recruits these factors, but it also actively controls their function as chromatin assembles. Therefore, control of PCNA-loading onto chromatin is fundamental for various replication-coupled reactions.

Three different conserved protein complexes are in charge of loading/unloading PCNA (Kupiec 2016) (Figure 5.1). PCNA is loaded onto DNA at template-primer junctions by RFC, a heteropentameric AAA+ protein complex consisting of the Rfc1-5 subunits, in an ATP-dependent process (Kelch 2011; Bowman, O'Donnell, and Kuriyan 2004; Gomes and Burgers 2001; Hedglin, Kumar, and Benkovic 2013; Yao and Donnell 2012). Elg1-RLC, which forms a hetero-pentameric complex by sharing four small Rfc subunits (Rfc 2-5), is the major unloader of PCNA as shown by many *in vivo* studies (Kanellis 2003; Kubota et al. 2013; Parnas et al. 2010). However, some *in vitro* studies have shown that human RFC can unload PCNA from singly nicked circular plasmid and fully replicated SV40 plasmid DNA, suggesting PCNA unloading roles of RFC (Yao et al. 1996; Cai et al. 1996; Shibahara and Stillman 1999). However, they do not demonstrate that RFC acts as the major PCNA unloader under normal *in*

vivo conditions, and the results of the former experiments were not reproducible (Bylund and Burgers 2005). It is difficult to assess the role of RFC in unloading of PCNA *in vivo*, as it is needed for loading PCNA.

Eukaryotic cells also have another alternative RFC complex known as Ctf18-RLC, which forms a hetero-heptameric complex by sharing four small Rfc subunits (Rfc 2-5) and two additional subunits Ctf8 and Dcc1 (Kanellis 2003; Bellaoui et al. 2003; Ben-Aroya et al. 2003; Hanna et al. 2001; Naiki et al. 2001) (Figure 5.1). Ctf18-RLC catalyses the ATP-dependent loading of PCNA according to many biochemical studies (Bermudez et al. 2003; Fujisawa et al. 2017; Shiomi et al. 2004). It was shown to load PCNA only onto primed and gapped DNA but not onto double-stranded nicked or single-stranded circular DNAs (Shiomi et al. 2004) (Figure 5.1). Also, in fission yeast, inactivation of Ctf18-RFC by the deletion of *ctf18*, *dcc1* or *ctf8* is lethal in a temperature-sensitive mutant of *rfc (rfc1-44)* showing that Ctf18-RFC is essential in the absence of fully functional RFC. In contrast, *rfc1-44 elg1*Δ cells are viable and overproduction of Elg1 in *rfc1-44* is lethal, suggesting that Elg1-RFC has an opposing function to RFC (Kim et al. 2005). However, in an *in vitro* study, budding yeast Ctf18-RLC was found to be an efficient unloader of PCNA from DNA in a reaction requiring ATP hydrolysis, in the same reaction where RFC and Elg1-RLC were not (Bylund and Burgers 2005). However, *in vivo* studies do not support the idea of Ctf18-RLC being a major unloader of PCNA, since yeast cells lacking *ctf18* or human cells transfected with siRNAs targeting *CTF18* show approximately normal levels of PCNA on chromatin in an unperturbed S phase (Kubota et al. 2011; Lee et al. 2013). Thus, due to its association with both loading and unloading of PCNA being shown by various

studies, after having investigated Elg1, I wanted to explore the role of Ctf18, as an alternative PCNA unloader/loader in replication fork collapse and RDR at *RTS1*.

Ctf18-RLC has distinct functions in checkpoint signalling and the establishment of sister chromatid cohesion and faithful chromosome transmission, as shown from the studies in budding yeast (Naiki et al. 2001; Mayer et al. 2001; Kubota et al. 2011; Wade et al. 2017). Ctf18 mutants were identified in screens for genes important for preventing chromosome loss (chromosome transmission fidelity); loss of any of the 3 genes (*ctf18*, *dcc1* or *ctf8)* leads to precocious sister chromatid separation accompanied by a pre-anaphase accumulation of cells dependent on the spindle assembly checkpoint (Hanna et al. 2001; Mayer et al. 2001). Studies in yeast and humans show that Ctf18 has a role in establishment of cohesion as it is needed for acetylation of the Smc3 (Psm3 in fission yeast) subunit of cohesion by Eco1 (Eso1 in fission yeast; Esco1-2 in humans), which is recruited by PCNA (Lengronne et al. 2006; Borges et al. 2013; Terret et al. 2009). These acetyltransferases are shown to promote cohesin stabilization in mammals and fission yeast by preventing Wapl/Wpl (destabilization factor) from acting on it (Gandhi et al. 2006; Feytout et al. 2011).

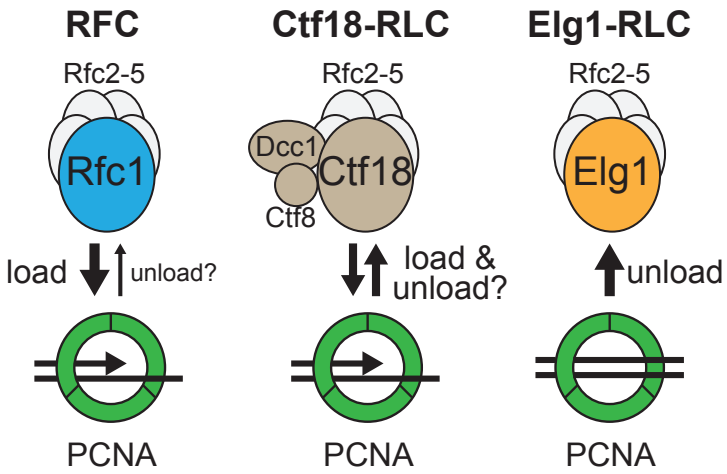

Figure 5.1 PCNA loaders and unloaders
Schematic representation of the protein complexes in charge of loading/unloading PCNA**.** All complexes share the Rfc2-5 subunits (in grey) (See section 5.1 for details).

5.2 Results

5.2.1 Ctf18 constrains Elg1 dependent recombination

To investigate whether Ctf18 is needed for the recombination that is induced by RF blockage at *RTS1,* I made use of the *RTS1*-based direct repeat recombination reporter, discussed in earlier chapters, which consists of two *ade6*$^{-}$ heteroalleles with an intervening *his3*$^{+}$ gene inserted at the *ade6* locus on chromosome 3 (Figure 5.2a). I crossed a *ctf18*Δ mutant into both *RTS1-IO* and *-AO* strains of wild-type and *elg1*Δ background and measured the effect on recombinant frequency (Figure 5.2b). In the *RTS1-IO* background, there was a minor but significant increase (~1.5-fold; $p<0.001$) in deletions, with no significant change in gene conversions in the *ctf18*Δ mutant, compared to the wild-type. In the *elg1*Δ *ctf18*Δ double mutant, there was a decrease in gene conversions (~1.8-fold, $p<0.0001$) with no change in deletions, compared to the wild type. In the *RTS1-AO* background*,* surprisingly, loss of Ctf18 results in a ~2-fold increase in direct repeat recombination ($p<0.0001$). Importantly, an *elg1*Δ *ctf18*Δ double mutant exhibits the same hypo-recombination as an *elg1*Δ single mutant showing that the hyper-recombination in a *ctf18*Δ single mutant is entirely dependent on Elg1 (Figure 5.2b). These data suggest that the level of direct repeat recombination is affected by the balance between Ctf18-dependent loading of PCNA, which counters the unloading mediated by Elg1. The former acts to suppress inter-repeat recombination whereas the latter promotes it.

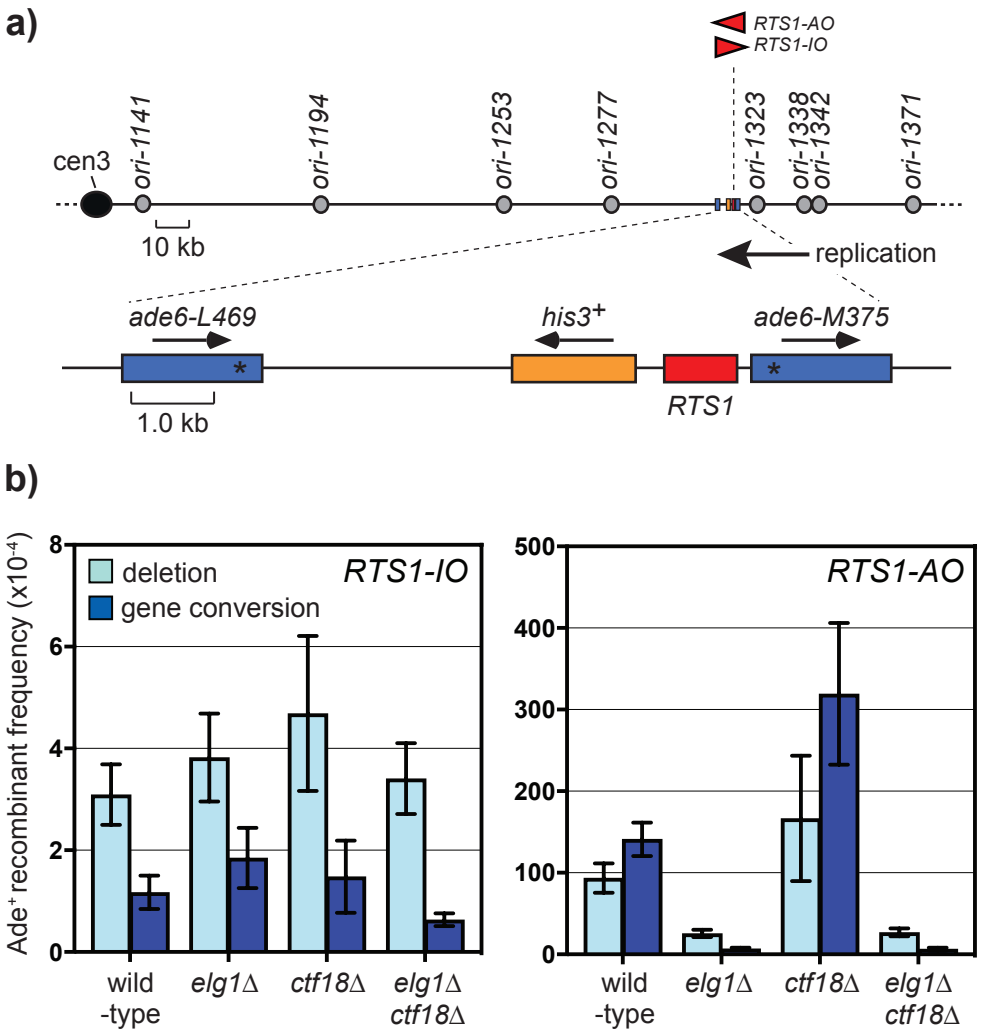

Figure 5.2 Ctf18 constrains Elg1 dependent recombination
a) Schematic showing the location of the *ade6*- intra-chromosomal recombination reporter and *RTS1* in relation to nearby replication origins (grey circles) at the endogenous *ade6* locus on chromosome 3. (b) Bar charts showing the effect of *elg1*Δ, *ctf18*Δ and *elg1*Δ *ctf18*Δ on the frequency and type of Ade+ recombinants in *RTS1-IO* and *RTS1-AO* strains. In order of presentation the strains are MCW4712, MCW7706, MCW8404, MCW8408, MCW4713, MCW7708, MCW8406, MCW8410. Error bars represent standard deviation. Ade+ recombinant frequency with statistical analysis is also shown in Table 1.

5.2.2 2D gel analysis reveals no major difference in the profile of replication intermediates at and around *RTS1* in a *ctf18*Δ mutant

I performed native two-dimensional (2D) gel electrophoresis for the analysis of replication intermediates at and surrounding *RTS1-AO* in the *EcoNI* restriction fragment that encompasses the *RTS1* site, in wild-type and *ctf18*Δ mutant strains (Figure 5.3a). It was important to ascertain whether the *RTS1* barrier strength remained the same, and to assess whether the hyperrecombination in *ctf18*Δ mutant correlates with increased replication restart and decrease in replication termination at the barrier. 2D gel analysis reveals no major difference in the profile of replication intermediates at and around *RTS1* between wild-type and *ctf18*Δ strains (Figure 5.3b). Similar levels of replication fork blockage signal confirm that *RTS1-AO* barrier strength is not changed in the *ctf18*Δ mutant, implying that the increase in recombination seen in this mutant is not due to an increase in barrier strength. The accumulation of double Y-shaped DNA molecules resulting from merging of the opposing forks with the forks held at the barrier, and large Y-shaped molecules that represent forks that have restarted and progressed beyond the barrier, are both similar in the two strains (Figure 5.3b and c). The 2D gel analysis thus does not reveal any significant difference in fork restart and replication past the barrier in a *ctf18*Δ mutant.

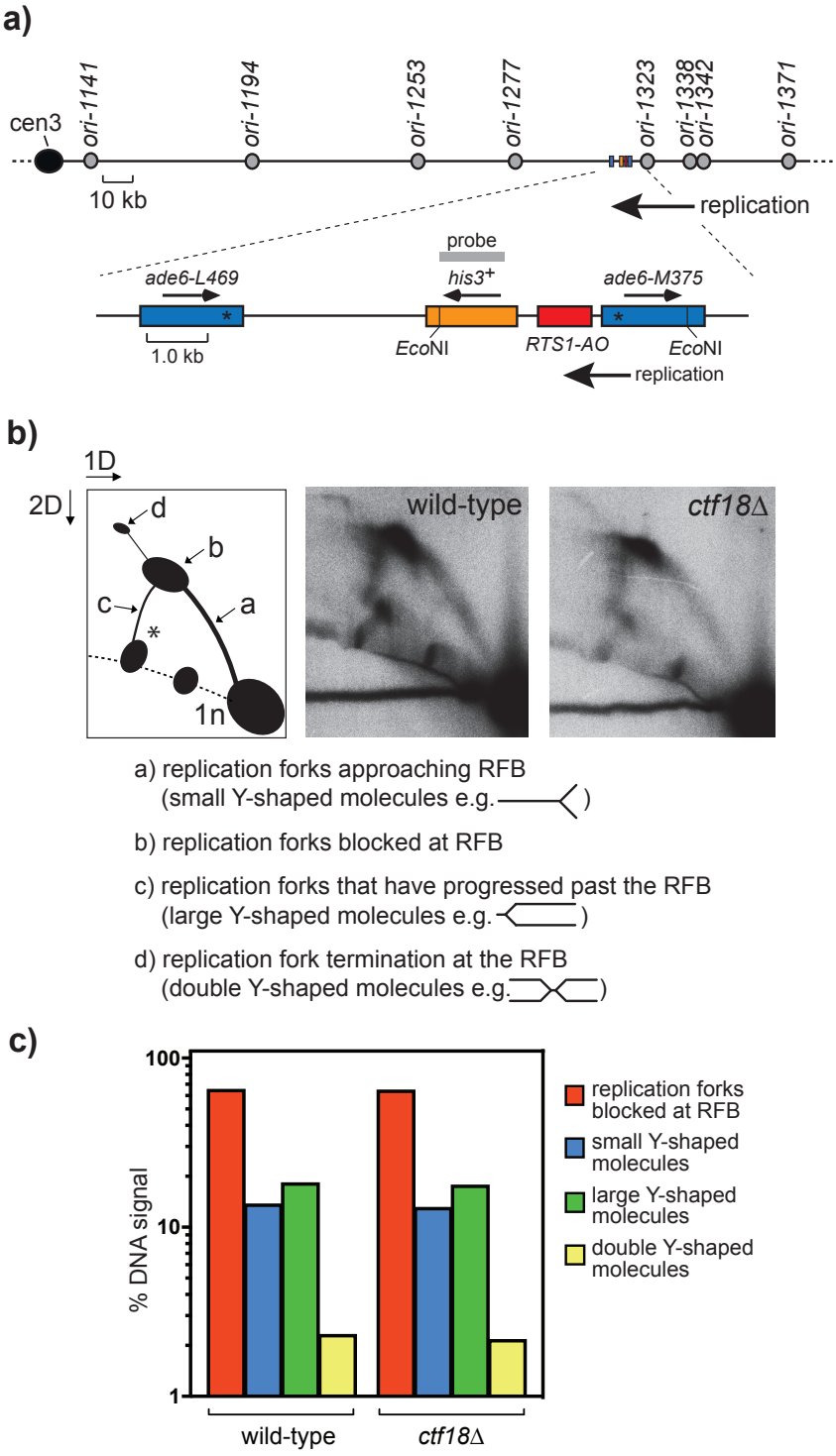

Figure 5.3 2D gel analysis of replication intermediates at and around *RTS1* shows no major difference between wild-type and *ctf18*Δ

a) Schematic showing the relative position of *RTS1* on chromosome 3, and the restriction fragment and probe used for 2D gel analysis. b) 2D gel analysis of replication intermediates within the *Eco*NI fragment. The panel on the left is a guide for interpreting the 2D gels ('∗' indicates a signal seen as an artefact in this experiment). c) Quantification of the 2D gels displayed as bar charts. The DNA was extracted from asynchronously growing cultures of the strains MCW 4713 (wild-type) and MCW8410 (*ctf18*Δ). This data is based on single experiment.

5.2.3 Recruitment of Rad52 at the RTS1 barrier is not reduced in a *ctf18*Δ mutant

I used the live cell imaging experimental system described in Chapter 4 to directly assess the effect of *ctf18*Δ on recombination protein recruitment at *RTS1* (Figure 5.4a). I analysed the presence of Rad52 foci and their co-localization with *lacO*-LacI foci in asynchronous cultures of wild-type and *ctf18*Δ strains containing either *RTS1-IO* or *RTS1-AO*, by snapshot imaging. For each strain, cells with a detectable *lacO*-LacI focus were analysed for the presence and localisation of Rad52 foci from three independent cultures. I considered only cells with *lacO*-LacI foci for this analysis.

Compared to the wild-type, there is no significant difference in spontaneous Rad52 foci in the absence of Ctf18 (*RTS1-IO* Figure 5.4b). As seen in Chapter 4, *RTS1-AO* causes an overall increase in the percentage of cells with Rad52 foci in wild-type cells, with most or all of the additional foci co-localizing with the RFB (Figure 5.4b). There was no significant difference in the percentage of cells with Rad52-YFP foci or Rad52 foci co-localizing with the barrier in the *ctf18*Δ mutant containing *RTS1-AO* compared to wild-type (Figure 5.4b). Thus, *ctf18*Δ does not seem to affect the efficient recruitment of Rad52 at *RTS1*. However, a different picture emerged when the cells were staged, based on their length and number of *lacO*-LacI foci, into two groups: 1) M phase to early G2 phase cells; 2) late G2 phase cells (Figure 5.4c). This analysis revealed that there was no significant change in the number of M phase to early G2 phase cells with Rad52 foci co-localizing at the RFB in the *ctf18*Δ mutant compared to wild-type, whereas there were significantly more of late G2 phase cells with co-localizing foci in the mutant ($p<0.03$) (Figure 5.4c). This observation is reminiscent of a previous report from budding yeast, where spontaneous and DNA

trinucleotide repeat induced Rad52 foci were seen to persist late into G_2/M in *ctf18*Δ cells (Gellon et al. 2011).

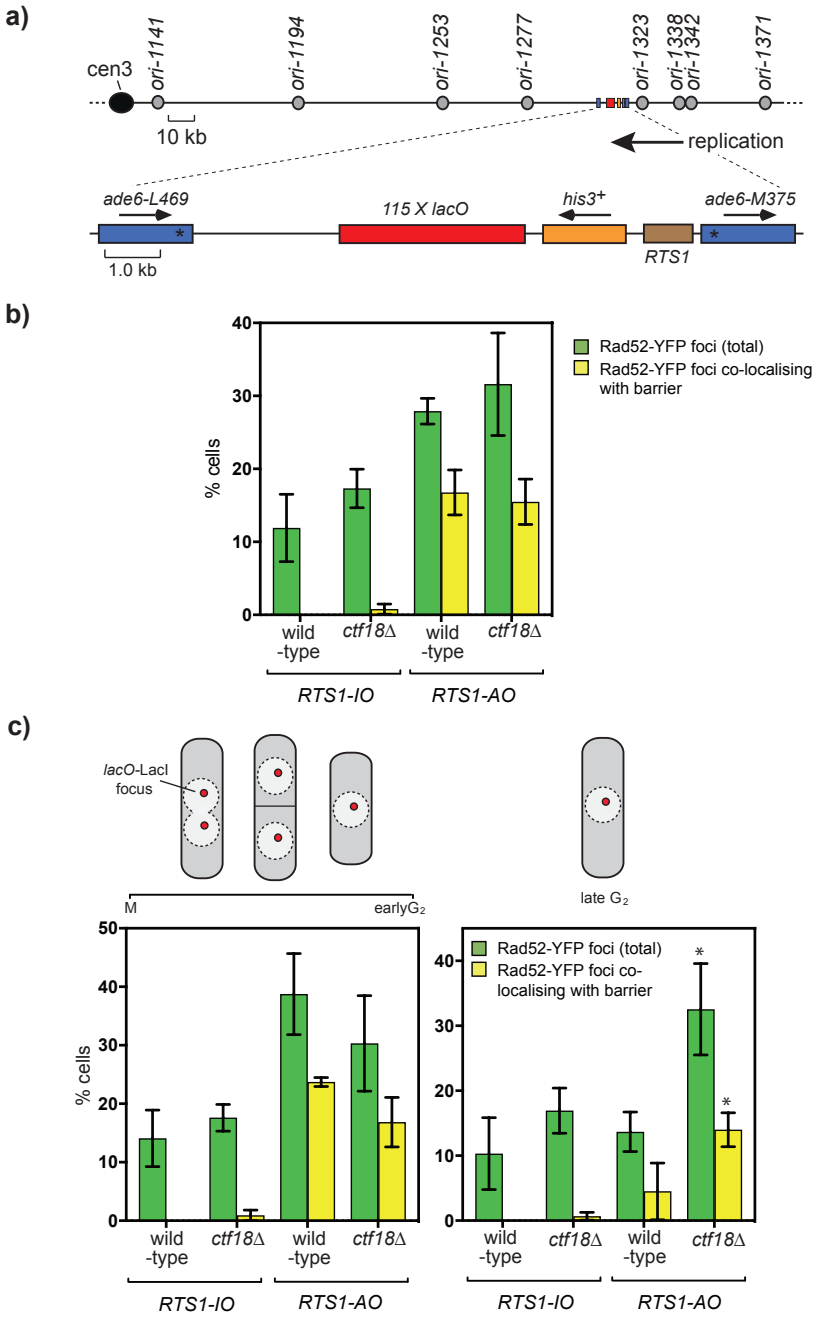

Figure 5.4 Effect of *ctf18*Δ on the frequency of Rad52 foci and their co-localization at the *RTS1* barrier
a) Schematic showing the modification of the direct repeat recombination reporter for live-cell imaging. b) Bar chart showing the percentage of cells with total Rad52-YFP foci and Rad52-YFP foci co-localizing with *lacO*-LacI-tdKatushka2 focus for wild-type and *ctf18*Δ strains with *RTS1-IO* and *RTS1-AO*. c) Data from 'b' re-analysed by dividing the cells into two groups (M-earlyG_2 and late G_2) on the basis of cell length and morphology. The strains are MCW6712 (n=523), MCW8537 (n=899), MCW7065 (n=671), MCW8539 (n=631). Error bars represent standard deviation. Significant changes compared to the wild-type strain are indicated. P-values were calculated using the Mann-Whitney test (ns $p>0.05$, *$p<0.05$).

5.2.4 Changed dynamics of Rad52 recruitment at *RTS1* in *ctf18*Δ cells

I decided to complement the snapshot analysis with time-lapse microscopy to monitor recombination protein recruitment to the RFB in individual cells and in real time. Cells were monitored from the start of S phase up to 90 minutes, following and recording the number of timepoints that Rad52-YFP foci appeared in individual cells at five-minute intervals (Figure 5.5).

Time-lapse imaging of wild-type cells reveals a consistent pattern of PCNA focus appearance 10-15 minutes post anaphase marking the start of S phase. Rad52 foci that co-localise with *RTS1-AO* start to appear about 10 minutes later (Nguyen et al. 2015) (Figure 5.6). The percentage of cells with co-localising Rad52 focus rises sharply and at a given time 60% of cells have a co-localizing focus. In the *ctf18*Δ mutant, despite all cells exhibiting a Rad52 focus at one or more time points during the time-course like in the wild-type strain, the overall percentage of cells with a co-localizing focus is less by ~1.2-fold (Figure 5.5 and 5.6b). This means that *ctf18*Δ cells exhibit more and/or longer lived spontaneous Rad52 foci (i.e. non-colocalizing foci) than wild-type cells (Figure 5.6c). The Rad52 foci that co-localise with *RTS1-AO* appear 10 minutes later in the *ctf18*Δ mutant than in the wild-type, but unlike in the wild-type (or *elg1*Δ mutant), the percentage of cells with a co-localizing focus peaks at around 30% and then remains fairly constant for ~35 minutes (Figure 5.6a). More *ctf18*Δ cells have a co-localizing Rad52 focus at later stages of the cell cycle, which accords with the findings from the snapshot experiment. The greater number of cells with co-localizing foci at later time points could be due to new cells displaying late arising foci or existing foci persisting longer. Although Rad52 foci in general appear around the same time in the *ctf18*Δ mutant and wild-type cells (Figure 5.7a), there is

greater number of new cells displaying late arising foci at the barrier in *ctf18*Δ mutant (Figure 5.7b). This suggests that there may be more new cells displaying late arising foci in *ctf18*Δ mutant. However, the population of cells showing first Rad52 foci at the barrier do not show a significant shift in *ctf18*Δ mutant from the wild-type as per the Mann-Whitney test.

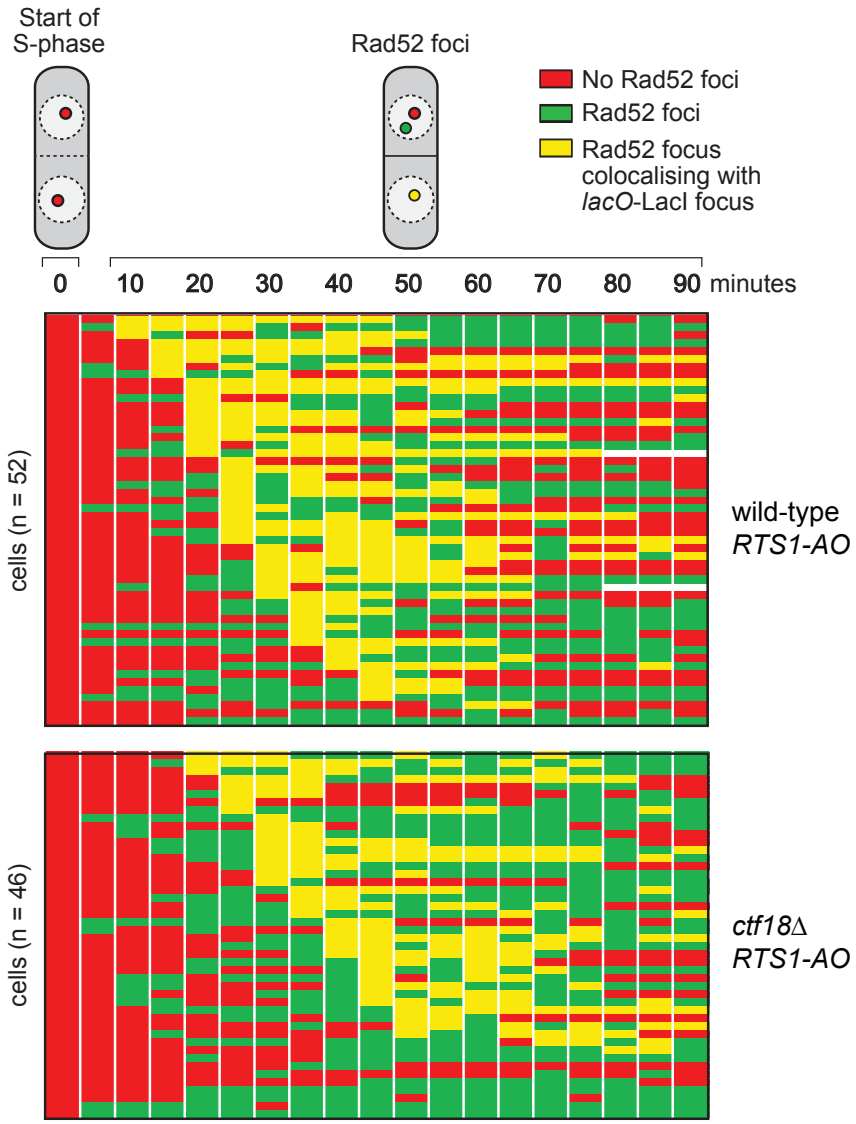

Figure 5.5 Tracking Rad52-YFP focus co-localization at *RTS1* by time-lapse microscopy in wild-type and *ctf18*Δ cells

Analysis of time-lapse movies. The presence of a Rad52 focus and whether it co-localizes with the *lacO*-LacI-tdKatushka2 focus is recorded every 5 minutes for 90 minutes post S-phase start in each cell. The *RTS1-AO* wild-type strain is MCW7065 (n=52), the *RST1-AO ctf18*Δ strain is MCW8539 (n=46). The top panel is a schematic of a *S. pombe* cell at various stages post S-phase with nuclear *lacO*-LacI foci in red, Rad52 foci in green and co-localizing foci in yellow.

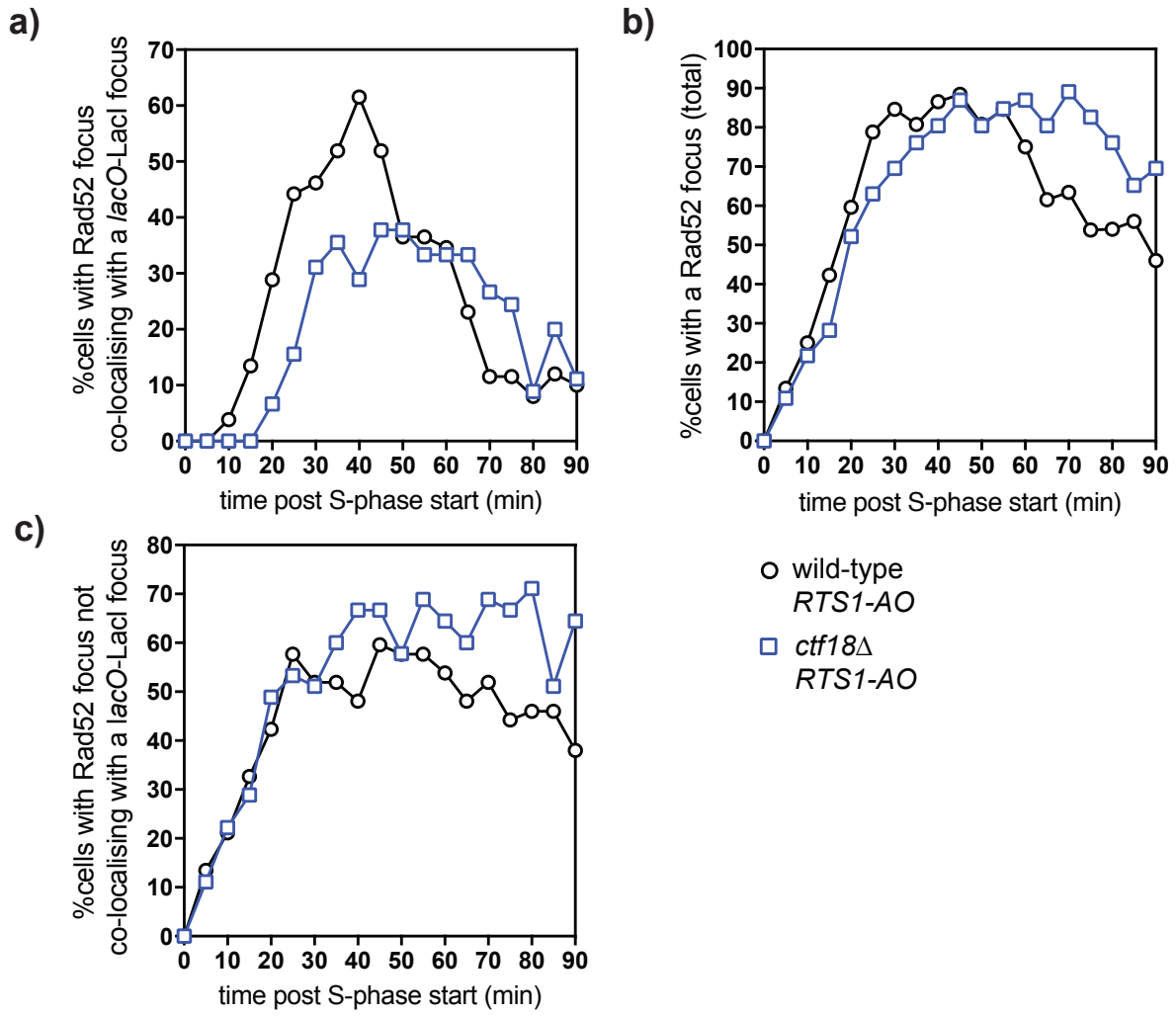

Figure 5.6 Loss of Ctf18 causes a change in the dynamics of recruitment of Rad52 at the *RTS1* barrier
Line graphs of the percentage of cells with a) Rad52-YFP focus that co-localizes with the *lacO*-LacI focus, b) any Rad52-YFP focus and c) Rad52-YFP focus not co-localizing with the *lacO*-LacI focus, during the first 90 minutes post S-phase start. The *RTS1-AO* wild-type strain is MCW7065 (n=52), the *RST1-AO ctf18*Δ strain is MCW8539 (n=46).

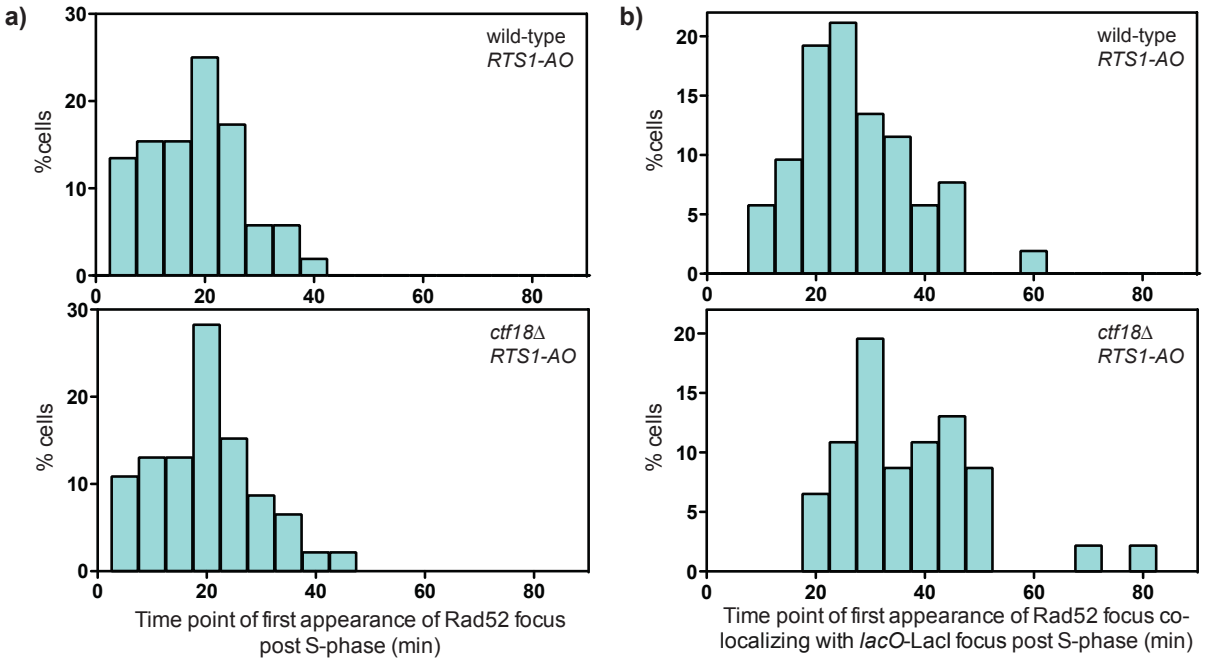

Figure 5.7 Analysis of time of appearance of Rad52-YFP foci in *ctf18*Δ versus wild-type strains
a) Histogram showing the percentage of cells with a given time point of first appearance of Rad52 focus, during the first 90 minutes post S-phase start. b) Histogram showing the percentage of cells with a given time point of first appearance of Rad52 focus co-localising with *lacO*-LacI, during the first 90 minutes post S-phase start. The *RTS1-AO* wild-type strain is MCW7065 (n=52), the *RST1-AO ctf18*Δ strain is MCW8539 (n=46).

5.2.5 Analysing PCNA foci in cells lacking Ctf18

There have been no reports of PCNA accumulation on the DNA in *ctf18*Δ cells *in vivo*, except in HU-treated budding yeast cells where PCNA accumulated with other components of the replisome progression complex, due to a probable defect in activating Rad53 checkpoint kinase (Kubota et al. 2011). I wanted to investigate whether there is any effect of the loss of *ctf18* on the persistence of PCNA on DNA in undisrupted cells. I used time lapse microscopy to analyse PCNA throughout the cell cycle visualizing it with an ECFP tag in asynchronously growing cultures of wild-type and *ctf18*Δ mutant strains (Figure 5.8a).

PCNA foci tend to appear slightly later (~ 5 minutes) after anaphase in a *ctf18*Δ mutant than in wild-type but persist longer (Figure 5.8b). I also followed the spatio-temporal patterns of PCNA foci (Figure 5.8a). As reported in Chapter 3, in wild-type cells, PCNA foci form successive distinguishable patterns during S phase that can be classified into various stages. In stage a, bright patches appear in the extranucleolar region without filling it entirely. In stage b, the bright patches extend and fill the entire extranucleolar space. Stage c shows bright spots at the edge of the nucleolus and smaller spots in the rest of the nucleus. Finally, in stage d, only a few bright spots located at the edges of the nucleolus are observed, that gradually diminish. I observed similar patterns of PCNA foci in *ctf18*Δ cells and, unlike in an *elg1*Δ mutant, did not see any cells displaying unusually bright blobs in late S-phase. However, each of the stages of PCNA foci (i.e. a - d) persisted longer in a *ctf18*Δ mutant than in wild-type cells (Figure 5.8a). The longer persistence of PCNA foci, as with Rad52 foci, may be related to a generally longer S phase in a *ctf18*Δ mutant. There have been no previous reports of S phase delay with *ctf18*Δ in yeast. However, as mentioned above, single molecule experiments in human cells have shown that replication dynamics in human cells are highly attuned to the acetylation of Smc3, and Ctf18 appears to control fork velocity through its ability to promote Smc3 acetylation (Terret et al. 2009).

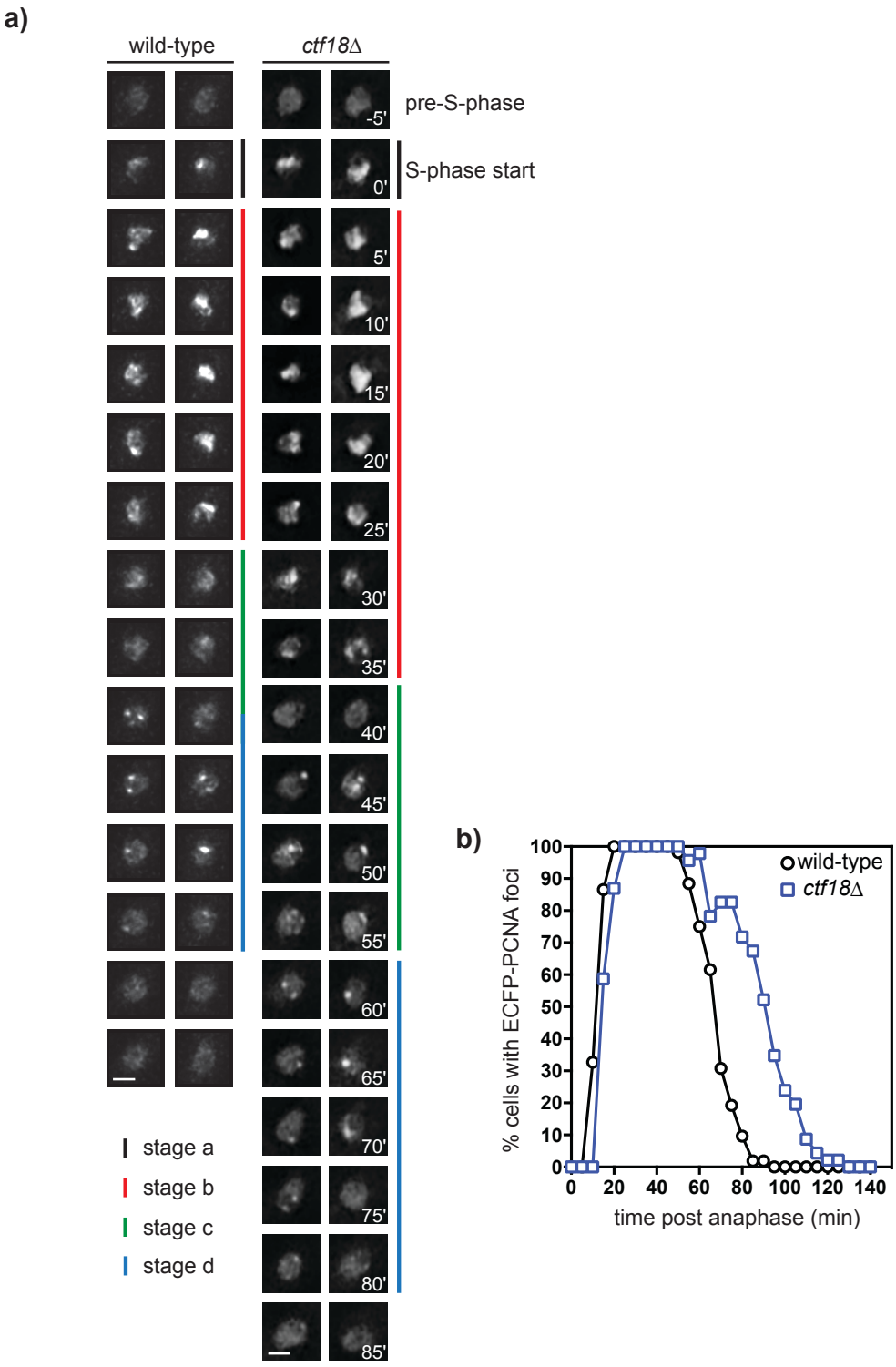

Figure 5.8 Prolonged persistence of PCNA foci in cells lacking Ctf18
a) Images from time-lapse microscopy showing ECFP-PCNA nuclear fluorescence that form successive distinguishable patterns classified into four different stages. Images of nuclei from four different time-lapse series are shown (two for wild-type and two for *ctf18*Δ). Scale bar = 2μm. b) Line graph of the percentage of cells with ECFP-PCNA foci in the cell cycle following anaphase at five-minute intervals, showing longer persistence of ECFP-PCNA foci in *ctf18*Δ cells compared to wild-type. The wild-type strain is MCW7065 (n=52) and the *ctf18*Δ strain is MCW8539 (n=46). The data are from a single experiment.

5.2.6 Effect of *ctf18*Δ on template switching downstream of *RTS1*

Forks restarted from *RTS1* remain prone to recombination as they progress from the RFB (Iraqui et al. 2012; Nguyen et al. 2015; Lambert et al. 2010), thus heightened genomic rearrangements at sites downstream of *RTS1-AO* are indicators of restarted fork progression. I measured the effect of *ctf18*Δ on template switching associated with restarted replication 12.4kb downstream of *RTS1* using the *ade6*$^{-}$ direct repeat reporter (Figure 5.9b). With *RTS1-IO, ctf18*Δ mutant again shows higher levels of spontaneous recombination compared to wild-type cells (see also Figure 5.2b). With *RTS1-AO,* the *ctf18*Δ mutant exhibited a ~4-fold increase in deletions and ~7-fold increase in gene conversions. Compared with wild-type these increases in template switching are greater than those seen when direct repeat recombination is measured at the barrier (Figure 5.2b). Surprisingly, unlike in wild-type cells, deleting *oriIII-1253* did not result in a noticeable increase in the level of *RTS1-AO*-induced recombinants in the *ctf18*Δ mutant, with only a minor increase (~1.3-fold; p=0.032) in gene conversions. In fact, the frequency of deletions was reduced by ~1.8-fold (p= 0.005) compared to a *ctf18*Δ mutant with *ori-1253*$^{+}$, and ~4.8-fold (p<0.0001) compared to the wild-type *ori-1253*Δ strain (Figure 5.9b). Altogether these data give a mixed view on Ctf18's role in template switching. In an *ori-1253*$^{+}$ background it appears to be required to limit template switching, whereas in an *ori-1253*Δ background it seems to promote template switching.

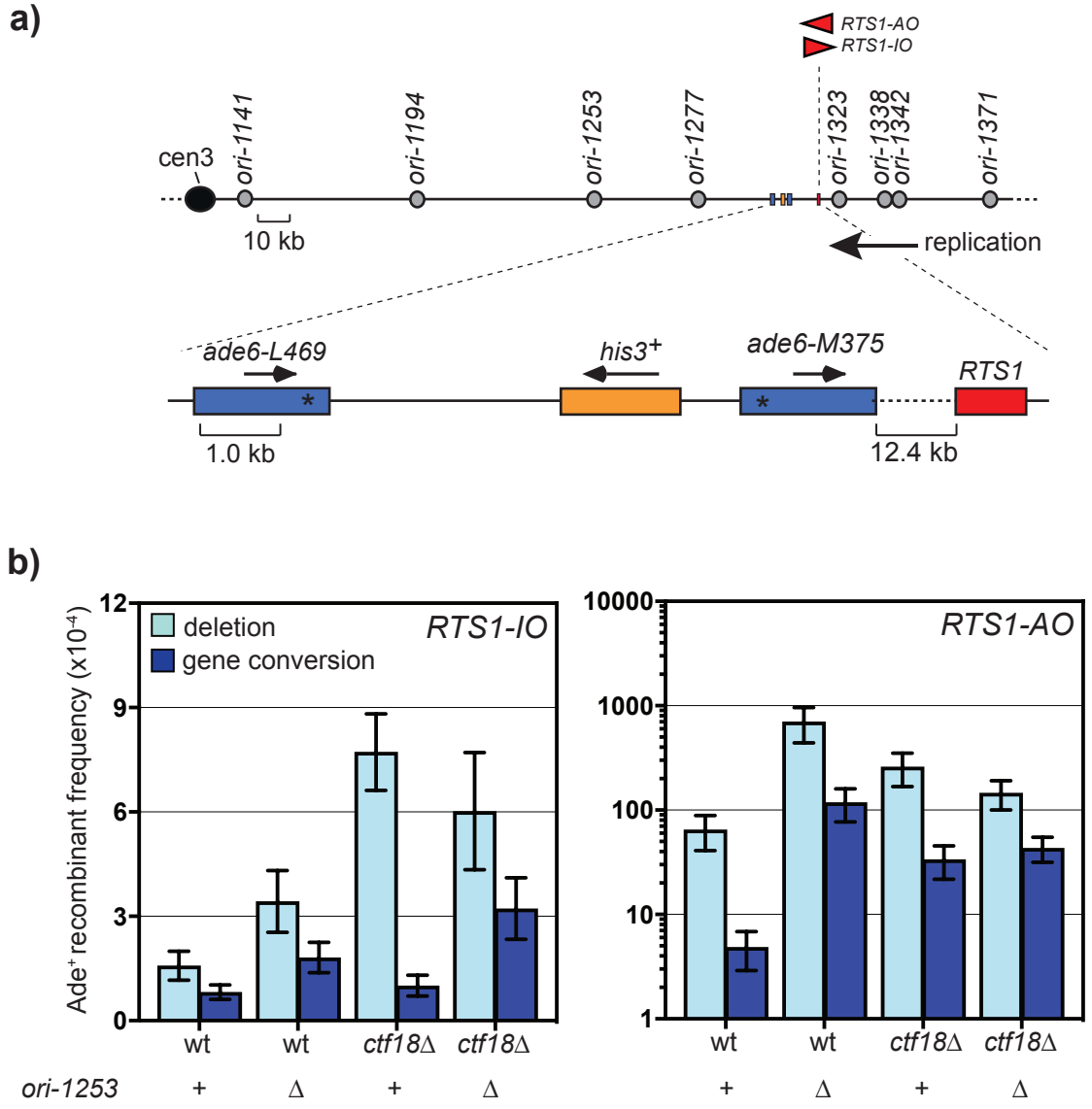

Figure 5.9 Effect of loss of Ctf18 on template switching 12.4kb downstream of *RTS1*
a) Schematic showing the location of *RTS1* and *ade6*$^{-}$ recombination reporter in relation to nearby replication origins (grey circles) on chromosome 3. Direction of replication indicates the direction of the recombination dependent restarted fork through the *ade6*$^{-}$ direct repeat reporter. b) Bar charts showing the frequency and type of Ade^{+} recombinants in MCW7257, MCW7293, MCW8597, MCW8822, MCW7259, MCW7295, MCW8598, MCW8763 (note the log scale in the bar chart for *RTS1-AO*). Error bars represent standard deviation. Ade^{+} recombinant frequency with statistical analysis is also shown in Table 1.

5.3 Discussion

In this chapter I investigated the role of Ctf18 as an alternative unloader or a loader of PCNA in RDR at *RTS1*. I observed ~2-fold increase in *RTS1*-induced direct repeat recombination at the barrier, which interestingly was completely dependent upon *elg1*. I suggested earlier that Elg1 promotes *RTS1*-induced recombination by unloading PCNA from the DNA and thereby limiting Fbh1 activity either by preventing its recruitment and/or enabling efficient Rad52 recruitment. My finding that Ctf18 suppresses Elg1-dependent recombination allows me to extend this model. I propose that Ctf18 suppresses recombination by promoting the loading of PCNA at the RFB, which, in turn, promotes Fbh1 recruitment/activity. Elg1 promotes recombination at collapsed RFs by unloading PCNA from the DNA which counteracts the loading activity of Ctf18. In the absence of Elg1, PCNA persists on the DNA acting as a platform for the recruitment of Fbh1 and/or a block to the recruitment of Rad52 (Figure 5.10). Increased loading of PCNA by Ctf18 in the absence of Elg1 to unload it, could result in increased recruitment of Fbh1 leading to suppression of *RTS1*-induced recombination. As mentioned earlier, overexpression of Fbh1 has previously been reported to suppress *RTS1-AO*-induced recombination (Lorenz et al. 2009) and, therefore, it is reasonable to think that modulating the amount of Fbh1 at the RFB, through a balancing act between Ctf18 and Elg1 loading and unloading PCNA, could account for the observed changes in direct repeat recombination. In the future, it will be important to investigate the genetic interaction between *ctf18*Δ and *fbh1*Δ to test my hypothesis. If the hyperrecombination of *ctf18*Δ is due to increased unloading of PCNA by Elg1, and thus reduced recruitment of Fbh1, a *ctf18*Δ *fbh1*Δ double mutant

should exhibit exactly the same level of direct repeat recombination as in a *fbh1*Δ single mutant (i.e. the interaction between *ctf18*Δ and *fbh1*Δ should be epistatic).

Even though a *ctf18*Δ mutant exhibits a ~2-fold increase in direct repeat recombination at the *RTS1-AO* barrier, live cell imaging experiments did not reveal an increase in the percentage of cells with a Rad52 focus co-localizing with the RFB. This suggests that for any given recombination event at the barrier there is a greater chance that it would give rise to an Ade^+ recombinant (i.e. there is a greater chance of inter-repeat recombination). This could be due entirely to reduced Fbh1 recruitment and/or activity at the RFB, which might favour the production of longer and more promiscuous Rad51 nucleofilaments. Alternatively, it may be associated with the role of Ctf18 in maintaining genome stability reported before, where it was reported to be associated with stabilizing trinucleotide repeats (Gellon et al. 2011). The aforementioned epistasis experiment between *ctf18*Δ and *elg1*Δ should help to distinguish between these possibilities. Although I did not observe any decrease in the recruitment of Rad52 at the barrier as such in a *ctf18*Δ mutant, I did find that the temporal dynamics of the protein recruitment was changed. Whilst non-colocalizing Rad52 foci appeared with similar timing following the start of S phase in both wild-type and *ctf18*Δ mutant cells, foci that co-localized with the RFB appeared later in the mutant ones. This appeared to have a knock-on effect, as a greater percentage of late G2 phase cells exhibited a co-localizing Rad52 focus in the *ctf18*Δ mutants. This altered temporal pattern of Rad52 recruitment to the RFB is most likely caused by a general reduction in replication fork velocity in the *ctf18*Δ mutant (Terret et al. 2009), which would result in replication forks arriving later at the RFB. A general reduction in replication fork velocity would also lead to a longer S phase and could account for the extended

duration of PCNA foci I observed in the *ctf18*Δ mutant. In future experiments it will be important to more directly assess fork velocity in the *ctf18*Δ mutant in *S. pombe* by DNA fibre experiments (Kaykov and Nurse 2015).

A seemingly conflicting finding of my study was the effect of *ori-1253* deletion on template switch recombination downstream of *RTS1-AO* in a *ctf18*Δ mutant. In an *ori-1253*$^{+}$ strain, loss of *ctf18* resulted in an increase in template switching, suggesting that Ctf18 constrains this process. Conceivably it could do this through its role in promoting cohesion and/or by affecting the recruitment of factors such as Fbh1 and Srs2 to the restarted fork through its PCNA loading function. Indeed, recent work from our group has shown that both Fbh1 and Srs2 strongly limit template switching associated with restarted replication (Jalan et al, unpublished data). However, unlike in a wild-type strain, deletion of *ori-1253* in a *ctf18*Δ mutant resulted in no increase in template switch recombination, instead it appears to slightly suppress it. Importantly, the frequency of template switch recombination in a *ctf18*Δ *ori-1253*Δ mutant was significantly less than in the comparable wild-type (*ori-1253*Δ) strain. This finding suggests that Ctf18 is needed to promote template switching. One explanation that could reconcile the seemingly conflicting results concerning Ctf18's role in constraining or promoting template switch recombination, relates back to the effect of *ctf18*Δ on general replication fork velocity (Terret et al. 2009). This would not only result in a delay in arrival of the first replication fork at the RFB, but would also delay the arrival of the oncoming replication fork (i.e. fork convergence at the barrier would occur later). For example, with *RTS1* at the *ade6* locus on chromosome 3 (Figure 5.2a), the telomere proximal replication fork moving at 3 kb/min would reach the barrier between 2.6 – 18.5 minutes following the start of S phase (depending on which

replication origin fired), whereas the oncoming centromere proximal fork would arrive between 17 – 62 minutes (Nguyen et al. 2015). If the fork velocity was only 1 kb/min these times would change to 7.8 – 55.5 minutes for the telomere proximal fork and 51 – 186 minutes for the centromere proximal fork. This means that the window of time between the first fork arriving at the RFB and second fork converging with it tends to increase the slower the replication forks are moving (e.g., in the ~80% of cells in which *ori-1253* fires and where either *ori-1323*, *ori-1338* or *ori-1342* also fires, the window expands from 16 - 22.5 minutes to 48 - 67.5 minutes). If we assume that RDR itself is not similarly slowed down in a *ctf18*Δ mutant, then the increase in recombination at *RTS1-AO* and downstream of it may be due to a general delay in fork convergence which would allow more time for recombination to occur. In essence, *ctf18*Δ would have a similar effect as deleting *ori-1253* on the frequency of recombination. If true, then *ctf18*Δ and *ori-1253*Δ should exhibit an epistatic interaction for *RTS1-AO*-induced recombination, which is almost the case at the *ade6*$^{-}$ direct repeat reporter 12.4 kb downstream of the RFB. In fact, as stated above, template switch recombination is significantly less in a *ctf18*Δ *ori-1253*Δ mutant than in wild-type (*ori-1253*Δ), which means that, in addition to promoting replication fork velocity, Ctf18 also promotes template switch recombination associated with restarted DNA replication. Exactly how it would do this is unclear, although it might relate to Ctf18's ability to unload PCNA (Bylund and Burgers 2005).

I have not investigated the role of RFC in RDR at *RTS1,* but it would be interesting to do so in the future, considering its role in loading and unloading PCNA as implicated by some *in vitro* studies (Yao et al. 1996; Cai et al. 1996; Shibahara and Stillman 1999. I had made the *RTS1*-based direct repeat recombination reporter strain

in the ts mutant background of *rfc (rfc1-44)* but was unable to carry out the assay due to time constrains. One could also investigate the *rfc1-44 elg1*Δ *ctf18*Δ mutant for its effect on RDR at *RTS1*, as it is a viable strain (Kim et al. 2005).

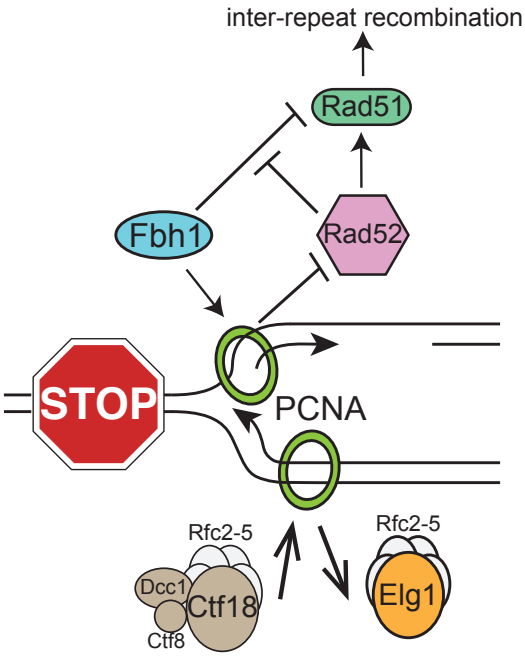

Figure 5.10 Hypothetical model encompassing the roles of Elg1 and Ctf18 in recombination at collapsed RFs
Elg1 promotes recombination at collapsed RFs by unloading PCNA from the DNA which counteracts the loading activity of Ctf18. In the absence of Elg1, PCNA persists on the DNA acting as a platform for the recruitment of the anti-recombinase Fbh1 and/or a block to the recruitment of Rad52.

6 The importance of Rad51 and its mediators in restarting collapsed RFs

6.1 Introduction

According to the model of RDR proposed by our lab, the fork collapsed at *RTS1* undergoes fork reversal and strand resection generates a ssDNA tail onto which RPA, Rad52 and Rad51 sequentially load (Sun et al. 2008). Strand invasion follows, creating a D-loop onto which replication proteins assemble and commence DNA synthesis. Replication continues with the invading DNA strand remaining connected to the reversed fork structure from where it originated. Lagging strand synthesis can convert the reversed fork into a fully ligated four-way DNA/Holliday junction, which can branch migrate behind the D-loop (Nguyen et al. 2015). The D-loop on dissociation is capable of reforming a reversed fork, facilitating reloading of HR proteins, which could then catalyse HR at sites distant from *RTS1*.

The reengagement of the nascent strands with the parental DNA duplex seems to be vital for the process of RDR. Rad51 is proposed to play a key role in this process by catalysing the strand invasion of a nascent strand into the parental DNA duplex (Brouwer et al. 2018; Xu et al. 2017). Rad51 requires a number of other proteins, including the Rad51 mediators, to facilitate formation and functional activation of a nucleofilament that is fundamental for the homology search and strand invasion steps of HR. There are three so-called Rad51 mediator complexes in *S. pombe*, Rad55-Rad57, Rdl1-Rlp1-Sws1 and Swi5-Sfr1, and they facilitate Rad51 assembly via different mechanisms (Symington 2002; Akamatsu et al. 2003; Akamatsu et al. 2007; Gaines et al. 2015).

A previous student in the lab (Michael Nguyen) investigated the role of the aforementioned mediators in *RTS1* induced direct repeat recombination (Figure 6.1). Rad55 and Rad57 were found to be needed for both spontaneous and *RTS1* induced

recombination. Deletion of either *rad55* or *rad57* abolished both spontaneous and *RTS1*-induced gene conversions. Importantly, the reductions in gene conversions and deletions were similar to a *rad51*Δ mutant with the exception that there was a lower frequency of *RTS1-AO*-induced deletions in both *rad55*Δ and *rad57*Δ single mutants compared to a *rad51*Δ single mutant. It was later inferred through epistasis analysis that the loading of Rad51 onto DNA in the absence of the mediators has a role in suppressing Rad51-independent deletions even when its ability to promote gene conversions is impaired (Nguyen 2014, DPhil thesis).

Rdl1, Rlp1, and Sws1 were also found to promote *RTS1* induced direct repeat recombination, though not to the same extent as Rad55-Rad57 (Figure 6.1). In the absence of *rdl1*, *rlp1* or *sws1*, the frequency of spontaneous gene conversions was slightly reduced in each of the mutants compared to wild-type, but not to the same extent as in *rad51*Δ, *rad55*Δ and *rad57*Δ mutants. Moreover, spontaneous deletions did not increase like they did in *rad51*Δ, *rad55*Δ and *rad57*Δ mutants. However, Rdl1, Rlp1 and Sws1 were required for most of the *RTS1-AO*-induced gene conversions and promoted *RTS1-AO*-induced deletions to the same extent as Rad55 and Rad57. Compared to the other mediator mutants, *sfr1*Δ and *swi5*Δ had only a modest impact on spontaneous and *RTS1-AO*-induced recombination, suppressing spontaneous deletions and promoting *RTS1-AO*-induced recombination (Figure 6.1). Epistasis analysis with *rad55*Δ *rdl1*Δ and *rad55*Δ *swi5*Δ revealed that the Rad51 mediators function in the same pathway for promoting RF block-induced recombination (Nguyen 2014, DPhil Thesis). As the Rad51 mediators were required for direct repeat recombination at the barrier, I wanted to see whether the same was true for template switch recombination associated with restarted replication. I anticipated that some or

all of the mediators would be required for promoting Rad51-dependent replication restart following fork collapse at the *RTS1* barrier and, therefore, template switch recombination downstream of the RFB would be reduced. However, my findings were not consistent with this simple hypothesis.

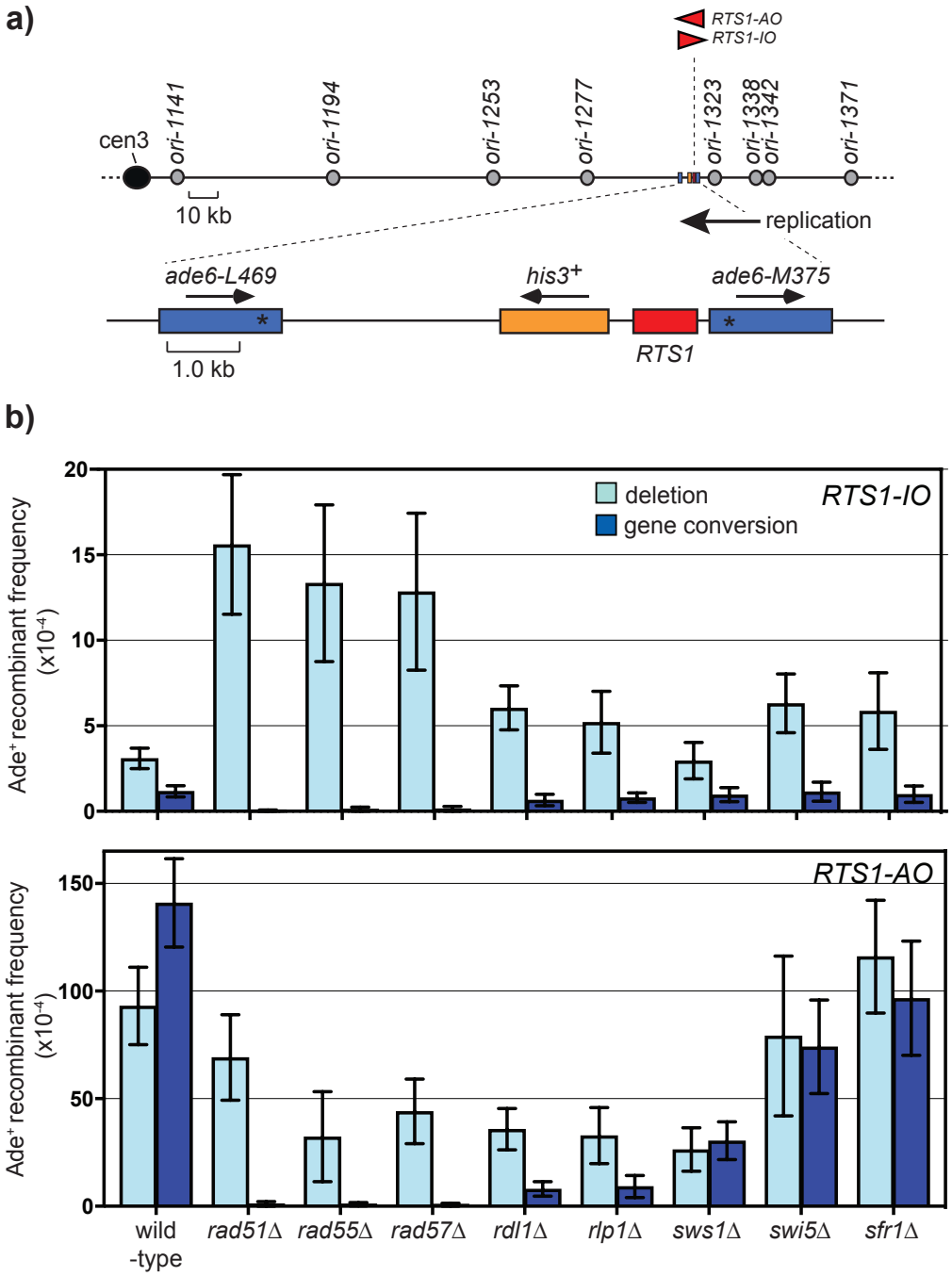

Figure 6.1 Role of Rad51 and Rad51 mediators in *RTS1*-induced direct repeat recombination
a) Schematic showing the location of the *ade6*- intra-chromosomal recombination reporter and *RTS1* in relation to nearby replication origins (grey circles) at the endogenous *ade6* locus on chromosome 3. (b) Bar charts showing the frequency and type of Ade+ recombinants in MCW4712, MCW1691, MCW2650, MCW6539, MCW6501, MCW6505, MCW6503, MCW2647, MCW6497, MCW4713, MCW1692, MCW2655, MCW6454, MCW6468, MCW6507, MCW6470, MCW2653, MCW6499. Error bars represent standard deviation. The data is from Nguyen 2014, DPhil thesis.

6.2 Results

6.2.1 Rad55, Swi5 and Rdl1 are not essential for template switching associated with restarted replication downstream of *RTS1-AO*

I investigated one factor from each of the mediator complexes Rad55-Rad57, Rdl1-Rlp1-Sws1 and Swi5-Sfr1 for their importance in template switching associated with the restarted fork at the *ade6*$^{-}$ direct repeat reporter positioned 12.4 kb downstream of *RTS1* (Figure 6.2a). In the case of spontaneous recombination (measured in *RTS1-IO* strains), *rad55*Δ, *swi5*Δ and *rdl1*Δ each had almost the same effect as they had when the direct repeat reporter was positioned at the barrier site (compare the data in Figure 6.1b and 6.2b). In the absence of *rad55,* the spontaneous gene conversions were again abolished, and the deletions increased (~5-fold) indicating repair of spontaneous lesions occurring through a more mutagenic, Rad51-independent pathway. In the absence of *swi5* or *rdl1*, there was no significant change in the level of spontaneous gene conversions (p=0.167 for *swi5*Δ; p=0.288 for *rdl1*Δ). However, the level of deletions rose by 2-fold (p<0.0001) in the *swi5*Δ mutant and by ~3.5-fold (p<0.0001) in *rdl1*Δ. In the strains with *RTS1-AO*, although the gene conversions are reduced ~2.7-fold (p<0.0001) in a *rad55*Δ mutant and ~1.7-fold (p<0.0001) in a *rdl1*Δ mutant, surprisingly the deletions are not reduced in the absence of *rad55*, *swi5* or *rdl1* (Figure 6.2b). Since the deletions come from template switching associated with restarted replication, these data suggest that the process of fork restart can operate without these mediator proteins.

It was previously proposed that Rad55-Rad57 and Swi5-Sfr1 operate in independent pathways to promote Rad51 activity in fission yeast (Akamatsu et al. 2007; Akamatsu et al. 2003). Hence, to test if one complex performs the function of promoting Rad51 in the absence of the other, I checked the effect of a *rad55*Δ *swi5*Δ

double mutant on direct repeat recombination at this site (Figure 6.3). However, this mutant exhibited a minor increase in the frequencies of spontaneous and *RTS1-AO*-induced recombination as a *rad55*Δ single mutant, with ~2.5-fold (p=0.01) and ~1.8-fold (p=0.004) increase in deletions, respectively. I also tested whether there was an increase in the level of template switching upon deletion of *ori-1253* and observed an enhanced level of recombination similar to wild-type in each of the mutants, albeit gene conversions are reduced by at least 10-fold when *rad55* is missing (Figure 6.3). These data provide further evidence that replication restart is happening in the absence of both known Rad51 mediator pathways in *S. pombe* (i.e. Rad55-Rad57 and Swi5-Sfr1), albeit, the ability of template switching to give rise to gene conversions is affected by the absence of Rad55 and Rdl1.

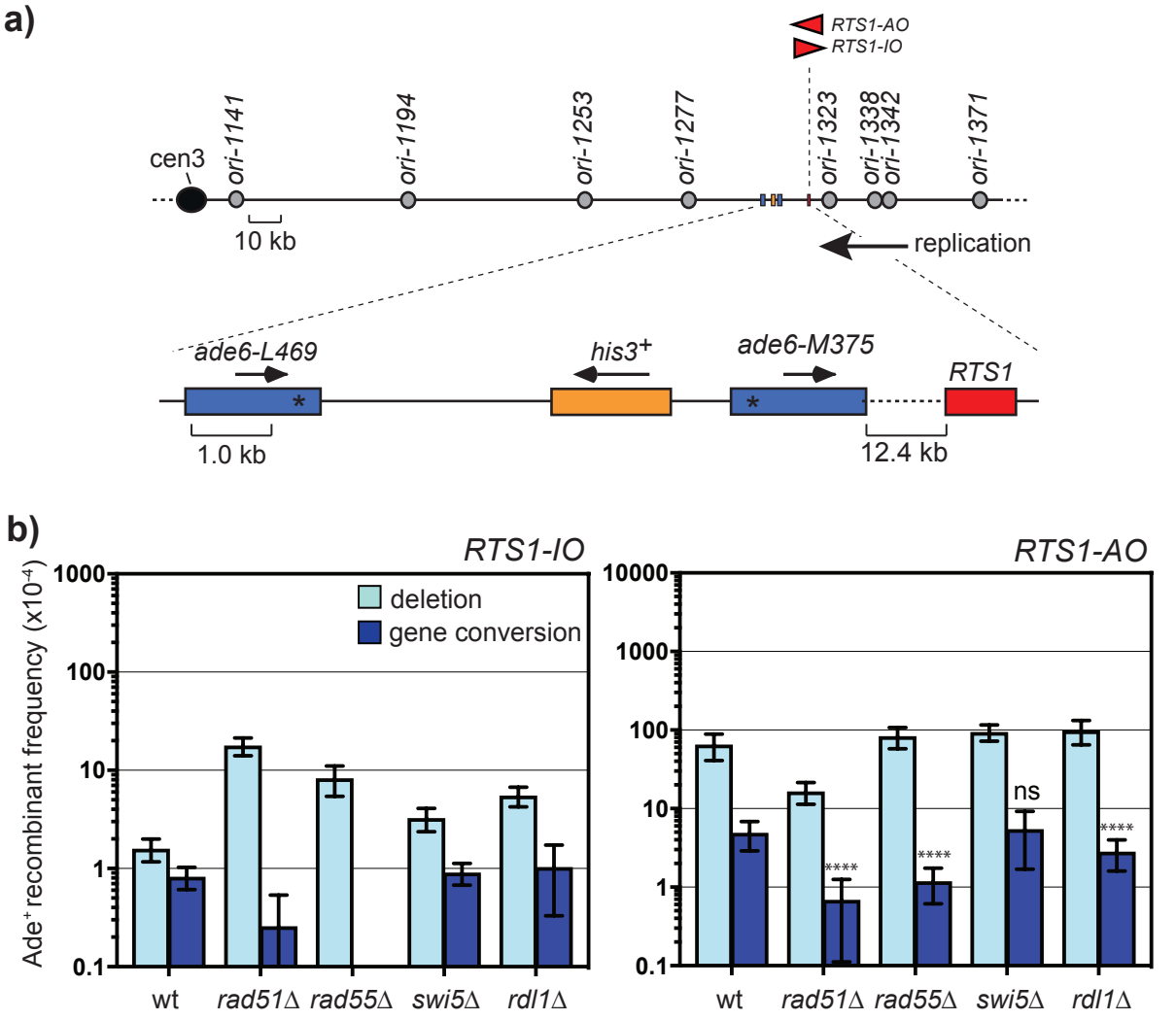

Figure 6.2 Rad55, Swi5 and Rdl1 are not essential for template switching associated with restarted replication downstream of *RTS1-AO*

a) Schematic showing the location of *RTS1* and *ade6*$^{-}$ recombination reporter in relation to nearby replication origins (grey circles) at the endogenous *ade6* locus on chromosome 3. The arrow depicting the direction of replication indicates the direction of the recombination dependent restarted fork through *ade6*$^{-}$ direct repeat reporter. b) Bar charts showing the frequency and type of Ade^{+} recombinants in MCW7257, MCW7812, MCW7588, MCW7555, MCW8931, MCW7259, MCW7814, MCW7590, MCW7557, MCW9140. Error bars represent standard deviation. Significant changes compared to the wild-type strain are indicated. P-values were calculated using the Shapiro-Wilk normality test (ns $p>0.05$, * $p<0.05$, ** $p<0.01$, *** $p<0.001$, **** $p<0.0001$). Ade^{+} recombinant frequency with statistical analysis is also shown in Table 1.

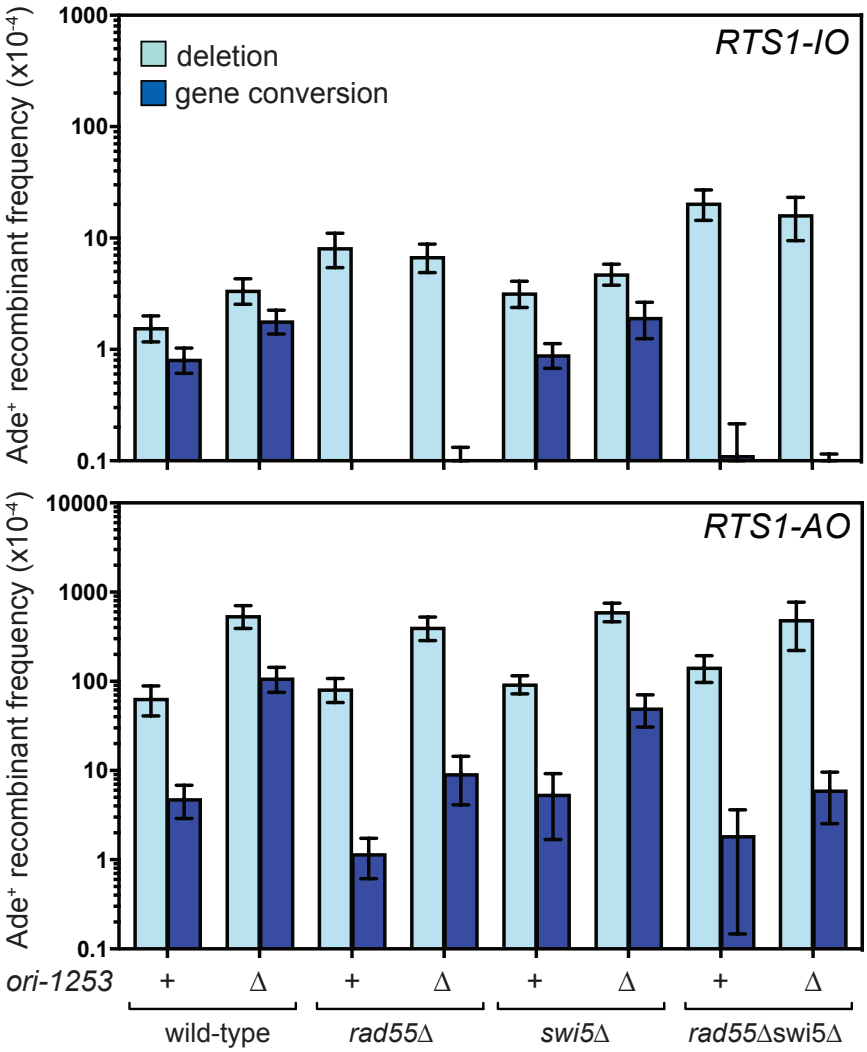

Figure 6.3 Effect of *rad55*Δ*swi5*Δ is similar to the effect of *rad55*Δ on direct repeat recombination 12.4 kb downstream of *RTS1*.
Bar charts showing the frequency and type of Ade$^+$ recombinants in MCW7257, MCW7293, MCW7588, MCW7592, MCW7555, MCW7559, MCW7607, MCW7611, MCW7259, MCW7295, MCW7590, MCW7594, MCW7557, MCW7561, MCW7609, MCW7613. Error bars represent standard deviation. Ade$^+$ recombinant frequency with statistical analysis is also shown in Table 1.

6.2.2 Rad51, Rad54 and Rad54's ATPase activities are needed to promote template switch recombination downstream of *RTS1*

Having found that some of Rad51's key mediator proteins are not required for template switch recombination downstream of *RTS1*, I next determined what effect *rad51* deletion has (Figure 6.4). Consistent with previous unpublished work from the lab, I found that a *rad51*Δ mutant exhibited essentially the same level of deletions and gene conversions in the presence of both *RTS1-IO* and *RTS1-AO*. This result indicates that Rad51 is required for template switching downstream of *RTS1*, which would be expected given its importance for promoting replication restart (Lambert et al. 2010).

Another important recombination protein that supports Rad51 activity is the Snf2 family DNA-dependent ATPase Rad54. Rad54 has multiple roles in recombination including: stimulation of Rad51's DNA strand exchange activity (Petukhova et al. 1998; Petukhova et al. 1999; Mazin et al. 2000; Mazin et al. 2003; Sigurdsson et al. 2002); dissociation of Rad51 from the DNA following strand exchange to permit nascent DNA synthesis (Solinger et al. 2002; Li and Heyer 2009); chromatin remodelling (Alexeev et al. 2003); and branch migration of Holliday junctions (Bugreev et al. 2006). Previous work in the lab by Michael Nguyen and Fikret Osman had shown that when *RTS1-AO* is positioned within the *ade6*$^{-}$ reporter, Rad54 is needed to promote Rad51-dependent gene conversions and deletions (unpublished data). I investigated Rad54 for its importance in direct repeat recombination 12.4 kb downstream of *RTS1* (Figure 6.4). Similar to a *rad51*Δ mutant, a *rad54*Δ mutant displays only residual levels of both spontaneous and *RTS1-AO*-induced gene conversions. The level of deletions in the *RTS1-AO rad54*Δ strain is also the same as in the equivalent *rad51*Δ strain. However, the frequency of spontaneous deletions in a *rad54*Δ mutant, although higher than wild-type, was not as high as in a *rad51*Δ mutant and, if this is taken into account, then the

level of deletions in the *RTS1-AO rad54*Δ strain is higher than the spontaneous level implying that there is some residual template switching in this mutant. To further investigate Rad54's role, I also measured spontaneous recombination and template switching in a *rad54*^{K300A} mutant (Figure 6.4). Lysine 300 is a critical conserved amino acid in Rad54's Walker A ATPase domain, and previous studies have shown that the equivalent mutation in budding yeast and murine Rad54 abolishes its ATPase activity but not its ability to promote Rad51 loading onto DNA (Wolner and Peterson 2005; Agarwal et al. 2011; Petukhova et al. 1999; Heyer et al. 2006). I found no significant difference for recombination frequencies in a *rad54*^{K300A} mutant compared to a *rad54*Δ mutant. These data indicate that Rad54's ATPase activity is required for promoting template switch recombination associated with restarted replication.

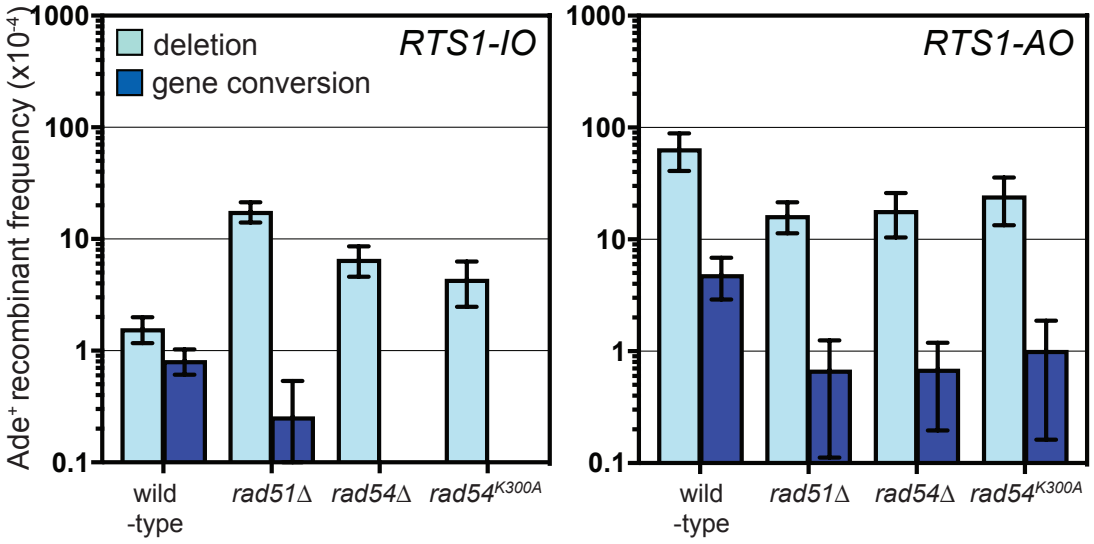

Figure 6.4 Importance of Rad54 and its ATPase activity in direct repeat recombination 12.4 kb downstream of *RTS1*
Bar charts showing the frequency and type of Ade$^+$ recombinants in MCW7257, MCW7812, MCW9030, MCW9006, MCW7259, MCW7814, MCW9013, MCW9008. Error bars represent standard deviation. Ade$^+$ recombinant frequency with statistical analysis is also shown in Table 1.

6.2.3 Investigating if *rad51*Δ is truly defective for RDR from *RTS1*

Given my observation that the mediator proteins, which facilitate formation and functional activation of the Rad51 nucleofilament, are not essential for direct repeat recombination downstream of *RTS1*, I wanted to check if *rad51*Δ is truly defective for RDR at *RTS1*. I reasoned that any residual restart activity in a *rad51*Δ mutant would be easier to detect if allowed more time to act before arrival of the oncoming replication fork. It should also be easier to detect if the direct repeat reporter was positioned closer to the RFB, as the restarted fork would have less distance to travel. With this is in mind, I measured the effect of *rad51*Δ on template switching at *RTS1* and at a distance of 0.2 kb and 12.4 kb downstream of it. I also performed these experiments in both *oriIII-1253*$^+$ and *oriIII-1253*Δ backgrounds (Figures 6.5 – 6.7).

We have seen before that when the *ade6*$^{-}$ repeats flank the barrier, both spontaneous and *RTS1*-induced gene conversions are abolished with *rad51*Δ (Figure 6.5). Conversely, the spontaneous deletions increase 5-fold and the *RTS1*-induced deletions decrease only 1.3-fold in the *rad51*Δ mutant. Unlike deletions, which can be formed in a Rad51-independent manner, gene conversions require strand invasion activity of Rad51 (Doe et al. 2004; Lorenz et al. 2009). I checked the effect of deleting *oriIII-1253* in the wild-type strain with *RTS1-AO* and observed that it causes ~1.7-fold increase in deletions and ~1.9-fold ($p<0.0001$) increase in gene conversions ($p<0.0001$) as more time is allowed for recombination before fork merging (Nguyen et al 2015). However, in the *rad51*Δ mutant, *oriIII-1253*Δ had little effect on the frequency of recombinants and instead a ~1.2-fold decrease in deletions was observed ($p=0.01$). In this case, recombination could be stimulated by fork convergence by a process mediated by Rad52 like IFSA (Morrow et al. 2017) where, during RF convergence, the *ade6* repeat on the 3'-ended ssDNA tail of the regressed fork anneals to the complementary ssDNA of the other *ade6* repeat that is exposed in the lagging strand gap of the incoming fork. There is thus a balance between the recombination curbed and stimulated by RF convergence (i.e. recombinants can stem from RDR, which is promoted by *oriIII-1253*Δ, or from IFSA, which is reduced by *oriIII-1253*Δ).

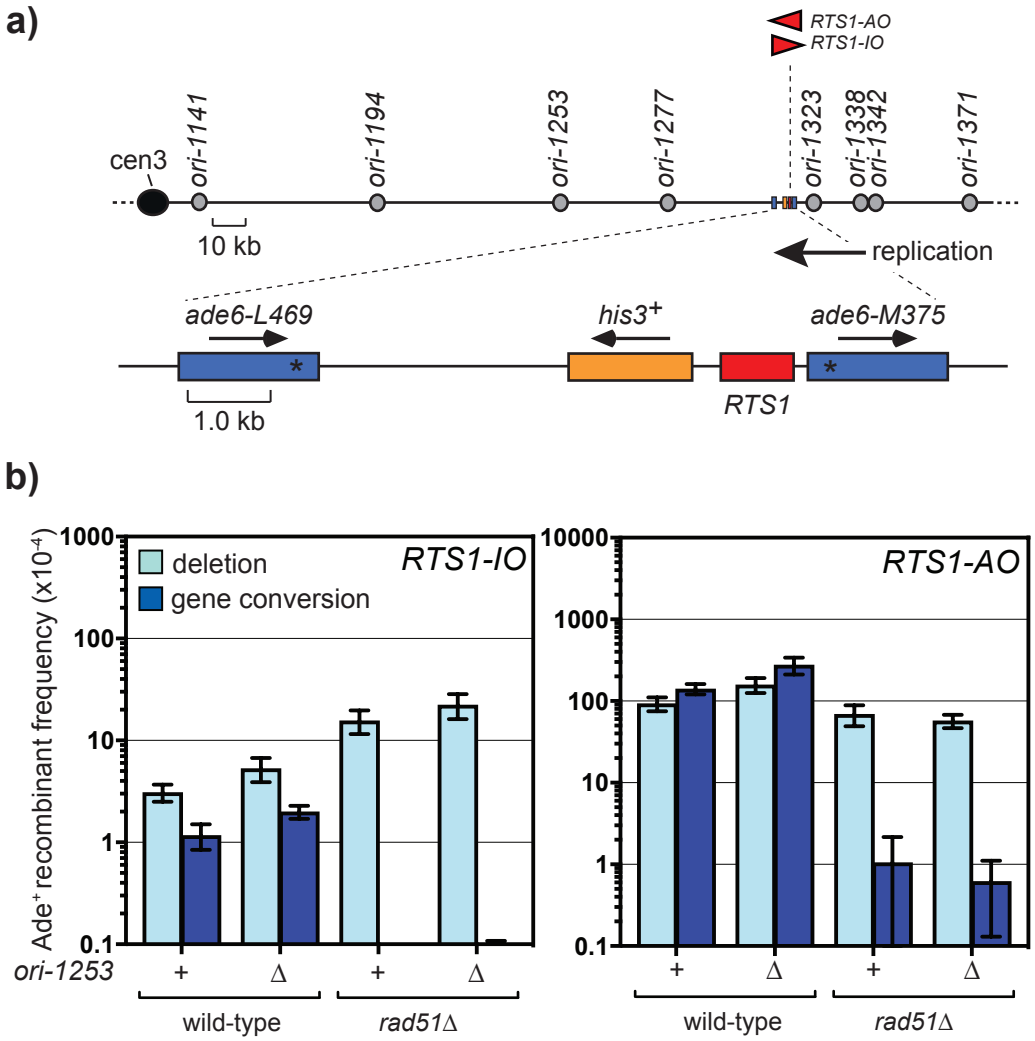

Figure 6.5 Effect of *rad51*Δ on the frequency of *RTS1*-induced direct repeat recombination
a) Schematic showing the location of the *ade6*- intra-chromosomal recombination reporter and *RTS1* in relation to nearby replication origins (grey circles) at the endogenous *ade6* locus on chromosome 3. b) Bar charts showing the frequency and type of Ade+ recombinants in MCW4712, MCW6894, MCW1691, MCW8837, MCW4713, MCW6778, MCW1692, MCW8835. Error bars represent standard deviation. Ade+ recombinant frequency with statistical analysis is also shown in Table 1.

When the *ade6*$^{-}$ reporter is placed 0.2 kb downstream of *RTS1*, with *RTS1-IO*, the recombinants are similar to the background level of spontaneous recombination; however, with *RTS1-AO*, the total recombinants increase by ~3.5-fold more than when the barrier is positioned between the *ade6*$^{-}$ repeats and more than 80% of these are deletions [Nguyen et al. 2015 and Figure 6.6 (my data)]. Allowing more time for fork restart and template switching downstream of *RTS1*, by the deletion of *oriIII-1253*, in the wild-type causes a doubling of gene conversions ($p<0.0001$) but deletions are reduced by half ($p<0.0001$), which suggests that some deletions may rely on fork convergence (Figure 6.6b). In the absence of *rad51,* with *RTS1-AO*, the gene conversions decrease by ~7-fold ($p<0.0001$) and deletions by ~2-fold ($p<0.0001$), nevertheless they are much higher than in the equivalent strains with *RTS1-IO* (38-fold increase in deletions; 827-fold increase in conversions). Like at the “0 kb” reporter, deletion of *oriIII-1253* has little effect on the frequency of recombination in a *rad51*Δ mutant with *RTS1-AO* (Figure 6.6b). If we assume that the induced levels of recombination at the 0.2 kb reporter depend on replication being restarted, then these data clearly indicate that there is a Rad51-independent pathway of restarting collapsed replication forks in fission yeast. Moreover, replication that is restarted by this pathway is prone to template switching, albeit these template switch events are much less likely to generate gene conversions than when replication is restarted by the Rad51-dependent pathway. Recent work from Anastasiya Kiskevich in our lab has shown that the Rad51-independent pathway depends on Rad52 (unpublished data).

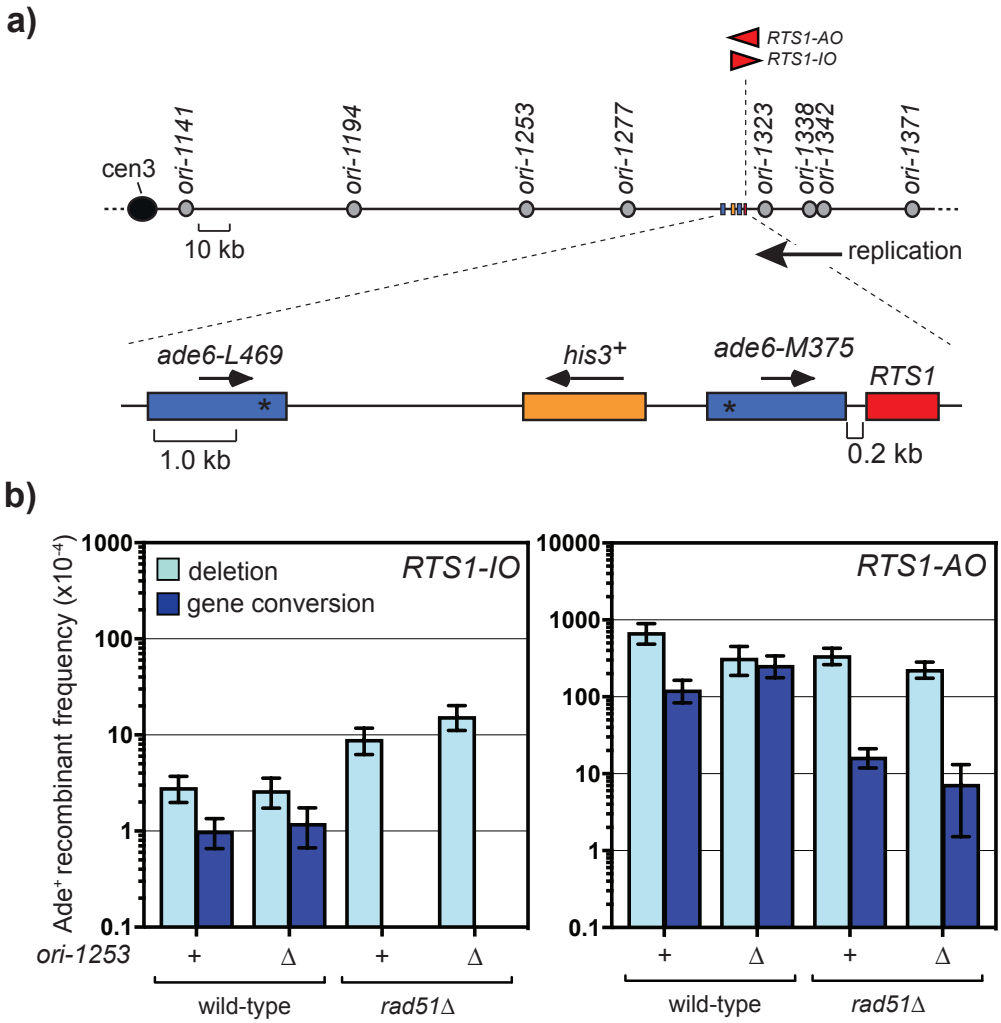

Figure 6.6 Effect of *rad51*Δ on template switching 0.2kb downstream of *RTS1*
a) Schematic showing the location of the *ade6*- intra-chromosomal recombination reporter and *RTS1* in relation to nearby replication origins (grey circles) at the endogenous *ade6* locus on chromosome 3. b) Bar charts showing the frequency and type of Ade+ recombinants in MCW7132, MCW7415, MCW8788, MCW8792, MCW7134, MCW7417, MCW8790, MCW8793. Error bars represent standard deviation. Ade+ recombinant frequency with statistical analysis is also shown in Table 1.

When the *ade6*- reporter is placed 12.4 kb downstream of *RTS1*, we know that the frequency of recombination with *RTS1-IO*, which is comparable to the spontaneous level, increases ~29-fold with *RTS1-AO* (Nguyen et al. 2015) and my data (Figure 6.7). The majority of recombinants at this site (~92%) are deletions, however, there is also a clear increase (~6-fold) in gene conversions. With *ori-1253*Δ, the frequency of recombination is ~12-fold higher than in the *RTS1* strain containing

oriIII-1253^{+}. In the absence of *rad51*, there is no induced level of recombinants at this site. However, when I deleted *oriIII-1253*, significant levels of induced recombinants were formed with ~38-fold ($p<0.0001$) increase in deletions and ~17-fold ($p<0.0001$) increase in gene conversions. This suggests that, whilst replication restart might be initiated relatively quickly by Rad52, the restarted fork moves quite slowly and will only reach the 12.4kb reporter if given sufficient time (by delaying the arrival of the oncoming fork).

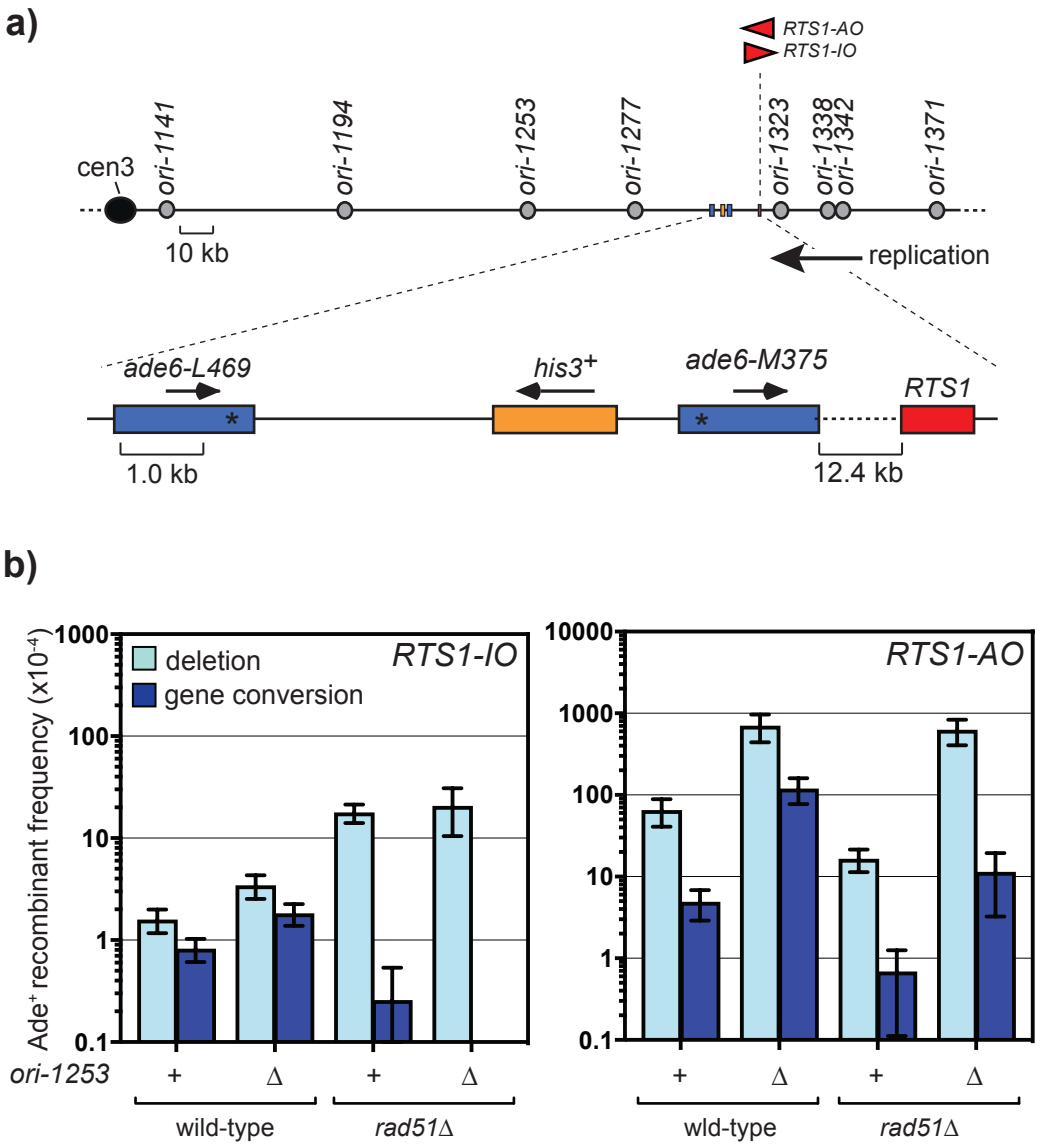

Figure 6.7 Effect of *rad51*Δ on template switching 12.4kb downstream of *RTS1*
a) Schematic showing the location of the *ade6*$^{-}$ intra-chromosomal recombination reporter and *RTS1* in relation to nearby replication origins (grey circles) at the endogenous *ade6* locus on chromosome 3. b) Bar charts showing the frequency and type of Ade^{+} recombinants in MCW7257, MCW7293, MCW7812, MCW8766, MCW7259, MCW7295, MCW7814, MCW8765. Error bars represent standard deviation. Ade^{+} recombinant frequency with statistical analysis is also shown in Table 1.

6.2.4 Further investigation on the effect of *rad51*Δ on replication restart and associated template switching using a modified reporter system

In order to confirm the observation that *rad51*Δ strains can perform replication restart and thus give rise to template switching 12.4kb downstream of *RTS1*, I repeated the investigation using Reporter System 2 described in Section 4.2.2 (Figure 6.8a). This system is a modification of the standard 12.4 kb *ade6*$^{-}$ direct repeat reporter (Reporter System 1) in which an adjacent *kanMX6* cassette has been swapped to *ura4MX4*. The *ura4*$^{+}$ gene can be used to assess mutagenesis by measuring the frequency of cell resistance to 5-FOA resulting from loss of *ura4*+ function and, therefore, with Reporter System 2 both template switch recombination and mutagenesis can be monitored at neighbouring genomic sites in the same strain.

With Reporter System 2, the frequencies of *ade6*$^{-}$ direct repeat recombination for the wild-type and *rad51*Δ strains are generally consistent with what I observed with Reporter System 1, except for strains with *RTS1-AO* and *oriIII-1253*$^{+}$, which exhibit significantly higher levels of recombination than the equivalent Reporter System 1 strains (Figure 6.8b) (see Discussion for a potential explanation). The level of deletions increased by ~4.3-fold ($p<0.0001$) for both wild-type and *rad51*Δ*, RTS1-AO* strains with *ori-1253.* The level of gene conversions increased by ~4.5-fold ($p<0.0001$) and ~4-fold ($p=0.04$) for wild-type and *rad51*Δ*, RTS1-AO* strains respectively, with *ori-1253*Δ. Nevertheless, deletion of *rad51* causes the same fold reduction in gene conversions ~9.7-fold in an ori-1253+ background and ~6.6-fold in an ori-1253Δ

background) and deletions (~4.2-fold in an ori-1253+ background and ~1.6-fold in an ori-1253Δ background) as seen with Reporter System 1.

The frequency of FOA resistant colonies for the wild-type is spontaneously higher than reported before (Iraqui et al. 2012) and it increases ~280-fold with *RTS1-AO* (Figure 6.8c). The spontaneous frequency of FOA resistant colonies is increased (~8-fold, $p<0.001$) in *rad51*Δ mutant due to more mutagenic repair of spontaneous lesions, which is increased ~115-fold with *RTS1-AO*. The frequency unexpectedly comes down in an *ori-1253*Δ strain for both wild-type and *rad51*Δ mutant. Providing more time with *ori-1253*Δ counterintuitively decreases these events suggesting that it is needed (see Discussion for a potential explanation). If we assume that the mechanisms that give rise to spontaneous (i.e. *RTS1-IO*) and *RTS1-AO*-induced levels of FOA resistant colonies are distinct then their effects should be additive. In that case, the increase in FOA resistant colonies in a *rad51*Δ mutant (*RTS1-AO* and *ori-1253*Δ) is more than in the equivalent wild-type strain. Thus, the data shows that Rad51 is required to supress the formation of FOA resistant colonies.

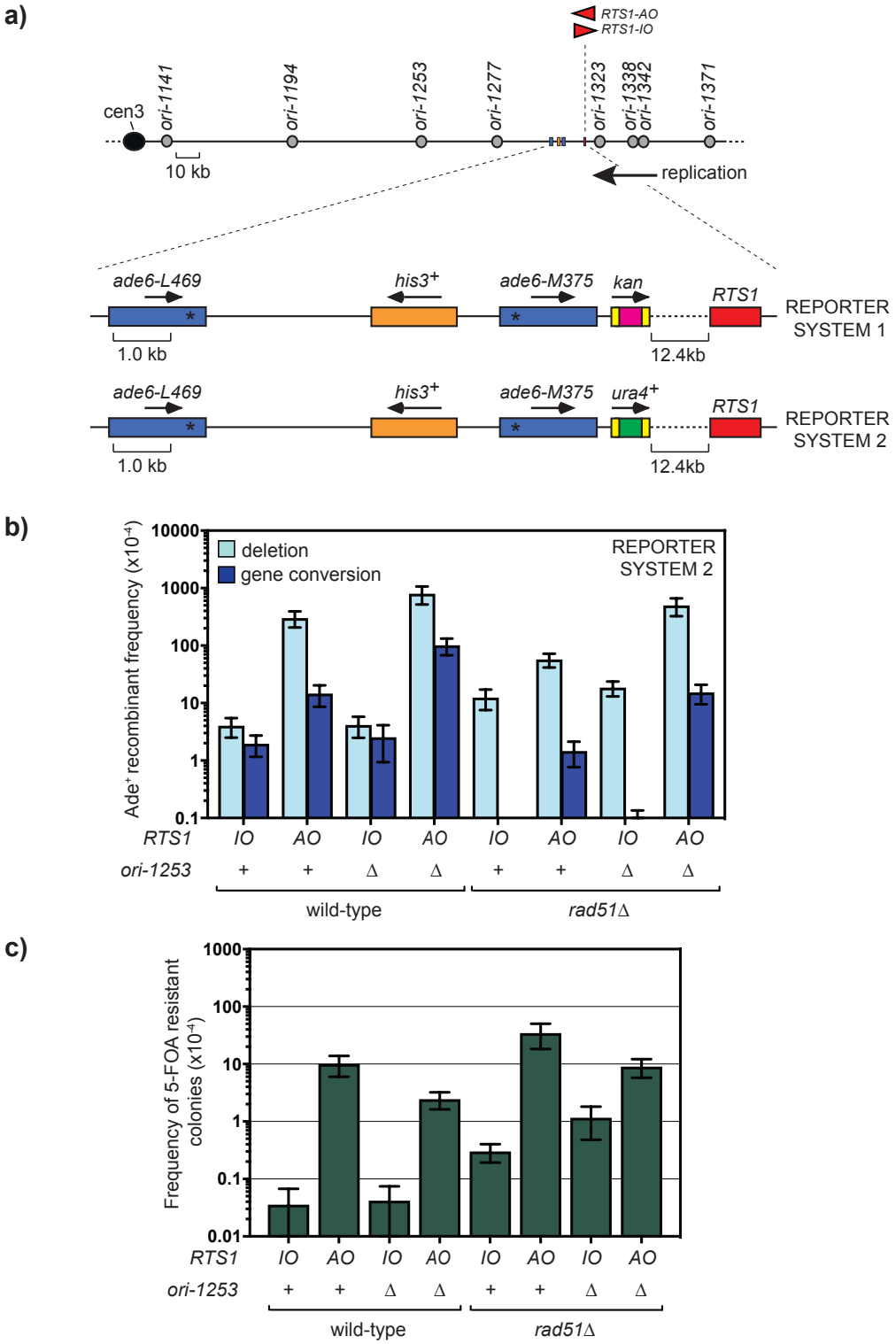

Figure 6.8 Effect of *rad51*Δ on template switching and mutagenesis downstream of *RTS1*
a) Schematic showing the location of *RTS1* and *ade6*- recombination reporter with and without *ura4*+ reporter in relation to nearby replication origins (grey circles) at the endogenous *ade6* locus on chromosome 3. The arrow depicting the direction of replication indicates the direction of the recombination dependent restarted fork through *ade6*- direct repeat reporter. b) Bar charts showing the frequency and type of Ade+ recombinants in MCW9036, MCW9039, MCW8700, MCW8888, MCW9028, MCW9004, MCW9000, MCW9002. c) Bar charts showing the frequency of 5-FOA resistance in the same strains. Error bars represent standard deviation. Ade+ recombinant frequency with statistical analysis is also shown in Table 1.

6.2.5 Investigating if Exo1 impedes Rad51-independent replication restart

Exo1 is a multifunctional 5'-3' exonuclease and DNA structure-specific DNA endonuclease, identified as a member of the Rad2 family of proteins (Szankasi and Smith 1995). It is important for mitotic and meiotic recombination, Okazaki fragment processing and telomere maintenance (Tsang et al. 2014). Exo1 has been shown to be recruited to stalled replication forks and counteract fork reversal by generating ss-DNA intermediates (Cotta-Ramusino et al. 2005). At *RTS1*, Exo1 is responsible for the resection behind the collapsed replication fork and aids in the recruitment of Rad52, thus promoting RDR (Tsang et al. 2014; Teixeira-Silva et al. 2017; Osman et al. 2016).

As mentioned above, unpublished work from the Whitby lab has shown that the Rad51-independent pathway of replication restart depends on Rad52. Indeed, the increased level of direct repeat recombination seen in a *rad51*Δ mutant 12.4kb downstream of *RTS1-AO* in a *ori-1253*Δ background is greatly suppressed by *rad52*Δ (Whitby lab unpublished data). However, I wanted to investigate whether there were any factors that might be limiting Rad52-mediated replication restart. It was recently reported that the DNA binding activity of Rad51 protects arrested replication forks from Exo1 mediated fork resection (Ait Saada et al. 2017). One way in which Rad52 might promote replication restart without Rad51 is by catalysing "inverse strand exchange" (Mazina et al. 2017; Kwon and Sung 2017). In this process Rad52 binds to a dsDNA (preferably one with a short ssDNA tail) and uses it to "invade" a homologous ssDNA molecule. Thus, in the absence of *rad51*, the Rad52-mediated pathway may be inhibited through the action of Exo1. If this is true, getting rid of *exo1* in a *rad51*Δ mutant might promote the Rad52 mediated pathway.

In strains where the *ade6*$^{-}$ repeats flank the barrier, there is ~2-fold reduction in both *RTS1-AO* induced gene conversions and deletions in an *exo1*Δ mutant compared to the wild-type (Figure 6.9). This is presumably due to a loss of DNA resection at the fork which would result in a shorter ssDNA tail onto which recombination proteins could load (Osman et al. 2016; Tsang et al. 2014; Zhu et al. 2008). Contrary to the idea that unfettered Exo1 activity might suppress Rad51-independent recombination, I observed no significant difference between a *rad51*△ single mutant and *exo1*Δ *rad51*Δ double mutant in the frequency of *RTS1-AO*-induced recombination either at the RFB ($p=0.37$ for deletions; $p=0.98$ for gene conversions) or at the reporter positioned 12.4 kb downstream of it ($p=0.2$ for deletions; $p=0.06$ for gene conversions) (Figure 6.9) Thus, it does not appear that Exo1 has a major negative effect on the ability of Rad52 to catalyse replication restart without Rad51.

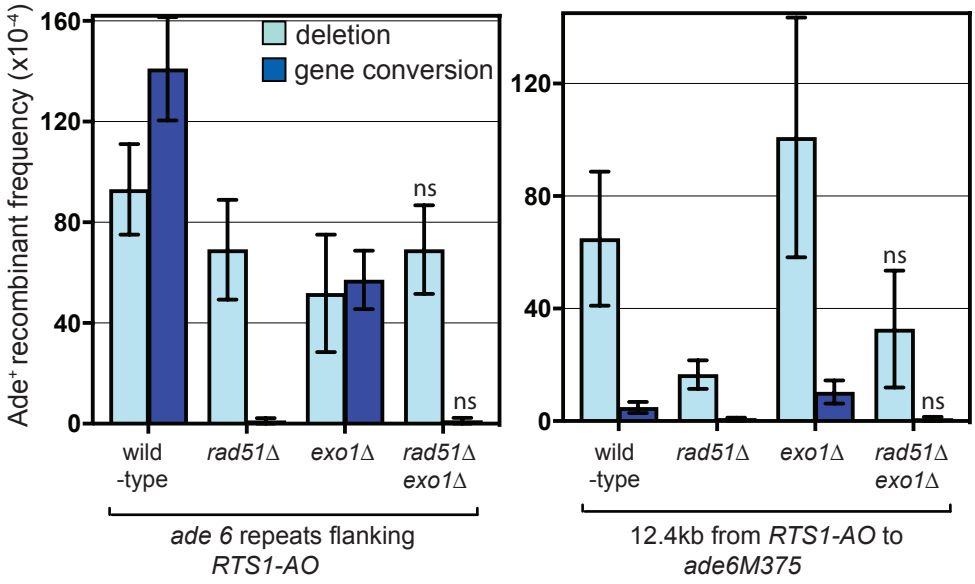

Figure 6.9 Effect of *exo1*Δ on Rad51-independent direct repeat recombination at and downstream of *RTS1-AO*
Bar charts showing the frequency and type of Ade+ recombinants in MCW4713, MCW1692, FO1742, MCW8950, MCW7259, MCW7814, MCW8218, MCW9034. Error bars represent standard deviation. Significant changes compared to the *rad51*Δ strains are indicated. P-values were calculated using the Shapiro-Wilk normality test (ns p>0.05, *p<0.05, **p<0.01, ***p<0.001). Ade+ recombinant frequency with statistical analysis is also shown in Table 1.

6.3 Discussion

Previous studies in both budding yeast and fission yeast have concluded that most RDR (either BIR in budding yeast or RDR from *RTS1* in fission yeast) depends on Rad51 (Sakofsky and Malkova 2017; Lambert et al. 2010; Ait Saada et al. 2017). Indeed, using both genetic assays and 2D gel analysis of replication intermediates, Lambert and co-workers previously concluded that there is very little if any replication restart from *RTS1* in a *rad51*Δ mutant (Lambert et al. 2010; Ait Saada et al. 2017). A Rad51-independent pathway of BIR in budding yeast, which depends on Rad52, Rad59, Mre11-Rad50-Xrs2 complex and Rdh54, was described more than 20 years ago (Malkova et al. 1996; Signon et al. 2001). However, it has remained poorly studied probably due to the fact that it was found to be a very inefficient pathway. The recent

findings that mammalian Rad52 localizes to sites of replication stress and facilitates the restart of collapsed forks by BIR independent of Rad51 and BRCA2 (Sotiriou et al. 2016), and is important for mitotic DNA synthesis activated by replication stress (MiDAS), by mediating DNA annealing from a collapsed replication fork into regions of micro-homology facilitating rapid completion of DNA synthesis (Bhowmick et al. 2016) has reawakened interest in the Rad51-independent pathway of replication restart.

In this chapter I have provided evidence that a seemingly robust Rad51-independent pathway of replication restart can operate following replication fork collapse at the *RTS1* RFB. However, this conclusion is based on an indirect measure of replication restart in which restart efficiency is inferred from the frequency of template switching that occurs downstream of the site of fork collapse and, therefore, it will be important in the future to verify my findings using a more direct physical assay to measure restart efficiency as discussed in Chapter 4. The first efforts to provide this direct evidence have recently been made in the Whitby lab, when 2D gel experiments revealed very little difference in the profile of replication intermediates at and around the *RTS1* barrier from wild-type and *rad51*Δ strains, suggesting that replication restart is reasonably efficient without Rad51 (unpublished data). The apparent contradictions with the studies from Lambert and co-workers (Lambert et al 2010) may be explained by the fact that in their studies the *RTS1* barrier protein, Rtf1, is overexpressed, whereas in the Whitby lab Rtf1 is expressed from its normal endogenous promoter. Conceivably Rad51-independent restart may be less able to promote restart at *RTS1* when there are excessive amounts of Rtf1 protein binding to the site.

One of the intriguing findings of my study is the differing effect of *ori-1253* deletion on the frequency of direct repeat recombination at and downstream of *RTS1*-

AO in a *rad51*Δ mutant. At the RFB and 0.2 kb downstream of it, deletion of *ori-1253* had little or no effect on the frequency of recombination, whereas at the 12.4 kb reporter site the frequency of recombination increased dramatically. The reason for this difference remains uncertain, however one plausible interpretation of these data is that Rad51-independent restart is much faster to initiate than the Rad51-dependent mechanism, perhaps because it does not depend on the formation of an elaborate Rad51 nucleofilament. Indeed, it might be fast enough to enable all cells to initiate restart and progress the restarted replication to the 0.2 kb reporter site before the arrival of the oncoming fork that originates from *ori-1253*. In this scenario, deleting *ori-1253* would not be needed to provide a sufficient window of time for maximal levels of restart to occur. Following on from this logic, the failure to detect *RTS1-AO*-induced template switching at the 12.4 kb reporter site in a *rad51*Δ *ori-1253*+ strain, and ability to detect it at reasonably high levels in a *rad51*Δ *ori-1253*Δ strain would imply that the progression of the restarted replication away from its site of initiation is much slower than the initiation process itself. As discussed below, the slow progression of Rad51-independent restarted replication may stem from an inhibitory effect of Rad55-Rad57.

My finding that template switch recombination, downstream of *RTS1*, is reasonably efficient in the absence of Rad55, Rdl1 and Swi5 suggested that either Rad51-dependent replication restart can operate without these mediators or that Rad51-independent restart is more efficient when they are absent. To determine which of these possibilities is correct one could test whether template switch recombination in a *rad55*Δ mutant depends on Rad51. If it does, then this would suggest that Rad51 can promote restart without Rad55. However, if a *rad55*Δ*rad51*Δ double mutant exhibits similar levels of template switching as a *rad55*Δ mutant, then this would

suggest that Rad55 inhibits the Rad51 independent restart pathway. This experiment is currently in progress (at the time of writing) but the initial findings indicate that Rad55 appears to be inhibiting the Rad51-independent restart pathway (Whitby lab unpublished data). Interestingly, Rad55-Rad57 has been shown to physically interact with Rad52 in both budding yeast and fission yeast (Gaines et al. 2015; Vo et al. 2016) and, therefore, it is possible that in the absence of Rad51 Rad55-Rad57 binds to Rad52 and inhibits its ability to promote efficient progression of restarted replication (Figure 6.10).

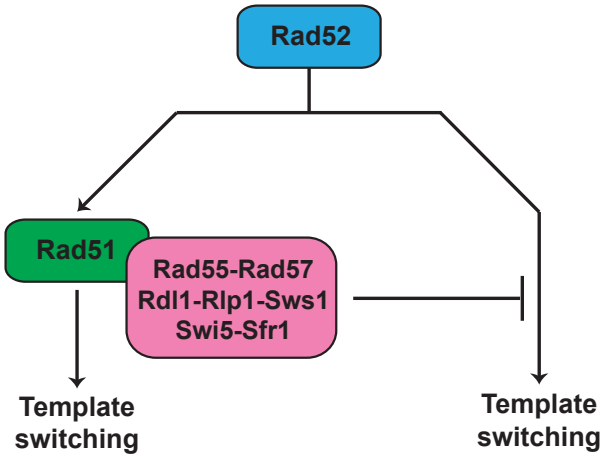

Figure 6.10 Model showing two different RDR pathways in fission yeast.
Rad52 is required for both pathways and is inhibited by the Rad51 mediator complex Rad55-Rad57 (possibly acting together with Rdl1-Rlp1-Sws1 and Swi5-Sfr1). The Rad51 pathway depends on Rad55-Rad57 and to a lesser extent on Rdl1-Rlp1-Sws1 and Swi5-Sfr1.

An intriguing feature of the Rad51-independent replication restart pathway is its ability to promote deletions without generating the same level of gene conversions as seen with the Rad51-dependent pathway. Template switching is thought to occur when the restarted replication, progressing in the form of a migrating D-loop, collapses (Nguyen et al 2015). Collapse would involve the dissociation of the D-loop releasing

its invading DNA strand. Presumably Rad51 and/or Rad52 would catalyse the re-invasion of the DNA strand so that DNA synthesis could continue. It is at this step that template switching would occur if the strand re-invades at an ectopic site. At the *ade6*$^{-}$ direct repeat reporter, used in my studies, a single template switch event from *ade6-M375* to *ade6-L469* would result in a deletion, whereas a gene conversion would require two template switch events - the first from *ade6-M375* to *ade6-L469* and the second from *ade6-L469* back to *ade6-M375* (Jalan et al. 2019). It would seem that such consecutive template switch events occur less frequently in the Rad51-independent pathway than they do in the Rad51-dependent pathway. In order to understand why consecutive template switch events may be less frequent in the Rad51-independent pathway, it will be necessary to establish the mechanism by which Rad52 promotes replication restart without Rad51. *In vitro* Rad52 is capable of catalysing D-loop formation, ssDNA annealing and inverse strand exchange (Kagawa et al. 2001; Stasiak et al. 2000; Fortin and Symington 2002; Mortensen et al. 1996; Mazina et al. 2017; Reddy et al. 1997). Future biochemical studies, using purified proteins, will be needed to determine whether one, or a combination, of these activities is sufficient for Rad52 to restart replication without Rad51.

During the course of my investigation I studied template switching downstream of *RTS1* using two different but related reporter constructs (Reporter System 1 and Reporter System 2). Whilst both reporters yielded similar levels of recombinants in *ori-1253*Δ strains, in *ori-1253*$^{+}$ background Reporter System 2 yielded consistently higher levels of recombinants than Reporter System 1. The reason for this difference remains unclear. However, a potential explanation stems from the fact that the Reporter System 2 *ori-1253*$^{+}$ strains were derived from a Reporter System 2 *ori-1253*Δ strain. It

is known that origin function is determined by both genetic and epigenetic processes and the accessibility of replication origins to initiation factors is regulated by epigenetic mechanisms (Méchali et al. 2013; Antequera 2004; Knott et al. 2009). It is therefore possible that deletion of *ori-1253* might have caused a change in the local chromatin environment which regulates the DNA replication program at the level of origin selection and activation (Eaton et al. 2011; Demczuk et al. 2012; Dorn and Cook 2011; Ding and MacAlpine 2011). It is conceivable that the re-introduction of *ori-1253* by genetic crossing does not fully re-establish the correct epigenetic environment for it to fire at full efficiency. Studies are on-going to determine the frequency of recombination in *ori-1253*$^{+}$ strains where Reporter System 2 has been introduced *de novo* via targeted integration.

Another intriguing finding from using Reporter System 2 was that the spontaneous and *RTS1-AO*-induced frequencies of FOA resistant colonies were much higher than expected based on data from similar experiments reported in the literature (Mayle et al. 2015; Iraqui et al. 2012). Moreover, the frequency of *RTS1-AO*-induced FOA resistant colonies was significantly higher in an *ori-1253*$^{+}$ background compared to *ori-1253*Δ, even though template switch recombination, adjacent to the *ura4* gene, was higher when *ori-1253* was deleted. The strains containing Reporter System 2 also contain a hygromycin resistance cassette positioned just upstream of *RTS1* (Figure 6.11). This cassette is flanked by promoter and terminator DNA sequences (“MX” DNA) that are homologous to the sequences surrounding *ura4*. Therefore a type of multi-invasion recombination, similar to that recently reported in budding yeast (Piazza et al. 2017; Piazza and Heyer 2018) could occur during the initiation of RDR. Multi-invasion recombination (MIR) has been reported to result in a chromosomal

rearrangement called multi-invasion-induced rearrangement whereby translocation between intact chromosomes is induced by a lesion on a third chromosome, occurring as a result of a broken DNA end simultaneously invading two intact donors (Piazza et al. 2017). In the case of Reporter System 2, an intra-chromosomal multi-invasion event could lead to the replacement of the *ura4+* gene with the *hyg* gene. This type of genomic rearrangement would be described as a “dispersed duplication with deletion” and, in a recent study, it was reported that 8.5% of subjects with autism spectrum disorder and other developmental abnormalities had more than one of this type of rearrangement in their genome (Collins et al. 2017). Preliminary analysis by Dr Judith Oehler in the Whitby lab has confirmed that the majority of FOA resistant colonies that are formed in wild-type and *rad51*Δ strains with *RTS1-AO* are indeed where *ura4* has been deleted and replaced by *hyg* (unpublished work).

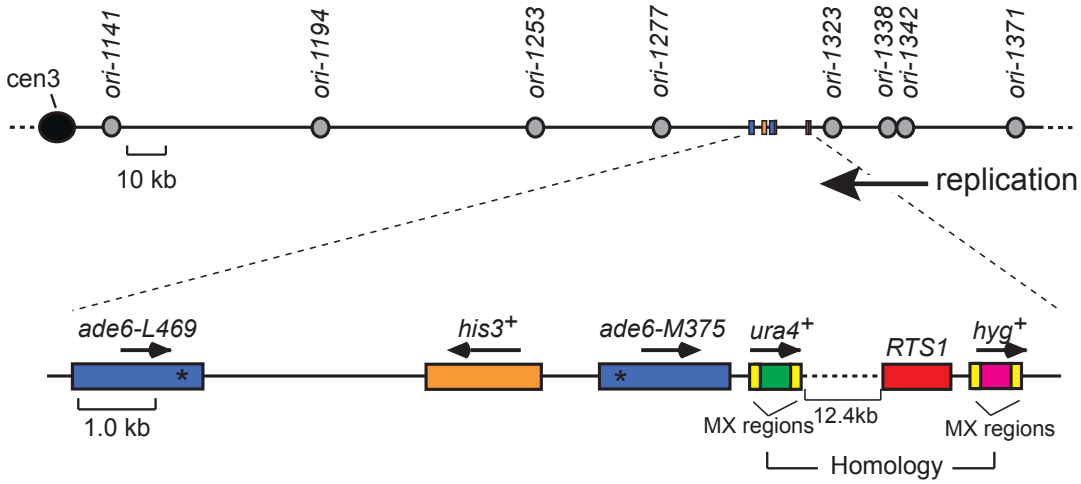

Figure 6.11 Homology between regions upstream and downstream of *RTS1* that may be used for multi-invasion recombination
Schematic showing the location of *RTS1* (with adjacent *hyg*MX cassette) and *ade6*$^{-}$ direct repeat (with adjacent *ura4*$^{+}$ gene flanked by MX DNA), in relation to nearby replication origins (grey circles) at the endogenous *ade6* locus on chromosome 3. The arrow depicting the direction of replication indicates the direction of the recombination dependent restarted fork through *ura4*$^{+}$ and *ade6*$^{-}$ direct repeat reporters.

A hypothetical model can be proposed for this event (Figure 6.12). Replication fork collapse at *RTS1* would lead to fork reversal and strand resection generating a ssDNA tail onto which RPA, Rad52 and Rad51 would sequentially load (W. Sun et al. 2008). Strand invasion of the ssDNA tail at the homologous sequences flanking *ura4* would create a MIR intermediate. This multi-invasion intermediate could be resolved by DNA structure-specific nucleases resulting in the deletion of *ura4* and its replacement by *hyg*. The increased frequency of FOA resistant colonies in *ori-1253*$^{+}$ cells compared to *ori-1253*Δ cells suggests that replication fork convergence may promote this type of rearrangement. Possibly the multi-invasion intermediate is stabilised by the arrival of the oncoming replication fork through the ligation of the 3' end of the invading DNA strand to the 5' end of the oncoming fork's lagging nascent strand (Figure 6.12).

MIR is thought to be dependent on Rad51 being a consequence of the multiplexed homology search (also referred to as inter-segmental contact sampling) that Rad51 catalyses (Forget and Kowalczykowski 2012). Indeed Rad51, together with Rad54, has been shown to catalyse the formation of multi-invasion intermediates *in vitro* (Wright and Heyer 2014). However, my finding that a *rad51*Δ mutant is more efficient at generating FOA resistant colonies, in which the *ura4* gene has been deleted and replaced by *hyg*, suggests that MIR can be catalysed without Rad51. In future studies it will be important to determine whether MIR can be catalysed directly by Rad52. It will also be interesting to investigate what factors limit the occurrence of this potentially deleterious genome rearrangement. In budding yeast Sgs1-Top3-Rmi1, Srs2 and Mph1 inhibit MIR (Piazza et al. 2017) and, therefore, current studies in the Whitby lab are investigating whether the equivalent factors in fission yeast limit the occurrence of the dispersed duplication with deletion rearrangement that stems from an aberrant attempt to restart replication.

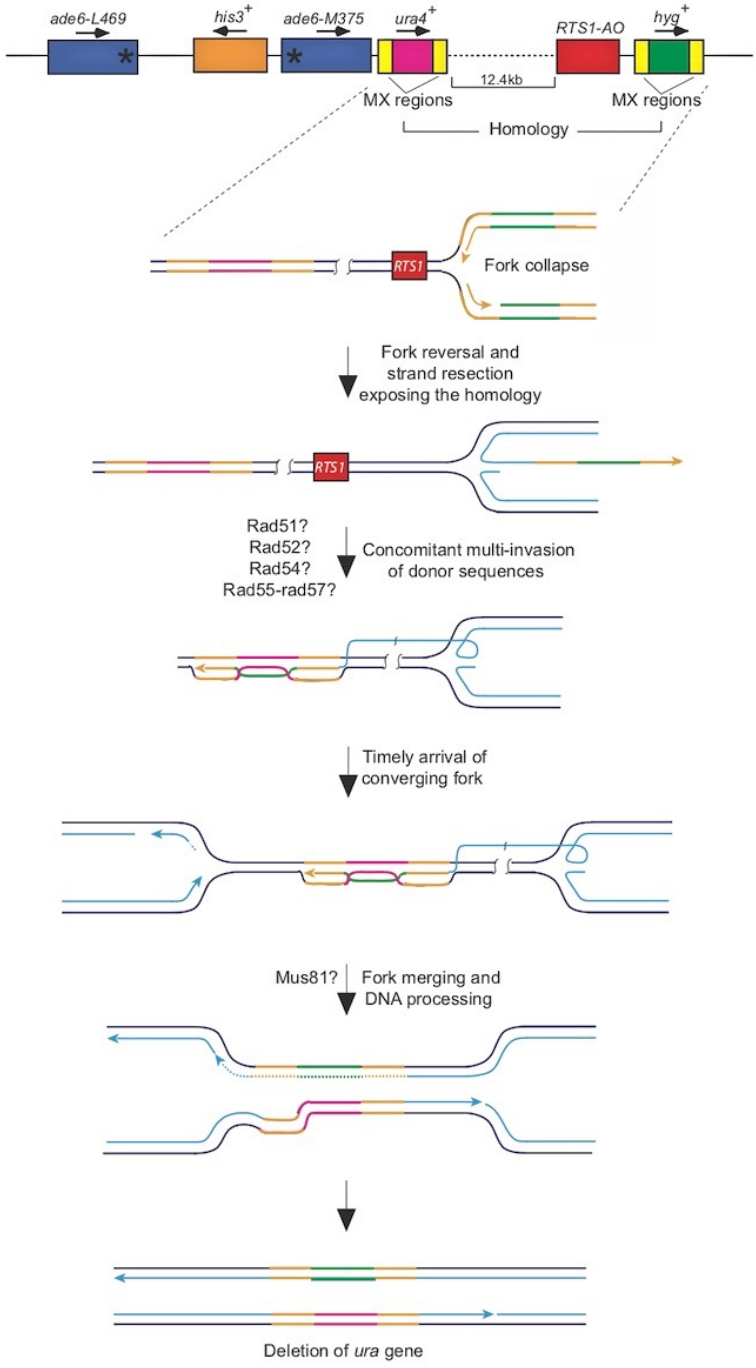

Figure 6.12 A hypothetical model for multi-invasion recombination leading to the loss of a *ura4* gene following replication fork collapse at a nearby site
Parental DNA strands are shown in black and nascent strands in light blue. Light blue arrows show the direction of replication. The patches of DNA highlighted in yellow represent homologous 'MX' regions. Fork reversal and strand resection, following fork collapse at *RTS1,* allows recombination proteins to bind to MX region DNA behind the RFB. The recombination proteins then catalyse strand invasion of the two homologous donor sequences concomitantly forming a multi-invasion recombination intermediate. This intermediate may be stabilised by the arrival of the oncoming replication fork through the ligation of the 3' end of the invading DNA strand to the 5' end of the oncoming fork's lagging nascent strand. However, the replacement of the *ura4* gene between the two homologous donor sequences with the hygromycin resistance gene flanked by the same homologous sequences on the invading strand would depend on a nuclease(s) making appropriate cuts at the junction points of the multi-invasion intermediate.

7 Concluding remarks

Replication fork collapse is thought to involve either replisome remodelling and/or disassembly, which paves the way for HR proteins to restart replication by RDR (Ahn et al. 2005; Lambert and Carr 2005; Lambert et al. 2010). RDR is essential for completing DNA synthesis and avoiding mitotic catastrophe. Despite their importance, the molecular details of RF collapse and RDR are poorly understood. The main aim of my project was to discover whether active disassembly of the replisome was necessary for RDR to occur, with specific focus on PCNA, which is an integral component of the replisome and acts as a processivity factor for the replicative DNA polymerases. It is a homotrimeric ring that is actively loaded onto DNA by RFC and needs to be unloaded from the DNA after the replication of each Okazaki fragment. The Elg1 protein forms an RFC-like complex that is known to unload PCNA from the DNA (Parnas et al. 2010; Kubota et al. 2013; Aurèle Piazza and Heyer 2018). In order to understand whether active unloading of PCNA from DNA is needed for RDR to occur, I investigated the role of Elg1 in RDR induced by the polar *RTS1* RFB. I discovered that Elg1 is needed for direct repeat recombination induced by *RTS1* at the *ade6* locus on Chromosome 3. With further observations that PCNA persists on the DNA much later in the cell cycle in an *elg1*Δ mutant, and that a disassembly-prone PCNA mutant suppresses *elg1*Δ induced hypo-recombination, I was able to draw a strong correlation between Elg1's role in promoting *RTS1*-induced recombination and unloading PCNA from the blocked fork, thus, suggesting that PCNA unloading is critical for efficient RDR.

Apart from showing that Elg1 was needed for recombination induced from a collapsed fork, I was also able to demonstrate that Elg1 is capable of supressing recombination, given the circumstances are different. I observed that Elg1 was needed to suppress recombination when *RTS1* is replaced by *ter2X3* which has been reported

to only transiently stall forks without inducing fork collapse, and when *RTS1* is placed at a sub-telomeric site on chromosome 1, where there is limited *RST1*-induced recombination due to high fork convergence. This finding supported previous reports of Elg1 being needed to both promote (Ogiwara et al. 2007) and suppress (Ben-Aroya et al. 2003) recombination in budding yeast. However, it still remains to be clarified what determines the dual role of Elg1 in recombination. It may be through its role in PCNA unloading or via a role that is independent of its interaction with PCNA (Parnas et al. 2011; Parnas et al. 2010; Davidson and Brown 2008).

Along with its function as a polymerase clamp, PCNA is known for its striking ability to interact with multiple factors required for DNA replication, DNA repair, cell cycle regulation and chromatin assembly (Moldovan et al. 2007; Gazy and Kupiec 2012; Moldovan et al. 2006; Maga and Hübscher 2003). It is possible that the prolonged presence of PCNA at the RFB in an *elg1*Δ mutant could be affecting the frequency of inter-repeat recombination, either directly or indirectly through its interacting partners. I was thus inclined to test some candidate PCNA interacting factors, like Srs2, Fml1, Eso1 and Fbh1, which are implicated in *RTS1*-induced recombination, for their role in the hypo-recombination phenotype of an *elg1*Δ mutant. I was able to succesfully identify the helicase Fbh1 as the factor responsible for supressing the majority of the direct repeat recombination promoted by Elg1 at *RTS1*. PCNA recruits FBH1 to sites of DNA replication and DNA damage in humans (Bacquin et al. 2013), but the PCNA interacting motifs in human FBH1 do not appear to be conserved in fission yeast Fbh1. Thus, it remains to be determined whether increased retention of PCNA at the barrier leads to greater Fbh1 recruitment or facilitates its activity by some other means.

Furthermore, it was unclear whether increased Fbh1 activity at the RFB only limits ectopic recombination or whether it is also a barrier to efficient replication restart. In Chapter 4, I went on to establish by snap shot and time-lapse imaging, that Elg1 is indeed required for the efficient recruitment of both Rad51 and Rad52 to the *RTS1* barrier. This correlates with the reduction in both Rad51-dependent and Rad51-independent direct repeat recombination in an *elg1*Δ mutant and suggests that replication restart is likely to be delayed and/or impaired. *fbh1* overexpression is known to reduce DNA damage-induced Rad51 foci while having no effect on Rad52 foci formation (Lorenz et al. 2009). Thus, the observed reduced number of Rad52 foci at *RTS1* in an *elg1*Δ mutant points towards the possibility that Elg1 counteracts Fbh1 not by limiting its recruitment to the RFB, but by ensuring that its key antagonist Rad52 is efficiently recruited. Moreover, I also observed that presence of PCNA at the barrier correlated with the reduction of the co-localization of Rad52 in an *elg1*Δ mutant, suggesting that PCNA accumulated at the barrier either recruits factors that inhibit Rad52 recruitment, or inhibits processing of the fork that is necessary for Rad52 recruitment.

In Chapter 5, I investigated Ctf18 as a prospective loader/unloader of PCNA in RDR at *RTS1* as it has been implicated in both functions by various studies (V. P. Bermudez et al. 2003; Fujisawa et al. 2017; Shiomi et al. 2004; Bylund and Burgers 2005). I made a significant discovery that Ctf18 suppresses Elg1-dependent recombination. This enabled me to devise a model encompassing the roles of Elg1 and Ctf18 in recombination at collapsed RFs. Elg1 promotes recombination at collapsed RFs by unloading PCNA from the DNA which counteracts the loading activity of Ctf18. In the absence of Elg1, PCNA persists on the DNA acting as a platform for the recruitment of Fbh1 and/or a block to the recruitment of Rad52. It will

be important to investigate the genetic interaction between *ctf18*Δ and *fbh1*Δ to test my hypothesis.

The final chapter of my thesis covers another important mechanistic aspect of RDR. By the use of genetic assays, I have made some interesting revelations about the poorly understood Rad51-independent pathway of RDR. Given that previous studies in both budding yeast and fission yeast have concluded that most RDR depends on Rad51 (Sakofsky and Malkova 2017; Lambert et al. 2010; Ait Saada et al. 2017), my findings could contribute towards a change in this narrative. I have provided evidence that a seemingly robust Rad51-independent pathway of replication restart can operate following replication fork collapse at the *RTS1* RFB. My data indicate that Rad51-independent replication restart initiates faster than the Rad51-dependent mechanism, possibly because it does not involve an elaborated Rad51 nucleofilament formation. However, the restarted fork in the Rad51-independent pathway progresses slower compared to the Rad51 dependent restarted fork. Mediators of Rad51 were an important part of my investigation and there is indication that mediators like Rad55-Rad57 bind to Rad52 and thus inhibit its ability to promote efficient progression of restarted RFs. Using a genetic reporter, I observed template switch events during the progression of the restarted fork, probably due to frequent dissociation of the migrating D-loop and re-invasion of the DNA strand. Template switch occurs when the dissociated nascent strand re-invades at an ectopic site, with a single template switch giving rise to deletions and consecutive template switch events giving rise to gene conversions. An interesting feature of the Rad51-independent replication restart pathway is that it generates deletions but relatively few gene conversions as compared with the Rad51-dependent pathway. In future studies it will be important to investigate the nature of the restarted fork by establishing the

mechanism by which Rad52 promotes replication restart without Rad51 and determining what biochemical activities of Rad52 are involved. This is especially important in the light of recent findings in mammalian cells that Rad52 localizes to sites of oncogene-induced replication stress where it facilitates the restart of collapsed forks by BIR independently of Rad51 and BRCA2 (Sotiriou et al. 2016), and also drives mitotic DNA synthesis (MiDAS) to help prevent incomplete replication impeding successful chromosome segregation (Bhowmick et al. 2016).

Along with many interesting revelations, there are also many unanswered questions that have been discussed in the different chapters of this thesis. However two key immediate goals are: 1) direct analysis of the recruitment of proteins like Fbh1 to the *RTS1* RFB and its interaction with PCNA by employing methods like chromatin immunoprecipitation (ChIP), co-immunoprecipitation (co-IP) and pull-down assays; 2) establishing a more direct measure of replication restart efficiency from the *RTS1* RFB, using physical assays like DNA fibre analysis or DNA combing, which would enable proper calibration of my template switch data and provide a definitive measure of how much restart actually happens without Elg1 and Rad51 (Kaykov and Nurse 2015; Patel et al. 2006). Better understanding of the process of replication restart from collapsed forks is important as they are associated with genomic rearrangements (Morrow et al. 2017; Nguyen et al. 2015; Ahn et al. 2005; Lambert et al. 2005; Lambert et al. 2010; Mizuno et al. 2009; Iraqui et al. 2012) which are the hallmarks of many diseases including cancer. Therefore, understanding the nature of the restarted fork may eventually open new doors for treating cancer and other diseases.

Appendix

Table 1: Direct repeat recombinant frequencies *(RTS1)*

Genotype and Strain no.	*RTS1* orientation[a]	Position of direct repeat relative to *RTS1*[b]	Number of colonies analysed	Ade$^+$ His$^-$ recombinant frequency (X10^{-4})[c]		Ade$^+$ His$^+$ recombinant frequency (X10^{-4})[c]	
				Mean	*P* value[d]	Mean	*P* value[d]
wild-type MCW 4712	IO	Flanking	44	3.09 (±0.59)	-	1.17 (±0.33)	-
wild-type MCW 4713	AO	Flanking	51	93.09 (±17.97)	<0.0001[f]	141 (±20.56)	<0.0001[f]
ori-1253Δ MCW 6894	IO	Flanking	9	5.31 (±1.42)	0.0001[f]	1.99 (±0.29)	<0.0001[f]
ori-1253Δ MCW 6778	AO	Flanking	8	158.1 (±32.49)	<0.0001[g]	275.9 (±64.41)	<0.0001[g]
wild-type MCW 7132	IO	0.2 kb downstream	9	2.85 (±0.86)	0.304[f]	1.00 (±0.34)	0.166[f]
wild-type MCW 7134	AO	0.2 kb downstream	13	688.4 (±203.1)	<0.0001[h]	123.6 (±40.11)	<0.0001[h]
ori-1253Δ MCW 7415	IO	0.2 kb downstream	13	2.65 (±0.92)	0.610[h]	1.20 (±0.54)	0.331[h]
ori-1253Δ MCW 7417	AO	0.2 kb downstream	10	320.8 (±130.3)	<0.0001[i]	258.7 (±81.95)	<0.0001[i]
wild-type MCW 7257	IO	12.4 kb downstream	40	1.58 (±0.42)	<0.0001[f]	0.82 (±0.21)	<0.0001[f]
wild-type MCW 7259	AO	12.4 kb downstream	47	64.8 (±23.82)	<0.0001[j]	4.87 (±1.97)	<0.0001[j]
ori-1253Δ MCW 7293	IO	12.4 kb downstream	38	3.43 (±0.89)	<0.0001[j]	1.81 (±0.44)	<0.0001[j]
ori-1253Δ MCW 7295	AO	12.4 kb downstream	40	701.9 (±261.3)	<0.0001[k]	118.4 (±41.32)	<0.0001[k]
elg1Δ MCW 7706	IO	Flanking	51	3.82 (±0.86)	<0.0001[f]	1.85 (±0.59)	<0.0001[f]
elg1Δ	AO	Flanking	41	25.27 (±4.47)	<0.0001[g]	6.87 (±1.17)	<0.0001[g]

MCW 7708							
pof3Δ MCW 7710	IO	Flanking	15	5.21 (±1.42)	<0.0001[f]	2.02 (±0.73)	<0.0001[f]
pof3Δ MCW 7712	AO	Flanking	25	103.8 (±33.94)	0.1494[g]	60.76 (±29.79)	<0.0001[g]
ctf18Δ MCW 8404	IO	Flanking	17	4.69 (±1.52)	<0.001[f]	1.48 (±0.71)	0.099[f]
ctf18Δ MCW 8406	AO	Flanking	28	166.3 (±76.92	<0.0001[g]	319.3 (±86.91)	<0.0001[g]
elg1Δ ctf18Δ MCW 8408	IO	Flanking	17	3.41 (±0.70)	0.0836[f]	0.63 (±0.13)	<0.0001[f]
elg1Δ ctf18Δ MCW 8410	AO	Flanking	18	26.64 (±4.79)	<0.0001[g]	6.42 (±1.78)	<0.0001[g]
srs2Δ FO 1748	IO	Flanking	17	9.38 (±2.37)	<0.0001[f]	12.19 (±5.35)	<0.0001[f]
srs2Δ FO 1750	AO	Flanking	19	444 (±120.4)	<0.0001[g]	1078 (±229.8)	<0.0001[g]
elg1Δ srs2Δ MCW 8328	IO	Flanking	17	10.87 (±1.94)	<0.0001[f]	17.11 (±1.93)	<0.0001[f]
elg1Δ srs2Δ MCW 8330	AO	Flanking	18	111.2 (±27.55)	0.0161[g]	82.71 (±14.05)	<0.0001[g]
fbh1Δ FO 1816	AO	Flanking	30	1908 (±394.2)	<0.0001[g]	651 (±217.8)	<0.0001[g]
elg1Δ fbh1Δ MCW 8946	AO	Flanking	12	2066 (±844.9)	<0.0001[g]	395.1 (±124.9)	<0.0001[g]
fml1Δ MCW 4752	AO	Flanking	7	146.1 (±50.45)	0.0318[g]	17.87 (±10.19)	<0.0001[g]
elg1Δ fml1Δ MCW 8431	AO	Flanking	9	49.22 (±19.52)	<0.0001[g]	2.0 (±1.0)	<0.0001[g]
wpl1Δ MCW 8919	IO	Flanking	5	3.96 (±0.91)	0.005[f]	1.45 (±0.63)	0.39[f]
wpl1Δ MCW 8920	AO	Flanking	5	107 (±25.87)	0.117[g]	94.98 (±46.23)	0.09[g]

elg1Δ wpl1Δ MCW 8995	IO	Flanking	10	3.82 (±0.80)	0.002[f]	1.38 (±0.32)	0.08[f]
elg1Δ wpl1Δ MCW 8998	AO	Flanking	7	29.66 (±4.71)	<0.0001[g]	15.31 (±5.09)	<0.0001[g]
ctf18Δ MCW 8597	IO	12.4 kb downstream	10	7.72 (±1.10)	<0.0001[j]	1.01 (±0.30)	0.026[j]
ctf18Δ MCW 8598	AO	12.4 kb downstream	9	259.9 (±91.59)	<0.001[k]	33.57 (±11.77)	<0.0001[k]
ctf18Δ ori-1253Δ MCW 8822	IO	12.4 kb downstream	14	6.02 (±1.68)	0.011[l]	3.22 (±0.88)	<0.0001[l]
ctf18Δ ori-1253Δ MCW 8763	AO	12.4 kb downstream	36	145.5 (±45.38)	0.005[m]	43.2 (±11.62)	0.032[m]
rad51Δ MCW 1691	IO	Flanking	44	15.6 (±4.08)	<0.0001[f]	0.02 (±0.06)	<0.0001[f]
rad51Δ MCW 1692	AO	Flanking	45	69.12 (±19.85)	<0.0001[g]	1.05 (±1.11)	<0.0001[g]
rad51Δ ori-1253Δ MCW 8837	IO	Flanking	13	22.31 (±6.13)	<0.0001[n]	0.05 (±0.05)	.040[n]
rad51Δ ori-1253Δ MCW 8835	AO	Flanking	10	57.29 (±10.56)	0.014[o]	0.62 (±0.49)	0.065[o]
rad51Δ MCW 8788	IO	0.2 kb downstream	17	9.01 (±2.77)	<0.0001[h]	0.02 (±0.02)	<0.0001[h]
rad51Δ MCW 8790	AO	0.2 kb downstream	13	344.8 (±81.79)	<0.0001[i]	16.54 (±4.62)	<0.0001[i]
rad51Δ ori-1253Δ MCW 8792	IO	0.2 kb downstream	14	15.65 (±4.52)	<0.0001[p]	0.03 (±0.06)	0.379[p]
rad51Δ ori-1253Δ MCW 8793	AO	0.2 kb downstream	14	228.9 (±55.06)	<0.001[q]	7.33 (±5.81)	<0.0001[q]
rad51Δ MCW 7812	IO	12.4 kb downstream	15	17.73 (±3.66)	<0.0001[j]	0.26 (±028)	<0.0001[j]
rad51Δ MCW 7814	AO	12.4 kb downstream	13	16.44 (±5.09)	<0.0001[k]	0.68 (±0.57)	0.0001[k]

rad51Δ ori-1253Δ MCW 8766	IO	12.4 kb downstream	19	20.63 (±10.15)	0.261[r]	0 (±0)	0.003[r]
rad51Δ ori-1253Δ MCW 8765	AO	12.4 kb downstream	17	622 (±215.1)	<0.0001[s]	11.33 (±8.09)	<0.0001[s]
rad55Δ MCW 7588	IO	12.4 kb downstream	18	8.25 (±2.82)	<0.0001[j]	0.01 (±0.02)	<0.0001[j]
rad55Δ MCW 7590	AO	12.4 kb downstream	19	82.61 (±24.85)	0.0085[k]	1.18 (±0.56)	<0.0001[k]
rad55Δ ori-1253Δ MCW 7592	IO	12.4 kb downstream	18	6.86 (±1.95)	0.095[t]	0.07 (±0.06)	<0.001[t]
rad55Δ ori-1253Δ MCW 7594	AO	12.4 kb downstream	22	406.9 (±120.1)	<0.0001[u]	9.29 (±5.17)	<0.0001[u]
swi5Δ MCW 7555	IO	12.4 kb downstream	21	3.23 (±0.86	<0.0001[j]	0.90 (±0.22)	0.167[j]
swi5Δ MCW 7557	AO	12.4 kb downstream	18	94.01 (±21.81)	<0.0001[k]	5.45 (±3.76)	<0.542[k]
swi5Δ ori-1253Δ MCW 7559	IO	12.4 kb downstream	23	4.8 (±1.03)	<0.0001[v]	1.95 (±0.70)	<0.0001[v]
swi5Δ ori-1253Δ MCW 7561	AO	12.4 kb downstream	24	608 (±141.9)	<0.0001[w]	50.68 (±20.03)	<0.0001[w]
rad55Δ swi5Δ MCW 7607	IO	12.4 kb downstream	5	20.73 (±6.30)	0.002[j]	0.11 (±0.10)	<0.0001[j]
rad55Δ swi5Δ MCW 7609	AO	12.4 kb downstream	9	145.5 (±48.44)	<0.001[k]	1.88 (±1.73)	<0.0001[k]
rad55Δ swi5Δ ori-1253Δ MCW 7611	IO	12.4 kb downstream	8	16.33 (±6.87)	0.272[x]	0.03 (±0.08)	0.146[x]
rad55Δ swi5Δ ori-1253Δ MCW 7613	AO	12.4 kb downstream	10	497.8 (±275.5)	0.003[y]	6.08 (±3.53	0.005[y]
rdl1Δ MCW 8931	IO	12.4 kb downstream	14	5.50 (±1.26)	<0.0001[j]	1.03 (±0.70)	0.288[j]
rdl1Δ MCW 9140	AO	12.4 kb downstream	26	98.46 (±33.82	<0.0001[k]	2.80 (±1.20)	<0.0001[k]
rad54Δ MCW 9030	IO	12.4 kb downstream	14	6.60 (±1.99)	<0.0001[j]	0.03 (±0.54)	<0.0001[j]
rad54Δ	AO	12.4 kb	13	18.17	<0.0001[k]	0.70	<0.0001[k]

MCW 9013		downstream		(±7.73		(±0.50)	
rad54^{K300A} MCW 9006	IO	12.4 kb downstream	14	4.38 (±1.91)	0.0001[j]	0.00 (±0.01)	<0.0001[j]
rad54^{K300A} MCW 9008	AO	12.4 kb downstream	17	24.53 (±11.14	<0.0001[k]	1.02 (±0.86)	<0.0001[k]
exo1Δ FO1742	AO	Flanking	21	51.80 (±23.30)	<0.001[g]	57.1 (±11.60)	<0.001[g]
rad51Δ exo1Δ MCW 8950	AO	Flanking	16	69.2 (±17.58)	<0.001[g]	1.11 (±1.17)	<0.001[g]
exo1Δ MCW 8218	AO	12.4 kb downstream	12	100.75 (±42.63)	<0.01[k]	10.32 (±4.12)	<0.001[k]
rad51Δ exo1Δ MCW 9034	AO	12.4 kb downstream	11	32.60 (±20.80)	<0.001[k]	0.65 (±0.88)	<0.001[k]
5kb spacer[e] MCW 8023	AO	Flanking	8	827.9 (±379.2)	<0.001[g]	206 (±148.6)	0.256[g]
rad51Δ 5kb spacer[e] MCW 8136	AO	Flanking	11	778 (±217.50)	0.720[aa]	7.87 (±5.37)	0.007[aa]
elg1Δ 5kb spacer[e] MCW 8941	AO	Flanking	17	90.06 (±39.47)	<0.001[aa]	9.40 (±4.63)	0.0076[aa]
rad51Δ elg1Δ 5kb spacer[e] MCW 8943	AO	Flanking	10	397.10 (±143)	0.0145 [aa]	0.00 (±0.00)	0.0057[aa]
sub-telomeric site on chromosome I[§] wild type MCW 6472	-	Flanking	7	0.051 (±0.04)	-	0.71 (±0.17)	-
sub-telomeric site on chromosome I[§] wild type MCW 6557	IO	Flanking	8	0.67 (±0.24)	<0.0001[bb]	3.91 (±0.79)	<0.0001[bb]
sub-telomeric site on chromosome I[§] wild type MCW 6474	AO	Flanking	10	0.95 (±0.35)	0.085[cc]	4.46 (±0.81)	0.167[cc]
sub-telomeric site on	-	Flanking	10	3.62	<0.0001[bb]	1.29	0.004[bb]

chromosome I[§] *elg1Δ* MCW 8204				(±0.76)		(±0.48)	
sub-telomeric site on chromosome I[§] *elg1Δ* MCW 8206	IO	Flanking	8	4.83 (±0.52)	<0.0001[cc]	1.19 (±0.21)	<0.0001[cc]
sub-telomeric site on chromosome I[§] *elg1Δ* MCW 8208	AO	Flanking	10	3.71 (±0.56)	<0.0001[dd]	1.93 (±0.32)	<0.0001[dd]
wild-type[#] MCW 9036	IO	12.4 kb downstream	32	3.98 (±1.49)	-	1.95 (±0.78)	-
wild-type[#] MCW 9039	AO	12.4 kb downstream	42	299.3 (±93.29)	<0.001[ee]	14.51 (±5.88)	<0.001[ee]
ori-1253Δ[#] MCW 8700	IO	12.4 kb downstream	18	3.98 (±1.61)	0.754[ee]	2.23 (±1.23)	0.148[ee]
ori-1253Δ[#] MCW 8888	AO	12.4 kb downstream	23	792.5 (±273.3)	<0.001[ff]	100.3 (±32.35)	<0.001[ff]
elg1Δ[#] MCW 9026	IO	12.4 kb downstream	11	3.059 (±1.24)	0.072[ee]	0.65 (±0.32)	<0.001[ee]
elg1Δ[#] MCW 8992	AO	12.4 kb downstream	13	12.06 (±8.28)	<0.001[ff]	0.72 (±0.23)	<0.001[ff]
elg1Δ *ori-1253Δ*[#] MCW 8988	IO	12.4 kb downstream	12	3.78 (±1.6)	0.74[gg]	0.71 (±0.56)	<0.001[gg]
elg1Δ *ori-1253Δ*[#] MCW 8990	AO	12.4 kb downstream	10	74.31 (±26.4)	<0.001[hh]	6.26 (±3.65)	<0.001[hh]
rad51Δ[#] MCW 9028	IO	12.4 kb downstream	22	12.37 (±4.79)	<0.0001[ee]	0.01 (±0.03)	<0.0001[ee]
rad51Δ[#] MCW 9004	AO	12.4 kb downstream	24	70.79 (±29.72)	<0.001[ff]	1.50 (±0.77)	<0.001[ff]
rad51Δ *ori-1253Δ*[#] MCW 9000	IO	12.4 kb downstream	20	18.35 (±5.30)	<0.001[gg]	0.03 (±0.10	0.718[gg]

rad51Δ *ori-1253Δ*[#] MCW 9002	AO	12.4 kb downstream	22	495 (±170.7)	<0.001[hh]	15.16 (±5.67)	<0.001[hh]
PCNA-D150E MCW 9183	IO	flanking	21	17.74 (±8.59)	<0.001[f]	8.88 (±3.02)	<0.001[f]
elg1Δ PCNA-D150E MCW 9187	IO	flanking	23	18.19 (±3.96)	0.830[ii]	11.06 (±2.74)	0.016[ii]
PCNA-D150E MCW 9185	AO	Flanking	17	113.5 (±56.36)	0.160[g]	177.1 (±78.91)	0.079[g]
elg1Δ PCNA-D150E MCW 9189	AO	Flanking	14	126.7 (±33.08)	0.561[jj]	151.3 (±34)	0.789[jj]

a-*RTS1* is integrated at the ade6 locus either between a direct repeat of ade6- alleles or replacing ade6, except for strains marked §. In strains without *RTS1*, the ade6 gene is deleted from its normal locus; b-The different positions of the ade6$^-$ direct repeat recombination reporters are shown in Figure 6.5, Fig.6.6 and Fig.6.7; c-The values in parentheses are the standard deviations about the mean; d-P values are derived from independent-sample t-tests comparing the mean values as indicated; e-strain with *RTS1* integrated at the ade6 locus between a direct repeat of ade6$^-$ alleles, with a 5kb spacer DNA inserted on the centromere-proximal side of *RTS1*; f-compared to the equivalent mean recombinant frequency of MCW 4712; g-compared to the equivalent mean recombinant frequency of MCW 4713; h-compared to the equivalent mean recombinant frequency of MCW 7132; i-compared to the equivalent mean recombinant frequency of MCW 7134; j-compared to the equivalent mean recombinant frequency of MCW 7257; k-compared to the equivalent mean recombinant frequency of MCW 7259; l-compared to the equivalent mean recombinant frequency of MCW 8597; m-compared to the equivalent mean recombinant frequency of MCW 8598; n-compared to the equivalent mean recombinant frequency of MCW 1691; o-compared to the equivalent mean recombinant frequency of MCW 1692; p-compared to the equivalent mean recombinant frequency of MCW 8788; q-compared to the equivalent mean recombinant frequency of MCW 8790; r-compared to the equivalent mean recombinant frequency of MCW 7812; s-compared to the equivalent mean recombinant frequency of MCW 7814; t-compared to the equivalent mean recombinant frequency of MCW 7588; u-compared to the equivalent mean recombinant frequency of MCW 7590; v-compared to the equivalent mean recombinant frequency of MCW 7555; w-compared to the equivalent mean recombinant frequency of MCW 7557; x-compared to the equivalent mean recombinant frequency of MCW 7607; y-compared to the equivalent mean recombinant frequency of MCW 7609; z-compared to the equivalent mean recombinant frequency of MCW 8931; aa-compared to the equivalent mean recombinant frequency of MCW 8023; bb-compared to the equivalent mean recombinant frequency of MCW 6472; cc-compared to the equivalent mean recombinant frequency of MCW 6557; dd-compared to the equivalent mean recombinant frequency of MCW 6474; ee-compared to the equivalent mean recombinant frequency of MCW 9036; ff-compared to the equivalent mean recombinant frequency of MCW 9039; gg-compared to the equivalent mean recombinant frequency of MCW 8700; hh-compared to the equivalent mean recombinant frequency of MCW 8888; ii-compared to the equivalent mean recombinant frequency of MCW 9183; jj-compared to the equivalent mean recombinant frequency of MCW 9185; §- strain with *RTS1* between a direct repeat of ade6$^-$ alleles placed at a sub-telomeric site on chromosome1; #- strain with reporter system 2 (ade6$^-$ direct repeat reporter adjacent to a *ura4*$^+$ reporter) as shown in Figure 6.8a

Table 2:Direct repeat recombination *(Ter2*x3*)*

Genotype and Strain no.	*Ter2*X3 orientation[a]	Position of direct repeat relative to *Ter2*X3	Number of colonies analysed	Ade$^+$ His$^-$ recombinant frequency (X10^{-4})[b]		Ade$^+$ His$^+$ recombinant frequency (X10^{-4})[b]		% gene conversion[b]
				Mean	*P* value[c]	Mean	*P* value[c]	
wild-type MCW 7045	1	Flanking	31	5.06 (±1.32)	-	1.18 (±0.37)	-	18.45
wild-type MCW 7046	2	Flanking	33	4.51 (±0.96)	0.061[d]	1.38 (±0.34)	0.060[d]	25.35
elg1Δ MCW 8130	1	Flanking	13	6.80 (±0.82)	<0.0001[d]	2.26 (±0.67)	<0.0001[d]	22.05
elg1Δ MCW 8132	2	Flanking	17	6.48 (±0.79)	<0.0001[e]	5.58 (±1.42)	<0.0001[e]	45.77

a-*Ter2*X3 is integrated at the ade6 locus between a direct repeat of ade6- alleles; b-The values in parentheses are the standard deviations about the mean; c-P values are derived from independent-sample t-tests comparing the mean values as indicated; d-compared to the equivalent mean recombinant frequency of MCW 7045; e-compared to the equivalent mean recombinant frequency of MCW 7046.

Table 3:direct repeat recombination frequencies (*RTS1* live-cell imaging)

Genotype and Strain no	*RTS1* orientation[a]	Number of colonies analysed	Ade$^+$ His$^-$ recombinant frequency (X10^{-4})[b]		Ade$^+$ His$^+$ recombinant frequency (X10^{-4})[b]		% gene conversion[b]
			Mean	*P* value[c]	Mean	*P* value[c]	
wild type, 115X*lacO* LacI, Rad52-YFP, ECFP-PCNA MCW 6712	IO	7	1.71 (±0.15)	-	0.25 (±0.08)	-	12.91
wild type, 115X*lacO* LacI, Rad52-YFP, ECFP-PCNA MCW 7065	AO	5	174.4 (±17.29)	<0.0001[d]	73.14 (±8.88)	<0.0001[d]	29.6
elg1Δ, 115X*lacO* LacI, Rad52-YFP, ECFP-PCNA MCW 7969	IO	8	1.14 (±0.19)	<0.0001[d]	0.34 (±0.14)	0.199[d]	22.3

elg1Δ, 115X*lacO* LacI, Rad52-YFP, ECFP-PCNA MCW 7965	AO	6	29.31 (±2.76)	<0.0001[e]	11.14 (±2.65)	<0.0001[e]	27.38
wild type, 115X*lacO* LacI, Rad52-YFP MCW 6395	IO	10	2.24 (±0.98)	-	0.40 (±0.13)	-	16.42
wild type, 115X*lacO* LacI, Rad52-YFP MCW 6556	AO	7	234.8 (±54.63)	<0.0001[f]	105.1 (±16.7)	<0.0001[f]	31.58
elg1Δ, 115X*lacO* LacI, Rad52-YFP MCW 8484	IO	10	2.98 (±0.44)	0.047[f]	0.41 (±0.06)	<0.844[f]	12.73
elg1Δ, 115X*lacO* LacI, Rad52-YFP MCW 8486	AO	10	31.11 (±3.10)	<0.0001[g]	10.07 (±2.25)	<0.0001[g]	24.46

a-*RTS1* is integrated at the ade6 locus between a direct repeat of ade6^{-} alleles; b-The values in parentheses are the standard deviations about the mean; c-P values are derived from independent-sample t-tests comparing the mean values as indicated; d-compared to the equivalent mean recombinant frequency of MCW 6712; e-compared to the equivalent mean recombinant frequency of MCW 7065; f-compared to the equivalent mean recombinant frequency of MCW 6395; g-compared to the equivalent mean recombinant frequency of MCW 6556;

Table 4: List of *S. pombe* strains used in this study

Strain number	Mating type	Genotype	
FO 1748	h^+	*srs2Δ::ura4+ ura4-D18 leu1-32 his3-D1 arg3-D4 ade6-L469/pUC8/his3+/RTS1-IO/ade6-M375*	Lab strain
FO 1750	$h^{-\ smt0}$	*srs2Δ::ura4+ ura4-D18 leu1-32 his3-D1 arg3-D4 ade6-L469/pUC8/his3+/RTS1-AO/ade6-M375*	Lab strain
MCW 1691	h^+	*rad51Δ::arg3+ ade6-M375 int::pUC8/ his3+/RTS1-IO/ ade6 -L469 ura4-D18 leu1-32 his3-D1 arg3-D4*	Lab strain
MCW 1692	h^+	*rad51Δ::arg3+ ade6-M375 int::pUC8/ his3+/RTS1-AO/ ade6 -L469 ura4-D18 leu1-32 his3-D1 arg3-D4*	Lab strain
MCW 4712	h^+	*ade6-M375 int::pUC8/his3+/RTS1-IO/ade6-L469 ura4-D18 leu1-32 his3-D1 arg3-D4*	Lab strain
MCW 4713	h^+	*ade6-M375 int::pUC8/his3+/RTS1-AO/ade6-L469 ura4-D18 leu1-32 his3-D1 arg3-D4*	Lab strain
MCW 4752	h^+	*fml1Δ::hphMX4 ade6-M375 int::pUC8/his3+/RTS1-AO/ade6-L469 ura4-D18 leu1-32 his3-D1 arg3-D4*	Lab strain
MCW 6472	$h^{-\ smt0}$	*ade6-D20 ChrI(80,355-80,423)::ade6-L469/pUc8/his3+/ade6-M375-KanMX ura4-D18 leu1-32 his3-D1*	Lab strain
MCW 6474	$h^{-\ smt0}$	*ade6-D20 ChrI(80,355-80,423)::ade6-L469/pUc8/his3+/RTS1-AO/ade6-M375-KanMX ura4-D18 leu1-32 his3-D1 arg3-D4*	Lab strain
MCW 6556	h^+	*ade6-M375 int::pUC8/lacO115/his3+/RTS1-AO/ade6-L469 lys1-::Pnmt41-NLS-lacI-tdKatushka2-hphMX4 rad52+::YFP- kanMX6 ura4-D18 his3-D1 leu1-32 arg3-D4*	Lab strain
MCW 6557	h^+	*ade6-D20 ChrI(80,355-80,423)::ade6-L469/pUc8/his3+/RTS1-IO/ade6-M375-KanMX ura4-D18 leu1-32 his3-D1*	Lab strain
MCW 6712	h^+	*ade6-M375 int::pUC8/lacO115/his3+/RTS1-IO/ade6-L469 lys1-::Pnmt41-NLS-lacI-tdKatushka2-hphMX4 rad52+::YFP- kanMX6 ura4-::pECFP-PCNA+ his3-D1 leu1-32 arg3-D4*	Lab strain
MCW 6778	h^+	*oriIII-1253Δ::natMX4 ade6-L469/pUC8/his3+/RTS1-AO/ade6-M375 ura4-D8 leu1-32 his3-D1 arg3-D4*	Lab strain
MCW 6894	h^+	*oriIII-1253Δ::natMX4 ade6-L469/pUC8/his3+/RTS1-IO/ade6-M375 ura4-D8 leu1-32 his3-D1 arg3-D4*	Lab strain
MCW 7045	h^+	*ade6-M375 int::pUC8/his3+/Ter orientation1/ade6-L469 ura4-D18 leu1-32 his3-D1 arg3-D4*	Lab strain
MCW 7046	h^+	*ade6-M375 int::pUC8/his3+/Ter orientation 2/ade6-L469 ura4-D18 leu1-32 his3-D1 arg3-D4*	Lab strain
MCW 7065	h^+	*ade6-M375 int::pUC8/lacO115/his3+/RTS1-AO/ade6-L469 lys1-::Pnmt41-NLS-lacI-tdKatushka2-hphMX4 rad52+::YFP- kanMX6 ura4-::pECFP-PCNA+ his3-D1 leu1-32 arg3-D4*	Lab strain
MCW 7132	$h^{-\ smt0}$	*ade6-M375 int::puc8/his3+/ade6-L469 int::RTS1- IO-hphMX4(0.2 kb from ade6-M375) ura4-D18 leu1-32 his3-D1 arg3-D4*	Lab strain
MCW 7134	$h^{-\ smt0}$	*ade6-M375 int::puc8/his3+/ade6-L469 int::RTS1- AO-hphMX4(0.2 kb from ade6-M375) ura4-D18 leu1-32 his3-D1 arg3-*	Lab strain
MCW 7257	h^+	*ade6Δ:: RTS1-IO-hphMX4 (12.4 kb from ade6) int::ade6-L469/pUC8/his3+/ade6-M375/kanMX6 ura4-D18 leu1-32 his3-D1 arg3-D4*	Lab strain
MCW 7259	h^+	*ade6Δ:: RTS1-AO-hphMX4 (12.4 kb from ade6) int::ade6-L469/pUC8/his3+/ade6-M375/kanMX6 ura4-D18 leu1-32 his3-D1*	Lab strain

		arg3-D4	
MCW 7293	h^+	*oriIII-1253Δ::natMX4 ade6:: RTS1-IO-hphMX4 (12.4 kb from ade6) int::ade6-L469/pUC8/his3+/ade6-M375/kanMX6 ura4-D18 leu1-32 his3-D1 arg3-D4*	Lab strain
MCW 7295	h^+	*oriIII-1253Δ::natMX4 ade6:: RTS1-AO-hphMX4 (12.4 kb from ade6) int::ade6-L469/pUC8/his3+/ade6-M375/kanMX6 ura4-D18 leu1-32 his3-D1 arg3-D4*	Lab strain
MCW 7415	$h^{-\ smt0}$	*oriIII-1253Δ::natMX4 ade6-M375 int::pUC8/ his3+/ ade6-L469 int::RTS1-IO-hphMX4 (0.2 kb from ade6-M375)ura4-D18 leu1-32 his3-D1 arg3-D4*	Lab strain
MCW 7417	$h^{-\ smt0}$	*oriIII-1253Δ::natMX4 ade6-M375 int::pUC8/ his3+/ ade6-L469 int::RTS1-AO-hphMX4 (0.2 kb from ade6-M375)ura4-D18 leu1-32 his3-D1 arg3-D4*	Lab strain
MCW 7555	h^+	*swi5Δ::ura4+ ade6Δ:: RTS1-IO-hphMX4 (12.4 kb from ade6) int::ade6-L469/pUC8/his3+/ade6-M375/kanMX6 ura4-D18 leu1-32 his3-D1 arg3-D4*	This study
MCW 7557	h^+	*swi5Δ::ura4+ ade6Δ:: RTS1-AO-hphMX4 (12.4 kb from ade6) int::ade6-L469/pUC8/his3+/ade6-M375/kanMX6 ura4-D18 leu1-32 his3-D1 arg3-D4*	This study
MCW 7559	h^+	*swi5Δ::ura4+ oriIII-1253Δ::natMX4 ade6:: RTS1-IO-hphMX4 (12.4 kb from ade6) int::ade6-L469/pUC8/his3+/ade6-M375/kanMX6 ura4-D18 leu1-32 his3-D1 arg3-D4*	This study
MCW 7561	h^+	*swi5Δ::ura4+ oriIII-1253Δ::natMX4 ade6:: RTS1-IO-hphMX4 (12.4 kb from ade6) int::ade6-L469/pUC8/his3+/ade6-M375/kanMX6 ura4-D18 leu1-32 his3-D1 arg3-D4*	This study
MCW 7588	h^+	*rad55Δ::arg3+ ade6Δ:: RTS1-IO-hphMX4 (12.4 kb from ade6) int::ade6-L469/pUC8/his3+/ade6-M375/kanMX6 ura4-D18 leu1-32 his3-D1 arg3-D4*	This study
MCW 7590	h^+	*rad55Δ::arg3+ ade6Δ:: RTS1-AO-hphMX4 (12.4 kb from ade6) int::ade6-L469/pUC8/his3+/ade6-M375/kanMX6 ura4-D18 leu1-32 his3-D1 arg3-D4*	This study
MCW 7592	h^+	*rad55Δ::arg3+ oriIII-1253Δ::natMX4 ade6:: RTS1-IO-hphMX4 (12.4 kb from ade6) int::ade6-L469/pUC8/his3+/ade6-M375/kanMX6 ura4-D18 leu1-32 his3-D1 arg3-D4*	This study
MCW 7594	h^+	*rad55Δ::arg3+ oriIII-1253Δ::natMX4 ade6:: RTS1-AO-hphMX4 (12.4 kb from ade6) int::ade6-L469/pUC8/his3+/ade6-M375/kanMX6 ura4-D18 leu1-32 his3-D1 arg3-D4*	This study
MCW 7607	h^+	*swi5Δ::ura4+ rad55Δ::arg3+ ade6Δ:: RTS1-IO-hphMX4 (12.4 kb from ade6) int::ade6-L469/pUC8/his3+/ade6-M375/kanMX6 ura4-D18 leu1-32 his3-D1 arg3-D4*	This study
MCW 7609	h^+	*swi5Δ::ura4+ rad55Δ::arg3+ ade6Δ:: RTS1-AO-hphMX4 (12.4 kb from ade6) int::ade6-L469/pUC8/his3+/ade6-M375/kanMX6 ura4-D18 leu1-32 his3-D1 arg3-D4*	This study
MCW 7611	h^+	*swi5Δ::ura4+ rad55Δ::arg3+ oriIII-1253Δ::natMX4 ade6:: RTS1-IO-hphMX4 (12.4 kb from ade6) int::ade6-L469/pUC8/his3+/ade6-M375/kanMX6 ura4-D18 leu1-32 his3-D1 arg3-D4*	This study
MCW 7613	h^+	*swi5Δ::ura4+ rad55Δ::arg3+ oriIII-1253Δ::natMX4 ade6:: RTS1-AO-hphMX4 (12.4 kb from ade6) int::ade6-L469/pUC8/his3+/ade6-M375/kanMX6 ura4-D18 leu1-32 his3-D1 arg3-D4*	This study

MCW 7638	h$^{-\ smt0}$	*ade6-M375 int::pUC8/lacO115/his3+/RTS1-AO/ade6-L469 lys1-::Pnmt41-NLS-lacI-tdKatushka2-hphMX4 rad52+::YFP- kanMX6 rad51+::ECFP-rad51+-arg3+ ura4-D18::rad51+- ura4+ his3-D1 leu1-32 arg3-D4*	Lab strain
MCW 7706	h$^+$	*elg1Δ::natMX6 ade6-M375 int::pUC8/his3$^+$/RTS1-IO/ade6-L469 ura4-D18 leu1-32 his3-D1 arg3-D4*	This study
MCW 7708	h$^+$	*elg1Δ::natMX4 ade6-M375 int::pUC8/his3$^+$/RTS1-AO/ade6-L469 ura4-D18 leu1-32 his3-D1 arg3-D4*	This study
MCW 7710	h$^+$	*pof3Δ::ura4MX6 ade6-M375 int::pUC8/his3$^+$/RTS1-IO/ade6-L469 ura4-D18 leu1-32 his3-D1 arg3-D4*	This study
MCW 7712	h$^+$	*pof3Δ::ura4MX6 ade6-M375 int::pUC8/his3$^+$/RTS1-AO/ade6-L469 ura4-D18 leu1-32 his3-D1 arg3-D4*	This study
MCW 7812	h$^+$	*rad51Δ::arg3$^+$ ade6Δ:: RTS1-IO-hphMX4 (12.4 kb from ade6) int::ade6-L469/pUC8/his3$^+$/ade6-M375/kanMX6 ura4-D18 leu1-32 his3-D1 arg3-D4*	Lab strain
MCW 7814	h$^+$	*rad51Δ::arg3$^+$ ade6Δ:: RTS1-AO-hphMX4 (12.4 kb from ade6) int::ade6-L469/pUC8/his3$^+$/ade6-M375/kanMX6 ura4-D18 leu1-32 his3-D1 arg3-D4*	Lab strain
MCW 7965	h$^+$	*elg1Δ::natMX6 ade6-M375 int::pUC8/lacO115/his3+/RTS1-AO/ade6-L469 lys1-::Pnmt41-NLS-lacI-tdKatushka2-hphMX4 rad52+::YFP- kanMX6 ura4-::pECFP-PCNA+ his3-D1 leu1-32 arg3-D4*	This study
MCW 7969	h$^+$	*elg1Δ::natMX6 ade6-M375 int::pUC8/lacO115/his3+/RTS1-IO/ade6-L469 lys1-::Pnmt41-NLS-lacI-tdKatushka2-hphMX4 rad52+::YFP- kanMX6 ura4-::pECFP-PCNA+ his3-D1 leu1-32 arg3-D4*	This study
MCW 8023	h$^+$	*ade6-M375 int::pUC8/5000 bp spacer/his3$^+$/RTS1-AO/ade6-L469 ura4-D18 his3-D1 leu1-32 arg3-D4*	Lab strain
MCW 8130	h$^+$	*elg1Δ::natMX6 ade6-M375 int::pUC8/his3$^+$/Ter orientation1/ade6-L469 ura4-D18 leu1-32 his3-D1 arg3-D4*	This study
MCW 8132	h$^+$	*elg1Δ::natMX6 ade6-M375 int::pUC8/his3$^+$/Ter orientation 2/ade6-L469 ura4-D18 leu1-32 his3-D1 arg3-D4*	This study
MCW 8136	h$^+$	*rad51Δ::arg3$^+$ ade6-M375 int::pUC8/5000 bp spacer/his3$^+$/RTS1-AO/ade6-L469 ura4-D18 his3-D1 leu1-32 arg3-D4*	Lab strain
MCW 8204	h$^+$	*elg1Δ::natMX6 ChrI(80,355-80,423)::ade6-L469/pUc8/his3$^+$/RTS1-IO/ade6-M375-KanMX ade6-D20 ura4-D18 leu1-32 his3-D1*	This study
MCW 8206	h$^+$	*elg1Δ::natMX6 ChrI(80,355-80,423)::ade6-L469/pUc8/his3$^+$/ade6-M375-KanMX ade6-D20 ura4-D18 leu1-32 his3-D1*	This study
MCW 8208	h$^+$	*elg1Δ::natMX6 ChrI(80,355-80,423)::ade6-L469/pUc8/his3$^+$/RTS1-AO/ade6-M375-KanMX ade6-D20 ura4-D18 leu1-32 his3-D1*	This study
MCW 8218	h$^{-\ smt0}$	*exo1Δ::ura4$^+$ ade6Δ:: RTS1-AO-hphMX4 (12.4 kb from ade6) int::ade6-L469/pUC8/his3$^+$/ade6-M375/kanMX6 ura4-D18 leu1-32 his3-D1 arg3-D4*	Lab strain
MCW 8328	h$^+$	*elg1Δ::natMX6 srs2Δ::ura4+ ade6-M375 int::pUC8/his3$^+$/RTS1-IO/ade6-L469 ura4-D18 leu1-32 his3-D1 arg3-D4*	This study

MCW 8330	h^+	*elg1Δ::natMX6 srs2Δ::ura4+ ade6-M375 int::pUC8/his3⁺/RTS1-AO/ade6-L469 ura4-D18 leu1-32 his3-D1 arg3-D4*	This study
MCW 8404	h^+	*ctf18Δ::natMX6 ade6-M375 int::pUC8/his3⁺/RTS1-IO/ade6-L469 ura4-D18 leu1-32 his3-D1 arg3-D4*	This study
MCW 8406	h^+	*ctf18Δ::natMX6 ade6-M375 int::pUC8/his3⁺/RTS1-AO/ade6-L469 ura4-D18 leu1-32 his3-D1 arg3-D4*	This study
MCW 8408	h^+	*ctf18Δ::natMX6 elg1Δ::kanMX6 ade6-M375 int::pUC8/his3⁺/RTS1-IO/ade6-L469 ura4-D18 leu1-32 his3-D1 arg3-D4*	This study
MCW 8410	h^+	*ctf18Δ::natMX6 elg1Δ::kanMX6 ade6-M375 int::pUC8/his3⁺/RTS1-AO/ade6-L469 ura4-D18 leu1-32 his3-D1 arg3-D4*	This study
MCW 8431	h^+	*fml1Δ::hphMX4 elg1Δ::natMX6 ade6-M375 int::pUC8/his3⁺/RTS1-AO/ade6-L469 ura4-D18 leu1-32 his3-D1 arg3-D4*	This study
MCW 8486	h^+	*elg1Δ::natMX6 ade6-M375 int::pUC8/lacO115/his3+/RTS1-AO/ade6-L469 lys1- ::Pnmt41-NLS-lacI-tdKatushka2-hphMX4 rad52+::YFP- kanMX6 ura4-D18 his3-D1 leu1-32 arg3-D4*	This study
MCW 8537	h^+	*ctf18Δ::natMX6 ade6-M375 int::pUC8/lacO115/his3+/RTS1-IO/ade6-L469 lys1- ::Pnmt41-NLS-lacI-tdKatushka2-hphMX4 rad52+::YFP- kanMX6 ura4-::pECFP-PCNA+ his3-D1 leu1-32 arg3-D4*	This study
MCW 8539	h^+	*ctf18Δ::natMX6 ade6-M375 int::pUC8/lacO115/his3+/RTS1-AO/ade6-L469 lys1- ::Pnmt41-NLS-lacI-tdKatushka2-hphMX4 rad52+::YFP- kanMX6 ura4-::pECFP-PCNA+ his3-D1 leu1-32 arg3-D4*	This study
MCW 8597	h^+	*ctf18Δ::natMX6 ade6Δ:: RTS1-IO-hphMX4 (12.4 kb from ade6) int::ade6-L469/pUC8/his3⁺/ade6-M375/kanMX6 ura4-D18 leu1-32 his3-D1 arg3-D4*	This study
MCW 8598	h^+	*ctf18Δ::natMX6 ade6Δ:: RTS1-AO-hphMX4 (12.4 kb from ade6) int::ade6-L469/pUC8/his3⁺/ade6-M375/kanMX6 ura4-D18 leu1-32 his3-D1 arg3-D4*	This study
MCW 8700	h^+	*oriIII-1253Δ::natMX4 ade6:: RTS1-IO-hphMX4 (12.4 kb from ade6) int::ade6-L469/pUC8/his3⁺/ade6-M375/ ura4MX ura4-D18 leu1-32 his3-D1 arg3-D4*	This study
MCW 8763	h^+	*ctf18Δ::natMX6 oriIII-1253Δ:: arg3⁺ ade6:: RTS1-IO-hphMX4 (12.4 kb from ade6) int::ade6-L469/pUC8/his3⁺/ade6-M375/kanMX6 ura4-D18 leu1-32 his3-D1 arg3-D4*	This study
MCW 8765	h^+	*rad51Δ::arg3⁺ oriIII-1253Δ::natMX4 ade6:: RTS1-IO-hphMX4 (12.4 kb from ade6) int::ade6-L469/pUC8/his3⁺/ade6-M375/kanMX6 ura4-D18 leu1-32 his3-D1 arg3-D4*	This study
MCW 8766	h^+	*rad51Δ::arg3⁺ oriIII-1253Δ::natMX4 ade6:: RTS1-AO-hphMX4 (12.4 kb from ade6) int::ade6-L469/pUC8/his3⁺/ade6-M375/kanMX6 ura4-D18 leu1-32 his3-D1 arg3-D4*	This study
MCW 8788	h^+	*rad51Δ::arg3⁺ ade6-M375 int::pUC8/ his3⁺/ ade6-L469 int::RTS1-IO-hphMX4 (0.2 kb from ade6-M375)ura4-D18 leu1-32 his3-D1 arg3-D4*	This study
MCW 8790	h^+	*rad51Δ::arg3⁺ ade6-M375 int::pUC8/ his3⁺/ ade6-L469 int::RTS1-AO-hphMX4 (0.2 kb from ade6-M375)ura4-D18 leu1-32 his3-D1 arg3-D4*	This study

MCW 8792	h^+	*rad51Δ::arg3$^+$ oriIII-1253Δ::natMX4 ade6-M375 int::pUC8/ his3$^+$/ ade6-L469 int::RTS1-IO-hphMX4 (0.2 kb from ade6-M375)ura4-D18 leu1-32 his3-D1 arg3-D4*	This study
MCW 8793	h^+	*rad51Δ::arg3$^+$ oriIII-1253Δ::natMX4 ade6-M375 int::pUC8/ his3$^+$/ ade6-L469 int::RTS1-AO-hphMX4 (0.2 kb from ade6-M375)ura4-D18 leu1-32 his3-D1 arg3-D4*	This study
MCW 8822	h^+	*ctf18Δ::natMX6 oriIII-1253Δ:: arg3$^+$ ade6:: RTS1-IO-hphMX4 (12.4 kb from ade6) int::ade6-L469/pUC8/his3$^+$/ade6-M375/kanMX6 ura4-D18 leu1-32 his3-D1 arg3-D4*	This study
MCW 8835	h^+	*rad51Δ::arg3$^+$ oriIII-1253Δ::natMX4 ade6-L469/pUC8/his3$^+$/RTS1-AO/ade6-M375 ura4-D8 leu1-32 his3-D1 arg3-D4*	This study
MCW 8837	h^+	*rad51Δ::arg3$^+$ oriIII-1253Δ::natMX4 ade6-L469/pUC8/his3$^+$/RTS1-IO/ade6-M375 ura4-D8 leu1-32 his3-D1 arg3-D4*	This study
MCW 8888	h^+	*oriIII-1253Δ::natMX4 ade6:: RTS1-AO-hphMX4 (12.4 kb from ade6) int::ade6-L469/pUC8/his3$^+$/ade6-M375/ ura4MX ura4-D18 leu1-32 his3-D1 arg3-D4*	Lab strain
MCW 8919	h^+	*wpl1Δ::kanR ade6-M375 int::pUC8/his3$^+$/RTS1-IO/ade6-L469 ura4-D18 leu1-32 his3-D1 arg3-D4*	This study
MCW 8920	h^+	*wpl1Δ::kanR ade6-M375 int::pUC8/his3$^+$/RTS1-AO/ade6-L469 ura4-D18 leu1-32 his3-D1 arg3-D4*	This study
MCW 8921	$h^{-\ smt0}$	*elg1Δ::natMX6 ade6-M375 int::pUC8/lacO115/his3+/RTS1-AO/ade6-L469 lys1- ::Pnmt41-NLS-lacI-tdKatushka2-hphMX4 rad52+::YFP- kanMX6 rad51+::ECFP-rad51+-arg3+ ura4-D18::rad51+- ura4+ his3-D1 leu1-32 arg3-D4*	This study
MCW 8931	h^+	*rdl1Δ::natMX6 ade6Δ:: RTS1-IO-hphMX4 (12.4 kb from ade6) int::ade6-L469/pUC8/his3$^+$/ade6-M375/kanMX6 ura4-D18 leu1-32 his3-D1 arg3-D4*	This study
MCW 8941	h^+	*elg1Δ::natMX6 ade6-M375 int::pUC8/5000 bp spacer/his3$^+$/RTS1-AO/ade6-L469 ura4-D18 his3-D1 leu1-32 arg3-D4*	This study
MCW 8943	h^+	*rad51Δ::arg3$^+$ rad51Δ::arg3$^+$ ade6-M375 int::pUC8/5000 bp spacer/his3$^+$/RTS1-AO/ade6-L469 ura4-D18 his3-D1 leu1-32 arg3-D4*	This study
MCW 8946	$h^{-\ smt0}$	*elg1Δ::natMX6 fbh1Δ::kanMX ade6-M375 int::pUC8/his3$^+$/RTS1-AO/ade6-L469 ura4-D18 leu1-32 his3-D1 arg3-D4*	This study
MCW 8950	h^+	*elg1Δ::natMX6 exo1Δ::ura4$^+$ ade6-M375 int::pUC8/his3$^+$/RTS1-AO/ade6-L469 ura4-D18 leu1-32 his3-D1 arg3-D4*	This study
MCW 8988	h^+	*elg1Δ::kanMX6 oriIII-1253Δ::natMX4 ade6:: RTS1-IO-hphMX4 (12.4 kb from ade6) int::ade6-L469/pUC8/his3$^+$/ade6-M375/ ura4MX ura4-D18 leu1-32 his3-D1 arg3-D4*	This study
MCW 8990	$h^{-\ smt0}$	*elg1Δ::kanMX6 oriIII-1253Δ::natMX4 ade6:: RTS1-AO-hphMX4 (12.4 kb from ade6) int::ade6-L469/pUC8/his3$^+$/ade6-M375/ ura4MX ura4-D18 leu1-32 his3-D1 arg3-D4*	This study
MCW 8992	h^+	*elg1Δ::kanMX6 ade6:: RTS1-AO-hphMX4 (12.4 kb from ade6) int::ade6-L469/pUC8/his3$^+$/ade6-M375/ ura4MX ura4-D18 leu1-32 his3-D1 arg3-D4*	This study
MCW 8995	h^+	*elg1Δ::natMX6 wpl1Δ::kanR ade6-M375 int::pUC8/his3$^+$/RTS1-IO/ade6-L469 ura4-D18 leu1-32 his3-D1 arg3-D4*	This study
MCW 8998	h^+	*elg1Δ::natMX6 wpl1Δ::kanR ade6-M375 int::pUC8/his3$^+$/RTS1-IO/ade6-L469 ura4-D18 leu1-32 his3-D1 arg3-D4*	This study

MCW 9000	h^+	*rad51Δ::arg3⁺ oriIII-1253Δ::natMX4 ade6:: RTS1-IO-hphMX4 (12.4 kb from ade6) int::ade6-L469/pUC8/his3⁺/ade6-M375/ ura4MX ura4-D18 leu1-32 his3-D1 arg3-D4*	This study
MCW 9002	h^+	*rad51Δ::arg3⁺ oriIII-1253Δ::natMX4 ade6:: RTS1-AO-hphMX4 (12.4 kb from ade6) int::ade6-L469/pUC8/his3⁺/ade6-M375/ ura4MX ura4-D18 leu1-32 his3-D1 arg3-D4*	This study
MCW 9004	$h^{-\ smt0}$	*rad51Δ::arg3⁺ ade6:: RTS1-AO-hphMX4 (12.4 kb from ade6) int::ade6-L469/pUC8/his3⁺/ade6-M375/ ura4MX ura4-D18 leu1-32 his3-D1 arg3-D4*	This study
MCW 9006	h^+	*rad54-K300A::natMX4 ade6Δ:: RTS1-IO-hphMX4 (12.4 kb from ade6) int::ade6-L469/pUC8/his3⁺/ade6-M375/kanMX6 ura4-D18 leu1-32 his3-D1 arg3-D4*	This study
MCW 9008	$h^{-\ smt0}$	*rad54-K300A::natMX4 ade6Δ:: RTS1-AO-hphMX4 (12.4 kb from ade6) int::ade6-L469/pUC8/his3⁺/ade6-M375/kanMX6 ura4-D18 leu1-32 his3-D1 arg3-D4*	This study
MCW 9013	$h^{-\ smt0}$	*rad54Δ::kanMX ade6Δ:: RTS1-AO-hphMX4 (12.4 kb from ade6) int::ade6-L469/pUC8/his3⁺/ade6-M375/kanMX6 ura4-D18 leu1-32 his3-D1 arg3-D4*	This study
MCW 9026		*elg1Δ::kanMX6 ade6:: RTS1-IO-hphMX4 (12.4 kb from ade6) int::ade6-L469/pUC8/his3⁺/ade6-M375/ ura4MX ura4-D18 leu1-32 his3-D1 arg3-D4*	This study
MCW 9028		*rad51Δ::arg3⁺ ade6:: RTS1-IO-hphMX4 (12.4 kb from ade6) int::ade6-L469/pUC8/his3⁺/ade6-M375/ ura4MX ura4-D18 leu1-32 his3-D1 arg3-D4*	This study
MCW 9030	h^+	*rad54Δ::kanMX ade6Δ:: RTS1-IO-hphMX4 (12.4 kb from ade6) int::ade6-L469/pUC8/his3⁺/ade6-M375/kanMX6 ura4-D18 leu1-32 his3-D1 arg3-D4*	This study
MCW 9034		*rad51Δ::arg3⁺ exo1Δ::ura4⁺ ade6Δ:: RTS1-AO-hphMX4 ade6-L469/pUC8/his3⁺/ade6-M375-KanMX-aim1 ura4-D18 leu1-32 his3-D1 arg3-D4 ade6-D1*	This study
MCW 9036	$h^{-\ smt0}$	*ade6:: RTS1-IO-hphMX4 (12.4 kb from ade6) int::ade6-L469/pUC8/his3⁺/ade6-M375/ ura4MX ura4-D18 leu1-32 his3-D1 arg3-D4*	This study
MCW 9039	h^+	*ade6:: RTS1-AO-hphMX4 (12.4 kb from ade6) int::ade6-L469/pUC8/his3⁺/ade6-M375/ ura4MX ura4-D18 leu1-32 his3-D1 arg3-D4*	This study
MCW 9140	h^+	*rdl1Δ::natMX6 ade6Δ:: RTS1-AO-hphMX4 (12.4 kb from ade6) int::ade6-L469/pUC8/his3⁺/ade6-M375/kanMX6 ura4-D18 leu1-32 his3-D1 arg3-D4*	This study
MCW 9183		*pcn1-D150E-NatMX4 ade6-M375 int::pUC8/his3⁺/RTS1-IO/ade6-L469 ura4-D18 leu1-32 his3-D1 arg3-D4*	This study
MCW 9185		*pcn1-D150E-NatMX4 ade6-M375 int::pUC8/his3⁺/RTS1-AO/ade6-L469 ura4-D18 leu1-32 his3-D1 arg3-D4*	This study
MCW 9187		*elg1Δ::KanMX6 pcn1-D150E-NatMX4 ade6-M375 int::pUC8/his3⁺/RTS1-IO/ade6-L469 ura4-D18 leu1-32 his3-D1 arg3-D4*	This study
MCW 9189		*elg1Δ::KanMX6 pcn1-D150E-NatMX4 ade6-M375 int::pUC8/his3⁺/RTS1-AO/ade6-L469 ura4-D18 leu1-32 his3-D1 arg3-D4*	This study

Table 5: list of plasmids used in this study

Plasmid	Source
pMW777	Lab stock
pMW921	Lab stock
pST1	Mutagenesis
pST2	Mutagenesis
pST3	Mutagenesis
pST4	Mutagenesis
pFOX2	Lab stock
pBZ142	Lab stock

Table 6: list of of oligonucleotides used in this study.

Oligonucleotide	Sequence (5'-3')
oMW 284	CTAGGATACAGTTCTCAC
oMW 633	TTATACATATGCTTGAAGCTAGATTTCAG
oMW 634	TAGGATCCTACTCCTCATCCTCCTCACC
oMW 706	AAAGGCCTCGCTTCTCGAG
oMW 707	AGCAGCATACGCTAAAATC
oMW 716	ATTTGATGTTTAAGCGATGG
oMW 717	AGAAGAAAGCGATCGATGAG
oMW 720	TCACTATACTTCATCCCAC
oMW 721	AGTTGGTTGCGTTATTCGAG
oMW 722	AAAACATGTTGACAAACCTG
oMW 784	AACTGCAGAATTCTTGTTAACGTAACTG
oMW 787	AAGAGCTCCTGCCATAGTATAT
oMW 921	TTTAGATGAATTCAAGGTG
oMW 922	ATTGATATCAGCTGAATAATTTTTCCAACCAAC
oMW 1625	TATAAAGCTTGGTGGTGAGGTAAACG
oMW 1783	GAAAGCTGAGAAACCTGTG

oMW 1784	TTGGTTTCAACTGGAGGAG
oMW 1785	ATACGGTTCATTGGAAGC
oMW 1786	ACGGGTTTACTAGGATTG
oMW 1882	GGTCTTACGGCGAGCCCAAAACG
oMW 1883	TTTGATAAGGCGTTCAGATTTATAC
oMW 1884	CATTACTCGAGAGTTATTAACTTTGAG
oMW 1885	CGTTGAAATTCGGCAGCA
oMW 1886	GCCTGCTGCAAATTTCAACGCA
oMW 1887	ATAGTAATAGTAGCATCGTATTCGATATC

Bibliography

Abid Ali, Ferdos, Ludovic Renault, Julian Gannon, Hailey L. Gahlon, Abhay Kotecha, Jin Chuan Zhou, David Rueda, and Alessandro Costa. 2016. “Cryo-EM Structures of the Eukaryotic Replicative Helicase Bound to a Translocation Substrate.” *Nature Communications* 7: 1–11. doi:10.1038/ncomms10708.

Admire, Anthony, Lisa Shanks, Nicole Danzl, Mei Wang, Ulli Weier, William Stevens, Elizabeth Hunt, and Ted Weinert. 2006. “Cycles of Chromosome Instability Are Associated with a Fragile Site and Are Increased by Defects in DNA Replication and Checkpoint Controls in Yeast.” *Genes and Development* 20 (2): 159–73. doi:10.1101/gad.1392506.

Agarwal, Sheba, Wiggert A. Van Cappellen, Aude Guénolé, Berina Eppink, Sam E.V. Linsen, Erik Meijering, Adriaan Houtsmuller, Roland Kanaar, and Jeroen Essers. 2011. “ATP-Dependent and Independent Functions of Rad54 in Genome Maintenance.” *Journal of Cell Biology* 192 (5): 735–50. doi:10.1083/jcb.201011025.

Aguilera, Andrés, and Tatiana García-Muse. 2013. “Causes of Genome Instability.” *Annual Review of Genetics* 47 (1): 1–32. doi:10.1146/annurev-genet-111212-133232.

Ahn, Jong Sook, Fekret Osman, and Matthew C Whitby. 2005. “Replication Fork Blockage by RTS1 at an Ectopic Site Promotes Recombination in Fission Yeast.” *The EMBO Journal* 24 (11): 2011–23. doi:10.1038/sj.emboj.7600670.

Ait Saada, Anissia, Sarah A.E. Lambert, and Antony M. Carr. 2018. “Preserving Replication Fork Integrity and Competence via the Homologous Recombination Pathway.” *DNA Repair* 71: 135-47. doi:10.1016/j.dnarep.2018.08.017.

Ait Saada, Anissia, Ana Teixeira-Silva, Ismail Iraqui, Audrey Costes, Julien Hardy, Giulia Paoletti, Karine Fréon, and Sarah A.E. Lambert. 2017. “Unprotected Replication Forks Are Converted into Mitotic Sister Chromatid Bridges.” *Molecular Cell* 66 (3): 398–410. doi:10.1016/j.molcel.2017.04.002.

Akamatsu, Yufuko, Dorota Dziadkowiec, Mitsunori Ikeguchi, Hideo Shinagawa, and Hiroshi Iwasaki. 2003. “Two Different Swi5-Containing Protein Complexes Are Involved in Mating-Type Switching and Recombination Repair in Fission Yeast.” *Proceedings of the National Academy of Sciences of the United States of America* 100 (26): 15770–75. doi:10.1073/pnas.2632890100.

Akamatsu, Yufuko, Yasuhiro Tsutsui, Takashi Morishita, M. D.Shahjahan P. Siddique,

Yumiko Kurokawa, Mitsunori Ikeguchi, Fumiaki Yamao, Benoit Arcangioli, and Hiroshi Iwasaki. 2007. “Fission Yeast Swi5/Sfr1 and Rhp55/Rhp57 Differentially Regulate Rhp51-Dependent Recombination Outcomes.” *EMBO Journal* 26 (5): 1352–62. doi:10.1038/sj.emboj.7601582.

Albala, J S, M P Thelen, C Prange, W Fan, M Christensen, L H Thompson, and G G Lennon. 1997. “Identification of a Novel Human RAD51 Homolog, RAD51B." *Genomics* 46 (3): 476–79. doi:10.1006/geno.1997.5062.

Alexeev, Andrei, Alexander Mazin, and Stephen C. Kowalczykowski. 2003. “Rad54 Protein Possesses Chromatin-Remodeling Activity Stimulated by the Rad51-SsDNA Nucleoprotein Filament.” *Nature Structural Biology* 10 (3): 182–86. doi:10.1038/nsb901.

Allers, Thorsten, and Michael Lichten. 2001. “Differential Timing and Control of Noncrossover and Crossover Recombination during Meiosis.” *Cell* 106 (1): 47–57. doi:10.1016/S0092-8674(01)00416-0.

Alvaro, David, Michael Lisby, and Rodney Rothstein. 2007. “Genome-Wide Analysis of Rad52 Foci Reveals Diverse Mechanisms Impacting Recombination.” *PLoS Genetics* 3 (12): 2439–49. doi:10.1371/journal.pgen.0030228.

Anand, Ranjith P., Susan T. Lovett, and James E. Haber. 2013. “Break-Induced DNA Replication.” *Cold Spring Harbor Perspectives in Biology* 5 (12): a010397. doi:10.1101/cshperspect.a010397.

Anand, Ranjith P., Olga Tsaponina, Patricia W. Greenwell, Cheng Sheng Lee, Wei Du, Thomas D. Petes, and James E. Haber. 2014. “Chromosome Rearrangements via Template Switching between Diverged Repeated Sequences.” *Genes and Development* 28 (21): 2394–2406. doi:10.1101/gad.250258.114.

Andersen, Sabrina L., Daniel T. Bergstralh, Kathryn P. Kohl, Jeannine R. LaRocque, Chris B. Moore, and Jeff Sekelsky. 2009. “Drosophila MUS312 and the Vertebrate Ortholog BTBD12 Interact with DNA Structure-Specific Endonucleases in DNA Repair and Recombination.” *Molecular Cell* 35 (1): 128–35. doi:10.1016/j.molcel.2009.06.019.

Antequera, Francisco. 2004. “Genomic Specification and Epigenetic Regulation of Eukaryotic DNA Replication Origins.” *The EMBO Journal* 23 (22): 4365–70. doi:10.1038/sj.emboj.7600450.

Antony, Edwin, Eric J. Tomko, Qi Xiao, Lumir Krejci, Timothy M. Lohman, and Tom Ellenberger. 2009. “Srs2 Disassembles Rad51 Filaments by a Protein-Protein Interaction Triggering ATP Turnover and Dissociation of Rad51 from DNA.” *Molecular Cell* 35 (1): 105–15. doi:10.1016/j.molcel.2009.05.026.

Arias, Emily E., and Johannes C. Walter. 2006. “PCNA Functions as a Molecular Platform to Trigger Cdt1 Destruction and Prevent Re-Replication.” *Nature Cell Biology* 8 (1): 84–90. doi:10.1038/ncb1346.

Arlt, Martin F., Thomas E. Wilson, and Thomas W. Glover. 2012. “Replication Stress and Mechanisms of CNV Formation.” *Current Opinion in Genetics and Development* 22 (3): 204–10. doi:10.1016/j.gde.2012.01.009.

Armstrong, Anthony A., Firaz Mohideen, and Christopher D. Lima. 2012. “Recognition of SUMO-Modified PCNA Requires Tandem Receptor Motifs in Srs2.” *Nature* 483 (7387): 59–65. doi:10.1038/nature10883.

Atkinson, John, and Peter McGlynn. 2009. “Replication Fork Reversal and the Maintenance of Genome Stability.” *Nucleic Acids Research* 37 (11): 3475–92. doi:10.1093/nar/gkp244.

Azvolinsky, Anna, Paul G. Giresi, Jason D. Lieb, and Virginia a. Zakian. 2009. “Highly Transcribed RNA Polymerase II Genes Are Impediments to Replication Fork Progression in Saccharomyces Cerevisiae.” *Molecular Cell* 34 (6): 722–34. doi:10.1016/j.molcel.2009.05.022.

Bachrati, Csanád Z., Rhona H. Borts, and Ian D. Hickson. 2006. “Mobile D-Loops Are a Preferred Substrate for the Bloom’s Syndrome Helicase.” *Nucleic Acids Research* 34 (8): 2269–79. doi:10.1093/nar/gkl258.

Bacquin, Agathe, Caroline Pouvelle, Nicolas Siaud, Mylène Perderiset, Sophie Salomé-Desnoulez, Carine Tellier-Lebegue, Bernard Lopez, Jean Baptiste Charbonnier, and Patricia L. Kannouche. 2013. “The Helicase FBH1 Is Tightly Regulated by PCNA via CRL4(Cdt2)-Mediated Proteolysis in Human Cells.” *Nucleic Acids Research* 41 (13): 6501–13. doi:10.1093/nar/gkt397.

Bakhoum, Samuel F., Bryan Ngo, Ashley M. Laughney, Julie Ann Cavallo, Charles J. Murphy, Peter Ly, Pragya Shah, et al. 2018. “Chromosomal Instability Drives Metastasis through a Cytosolic DNA Response.” *Nature* 553 (7689): 467–72. doi:10.1038/nature25432.

Balakrishnan, Lata, and Robert A. Bambara. 2013. “Okazaki Fragment Metabolism.”

Cold Spring Harbour Perspectives in Biology 5 (2): a010173. doi:10.1101/cshperspect.a010173.

Barbour, Leslie, and Wei Xiao. 2003. “Regulation of Alternative Replication Bypass Pathways at Stalled Replication Forks and Its Effects on Genome Stability: A Yeast Model.” *Mutation Research - Fundamental and Molecular Mechanisms of Mutagenesis* 532 (1–2): 137–55. doi:10.1016/j.mrfmmm.2003.08.014.

Bashkirov, V I, J S King, E V Bashkirova, J Schmuckli-Maurer, and W D Heyer. 2000. “DNA Repair Protein Rad55 Is a Terminal Substrate of the DNA Damage Checkpoints.” *Molecular and Cellular Biology* 20 (12): 4393–4404. doi:10.1128/MCB.20.12.4393-4404.2000.

Bell, Stephen D., and Michael R. Botchan. 2013. “The Minichromosome Maintenance Replicative Helicase.” *Cold Spring Harbor Perspectives in Biology* 5 (11): 1–12. doi:10.1101/cshperspect.a012807.

Bellaoui, Mohammed, Michael Chang, Jiongwen Ou, Hong Xu, Charles Boone, and Grant W. Brown. 2003. “Elg1 Forms an Alternative RFC Complex Important for DNA Replication and Genome Integrity.” *EMBO Journal* 22 (16): 4304–13. doi:10.1093/emboj/cdg406.

Bellelli, Roberto, Valerie Borel, Clare Logan, Jennifer Svendsen, Danielle E. Cox, Emma Nye, Kay Metcalfe, Susan M. O’Connell, Gordon Stamp, Helen R. Flynn, Ambrosius P. Snijders, Francois Lassailly, Andrew Jackson, and Simon J. Boulton. 2018. "Polε Instability Drives Replication Stress, Abnormal Development, and Tumoriogenesis." *Molecular Cell* 70 (4): 707-21. doi: 10.1016/j.molcel.2018.04.008.

Ben-Aroya, Shay, Amnon Koren, Batia Liefshitz, Rivka Steinlauf, and Martin Kupiec. 2003. “ELG1, a Yeast Gene Required for Genome Stability, Forms a Complex Related to Replication Factor C.” *Proceedings of the National Academy of Sciences of the United States of America* 100 (17): 9906–11. doi:10.1073/pnas.1633757100.

Bermudez, V. P., Y. Maniwa, I. Tappin, K. Ozato, K. Yokomori, and J. Hurwitz. 2003. “The Alternative Ctf18-Dcc1-Ctf8-Replication Factor C Complex Required for Sister Chromatid Cohesion Loads Proliferating Cell Nuclear Antigen onto DNA.” *Proceedings of the National Academy of Sciences* 100 (18): 10237–42. doi:10.1073/pnas.1434308100.

Bermudez, Vladimir P., Andrea Farina, Inger Tappin, and Jerard Hurwitz. 2010. “Influence of the Human Cohesion Establishment Factor Ctf4/AND-1 on DNA Replication.” *Journal of Biological Chemistry* 285 (13): 9493–9505. doi:10.1074/jbc.M109.093609.

Bernstein, K. A., R. J. D. Reid, I. Sunjevaric, K. Demuth, R. C. Burgess, and R. Rothstein. 2011. “The Shu Complex, Which Contains Rad51 Paralogues, Promotes DNA Repair through Inhibition of the Srs2 Anti-Recombinase.” *Molecular Biology of the Cell* 22 (9): 1599–1607. doi:10.1091/mbc.E10-08-0691.

Bernstein, Kara A., Serge Gangloff, and Rodney Rothstein. 2010. “The RecQ DNA Helicases in DNA Repair.” *Annual Review of Genetics* 44 (1): 393–417. doi:10.1146/annurev-genet-102209-163602.

Bhargava, Ragini, David O. Onyango, and Jeremy M. Stark. 2016. “Regulation of Single-Strand Annealing and Its Role in Genome Maintenance.” *Trends in Genetics* 32 (9): 566–75. doi:10.1016/j.tig.2016.06.007.

Bhowmick, Rahul, Sheroy Minocherhomji, and Ian D. Hickson. 2016. “RAD52 Facilitates Mitotic DNA Synthesis Following Replication Stress.” *Molecular Cell* 64 (6): 1117–26. doi:10.1016/j.molcel.2016.10.037.

Bienko, M. 2005. “Ubiquitin-Binding Domains in Y-Family Polymerases Regulate Translesion Synthesis.” *Science* 310 (5755): 1821–24. doi:10.1126/science.1120615.

Biswas, Subhrajit, and Deepak Bastia. 2008. “Mechanistic Insights into Replication Termination as Revealed by Investigations of the Reb1-Ter3 Complex of *Schizosaccharomyces pombe” Molecular and Cell Biology* 28 (22): 6844-57. doi:10.1128/MCB.01235-08.

Bochman, M. L., S. P. Bell, and A. Schwacha. 2008. “Subunit Organization of Mcm2-7 and the Unequal Role of Active Sites in ATP Hydrolysis and Viability.” *Molecular and Cellular Biology* 28 (19): 5865–73. doi:10.1128/MCB.00161-08.

Bochman, Matthew L., and Anthony Schwacha. 2008. “The Mcm2-7 Complex Has In Vitro Helicase Activity.” *Molecular Cell* 31 (2): 287–93. doi:10.1016/j.molcel.2008.05.020.

Boehm, Elizabeth M., Melissa S. Gildenberga, and M. Todd Washington. 2016. “Replication, The Many Roles of PCNA in Eukaryotic DNA” 39: 231–54. doi:10.1016/S2214-109X(16)30265-0.Cost-effectiveness.

Borges, Vanessa, Duncan J. Smith, Iestyn Whitehouse, and Frank Uhlmann. 2013. “An Eco1-Independent Sister Chromatid Cohesion Establishment Pathway in S. Cerevisiae.” *Chromosoma* 122 (1–2): 121–34. doi:10.1007/s00412-013-0396-y.

Bosco, Giovanni, and James E. Haber. 1998. “Chromosome Break-Induced DNA Replication Leads to Nonreciprocal Translocations and Telomere Capture.” *Genetics* 150 (3): 1037–47.

Botchan, Michael, and James Berger. 2010. “DNA Replication: Making Two Forks from One Prereplication Complex.” *Molecular Cell* 40 (6): 860–61. doi:10.1016/j.molcel.2010.12.014.

Bowman, Gregory D., Mike O’Donnell, and John Kuriyan. 2004. “Structural Analysis of a Eukaryotic Sliding DNA Clamp-Clamp Loader Complex.” *Nature* 429 (6993): 724–30. doi:10.1038/nature02585.

Branzei, Dana, Masayuki Seki, and Takemi Enomoto. 2004. “Rad18/Rad5/Mms2-Mediated Polyubiquitination of PCNA Is Implicated in Replication Completion during Replication Stress.” *Genes to Cells* 9 (11): 1031–42. doi:10.1111/j.1365-2443.2004.00787.x.

Branzei, Dana, Fabio Vanoli, and Marco Foiani. 2008. “SUMOylation Regulates Rad18-Mediated Template Switch.” *Nature* 456 (7224): 915–20. doi:10.1038/nature07587.

Brewer, Bonita J, and Walton L Fangman. 1988. “A Replication Fork Barrier at the 3 ’ End of Yeast Ribosomal RNA Genes” 55: 637–43.

Brouwer, Ineke, Tommaso Moschetti, Andrea Candelli, Edwige B Garcin, Mauro Modesti, Luca Pellegrini, Gijs JL Wuite, and Erwin JG Peterman. 2018. “Two Distinct Conformational States Define the Interaction of Human RAD51-ATP with Single-stranded DNA.” *The EMBO Journal* 37 (7): e98162. doi:10.15252/embj.201798162.

Bugreev, Dmitry V., Olga M. Mazina, and Alexander V. Mazin. 2006. “Rad54 Protein Promotes Branch Migration of Holliday Junctions.” *Nature* 442 (7102): 590–93. doi:10.1038/nature04889.

Bugreev, Dmitry V., Matthew J. Rossi, and Alexander V. Mazin. 2011. “Cooperation of RAD51 and RAD54 in Regression of a Model Replication Fork.” *Nucleic Acids Research* 39 (6): 2153–64. doi:10.1093/nar/gkq1139.

Burgers, Peter M. J. 2009. “Polymerase Dynamics at the Eukaryotic DNA Replication

Fork." *Journal of Biological Chemistry* 284 (7): 4041–45. doi:10.1074/jbc.R800062200.

Burrell, Rebecca a, Sarah E McClelland, David Endesfelder, Petra Groth, Marie-Christine Weller, Nadeem Shaikh, Enric Domingo, et al. 2013. "Replication Stress Links Structural and Numerical Cancer Chromosomal Instability." *Nature* 494 (7438): 492–96. doi:10.1038/nature11935.

Bylund, G. O., and P. M. J. Burgers. 2005. "Replication Protein A-Directed Unloading of PCNA by the Ctf18 Cohesion Establishment Complex." *Molecular and Cellular Biology* 25 (13): 5445–55. doi:10.1128/MCB.25.13.5445-5455.2005.

Bzymek, Malgorzata, Nathaniel H. Thayer, Steve D. Oh, Nancy Kleckner, and Neil Hunter. 2010. "Double Holliday Junctions Are Intermediates of DNA Break Repair." *Nature* 464 (7290): 937–41. doi:10.1038/nature08868.

Cai, J, F Uhlmann, E Gibbs, H Flores-Rozas, C G Lee, B Phillips, J Finkelstein, Nina Y Yao, Mike O'Donnell, and Jerard Hurwitz. 1996. "Reconstitution of Human Replication Factor C from Its Five Subunits in Baculovirus-Infected Insect Cells." *Pnas* 93 (23): 12896–901. doi:VL - 93.

Calzada, Arturo, Ben Hodgson, Masato Kanemaki, Avelino Bueno, and Karim Labib. 2005. "Molecular Anatomy and Regulation of a Stable Replisome at a Paused Eukaryotic DNA Replication Fork." *Genes and Development* 19 (16): 1905–19. doi:10.1101/gad.337205.

Cam, Eric Le, Eric Coı, Institut Gustave, and Cnrs Umr. 2018. "Rad52-Rad51 Association Is Essential to Protect Rad51 Filaments against Srs2, but Facultative for Filament Formation." *ELife* 51: 1–24. doi:10.7554/eLife.32744.

Cartwright, Richard, Alison M. Dunn, Paul J. Simpson, Cathryn E. Tambini, and John Thacker. 1998. "Isolation of Novel Human and Mouse Genes of the RecA/RAD51 Recombination-Repair Gene Family." *Nucleic Acids Research* 26 (7): 1653–59. doi:10.1093/nar/26.7.1653.

Cartwright, Richard, Cathryn E. Tambini, Paul J. Simpson, and John Thacker. 1998. "The XRCC2 DNA Repair Gene from Human and Mouse Encodes a Novel Member of the RecA/RAD51 Family." *Nucleic Acids Research* 26 (13): 3084–89. doi:10.1093/nar/26.13.3084.

Carvalho, Claudia M.B., and James R. Lupski. 2016. "Mechanisms Underlying Structural Variant Formation in Genomic Disorders." *Nature Reviews Genetics* 17

(4): 224–38. doi:10.1038/nrg.2015.25.

Cha, Rita S, and Nancy Kleckner. 2002. “ATR Homolog Mec1 Promotes Fork Progression, Thus Averting Breaks in Replication Slow Zones.” *Science (New York, N.Y.)* 297 (5581): 602–6. doi:10.1126/science.1071398.

Chan, Kin, and Dmitry A. Gordenin. 2015. “Clusters of Multiple Mutations: Incidence and Molecular Mechanisms.” *Annual Review of Genetics* 49 (1): 243–67. doi:10.1146/annurev-genet-112414-054714.

Chan, Kok Lung, Timea Palmai-Pallag, Songmin Ying, and Ian D. Hickson. 2009. “Replication Stress Induces Sister-Chromatid Bridging at Fragile Site Loci in Mitosis.” *Nature Cell Biology* 11 (6): 753–60. doi:10.1038/ncb1882.

Chan, Ying Wai, Kasper Fugger, and Stephen C. West. 2018. “Unresolved Recombination Intermediates Lead to Ultra-Fine Anaphase Bridges, Chromosome Breaks and Aberrations.” *Nature Cell Biology* 20 (1): 92–103. doi:10.1038/s41556-017-0011-1.

Chan, Ying Wai, and Stephen C. West. 2018. “A New Class of Ultrafine Anaphase Bridges Generated by Homologous Recombination.” *Cell Cycle* 17 (17): 2101-09. doi:10.1080/15384101.2018.1515555.

Chandramouly, Gurushankar, Amy Kwok, Bin Huang, Nicholas A. Willis, Anyong Xie, and Ralph Scully. 2013. “BRCA1 and CtIP Suppress Long-Tract Gene Conversion between Sister Chromatids.” *Nature Communications* 4: 1–12. doi:10.1038/ncomms3404.

Chen, Shuyan, Milan A. de Vries, and Stephen P. Bell. 2007. "Orc6 is required for dynamic recruitment of Cdt1 during repeated Mcm2–7 loading." *Genes and Development* 21: 2897–2907. doi:10.1101/gad.1596807

Chen, Zhucheng, Haijuan Yang, and Nikola P. Pavletich. 2008. “Mechanism of Homologous Recombination from the RecA-SsDNA/DsDNA Structures.” *Nature* 453 (7194): 489–94. doi:10.1038/nature06971.

Chilkova, Olga, Peter Stenlund, Isabelle Isoz, Carrie M. Stith, Pawel Grabowski, Else Britt Lundström, Peter M. Burgers, and Erik Johansson. 2007. “The Eukaryotic Leading and Lagging Strand DNA Polymerases Are Loaded onto Primer-Ends via Separate Mechanisms but Have Comparable Processivity in the Presence of PCNA.” *Nucleic Acids Research* 35 (19): 6588–97. doi:10.1093/nar/gkm741.

Chiu, Roland K., Jan Brun, Chantal Ramaekers, Jan Theys, Lin Weng, Philippe

Lambin, Douglas A. Gray, and Bradly G. Wouters. 2006. “Lysine 63-Polyubiquitination Guards against Translesion Synthesis-Induced Mutations.” *PLoS Genetics* 2 (7): 1070–83. doi:10.1371/journal.pgen.0020116.

Cho, Nam Woo, Robert L. Dilley, Michael A. Lampson, and Roger A. Greenberg. 2014. “Interchromosomal Homology Searches Drive Directional ALT Telomere Movement and Synapsis.” *Cell* 159 (1): 108–21. doi:10.1016/j.cell.2014.08.030.

Choe, Katherine N., and George Lucian Moldovan. 2017. “Forging Ahead through Darkness: PCNA, Still the Principal Conductor at the Replication Fork.” *Molecular Cell* 65 (3): 380–92. doi:10.1016/j.molcel.2016.12.020.

Chu, Wai Kit, and Ian D. Hickson. 2009. “RecQ Helicases: Multifunctional Genome Caretakers.” *Nature Reviews Cancer* 9 (9): 644–54. doi:10.1038/nrc2682.

Chung, Woo Hyun, Zhu Zhu, Alma Papusha, Anna Malkova, and Grzegorz Ira. 2010. “Defective Resection at DNA Double-Strand Breaks Leads to de Novo Telomere Formation and Enhances Gene Targeting.” *PLoS Genetics* 6 (5): 24. doi:10.1371/journal.pgen.1000948.

Church, George M., and Walter Gilbert. 1984. Genomic sequencing” *Proceedings of the National Academy of Sciences of the United States of America* 81 (7): 1991–95. doi:10.1073/pnas.81.7.1991.

Ciccia, Alberto, Amitabh V. Nimonkar, Yiduo Hu, Ildiko Hajdu, Yathish Jagadheesh Achar, Lior Izhar, Sarah A. Petit, et al. 2012. “Polyubiquitinated PCNA Recruits the ZRANB3 Translocase to Maintain Genomic Integrity after Replication Stress.” *Molecular Cell* 47 (3): 396–409. doi:10.1016/j.molcel.2012.05.024.

Clausen, Anders R., Scott A. Lujan, Adam B. Burkholder, Clinton D. Orebaugh, Jessica S. Williams, Maryam F. Clausen, Ewa P. Malc, et al. 2015. “Tracking Replication Enzymology in Vivo by Genome-Wide Mapping of Ribonucleotide Incorporation.” *Nature Structural and Molecular Biology* 22 (3): 185–91. doi:10.1038/nsmb.2957.

Cobb, Jennifer a., Lotte Bjergbaek, Kenji Shimada, Christian Frei, and Susan M. Gasser. 2003. “DNA Polymerase Stabilization at Stalled Replication Forks Requires Mec1 and the RecQ Helicase Sgs1.” *EMBO Journal* 22 (16): 4325–36. doi:10.1093/emboj/cdg391.

Cobb, Jennifer a., Thomas Schleker, Vanesa Rojas, Lotte Bjergbaek, José Antonio Tercero, and Susan M. Gasser. 2005. “Replisome Instability, Fork Collapse, and

Gross Chromosomal Rearrangements Arise Synergistically from Mec1 Kinase and RecQ Helicase Mutations." *Genes and Development* 19 (24): 3055–69. doi:10.1101/gad.361805.

Codlin, Sandra, and Jacob Z Dalgaard. 2003. "Complex Mechanism of Site-Specific DNA Replication Termination in Fission Yeast." *EMBO Journal* 22 (13): 3431-40. doi:10.1093/emboj/cdg330.

Coleman, Kate E., Miklós Békés, Jessica R. Chapman, Sarah B. Crist, Mathew J.K. Jones, Beatrix M. Ueberheide, and Tony T. Huang. 2017. "SENP8 Limits Aberrant Neddylation of Nedd8 Pathway Components to Promote Cullin-RING Ubiquitin Ligase Function." *ELife* 6: 1–27. doi:10.7554/eLife.24325.

Collins, Ryan L., Harrison Brand, Claire E. Redin, Carrie Hanscom, Caroline Antolik, Matthew R. Stone, Joseph T. Glessner, et al. 2017. "Defining the Diverse Spectrum of Inversions, Complex Structural Variation, and Chromothripsis in the Morbid Human Genome." *Genome Biology* 18 (1): 1–21. doi:10.1186/s13059-017-1158-6.

Cortes-Ledesma, Felipe, and Andr??s Aguilera. 2006. "Double-Strand Breaks Arising by Replication through a Nick Are Repaired by Cohesin-Dependent Sister-Chromatid Exchange." *EMBO Reports* 7 (9): 919–26. doi:10.1038/sj.embor.7400774.

Cortez, David. 2015. "Preventing Replication Fork Collapse to Maintain Genome Integrity." *DNA Repair* 32: 149–57. doi:10.1016/j.dnarep.2015.04.026.

Costantino, Lorenzo, 1, Sotirios K. Sotiriou, 1, Juha K. Rantala, 2, Simon Magin, et al. 2014. "Break-Induced Replication Repair of Damaged Forks Induces Genomic Duplications in Human Cells." *Science* 343: 88–91. doi:10.1038/nrm2852.

Cotta-Ramusino, Cecilia, Daniele Fachinetti, Chiara Lucca, Ylli Doksani, Massimo Lopes, José Sogo, and Marco Foiani. 2005. "Exo1 Processes Stalled Replication Forks and Counteracts Fork Reversal in Checkpoint-Defective Cells." *Molecular Cell* 17 (1): 153–59. doi:10.1016/j.molcel.2004.11.032.

Cox, Lynne S. 1997. "Who Binds Wins: Competition for PCNA Rings out Cell-Cycle Changes." *Trends in Cell Biology* 7 (12): 493–98. doi:10.1016/S0962-8924(97)01170-7.

Dalgaard, J. Z., and a. J S Klar. 2001. "Does S. Pombe Exploit the Intrinsic Asymmetry of DNA Synthesis to Imprint Daughter Cells for Mating-Type Switching?" *Trends*

in Genetics 17 (3): 153–57. doi:10.1016/S0168-9525(00)02203-4.

Dalgaard, J Z, and a J Klar. 2000. “Swi1 and Swi3 Perform Imprinting, Pausing, and Termination of DNA Replication in S. Pombe.” *Cell* 102 (6): 745–51. doi:10.1016/S0092-8674(00)00063-5.

Dalgaard, Jacob Z., Emma L. Godfrey, and Ramsay J. McFarlane. 2011. “Eukaryotic Replication Barriers : How, Why and Where Forks Stall.” doi:10.5772/20383.

Davidson, Marta B., and Grant W. Brown. 2008. “The N- and C-Termini of Elg1 Contribute to the Maintenance of Genome Stability.” *DNA Repair* 7 (8): 1221–32. doi:10.1016/j.dnarep.2008.04.001.

Davidson, Marta B., Yuki Katou, Andrea Keszthelyi, Tina L. Sing, Tian Xia, Jiongwen Ou, Jessica A. Vaisica, Neroshan Thevakumaran, Lisette Marjavaara, Chad L. Myers, Andrei Chabes, Katsuhiko Shirahige, and Grant W. Brown. 2012. “Endogenous DNA Replication Stress Results in Expansion of dNTP Pools and a Mutator Phenotype.” *EMBO Journal* 31 (4): 895-907. doi:10.1038/emboj.2011.485.

Davies, Adelina A., Diana Huttner, Yasukazu Daigaku, Shuhua Chen, and Helle D. Ulrich. 2008. “Activation of Ubiquitin-Dependent DNA Damage Bypass Is Mediated by Replication Protein A.” *Molecular Cell* 29 (5): 625–36. doi:10.1016/j.molcel.2007.12.016.

Davis, Allison P., and Lorraine S. Symington. 2001. “The Yeast Recombinational Repair Protein Rad59 Interacts with Rad52 and Stimulates Single-Strand Annealing.” *Genetics* 159 (2): 515–25.

Davis, Allison P, and Lorraine S Symington. 2004. “RAD51-Dependent Break-Induced Replication in Yeast.” *Molecular and Cellular Biology* 24 (6): 2344–51. doi:10.1128/MCB.24.6.2344.

De March, Matteo, and Alfredo De Biasio. 2017. “The Dark Side of the Ring: Role of the DNA Sliding Surface of PCNA.” *Critical Reviews in Biochemistry and Molecular Biology* 52 (6): 663–73. doi:10.1080/10409238.2017.1364218.

De March, Matteo, Nekane Merino, Susana Barrera-Vilarmau, Ramon Crehuet, Silvia Onesti, Francisco J. Blanco, and Alfredo De Biasio. 2017. “Structural Basis of Human PCNA Sliding on DNA.” *Nature Communications* 8: 1–7. doi:10.1038/ncomms13935.

De Piccoli, Giacomo, Yuki Katou, Takehiko Itoh, Ryuichiro Nakato, Katsuhiko

Shirahige, and Karim Labib. 2012. “Replisome Stability at Defective DNA Replication Forks Is Independent of S Phase Checkpoint Kinases.” *Molecular Cell* 45 (5): 696–704. doi:10.1016/j.molcel.2012.01.007.

De Tullio, Luisina, Kyle Kaniecki, Youngho Kwon, J. Brooks Crickard, Patrick Sung, and Eric C. Greene. 2017. “Yeast Srs2 Helicase Promotes Redistribution of Single-Stranded DNA-Bound RPA and Rad52 in Homologous Recombination Regulation.” *Cell Reports* 21 (3): 570–77. doi:10.1016/j.celrep.2017.09.073.

Deem, Angela, Krista Barker, Kelly VanHulle, Brandon Downing, Alexandra Vayl, and Anna Malkova. 2008. "Defective Break-Induced Replication Leads to Half-Crossovers in *Saccharomyces Cerevisiae*." *Genetics* 179 (4): 1845-60. doi:10.1534/genetics.108.087940.

Deem, Angela, Andrea Keszthelyi, Tiffany Blackgrove, Alexandra Vayl, Barbara Coffey, Ruchi Mathur, Andrei Chabes, and Anna Malkova. 2011. “Break-Induced Replication Is Highly Inaccurate.” *PLoS Biology* 9 (2). doi:10.1371/journal.pbio.1000594.

Demczuk, Agnieszka, Michel G. Gauthier, Ingrid Veras, Settapong Kosiyatrakul, Carl L. Schildkraut, Meinrad Busslinger, John Bechhoefer, and Paolo Norio. 2012. “Regulation of DNA Replication within the Immunoglobulin Heavy-Chain Locus during B Cell Commitment.” *PLoS Biology* 10 (7): 15. doi:10.1371/journal.pbio.1001360.

Deshpande, a M, and C S Newlon. 1996. “DNA Replication Fork Pause Sites Dependent on Transcription.” *Science* 272 (5264): 1030–33. doi:10.1126/science.272.5264.1030.

Ding, Queying, and David M. MacAlpine. 2011. “Defining the Replication Program through the Chromatin Landscape.” *Critical Reviews in Biochemistry and Molecular Biology* 46 (2): 165–79. doi:10.3109/10409238.2011.560139.

Doe, Claudette L., Fekret Osman, Julie Dixon, and Matthew C. Whitby. 2004. “DNA Repair by a Rad22-Mus81-Dependent Pathway That Is Independent of Rhp51.” *Nucleic Acids Research* 32 (18): 5570–81. doi:10.1093/nar/gkh853.

Donnianni, Roberto a, and Lorraine S Symington. 2013. “Break-Induced Replication Occurs by Conservative DNA Synthesis.” *Proceedings of the National Academy of Sciences of the United States of America* 110 (33): 13475–80. doi:10.1073/pnas.1309800110.

Dorn, Elizabeth Suzanne, and Jeanette Gowen Cook. 2011. “Nucleosomes in the Neighborhood: New Roles for Chromatin Modifications in Replication Origin Control.” *Epigenetics* 6 (5): 552–59. doi:10.4161/epi.6.5.15082.

Dosanjh, Manjit K., David W. Collins, Wufang Fan, Gregory G. Lennon, Joanna S. Albala, Zhiyuan Shen, and David Schild. 1998. “Isolation and Characterization of RAD51C, a New Human Member of the RAD51 Family of Related Genes.” *Nucleic Acids Research* 26 (5): 1179–84. doi:10.1093/nar/26.5.1179.

Downing, Brandon, Rachel Morgan, Kelly VanHulle, Angela Deem, and Anna Malkova. 2008. “Large Inverted Repeats in the Vicinity of a Single Double-Strand Break Strongly Affect Repair in Yeast Diploids Lacking Rad51.” *Mutation Research - Fundamental and Molecular Mechanisms of Mutagenesis* 645 (1–2): 9–18. doi:10.1016/j.mrfmmm.2008.07.013.

Dubarry, Marion, Conor Lawless, a Peter Banks, Simon Cockell, and David Lydall. 2015. “Genetic Networks Required to Coordinate Chromosome Replication by DNA Polymerases α, δ, and ε in Saccharomyces Cerevisiae.” *G3 Genes/ Genomes/ Genetics* 5 (10): 2187–97. doi:10.1534/g3.115.021493.

Dupaigne, Pauline, Cyrille Le Breton, Francis Fabre, Serge Gangloff, Eric Le Cam, and Xavier Veaute. 2008. “The Srs2 Helicase Activity Is Stimulated by Rad51 Filaments on DsDNA: Implications for Crossover Incidence during Mitotic Recombination.” *Molecular Cell* 29 (2): 243–54. doi:10.1016/j.molcel.2007.11.033.

Eaton, Matthew L., Joseph A. Prinz, Heather K. MacAlpine, George Tretyakov, Peter V. Kharchenko, and David M. MacAlpine. 2011. “Chromatin Signatures of the Drosophila Replication Program.” *Genome Research* 21 (2): 164–74. doi:10.1101/gr.116038.110.

Edenberg, Howard J., and Joel A. Huberman. 1975. "Eukaryotic Chromosome Replication" *Annual Review of Genetics* 9: 245-284. doi:10.1146/annurev.ge.09.120175.001333.

Eissenberg, Joel C., Rao Ayyagari, Xavier V. Gomes, and Peter M. J. Burgers. 1997. “Mutations in yeast proliferating cell nuclear antigen define distinct sites for interaction with DNA polymerase δ and DNA polymerase ε.” *Molecular and Cell Biology* 17 (11): 6367-78. doi:10.1128/MCB.17.11.6367.

Ekholm-Reed, Susanna, Juan Méndez, Donato Tedesco, Anders Zetterberg, Bruce

Stillman, and Steven I. Reed. 2004. “Deregulation of Cyclin E in Human Cells Interferes with Prereplication Complex Assembly.” *Journal of Cell Biology* 165 (6): 789–800. doi:10.1083/jcb.200404092.

Elango et al. 2017. “Break-Induced Replication Promotes Formation of Lethal Joint Molecules Dissolved by Srs2.” *Nature Communications* 8 (1). doi:10.1038/s41467-017-01987-2.

Elia, Andrew E.H., Alexander P. Boardman, David C. Wang, Edward L. Huttlin, Robert A. Everley, Noah Dephoure, Chunshui Zhou, Itay Koren, Steven P. Gygi, and Stephen J. Elledge. 2015. “Quantitative Proteomic Atlas of Ubiquitination and Acetylation in the DNA Damage Response.” *Molecular Cell* 59 (5): 867–81. doi:10.1016/j.molcel.2015.05.006.

Ellis, Nathan A., Joanna Groden, Tian Zhang Ye, Joel Straughen, David J. Lennon, Susan Ciocci, Maria Proytcheva, and James German. 1995. “The Bloom’s Syndrome Gene Product Is Homologous to RecQ Helicases.” *Cell* 83 (4): 655–66. doi:10.1016/0092-8674(95)90105-1.

Enemark, Eric J., and Leemor Joshua-Tor. 2006. “Mechanism of DNA Translocation in a Replicative Hexameric Helicase.” *Nature* 442 (7100): 270–75. doi:10.1038/nature04943.

Evrin, C., P. Clarke, J. Zech, R. Lurz, J. Sun, S. Uhle, H. Li, B. Stillman, and C. Speck. 2009. “A Double-Hexameric MCM2-7 Complex Is Loaded onto Origin DNA during Licensing of Eukaryotic DNA Replication.” *Proceedings of the National Academy of Sciences* 106 (48): 20240–45. doi:10.1073/pnas.0911500106.

Eydmann, T., E. Sommariva, T. Inagawa, S. Mian, a. J S Klar, and J. Z. Dalgaard. 2008. “Rtf1-Mediated Eukaryotic Site-Specific Replication Termination.” *Genetics* 180 (1): 27–39. doi:10.1534/genetics.108.089243.

Federley, Richard G., and Louis J. Romano. 2010. “DNA Polymerase: Structural Homology, Conformational Dynamics, and the Effects of Carcinogenic DNA Adducts.” *Journal of Nucleic Acids* 10. doi:10.4061/2010/457176.

Fekairi, Samira, Sarah Scaglione, Charly Chahwan, Ewan R. Taylor, Agnès Tissier, Stéphane Coulon, Meng Qiu Dong, et al. 2009. “Human SLX4 Is a Holliday Junction Resolvase Subunit That Binds Multiple DNA Repair/Recombination Endonucleases.” *Cell* 138 (1): 78–89. doi:10.1016/j.cell.2009.06.029.

Fekret Osman and Matthew C. Whitby. 2009. “Monitoring Homologous Recombination

Following Replication Fork Perturbation in the Fission Yeast Schizosaccharomyces Pombe." *Methods in Molecular Biology* 521:535–52. doi:10.1007/978-1-60327-817-5.

Feng, Z., S. P. Scott, W. Bussen, G. G. Sharma, G. Guo, T. K. Pandita, and S. N. Powell. 2011. "Rad52 Inactivation Is Synthetically Lethal with BRCA2 Deficiency." *Proceedings of the National Academy of Sciences* 108 (2): 686–91. doi:10.1073/pnas.1010959107.

Feytout, A., S. Vaur, S. Genier, S. Vazquez, and J.-P. Javerzat. 2011. "Psm3 Acetylation on Conserved Lysine Residues Is Dispensable for Viability in Fission Yeast but Contributes to Eso1-Mediated Sister Chromatid Cohesion by Antagonizing Wpl1." *Molecular and Cellular Biology* 31 (8): 1771–86. doi:10.1128/MCB.01284-10.

Fisher, A., T. S. Wang, and D. Korn. 1979. "Enzymological Characterization of DNA Polymerase alpha. Basic Catalytic Properties Processivity, and Gap Utilization of the Homogenous Enzyme from Human KB Cells 254 (13): 6128–37. http://www.jbc.org/content/254/13/6128.

Flood, Carrie L., Gina P. Rodriguez, Gaobin Bao, Arthur H. Shockley, Yoke Wah Kow, and Gray F. Crouse. 2015. "Replicative DNA Polymerase δ but Not ε Proofreads Errors in Cis and in Trans." *PLoS Genetics* 11 (3): 1–32. doi:10.1371/journal.pgen.1005049.

Forget, Anthony L., and Stephen C. Kowalczykowski. 2012. "Single-Molecule Imaging of DNA Pairing by RecA Reveals a Three-Dimensional Homology Search." *Nature* 482 (7385): 423–27. doi:10.1038/nature10782.

Fornander, Louise H., Axelle Renodon-Cornière, Naoyuki Kuwabara, Kentaro Ito, Yasuhiro Tsutsui, Toshiyuki Shimizu, Hiroshi Iwasaki, Bengt Nordén, and Masayuki Takahashi. 2014. "Swi5-Sfr1 Protein Stimulates Rad51-Mediated DNA Strand Exchange Reaction through Organization of DNA Bases in the Presynaptic Filament." *Nucleic Acids Research* 42 (4): 2358–65. doi:10.1093/nar/gkt1257.

Fortin, Gary S., and Lorraine S. Symington. 2002. "Mutations in Yeast Rad51 That Partially Bypass the Requirement for Rad55 and Rad57 in DNA Repair by Increasing the Stability of Rad51-DNA Complexes." *EMBO Journal* 21 (12): 3160–70. doi:10.1093/emboj/cdf293.

Fotedar, Rati, Romina Mossi, Patrick Fitzgerald, Tristan Rousselle, Giovanni Maga, Howard Brickner, Helen Messier, Shailaja Kasibhatla, Ulrich Hubscher, and Arun Fotedar. 1996. “A conserved domain of the large subunit of replication factor C binds PCNA and acts like a dominant negative inhibitor of DNA replication in mammalian cells.” *The EMBO Journal* 15 (16): 4423-33. doi:10.1002/j.1460-2075.1996.tb00815.x.

Frampton, Jonathan, Anja Irmisch, Catherine M. Green, Andrea Neiss, Michelle Trickey, Helle D. Ulrich, Kanji Furuya, Felicity Z. Watts, Antony M. Carr, and and Alan R. Lehmann. 2006. “Postreplication Repair and PCNA Modification in Schizosaccharomyces Pombe.” *Molecular Biology of the Cell* 17: 2976–85. doi:10.1091/mbc.E05.

Fricke, William M., and Steven J. Brill. 2003. “Slx1 - Slx4 Is a Second Structure-Specific Endonuclease Functionally Redundant with Sgs1 - Top3.” *Genes and Development* 17 (14): 1768–78. doi:10.1101/gad.1105203.

Fridman, Yearit, Niv Palgi, Daniel Dovrat, Shay Ben-Aroya, Philip Hieter, and Amir Aharoni. 2010. “Subtle Alterations in PCNA-Partner Interactions Severely Impair DNA Replication and Repair.” *PLoS Biology* 8 (10). doi:10.1371/journal.pbio.1000507.

Frigola, Jordi, Dirk Remus, Amina Mehanna, and John F. X. Diffley. 2013. "ATPase-dependent quality control of DNA replication origin licensing.” *Nature* 495 (74411): 339-343. doi:10.1038/nature11920

Fromme, J.C., and G.L. Verdine. 2004. “Base Excision Repair.” *Advances in Protein Chemistry* 69: 1–41. doi:10.1016/S0065-3233(04)69001-2.

Fugger, Kasper, Martin Mistrik, Kai J. Neelsen, Qi Yao, Ralph Zellweger, Arne Nedergaard Kousholt, Peter Haahr, et al. 2015. “FBH1 Catalyzes Regression of Stalled Replication Forks.” *Cell Reports* 10 (10): 1749–57. doi:10.1016/j.celrep.2015.02.028.

Fujisawa, Ryo, Eiji Ohashi, Kouji Hirota, and Toshiki Tsurimoto. 2017. “Human CTF18-RFC Clamp-Loader Complexed with Non-Synthesising DNA Polymerase ϵ Efficiently Loads the PCNA Sliding Clamp.” *Nucleic Acids Research* 45 (8): 4550–63. doi:10.1093/nar/gkx096.

Fullbright, George, Halley B. Rycenga, Jordon D. Gruber, and David T. Long. 2016. “P97 Promotes a Conserved Mechanism of Helicase Unloading during DNA

Cross-Link Repair." *Molecular and Cellular Biology* 36 (23): 2983–94. doi:10.1128/MCB.00434-16.

Fumasoni, Marco, Katharina Zwicky, Fabio Vanoli, Massimo Lopes, and Dana Branzei. 2015. "Error-Free DNA Damage Tolerance and Sister Chromatid Proximity during DNA Replication Rely on the Polα/Primase/Ctf4 Complex." *Molecular Cell* 57 (5). The Authors: 812–23. doi:10.1016/j.molcel.2014.12.038.

Gaines, William a., Stephen K. Godin, Faiz F. Kabbinavar, Timsi Rao, Andrew P. VanDemark, Patrick Sung, and Kara a. Bernstein. 2015. "Promotion of Presynaptic Filament Assembly by the Ensemble of S. Cerevisiae Rad51 Paralogues with Rad52." *Nature Communications* 6: 7834. doi:10.1038/ncomms8834.

Galanos, Panagiotis, Konstantinos Vougas, David Walter, Alexander Polyzos, Apolinar Maya-Mendoza, Emma J. Haagensen, Antonis Kokkalis, et al. 2016. "Chronic P53-Independent P21 Expression Causes Genomic Instability by Deregulating Replication Licensing." *Nature Cell Biology* 18 (7): 777–89. doi:10.1038/ncb3378.

Gambus, Agnieszka, Richard C. Jones, Alberto Sanchez-Diaz, Masato Kanemaki, Frederick van Deursen, Ricky D. Edmondson, and Karim Labib. 2006. "GINS Maintains Association of Cdc45 with MCM in Replisome Progression Complexes at Eukaryotic DNA Replication Forks." *Nature Cell Biology* 8 (4): 358–66. doi:10.1038/ncb1382.

Ganai, Rais A., Xiao-Ping Zhang, Wolf-Dietrich Heyer, and Erik Johansson. 2016. "Strand Displacement Synthesis by Yeast DNA Polymerase ε." *Nucleic Acids Research* 44 (17): 8229–40. doi:10.1093/nar/gkw556.

Gandhi, Rita, Peter J. Gillespie, and Tatsuya Hirano. 2006. "Human Wapl Is a Cohesin-Binding Protein That Promotes Sister-Chromatid Resolution in Mitotic Prophase." *Current Biology* 16 (24): 2406–17. doi:10.1016/j.cub.2006.10.061.

Garg, Parie, and Peter M J Burgers. 2005. "DNA Polymerases That Propagate the Eukaryotic DNA Replication Fork." *Critical Reviews in Biochemistry and Molecular Biology* 40 (2): 115–28. doi:10.1080/10409230590935433.

Gari, K., C. Decaillet, M. Delannoy, L. Wu, and A. Constantinou. 2008. "Remodeling of DNA Replication Structures by the Branch Point Translocase FANCM." *Proceedings of the National Academy of Sciences* 105 (42): 16107–12.

doi:10.1073/pnas.0804777105.

Gary, Ronald, Dale L. Ludwig, Helen L. Cornelius, Mark A. MacInnes, and Min S. Park. 1997. “The DNA Repair Endonuclease XPG Binds to Proliferating Cell Nuclear Antigen (PCNA) and Shares Sequence Elements with the PCNA-Binding Regions of FEN-1 and Cyclin-Dependent Kinase Inhibitor P21.” *Journal of Biological Chemistry* 272 (39): 24522–29. doi:10.1074/jbc.272.39.24522.

Gazy, Inbal, and Martin Kupiec. 2012. “The Importance of Being Modified: PCNA Modification and DNA Damage Response.” *Cell Cycle* 11 (14): 2620–23. doi:10.4161/cc.20626.

Gellon, Lionel, David F. Razidlo, Olive Gleeson, Lauren Verra, Danae Schulz, Robert S. Lahue, and Catherine H. Freudenreich. 2011. “New Functions of Ctf18-RFC in Preserving Genome Stability Outside Its Role in Sister Chromatid Cohesion.” *PLoS Genetics* 7 (2). doi:10.1371/journal.pgen.1001298.

Georgescu, Roxana E., Lance Langston, Nina Y. Yao, Olga Yurieva, Dan Zhang, Jeff Finkelstein, Tani Agarwal, and Mike E. O’Donnell. 2014. “Mechanism of Asymmetric Polymerase Assembly at the Eukaryotic Replication Fork.” *Nature Structural and Molecular Biology* 21 (8): 664–70. doi:10.1038/nsmb.2851.

Georgescu, Roxana E., Grant D. Schauer, Nina Y. Yao, Lance D. Langston, Olga Yurieva, Dan Zhang, Jeff Finkelstein, and Mike E. O’Donnell. 2015. “Reconstitution of a Eukaryotic Replisome Reveals Suppression Mechanisms That Define Leading/Lagging Strand Operation.” *ELife* 2015 (4): 1–20. doi:10.7554/eLife.04988.

Gilbert, D.M. 2004. "In Search of the Holy Replicator." *Nature Reviews Molecular Cell Biology* 5: 848–855. doi:10.1038/nrm1495.

Godin, Stephen, Adam Wier, Faiz Kabbinavar, Dominique S. Bratton-Palmer, Harshad Ghodke, Bennett Van Houten, Andrew P. Vandemark, and Kara A. Bernstein. 2013. “The Shu Complex Interacts with Rad51 through the Rad51 Paralogues Rad55-Rad57 to Mediate Error-Free Recombination.” *Nucleic Acids Research* 41 (8): 4525–34. doi:10.1093/nar/gkt138.

Gomes, Xavier V., and Peter M J Burgers. 2001. “ATP Utilization by Yeast Replication Factor C: I. ATP-Mediated Interaction with DNA and with Proliferating Cell Nuclear Antigen.” *Journal of Biological Chemistry* 276 (37): 34768–75. doi:10.1074/jbc.M011631200.

Gray, M D, J C Shen, a S Kamath-Loeb, a Blank, B L Sopher, G M Martin, J Oshima, and L a Loeb. 1997. “The Werner Syndrome Protein Is a DNA Helicase.” *Nature Genetics* 17 (1): 100–103. doi:10.1038/ng0997-100.

Greenfeder, S a, and C S Newlon. 1992. “A Replication Map of a 61-Kb Circular Derivative of Saccharomyces Cerevisiae Chromosome III.” *Molecular Biology of the Cell* 3 (9): 999–1013.

Guacci, V., J. Stricklin, M. S. Bloom, X. Gu , M. Bhatter, and D. Koshland. 2015. “A Novel Mechanism for the Establishment of Sister Chromatid Cohesion by the ECO1 Acetyltransferase.” *Molecular Biology of the Cell* 26 (1): 117–33. doi:10.1091/mbc.E14-08-1268.

Guo, Caixia, Tie Shan Tang, Marzena Bienko, Ivan Dikic, and Errol C. Friedberg. 2008. “Requirements for the Interaction of Mouse Polκ with Ubiquitin and Its Biological Significance.” *Journal of Biological Chemistry* 283 (8): 4658–64. doi:10.1074/jbc.M709275200.

Haering, Christian H., Doris Schoffnegger, Tatsuya Nishino, Wolfgang Helmhart, Kim Nasmyth, and Jan Löwe. 2004. “Structure and Stability of Cohesin’s Smc1-Kleisin Interaction.” *Molecular Cell* 15 (6): 951–64. doi:10.1016/j.molcel.2004.08.030.

Hanahan, Douglas, and Robert A Weinberg. 2011. “Hallmarks of Cancer: The next Generation.” *Cell* 144 (5): 646–74. doi:10.1016/j.cell.2011.02.013.

Handa, Tetsuya, Mai Kanke, Tatsuro S. Takahashi, Takuro Nakagawa, and Hisao M. asukata. 2012. "DNA Polymerization-Independent Functions of DNA Polymerase Epsilon in Assembly and Progression of the Replisome in Fission Yeast" *Molecular Biology of the Cell* 23 (16): 3240-53. doi:10.1091/mbc.E12-05-0339

Hanna, Joseph S, Evgueny S Kroll, Victoria Lundblad, and Forrest a Spencer. 2001. “Saccharomyces Cerevisiae CTF18 and CTF4 Are Required for Sister Chromatid Cohesion” *Molecular and Cellular Biology* 21 (9): 3144–58. doi:10.1128/MCB.21.9.3144.

Haracska, Lajos, Carlos A Torres-Ramos, Robert E Johnson, Satya Prakash, and Louise Prakash. 2004. “Opposing Effects of Ubiquitin Conjugation and SUMO Modification of PCNA on Replicational Bypass of DNA Lesions in Saccharomyces Cerevisiae.” *Molecular and Cellular Biology* 24 (10): 4267–74. doi:10.1128/MCB.24.10.4267-4274.2004.

Haruta, Nami, Yumiko Kurokawa, Yasuto Murayama, Yufuko Akamatsu, Satoru Unzai,

Yasuhiro Tsutsui, and Hiroshi Iwasaki. 2006. “The Swi5-Sfr1 Complex Stimulates Rhp51/Rad51 - and Dmc1-Mediated DNA Strand Exchange in Vitro.” *Nature Structural and Molecular Biology* 13 (9): 823–30. doi:10.1038/nsmb1136.

Hashimoto & Costanzo. 2011. “Studying DNA Replication Fork Stability in Xenopus Egg Extract” 745: 437–45. doi:10.1007/978-1-61779-129-1.

Hastings, P. J., Grzegorz Ira, and James R. Lupski. 2009. “A Microhomology-Mediated Break-Induced Replication Model for the Origin of Human Copy Number Variation.” *PLoS Genetics* 5 (1). doi:10.1371/journal.pgen.1000327.

Hays, S. L., A. A. Firmenich, and P. Berg. 1995. “Complex Formation in Yeast Double-Strand Break Repair: Participation of Rad51, Rad52, Rad55, and Rad57 Proteins.” *Proceedings of the National Academy of Sciences* 92 (15): 6925–29. doi:10.1073/pnas.92.15.6925.

Hedglin, Mark, Ravindra Kumar, and Stephen J. Benkovic. 2013. “Replication Clamps and Clamp Loaders.” *Cold Spring Harbor Perspectives in Biology* 5 (4): 1–19. doi:10.1101/cshperspect.a010165.

Heller, Ryan C, and Kenneth J Marians. 2006. “Replisome Assembly and the Direct Restart of Stalled Replication Forks.” *Nature Reviews. Molecular Cell Biology* 7 (12): 932–43. doi:10.1038/nrm2058.

Herzberg, K., V. I. Bashkirov, M. Rolfsmeier, E. Haghnazari, W. H. McDonald, S. Anderson, E. V. Bashkirova, J. R. Yates, and W.-D. Heyer. 2006. “Phosphorylation of Rad55 on Serines 2, 8, and 14 Is Required for Efficient Homologous Recombination in the Recovery of Stalled Replication Forks.” *Molecular and Cellular Biology* 26 (22): 8396–8409. doi:10.1128/MCB.01317-06.

Heyer, Wolf Dietrich, Xuan Li, Michael Rolfsmeier, and Xiao Ping Zhang. 2006. “Rad54: The Swiss Army Knife of Homologous Recombination?” *Nucleic Acids Research* 34 (15): 4115–25. doi:10.1093/nar/gkl481.

Hiasa, Hiroshi, and Kenneth J. Marians. 1994. “Tus Prevents Overreplication of OriC Plasmid DNA.” *Journal of Biological Chemistry* 269 (43): 26959–68. doi:10.1074/jbc.M104411200.

Hickson, Ian D. 2014. “The Dissolution of Double Holliday Junctions.” *Cold Spring Harbor Perspectives in Biology* 6 (7): a016477. doi:10.1101/cshperspect.a016477.

Higgins, N. P., K. Kato, and B. Strauss. 1976. “A Model for Replication Repair in

Mammalian Cells." *Journal of Molecular Biology* 101 (3): 417–25. doi:10.1016/0022-2836(76)90156-X.

Hills, Stephanie A., and John F X Diffley. 2014. "DNA Replication and Oncogene-Induced Replicative Stress." *Current Biology* 24 (10): R435–44. doi:10.1016/j.cub.2014.04.012.

Hishiki, Asami, Hiroshi Hashimoto, Tomo Hanafusa, Keijiro Kamei, Eiji Ohashi, Toshiyuki Shimizu, Haruo Ohmori, and Mamoru Sato. 2009. "Structural Basis for Novel Interactions between Human Translesion Synthesis Polymerases and Proliferating Cell Nuclear Antigen." *Journal of Biological Chemistry* 284 (16): 10552–60. doi:10.1074/jbc.M809745200.

Hoege, C, B Pfander, G L Moldovan, G Pyrowolakis, and S Jentsch. 2002. "RAD6-Dependent DNA Repair Is Linked to Modi Cation of PCNA by Ubiquitin and SUMO." *Nature* 419 (September): 135–41.

Hoffman, Charles S., Valerie Wood, and Peter A. Fantes. 2015. *"*An Ancient Yeast for Young Geneticists: A Primer on the Schizosaccharomyces pombe Model System." *Genetics* 201 (October): 403-23. doi:10.1534/genetics.115.181503.

Ilves, Ivar, Tatjana Petojevic, James J. Pesavento, and Michael R. Botchan. 2010. "Activation of the MCM2-7 Helicase by Association with Cdc45 and GINS Proteins." *Molecular Cell* 37 (2): 247–58. doi:10.1016/j.molcel.2009.12.030.

Inagawa, Takabumi, Tomoko Yamada-Inagawa, Trevor Eydmann, I Saira Mian, Teresa S Wang, and Jacob Z Dalgaard. 2009. "Schizosaccharomyces Pombe Rtf2 Mediates Site-Specific Replication Termination by Inhibiting Replication Restart." *Proceedings of the National Academy of Sciences of the United States of America* 106 (19): 7927–32. doi:10.1073/pnas.0812323106.

Ira, Grzegorz, Anna Malkova, Giordano Liberi, Marco Foiani, and James E. Haber. 2003. "Srs2 and Sgs1-Top3 Suppress Crossovers during Double-Strand Break Repair in Yeast." *Cell* 115 (4): 401–11. doi:10.1016/S0092-8674(03)00886-9.

Iraqui, Ismail, Yasmina Chekkal, Nada Jmari, Violena Pietrobon, Karine Fréon, Audrey Costes, and Sarah A E Lambert. 2012. "Recovery of Arrested Replication Forks by Homologous Recombination Is Error-Prone." *PLoS Genetics* 8 (10). doi:10.1371/journal.pgen.1002976.

Ito, Kentaro, Yasuto Murayama, Masayuki Takahashi, and Hiroshi Iwasaki. 2018. "Two Three-Strand Intermediates Are Processed during Rad51-Driven DNA

Strand Exchange." *Nature Structural and Molecular Biology* 25 (1): 29–36. doi:10.1038/s41594-017-0002-8.

J. Kramara, B. Osia, and A. Malkova. 2018. "Break-Induced Replication: The Where, The Why, and The How." *Trends in Genetics* 34 (7): 518–31. doi:10.1016/j.tig.2018.04.002.

Jain, Suvi, Neal Sugawara, John Lydeard, Moreshwar Vaze, Nicolas Tanguy Le Gac, and James E. Haber. 2009. "A Recombination Execution Checkpoint Regulates the Choice of Homologous Recombination Pathway during DNA Double-Strand Break Repair." *Genes and Development* 23 (3): 291–303. doi:10.1101/gad.1751209.

Jain, Suvi, Neal Sugawara, Anuja Mehta, Taehyun Ryu, and James E. Haber. 2016. "Sgs1 and Mph1 Helicases Enforce the Recombination Execution Checkpoint during DNA Double-Strand Break Repair in Saccharomyces Cerevisiae." *Genetics* 203 (2): 667–75. doi:10.1534/genetics.115.184317.

Jalan, Manisha, Judith Oehler, Carl A. Morrow, Fekret Osman, and Matthew C Whitby. 2019. "Factors Affecting Template Switch Recombination Associated with Restarted DNA Replication." *ELife* 8: 1-22. doi: 10.7554/eLife.41697.001.

Janke, Ryan, Kristina Herzberg, Michael Rolfsmeier, Jordan Mar, Vladimir I. Bashkirov, Edwin Haghnazari, Greg Cantin, John R. Yates, and Wolf Dietrich Heyer. 2010. "A Truncated DNA-Damage-Signaling Response Is Activated after DSB Formation in the G1 Phase of Saccharomyces Cerevisiae." *Nucleic Acids Research* 38 (7): 2302–13. doi:10.1093/nar/gkp1222.

Jin, Yong Hwan, Rao Ayyagari, Michael A. Resnick, Dmitry A. Gordenin, and Peter M. J. Burgers. 2003. "Okazaki Fragment Maturation in Yeast: II. Cooperation Between the Polymerase and 3′-5′-Exonuclease Activities of Pol δ in the Creation of a Ligatable Nick." *Journal of Biological Chemistry* 278 (3): 1626-33. doi:10.1074/jbc.M209803200.

Jin, Yong Hwan, Robyn Obert, Peter M. J. Burgers, Thomas A. Kunkel, Michael A. Resnick, and Dmitry A. Gordenin. 2001. "The 3'-5' Exonuclease of DNA Polymerase δ Can Substitute for the 5' Flap Endonuclease Rad27/Fen1 in Processing Okazaki Fragments and Preventing Genome Instability." *Proceedings of the National Academy of Sciences* 98 (9): 5122-27. doi:10.1073/pnas.091095198.

Johnson, Catherine, Vamsi K. Gali, Tatsuro S. Takahashi, and Takashi Kubota. 2016. "PCNA Retention on DNA into G2/M Phase Causes Genome Instability in Cells Lacking Elg1." *Cell Reports* 16 (3): 684–95. doi:10.1016/j.celrep.2016.06.030.

Johnson, R D, and L S Symington. 1995. "Functional Differences and Interactions among the Putative RecA Homologs Rad51, Rad55, and Rad57." *Molecular and Cellular Biology* 15 (9): 4843–50. doi:10.1128/MCB.15.9.4843.

Johnson, Robert E., Roland Klassen, Louise Prakash, and Satya Prakash. 2015. "A Major Role of DNA Polymerase δ in Replication of Both the Leading and Lagging DNA Strands." *Molecular Cell* 59 (2): 163–75. doi:10.1016/j.molcel.2015.05.038.

Jones, R. M., O. Mortusewicz, I. Afzal, M. Lorvellec, P. García, T. Helleday, and E. Petermann. 2013. "Increased Replication Initiation and Conflicts with Transcription Underlie Cyclin E-Induced Replication Stress." *Oncogene* 32 (32): 3744–53. doi:10.1038/onc.2012.387.

Kagawa, Wataru, Hitoshi Kurumizaka, Shukuko Ikawa, Shigeyuki Yokoyama, and Takehiko Shibata. 2001. "Homologous Pairing Promoted by the Human, Rad52 Protein." *Journal of Biological Chemistry* 276 (37): 35201–8. doi:10.1074/jbc.M104938200.

Kanellis. 2003. "Elg1 Forms an Alternative PCNA-Interacting RFC Complex Required to Maintain Genome Stability." *Current Biology* 13: 1583–95. doi: 10.1016/S0960-9822(03)00578-5.

Kang, Y.-H., W. C. Galal, A. Farina, I. Tappin, and J. Hurwitz. 2012. "Properties of the Human Cdc45/Mcm2-7/GINS Helicase Complex and Its Action with DNA Polymerase in Rolling Circle DNA Synthesis." *Proceedings of the National Academy of Sciences* 109 (16): 6042–47. doi:10.1073/pnas.1203734109.

Kang, Young Hoon, Chul Hwan Lee, and Yeon Soo Seo. 2010. "Dna2 on the Road to Okazaki Fragment Processing and Genome Stability in Eukaryotes." *Critical Reviews in Biochemistry and Molecular Biology* 45 (2): 71–96. doi:10.3109/10409230903578593.

Kaniecki, Kyle, Luisina De Tullio, Bryan Gibb, Youngho Kwon, Patrick Sung, and Eric C. Greene. 2017. "Dissociation of Rad51 Presynaptic Complexes and Heteroduplex DNA Joints by Tandem Assemblies of Srs2." *Cell Reports* 21 (11): 3166–77. doi:10.1016/j.celrep.2017.11.047.

Kans, J A, and R K Mortimer. 1991. "Nucleotide Sequence of the RAD57 Gene of

Saccharomyces Cerevisiae." *Gene* 105 (1): 139–40. doi:0378-1119(91)90527-I [pii].

Karakaidos, Panagiotis, Panayotis Zacharatos, Athanassios Kotsinas, Triantafillos Liloglou, Monica Venere, Richard A Ditullio Jr, Nikolaos G Kastrinakis, et al. 2005. "Activation of the DNA Damage Checkpoint and Genomic Instability in Human Precancerous Lesions." *Nature* 434: 907–13. doi:10.1038/nature03492.1.

Katz, Samantha S., Frederick S. Gimble, and Francesca Storici. 2014. "To Nick or Not to Nick: Comparison of I-SceI Single- And Double-Strand Break-Induced Recombination in Yeast and Human Cells." *PLoS ONE* 9 (2). doi:10.1371/journal.pone.0088840.

Kaufmann, Tanja, Irina Grishkovskaya, Anton A. Polyansky, Sebastian Kostrhon, Eva Kukolj, Karin M. Olek, Sebastien Herbert, et al. 2017. "A Novel Non-Canonical PIP-Box Mediates PARG Interaction with PCNA." *Nucleic Acids Research* 45 (16): 9741–59. doi:10.1093/nar/gkx604.

Kaykov, Atanas, and Paul Nurse. 2015. "The Spatial and Temporal Organization of Origin Firing during the S-Phase of Fission Yeast," *Genome Research* 1–12. doi:10.1101/gr.180372.114.Freely.

Kelch, Brian A., Debora L. Makino, Mike O'Donnell, and John Kuriyan. 2011. "How a DNA Polymerase Clamp Loader Opens a Sliding Clamp" *Science* 334 (December): 1675–81.

Kelman, Z, J K Lee, and J Hurwitz. 1999. "The Single Minichromosome Maintenance Protein of Methanobacterium Thermoautotrophicum DeltaH Contains DNA Helicase Activity." *Proceedings of the National Academy of Sciences of the United States of America* 96 (26): 14783–88. doi:10.1073/pnas.96.26.14783.

Kennedy, Richard D, and Alan D D Andrea. 2005. "The Fanconi Anemia / BRCA Pathway : New Faces in the Crowd." *Genes & Development* 19: 2925–40. doi:10.1101/gad.1370505.FA.

Keszthelyi, Andrea, Yasukazu Daigaku, Katie Ptasińska, Izumi Miyabe, and Antony M Carr. 2015. "Mapping Ribonucleotides in Genomic DNA and Exploring Replication Dynamics by Polymerase Usage Sequencing (Pu-Seq)." *Nature Protocols* 10 (11): 1786–1801. doi:10.1038/nprot.2015.116.

Khasanov, Fuat K., Albina F. Salakhova, Olga V. Chepurnaja, Vladimir G. Korolev, and Vladimir I. Bashkirov. 2004. "Identification and Characterization of the Rlp1+,

the Novel Rad51 Paralog in the Fission Yeast Schizosaccharomyces Pombe." *DNA Repair* 3 (10): 1363–74. doi:10.1016/j.dnarep.2004.05.010.

Khasanov, Fuat K., Galina V. Savchenko, Elena V. Bashkirova, Vladimir G. Korolev, Wolf Dietrich Heyer, and Vladimir I. Bashkirov. 1999. "A New Recombinational DNA Repair Gene from Schizosaccharomyces Pombe with Homology to Escherichia Coli RecA." *Genetics* 152 (4): 1557–72.

Kilkenny, Mairi L., Aline C. Simon, Jack Mainwaring, David Wirthensohn, Sandro Holzer, and Luca Pellegrini. 2017. "The Human CTF4-Orthologue AND-1 Interacts with DNA Polymerase a/Primase via Its Unique C-Terminal HMG Box." *Journal of the Royal Society Interface* 14 (136). doi:10.1098/rsob.170217.

Kim, Jane C., Samantha T. Harris, Teresa Dinter, Kartik A. Shah, and Sergei M. Mirkin. 2017. "The Role of Break-Induced Replication in Large-Scale Expansions of (CAG)n/(CTG)Nrepeats." *Nature Structural and Molecular Biology* 24 (1): 55–60. doi:10.1038/nsmb.3334.

Kim, Jiyoung, Kathryn Robertson, Katie J L Mylonas, Fiona C. Gray, Iryna Charapitsa, and Stuart a. MacNeill. 2005. "Contrasting Effects of Elg1-RFC and Ctf18-RFC Inactivation in the Absence of Fully Functional RFC in Fission Yeast." *Nucleic Acids Research* 33 (13): 4078–89. doi:10.1093/nar/gki728.

Kim, Woong, Eric J. Bennett, Edward L. Huttlin, Ailan Guo, Jing Li, Anthony Possemato, Mathew E. Sowa, et al. 2011. "Systematic and Quantitative Assessment of the Ubiquitin-Modified Proteome." *Molecular Cell* 44 (2): 325–40. doi:10.1016/j.molcel.2011.08.025.

Kitao, Saori, Akira Shimamoto, Makoto Goto, Robert W. Miller, William A. Smithson, Noralane M. Lindor, and Yasuhiro Furuichi. 1999. "Mutations in RECQL4 Cause a Subset of Cases of Rothmund-Thomson Syndrome." *Nature Genetics* 22 (1): 82–84. doi:10.1038/8788.

Klapstein, Kevin, Tom Chou, and Robijn Bruinsma. 2004. "Physics of RecA-Mediated Homologous Recognition." *Biophysical Journal* 87 (3): 1466–77. doi:10.1529/biophysj.104.039578.

Knott, Simon R V, Christopher J. Viggiani, Simon Tavar??, and Oscar M. Aparicio. 2009. "Genome-Wide Replication Profiles Indicate an Expansive Role for Rpd3L in Regulating Replication Initiation Timing or Efficiency, and Reveal Genomic Loci of Rpd3 Function in Saccharomyces Cerevisiae." *Genes and Development* 23 (9):

1077–90. doi:10.1101/gad.1784309.

Krejci, Lumir, Stephen Van Komen, Ying Li, Jana Villemain, Mothe Sreedhar Reddy, Hannah Klein, Thomas Ellenberger, and Patrick Sung. 2003. “DNA Helicase Srs2 Disrupts the Rad51 Presynaptic Filament.” *Nature* 423 (6937): 305–9. doi:10.1038/nature01577.

Krings, Gregor, and Deepak Bastia. 2004. “Swi1- and Swi3-Dependent and Independent Replication Fork Arrest at the Ribosomal DNA of Schizosaccharomyces Pombe.” *Proceedings of the National Academy of Sciences of the United States of America* 101 (39): 14085–90. doi:10.1073/pnas.0406037101.

Krogh, Berit Olsen, and Lorraine S. Symington. 2004. “Recombination Proteins in Yeast.” *Annual Review of Genetics* 38 (1): 233–71. doi:10.1146/annurev.genet.38.072902.091500.

Kubota, Takashi, Shin-ichiro Hiraga, Kayo Yamada, Angus I. Lamond, and Anne D. Donaldson. 2011. “Quantitative Proteomic Analysis of Chromatin Reveals That Ctf18 Acts in the DNA Replication Checkpoint.” *Molecular & Cellular Proteomics* 10 (7): M110.005561. doi:10.1074/mcp.M110.005561.

Kubota, Takashi, Kyungjae Myung, and Anne D. Donaldson. 2013. “Is PCNA Unloading the Central Function of the Elg1/ ATAD5 Replication Factor C-like Complex?” *Cell Cycle* 12 (16): 2570–79. doi:10.4161/cc.25626.

Kubota, Takashi, Kohei Nishimura, Masato T. Kanemaki, and Anne D. Donaldson. 2013. “The Elg1 Replication Factor C-like Complex Functions in PCNA Unloading during DNA Replication.” *Molecular Cell* 50 (2): 273–80. doi:10.1016/j.molcel.2013.02.012.

Kunkel, Thomas A., and Peter M. Burgers. 2008. “Dividing the Workload at a Eukaryotic Replication Fork.” *Trends in Cell Biology* 18 (11): 521–27. doi:10.1016/j.tcb.2008.08.005.

Kupiec, Martin. 2016. “Alternative Clamp Loaders/Unloaders.” *FEMS Yeast Research* 16 (7): 1–8. doi:10.1093/femsyr/fow084.

Kurokawa, Yumiko, Yasuto Murayama, Nami Haruta-Takahashi, Itaru Urabe, and Hiroshi Iwasaki. 2008. “Reconstitution of DNA Strand Exchange Mediated by Rhp51 Recombinase and Two Mediators.” *PLoS Biology* 6 (4): 836–48. doi:10.1371/journal.pbio.0060088.

Kwon, Youngho, and Patrick Sung. 2017. “Rad52, Maestro of Inverse Strand Exchange.” *Molecular Cell* 67 (1): 1–3. doi:10.1016/j.molcel.2017.06.015.

Lambert, Sarah, and Antony M. Carr. 2005. “Checkpoint Responses to Replication Fork Barriers.” *Biochimie* 87 (7): 591–602. doi:10.1016/j.biochi.2004.10.020.

———. 2013. “Replication Stress and Genome Rearrangements: Lessons from Yeast Models.” *Current Opinion in Genetics and Development* 23 (2): 132–39. doi:10.1016/j.gde.2012.11.009.

Lambert, Sarah, Ken’ichi Mizuno, Joël Blaisonneau, Sylvain Martineau, Roland Chanet, Karine Fréon, Johanne M. Murray, Antony M. Carr, and Giuseppe Baldacci. 2010. “Homologous Recombination Restarts Blocked Replication Forks at the Expense of Genome Rearrangements by Template Exchange.” *Molecular Cell* 39 (3): 346–59. doi:10.1016/j.molcel.2010.07.015.

Lambert, Sarah, Adam Watson, Daniel M. Sheedy, Ben Martin, and Antony M. Carr. 2005. “Gross Chromosomal Rearrangements and Elevated Recombination at an Inducible Site-Specific Replication Fork Barrier.” *Cell* 121 (5): 689–702. doi:10.1016/j.cell.2005.03.022.

Langston, L. D., D. Zhang, O. Yurieva, R. E. Georgescu, J. Finkelstein, N. Y. Yao, C. Indiani, and M. E. O’Donnell. 2014. “CMG Helicase and DNA Polymerase Form a Functional 15-Subunit Holoenzyme for Eukaryotic Leading-Strand DNA Replication.” *Proceedings of the National Academy of Sciences* 111 (43): 15390–95. doi:10.1073/pnas.1418334111.

Le, Siyuan, J. Kent Moore, James E. Haber, and Carol W. Greider. 1999. “RAD50 and RAD51 Define Two Pathways That Collaborate to Maintain Telomeres in the Absence of Telomerase.” *Genetics* 152 (1): 143–52.

Leach, Craig A., and W. Matthew Michael. 2005. “Ubiquitin/SUMO Modification of PCNA Promotes Replication Fork Progression in Xenopus Laevis Egg Extracts.” *Journal of Cell Biology* 171 (6): 947–54. doi:10.1083/jcb.200508100.

Lee, Kyoo Young, Haiqing Fu, Mirit I. Aladjem, and Kyungjae Myung. 2013. “ATAD5 Regulates the Lifespan of DNA Replication Factories by Modulating PCNA Level on the Chromatin.” *Journal of Cell Biology* 200 (1): 31–44. doi:10.1083/jcb.201206084.

Lemoine, Francene J., Natasha P. Degtyareva, Kirill Lobachev, and Thomas D. Petes. 2005. “Chromosomal Translocations in Yeast Induced by Low Levels of DNA

Polymerase: A Model for Chromosome Fragile Sites." *Cell* 120 (5): 587–98. doi:10.1016/j.cell.2004.12.039.

Lengronne, Armelle, John McIntyre, Yuki Katou, Yutaka Kanoh, Karl Peter Hopfner, Katsuhiko Shirahige, and Frank Uhlmann. 2006. "Establishment of Sister Chromatid Cohesion at the S. Cerevisiae Replication Fork." *Molecular Cell* 23 (6): 787–99. doi:10.1016/j.molcel.2006.08.018.

Lessard, Julie, and Guy Sauvageau. 2003. "Bmi-1 Determines the Proliferative Capacity of Normal and Leukaemic Stem Cells." *Nature* 423 (6937): 255–60. doi:10.1038/nature01572.

Li, Xuan, and Wolf Dietrich Heyer. 2009. "RAD54 Controls Access to the Invading 3′-OH End after RAD51-Mediated DNA Strand Invasion in Homologous Recombination in Saccharomyces Cerevisiae." *Nucleic Acids Research* 37 (2): 638–46. doi:10.1093/nar/gkn980.

Levin, David S., Wei Bai, Nina Yao, Michael O'Donnell, and Alan E. Tomkinson. 1997. "An interaction between DNA ligase I and proliferating cell nuclear antigen: implications for Okazaki fragment synthesis and joining." *Proceedings of the National Academy of Sciences of the United States of America*. 94 (24): 12863-68. doi:10.1073/pnas.94.24.12863.

Lim, D S, and P Hasty. 1996. "A Mutation in Mouse Rad51 Results in an Early Embryonic Lethal That Is Suppressed by a Mutation in P53." *Molecular and Cellular Biology* 16 (12): 7133–43. doi:10.1128/MCB.16.12.7133.

Lisby, Michael, Jacqueline H. Barlow, Rebecca C. Burgess, and Rodney Rothstein. 2004. "Choreography of the DNA Damage Response: Spatiotemporal Relationships among Checkpoint and Repair Proteins." *Cell* 118 (6): 699–713. doi:10.1016/j.cell.2004.08.015.

Liu, Jie, Ludovic Renault, Xavier Veaute, Francis Fabre, Henning Stahlberg, and Wolf Dietrich Heyer. 2011. "Rad51 Paralogues Rad55-Rad57 Balance the Antirecombinase Srs2 in Rad51 Filament Formation." *Nature* 479 (7372): 245–48. doi:10.1038/nature10522.

Liu, Nan, Jane E. Lamerdin, Robert S. Tebbs, David Schild, James D. Tucker, M. Richard Shen, Kerry W. Brookman, et al. 1998. "XRCC2 and XRCC3, New Human Rad51-Family Members, Promote Chromosome Stability and Protect against DNA Cross-Links and Other Damages." *Molecular Cell* 1 (6): 783–93.

doi:10.1016/S1097-2765(00)80078-7.

Llorente, Bertrand, Catherine E. Smith, and Lorraine S. Symington. 2008. “Break-Induced Replication: What Is It and What Is It For?” *Cell Cycle* 7 (7): 859–64. doi:10.4161/cc.7.7.5613.

Lorenz, Alexander, Fekret Osman, Victoria Folkyte, Sevil Sofueva, and Matthew C Whitby. 2009. “Fbh1 Limits Rad51-Dependent Recombination at Blocked Replication Forks.” *Molecular and Cellular Biology* 29 (17): 4742–56. doi:10.1128/MCB.00471-09.

Lorenz, Alexander, Fekret Osman, Weili Sun, Saikat Nandi, Roland Steinacher, and Matthew C. Whitby. 2012. “The Fission Yeast FANCM Ortholog Directs Non-Crossover Recombination during Meiosis.” *Science* 336 (6088): 1585–88. doi:10.1126/science.1220111.

Lou, Huiqiang, Makiko Komata, Yuki Katou, Zhiyun Guan, Clara C. Reis, Martin Budd, Katsuhiko Shirahige, and Judith L. Campbell. 2008. “Mrc1 and DNA Polymerase ε Function Together in Linking DNA Replication and the S Phase Checkpoint.” *Molecular Cell* 32 (1): 106–17. doi:10.1016/j.molcel.2008.08.020.

Lovett, Susan T. 1994. “Sequence of the RAD55 Gene of Saccharomyces Cerevisiae: Similarity of RAD55 to Prokaryotic RecA and Other RecA-like Proteins.” *Gene* 142 (1): 103–6. doi:10.1016/0378-1119(94)90362-X.

Lucca, Chiara, Fabio Vanoli, Cecilia Cotta-Ramusino, Achille Pellicioli, Giordano Liberi, James Haber, and Marco Foiani. 2004. “Checkpoint-Mediated Control of Replisome-Fork Association and Signalling in Response to Replication Pausing.” *Oncogene* 23 (6): 1206–13. doi:10.1038/sj.onc.1207199.

Lukas, Claudia, Velibor Savic, Simon Bekker-Jensen, Carsten Doil, Beate Neumann, Ronni Sølvhøj Pedersen, Merete Grøhfte, et al. 2011. “53BP1 Nuclear Bodies Form around DNA Lesions Generated by Mitotic Transmission of Chromosomes under Replication Stress.” *Nature Cell Biology* 13 (3): 243–53. doi:10.1038/ncb2201.

Lumpkin, Ryan J., Hongbo Gu, Yiying Zhu, Marilyn Leonard, Alla S. Ahmad, Karl R. Clauser, Jesse G. Meyer, Eric J. Bennett, and Elizabeth A. Komives. 2017. “Site-Specific Identification and Quantitation of Endogenous SUMO Modifications under Native Conditions.” *Nature Communications* 8 (1). doi:10.1038/s41467-017-01271-3.

Lydeard, John R., Suvi Jain, Miyuki Yamaguchi, and James E. Haber. 2007. “Break-Induced Replication and Telomerase-Independent Telomere Maintenance Require Pol32.” *Nature* 448 (7155): 820–23. doi:10.1038/nature06047.

Lydeard, John R., Zachary Lipkin-Moore, Yi Jun Sheu, Bruce Stillman, Peter M. Burgers, and James E. Haber. 2010. “Break-Induced Replication Requires All Essential DNA Replication Factors except Those Specific for Pre-RC Assembly.” *Genes and Development* 24 (11): 1133–44. doi:10.1101/gad.1922610.

Lyubimov, Artem Y., Melania Strycharska, and James M. Berger. 2011. “The Nuts and Bolts of Ring-Translocase Structure and Mechanism.” *Current Opinion in Structural Biology* 21 (2): 240–48. doi:10.1016/j.sbi.2011.01.002.

Macheret, Morgane, and Thanos D. Halazonetis. 2018. “Intragenic Origins Due to Short G1 Phases Underlie Oncogene-Induced DNA Replication Stress.” *Nature* 555 (7694): 112–16. doi:10.1038/nature25507.

Maculins, Timurs, Pedro Junior Nkosi, Hiroko Nishikawa, and Karim Labib. 2015. “Tethering of SCF^{Dia2} to the Replisome Promotes Efficient Ubiquitylation and Disassembly of the CMG Helicase.” *Current Biology* 25 (17): 2254–59. doi:10.1016/j.cub.2015.07.012.

Maga, Giovanni, and Ulrich Hübscher. 2003. “Proliferating Cell Nuclear Antigen (PCNA): A Dancer with Many Partners.” *Journal of Cell Science* 116 (15): 3051–60. doi:10.1242/jcs.00653.

Makovets, Svetlana, Ira Herskowitz, H Elizabeth, and Elizabeth H Blackburn. 2004. “Anatomy and Dynamics of DNA Replication Fork Movement in Yeast Telomeric Regions Anatomy and Dynamics of DNA Replication Fork Movement in Yeast Telomeric Regions.” *Molecular and Cellular Biology* 24 (9): 4019–31. doi:10.1128/MCB.24.9.4019.

Malkova, Anna, and Grzegorz Ira. 2013. “Break-Induced Replication: Functions and Molecular Mechanism.” *Current Opinion in Genetics and Development* 23 (3): 271–79. doi:10.1016/j.gde.2013.05.007.

Malkova, Anna, Maria L Naylor, Miyuki Yamaguchi, Grzegorz Ira, and James E Haber. 2005. “Replication Differs in Kinetics and Checkpoint Responses from RAD51 - Mediated Gene Conversion RAD51 -Dependent Break-Induced Replication Differs in Kinetics and Checkpoint Responses from RAD51 -Mediated Gene Conversion.” *Molecular and Cellular Biology* 25 (3): 933–44.

doi:10.1128/MCB.25.3.933.

Malkova et al. 1996. “Double-Strand Break Repair in the Absence of RAD51 in Yeast : A Possible Role for Break-Induced DNA Replication” 93 (July): 7131–36.

Mankouri, Hocine W., and Ian D. Hickson. 2007. “The RecQ Helicase-Topoisomerase III-Rmi1 Complex: A DNA Structure-Specific ‘Dissolvasome’?” *Trends in Biochemical Sciences* 32 (12): 538–46. doi:10.1016/j.tibs.2007.09.009.

Mannava, Sudha, Kalyana C. Moparthy, Linda J. Wheeler, Venkatesh Natarajan, Shoshanna N. Zucker, Emily E. Fink, Michael Im, et al. 2013. “Depletion of Deoxyribonucleotide Pools Is an Endogenous Source of DNA Damage in Cells Undergoing Oncogene-Induced Senescence.” *American Journal of Pathology* 182 (1): 142–51. doi:10.1016/j.ajpath.2012.09.011.

Manthei, Kelly A., and James L. Keck. 2013. “The BLM Dissolvasome in DNA Replication and Repair.” *Cellular and Molecular Life Sciences* 70 (21): 4067–84. doi:10.1007/s00018-013-1325-1.

Maradeo, Marie E., and Robert V. Skibbens. 2010. “Replication Factor C Complexes Play Unique Pro- and Anti-Establishment Roles in Sister Chromatid Cohesion.” *PLoS ONE* 5 (10): 1–9. doi:10.1371/journal.pone.0015381.

Maric, M., T. Maculins, G. De Piccoli, and K. Labib. 2014. “Cdc48 and a Ubiquitin Ligase Drive Disassembly of the CMG Helicase at the End of DNA Replication.” *Science* 346 (6208): 440-52. doi:10.1126/science.1253596.

Maric, Marija, Progya Mukherjee, Michael H. Tatham, Ronald Hay, and Karim Labib. 2017. “Ufd1-Npl4 Recruit Cdc48 for Disassembly of Ubiquitylated CMG Helicase at the End of Chromosome Replication.” *Cell Reports* 18 (13): 3033–42. doi:10.1016/j.celrep.2017.03.020.

Martín, Victoria, Charly Chahwan, Hui Gao, Véronique Blais, James Wohlschlegel, John R. Yates, Clare H. McGowan, and Paul Russell. 2006. “Sws1 Is a Conserved Regulator of Homologous Recombination in Eukaryotic Cells.” *EMBO Journal* 25 (11): 2564–74. doi:10.1038/sj.emboj.7601141.

Martino, Julieta, and Kara A. Bernstein. 2016. “The Shu Complex is a Conserved Regulator of Homologous Recombination.” *FEMS Yeast Research* 16 (6): 1-13. doi:10.1093/femsyr/fow073.

Matos, Joao, Miguel G. Blanco, Sarah Maslen, J. Mark Skehel, and Stephen C. West. 2011. “Regulatory Control of the Resolution of DNA Recombination Intermediates

during Meiosis and Mitosis.” *Cell* 147 (1): 158–72. doi:10.1016/j.cell.2011.08.032.

Mattock, Heidi, David P. Lane, and Emma Warbrick. 2001. “Inhibition of Cell Proliferation by the PCNA-Binding Region of P21 Expressed as a GFP Miniprotein.” *Experimental Cell Research* 265 (2): 234–41. doi:10.1006/excr.2001.5160.

Mayer, Melanie L., Steven P. Gygi, Ruedi Aebersold, and Philip Hieter. 2001. “Identification of RFC(Ctf18p, Ctf8p, Dcc1p): An Alternative RFC Complex Required for Sister Chromatid Cohesion in S. Cerevisiae.” *Molecular Cell* 7 (5): 959–70. doi:10.1016/S1097-2765(01)00254-4.

Mayle, Ryan, Ian M Campbell, Christine R Beck, Yang Yu, Marenda Wilson, Chad A Shaw, Lotte Bjergbaek, James R Lupski, and Grzegorz Ira. 2015. “Fork Breakage” 1 (6249): 742–47. doi:10.1126/science.aaa8391.Mus81.

Mazin, Alexander V., Andrei A. Alexeev, and Stephen C. Kowalczykowski. 2003. “A Novel Function of Rad54 Protein: Stabilization of the Rad51 Nucleoprotein Filament.” *Journal of Biological Chemistry* 278 (16): 14029–36. doi:10.1074/jbc.M212779200.

Mazin, Alexander V., Carole J. Bornarth, Jachen A. Solinger, Wolf Dietrich Heyer, and Stephen C. Kowalczykowski. 2000. “Rad54 Protein Is Targeted to Pairing Loci by the Rad51 Nucleoprotein Filament.” *Molecular Cell* 6 (3): 583–92. doi:10.1016/S1097-2765(00)00057-5.

Mazina, Olga M., Havva Keskin, Kritika Hanamshet, Francesca Storici, and Alexander V. Mazin. 2017. “Rad52 Inverse Strand Exchange Drives RNA-Templated DNA Double-Strand Break Repair.” *Molecular Cell* 67 (1): 19–29.e3. doi:10.1016/j.molcel.2017.05.019.

McDonald, Karin R., Amanda J. Guise, Parham Pourbozorgi-Langroudi, Ileana M. Cristea, Virginia A. Zakian, John A. Capra, and Nasim Sabouri. 2016. “Pfh1 Is an Accessory Replicative Helicase That Interacts with the Replisome to Facilitate Fork Progression and Preserve Genome Integrity.” *PLoS Genetics* 12 (9). doi:10.1371/journal.pgen.1006238.

McElhinny, Stephanie A. Nick, Dmitry A. Gordenin, Carrie M. Stith, Peter M.J. Burgers, and Thomas A Kunkel. 2008. “Division of Labor at the Eukaryotic Replication Fork.” *Molecular Cell* 30: 137–44. doi:10.1016/j.molcel.2014.11.004.

McIntyre, Justyna, and Roger Woodgate. 2015. “Regulation of Translesion DNA

Synthesis: Posttranslational Modification of Lysine Residues in Key Proteins." *DNA Repair* 29: 166–79. doi:10.1016/j.dnarep.2015.02.011.

Méchali, Marcel, Kazumasa Yoshida, Philippe Coulombe, and Philippe Pasero. 2013. "Genetic and Epigenetic Determinants of DNA Replication Origins, Position and Activation." *Current Opinion in Genetics and Development* 23 (2): 124–31. doi:10.1016/j.gde.2013.02.010.

Meister, Peter, Mickaël Poidevin, Stefania Francesconi, Isabelle Tratner, Patrick Zarzov, and Giuseppe Baldacci. 2003. "Nuclear Factories for Signalling and Repairing DNA Double Strand Breaks in Living Fission Yeast." *Nucleic Acids Research* 31 (17): 5064–73. doi:10.1093/nar/gkg719.

Meister, Peter, Angela Taddei, Aaron Ponti, Giuseppe Baldacci, and Susan M Gasser. 2007. "Replication Foci Dynamics: Replication Patterns Are Modulated by S-Phase Checkpoint Kinases in Fission Yeast." *The EMBO Journal* 26 (5): 1315–26. doi:10.1038/sj.emboj.7601538.

Melendy, T, and B Stillman. 1991. "Purification of DNA Polymerase-Delta As an Essential Simian Virus-40 DNA Replication Factor." *J Biol Chem* 266 (3): 1942–49.

Michel, Bénédicte, Hasna Boubakri, Zeynep Baharoglu, Marie LeMasson, and Roxane Lestini. 2007. "Recombination Proteins and Rescue of Arrested Replication Forks." *DNA Repair* 6 (7): 967–80. doi:10.1016/j.dnarep.2007.02.016.

Michel, Bénédicte, and Steven J. Sandler. 2017. "Replication Restart in Bacteria." *Journal of Bacteriology* 199 (13). doi:10.1128/JB.00102-17.

Miller, Kyle M, Ofer Rog, and Julia Promisel Cooper. 2006. "Semi-Conservative DNA Replication through Telomeres Requires Taz1." *Nature* 440 (7085): 824–28. doi:10.1038/nature04638.

Mimitou, Eleni P., and Lorraine S. Symington. 2009. "Nucleases and Helicases Take Center Stage in Homologous Recombination." *Trends in Biochemical Sciences* 34 (5): 264–72. doi:10.1016/j.tibs.2009.01.010.

Miron, Karin, Tamar Golan-Lev, Raz Dvir, Eyal Ben-David, and Batsheva Kerem. 2015. "Oncogenes Create a Unique Landscape of Fragile Sites." *Nature Communications* 6 (May): 1–7. doi:10.1038/ncomms8094.

Miyabe, Izumi, Thomas A. Kunkel, and Antony M. Carr. 2011. "The Major Roles of DNA Polymerases Epsilon and Delta at the Eukaryotic Replication Fork Are

Evolutionarily Conserved." *PLoS Genetics* 7 (12). doi:10.1371/journal.pgen.1002407.

Miyabe, Izumi, Ken'Ichi Mizuno, Andrea Keszthelyi, Yasukazu Daigaku, Meliti Skouteri, Saed Mohebi, Thomas A Kunkel, Johanne M Murray, and Antony M Carr. 2015. "Polymerase δ Replicates Both Strands after Homologous Recombination–Dependent Fork Restart." *Nature Structural & Molecular Biology* 22 (October): 1–8. doi:10.1038/nsmb.3100.

Mizuno, Ken'ichi, Sarah Lambert, Giuseppe Baldacci, Johanne M. Murray, and Antony M. Carr. 2009. "Nearby Inverted Repeats Fuse to Generate Acentric and Dicentric Palindromic Chromosomes by a Replication Template Exchange Mechanism." *Genes and Development* 23 (24): 2876–86. doi:10.1101/gad.1863009.

Mizuno, Ken'ichi, Izumi Miyabe, Stephanie a Schalbetter, Antony M Carr, and Johanne M Murray. 2013. "Recombination-Restarted Replication Makes Inverted Chromosome Fusions at Inverted Repeats." *Nature* 493 (7431): 246–49. doi:10.1038/nature11676.

Mohebi, Saed, Ken'Ichi Mizuno, Adam Watson, Antony M. Carr, and Johanne M. Murray. 2015. "Checkpoints Are Blind to Replication Restart and Recombination Intermediates That Result in Gross Chromosomal Rearrangements." *Nature Communications* 6: 6357. doi:10.1038/ncomms7357.

Mojardín, Laura, Enrique Vázquez, and Francisco Antequera. 2013. *"*Specification of DNA Replication Origins and Genomic Base Composition in Fission Yeasts." *Journal of Molecular Biology* 425 (23): 4706-13. doi: 10.1016/j.jmb.2013.09.023.

Moldovan, George Lucian, Donniphat Dejsuphong, Mark I R Petalcorin, Kay Hofmann, Shunichi Takeda, Simon J. Boulton, and Alan D. D'Andrea. 2012. "Inhibition of Homologous Recombination by the PCNA-Interacting Protein PARI." *Molecular Cell* 45 (1): 75–86. doi:10.1016/j.molcel.2011.11.010.

Moldovan, George Lucian, Boris Pfander, and Stefan Jentsch. 2006. "PCNA Controls Establishment of Sister Chromatid Cohesion during S Phase." *Molecular Cell* 23 (5): 723–32. doi:10.1016/j.molcel.2006.07.007.

Mpldovan, George-Lucian, Boris Pfander, ans Stefan Jentsch. 2007. "PCNA, the Maestro of the Replication Fork." *Cell* 129 (4): 665–79. doi:10.1016/j.cell.2007.05.003.

Moreno, Alberto, Jamie T. Carrington, Luca Albergante, Mohammed Al Mamun,

Emma J. Haagensen, Eirini-Stavroula Komseli, Vassilis G. Gorgoulis, Timothy J. Newman, and J. Julian Blow. 2016. “Unreplicated DNA Remaining from Unperturbed S Phases Passes through Mitosis for Resolution in Daughter Cells.” *Proceedings of the National Academy of Sciences* 113 (39): E5757–64. doi:10.1073/pnas.1603252113.

Morishita, Takashi, Takashi Morishita, Fumiko Furukawa, Fumiko Furukawa, Chikako Sakaguchi, Chikako Sakaguchi, Takashi Toda, et al. 2005. “Role of the *Schizosaccharomyces pombe* F-Box DNA Helicase in Processing Recombination Intermediates.” *Society* 25 (18): 8074–83. doi:10.1128/MCB.25.18.8074.

Morrow, Carl A, Michael O Nguyen, Andrew Fower, Io Nam Wong, Fekret Osman, Claire Bryer, and Matthew C Whitby. 2017a. “Inter-Fork Strand Annealing Causes Genomic Deletions during the Termination of DNA Replication.” *ELife* 6: 1–15. doi:10.7554/eLife.25490.

Morrow, Dwight M., Carla Connelly, and Philip Hieter. 1997. “‘Break Copy’ Duplication: A Model for Chromosome Fragment Formation in Saccharomyces Cerevisiae.” *Genetics* 147 (2): 371–82.

Mortensen, U. H., C. Bendixen, I. Sunjevaric, and R. Rothstein. 1996. “DNA Strand Annealing Is Promoted by the Yeast Rad52 Protein.” *Proceedings of the National Academy of Sciences* 93 (20): 10729–34. doi:10.1073/pnas.93.20.10729.

Mosig, Gisela. 1998. “Recombination and Recombination-Dependent Dna Replication in Bacteriophage T4.” *Annual Review of Genetics* 32 (1): 379–413. doi:10.1146/annurev.genet.32.1.379.

Moyer, S. E., P. W. Lewis, and M. R. Botchan. 2006. “Isolation of the Cdc45/Mcm2-7/GINS (CMG) Complex, a Candidate for the Eukaryotic DNA Replication Fork Helicase.” *Proceedings of the National Academy of Sciences* 103 (27): 10236–41. doi:10.1073/pnas.0602400103.

Mueser, Timothy C, Jennifer M Hinerman, Juliette M Devos, Ryan A Boyer, and Kandace J Williams. 2010. “Structural Analysis of Bacteriophage T4 DNA Replication : A Review in the Virology Journal Series on Bacteriophage T4 and Its Relatives.” *Virology Journal* 7 (1): 358-74. doi:10.1186/1743-422X-7-359.

Muñoz, Ivan M., Karolina Hain, Anne Cécile Déclais, Mary Gardiner, Geraldine W. Toh, Luis Sanchez-Pulido, Johannes M. Heuckmann, et al. 2009. “Coordination of Structure-Specific Nucleases by Human SLX4/BTBD12 Is Required for DNA

Repair." *Molecular Cell* 35 (1): 116–27. doi:10.1016/j.molcel.2009.06.020.

Murray, Johanne M, and Antony M Carr. 2008. "Smc5/6: A Link between DNA Repair and Unidirectional Replication?" *Nature Reviews. Molecular Cell Biology* 9 (2): 177–82. doi:10.1038/nrm2309.

Naiki, T, T Kondo, D Nakada, K Matsumoto, and K Sugimoto. 2001. "Chl12 (Ctf18) Forms a Novel Replication Factor C-Related Complex and Functions Redundantly with Rad24 in the DNA Replication Checkpoint Pathway." *Molecular and Cellular Biology* 21 (17): 5838–45. doi:10.1128/MCB.21.17.5838.

Nandi, Saikat, and Matthew C. Whitby. 2012. "The ATPase Activity of Fml1 Is Essential for Its Roles in Homologous Recombination and DNA Repair." *Nucleic Acids Research* 40 (19): 9584–95. doi:10.1093/nar/gks715.

Narayanan, Vidhya, Piotr A. Mieczkowski, Hyun Min Kim, Thomas D. Petes, and Kirill S. Lobachev. 2006. "The Pattern of Gene Amplification Is Determined by the Chromosomal Location of Hairpin-Capped Breaks." *Cell* 125 (7): 1283–96. doi:10.1016/j.cell.2006.04.042.

Nasmyth, Kim, and Christian H. Haering. 2005. "The Structure and Function of Smc and Kleisin Complexes." *Annual Review of Biochemistry* 74 (1): 595–648. doi:10.1146/annurev.biochem.74.082803.133219.

Navas, Tony A., Zheng Zhou, and Stephen J. Elledge. 1995. "DNA Polymerase ε Links the DNA Replication Machinery to the S Phase Checkpoint." *Cell* 80: 29-39. doi:10.1016/0092-8674(95)90448-4.

Naylor, Maria L, Ju-mei Li, Alex J Osborn, and Stephen J Elledge. 2009. "Mrc1 Phosphorylation in Response to DNA Replication Stress Is Required for Mec1 Accumulation at the Stalled Fork." *Proceedings of the National Academy of Sciences of the United States of America* 106 (31): 12765–70. doi:10.1073/pnas.0904623106.

Neo Pei Shan, Jacqueline. 2015. "The Importance of DNA Replication Termination and the MHF Complex to Genome Stability." PhD thesis, Oxford University, UK. https://ora.ox.ac.uk/objects/ora:11535.

Nethanel, Tamar, Tamar Zlotkin, and Gabriel Kaufmann. 1992. "Assembly of Simian Virus 40 Okazaki Pieces from DNA Primers Is Reversibly Arrested by ATP Depletion." *Journal of Virology* 66 (11): 6634–40.

Nguyen, Michael Ong. 2014. "Investigating the Molecular Mechanism of Replication

Restart in Fission Yeast." PhD thesis, Oxford University, UK. https://ora.ox.ac.uk/objects/ora:8935.

Nguyen, Michael Ong, Manisha Jalan, Carl a Morrow, Fekret Osman, and Matthew C Whitby. 2015. "Recombination Occurs within Minutes of Replication Blockage by *RTS1* Producing Restarted Forks That Are Prone to Collapse." *ELife* 4: 1–25. doi:10.7554/eLife.04539.

Nick McElhinny, Stephanie a, Grace E Kissling, and Thomas a Kunkel. 2010. "Differential Correction of Lagging-Strand Replication Errors Made by DNA Polymerases α and δ." *Proceedings of the National Academy of Sciences of the United States of America* 107 (49): 21070–75. doi:10.1073/pnas.1013048107.

Nielsen, Ida, Iben Bach Bentsen, Michael Lisby, Sabine Hansen, Kamilla Mundbjerg, Anni H. Andersen, and Lotte Bjergbaek. 2009. "A Flp-Nick System to Study Repair of a Single Protein-Bound Nick in Vivo." *Nature Methods* 6 (10): 753–57. doi:10.1038/nmeth.1372.

Nishinaka, T, a Shinohara, Y Ito, S Yokoyama, and T Shibata. 1998. "Base Pair Switching by Interconversion of Sugar Puckers in DNA Extended by Proteins of RecA-Family: A Model for Homology Search in Homologous Genetic Recombination." *Proceedings of the National Academy of Sciences of the United States of America* 95 (19): 11071–76. doi:10.1073/pnas.95.19.11071.

Noguchi, Eishi, Chiaki Noguchi, W Hayes McDonald, John R Yates, and Paul Russell. 2004. "Swi1 and Swi3 Are Components of a Replication Fork Protection Complex in Fission Yeast." *Molecular and Cellular Biology* 24 (19): 8342–55. doi:10.1128/MCB.24.19.8342-8355.2004.

Ogawa, Tomoko, Xiong Yu, Akira Shinohara, and Edward H. Egelman. 1993. "Similarity of the Yeast RAD51 Filament to the Bacterial RecA Filament." *Science* 259 (5103): 1896–99. doi:10.1126/science.8456314.

Ogiwara, Hideaki, Ayako Ui, Takemi Enomoto, and Masayuki Seki. 2007. "Role of Elg1 Protein in Double Strand Break Repair." *Nucleic Acids Research* 35 (2): 353–62. doi:10.1093/nar/gkl1027.

Okazaki, Koei, Noriko Okazaki, Kazuhiko Kume, Shigeki Jinno, Koichi Tanaka, and Hiroto Okayama. 1990. "High-Frequency Transformation Method and Library Transducing Vectors for Cloning Mammalian CDNAs by Trans-Complementation of Schizosaccharomyces Pombe." *Nucleic Acids Research* 18 (22): 6485–89.

doi:10.1093/nar/18.22.6485.

Osman, Fekret, Jong Sook Ahn, Alexander Lorenz, and Matthew C. Whitby. 2016. “The RecQ DNA Helicase Rqh1 Constrains Exonuclease 1-Dependent Recombination at Stalled Replication Forks.” *Scientific Reports* 6 (1): 22837. doi:10.1038/srep22837.

Osman, Fekret, Julie Dixon, Alexis R Barr, and Matthew C Whitby. 2005. “The F-Box DNA Helicase Fbh1 Prevents Rhp51-Dependent Recombination without Mediator Proteins.” *Molecular and Cellular Biology* 25 (18): 8084–96. doi:10.1128/MCB.25.18.8084-8096.2005.

Osman, Fekret, Julie Dixon, Claudette L. Doe, and Matthew C. Whitby. 2003. “Generating Crossovers by Resolution of Nicked Holliday Junctions: A Role for Mus81-Eme1 in Meiosis.” *Molecular Cell* 12 (3): 761–74. doi:10.1016/S1097-2765(03)00343-5.

Osman, Fekret, and Matthew C. Whitby. 2007. “Exploring the Roles of Mus81-Eme1/Mms4 at Perturbed Replication Forks.” *DNA Repair* 6 (7): 1004–17. doi:10.1016/j.dnarep.2007.02.019.

Ozeri-Galai, Efrat, Ronald Lebofsky, Ayelet Rahat, Assaf C. Bester, Aaron Bensimon, and Batsheva Kerem. 2011. “Failure of Origin Activation in Response to Fork Stalling Leads to Chromosomal Instability at Fragile Sites.” *Molecular Cell* 43 (1): 122–31. doi:10.1016/j.molcel.2011.05.019.

Pacek, Marcin, Antonin V. Tutter, Yumiko Kubota, Haruhiko Takisawa, and Johannes C. Walter. 2006. “Localization of MCM2-7, Cdc45, and GINS to the Site of DNA Unwinding during Eukaryotic DNA Replication.” *Molecular Cell* 21 (4): 581–87. doi:10.1016/j.molcel.2006.01.030.

Papouli, Efterpi, Shuhua Chen, Adelina a. Davies, Diana Huttner, Lumir Krejci, Patrick Sung, and Helle D. Ulrich. 2005. “Crosstalk between SUMO and Ubiquitin on PCNA Is Mediated by Recruitment of the Helicase Srs2p.” *Molecular Cell* 19 (1): 123–33. doi:10.1016/j.molcel.2005.06.001.

Park, Jung Mi, Seung Wook Yang, Kyung Ryun Yu, Seung Hyun Ka, Seong Won Lee, Jae Hong Seol, Young Joo Jeon, and Chin Ha Chung. 2014. “Modification of PCNA by ISG15 Plays a Crucial Role in Termination of Error-Prone Translesion DNA Synthesis.” *Molecular Cell* 54 (4): 626–38. doi:10.1016/j.molcel.2014.03.031.

Parker, Joanne L., Aleksandra B. Bielen, Ivan Dikic, and Helle D. Ulrich. 2007. “Contributions of Ubiquitin- and PCNA-Binding Domains to the Activity of Polymerase η in Saccharomyces Cerevisiae.” *Nucleic Acids Research* 35 (3): 881–89. doi:10.1093/nar/gkl1102.

Parnas, Oren, Rona Amishay, Batia Liefshitz, Adi Zipin-Roitman, and Martin Kupiec. 2011. “Elg1, the Major Subunit of an Alternative RFC Complex, Interacts with SUMO-Processing Proteins.” *Cell Cycle* 10 (17): 2894–2903. doi:10.4161/cc.10.17.16778.

Parnas, Oren, Adi Zipin-Roitman, Boris Pfander, Batia Liefshitz, Yuval Mazor, Shay Ben-Aroya, Stefan Jentsch, and Martin Kupiec. 2010. “Elg1, an Alternative Subunit of the RFC Clamp Loader, Preferentially Interacts with SUMOylated PCNA.” *EMBO Journal* 29 (15): 2611–22. doi:10.1038/emboj.2010.128.

Pascal, John M., Patrick J. O’Brien, Alan E. Tomkinson, and Tom Ellenberger. 2004. “Human DNA Ligase I Completely Encircles and Partially Unwinds Nicked DNA.” *Nature* 432 (7016): 473–78. doi:10.1038/nature03082.

Patel, Prasanta K., Benoit Arcangioli, Stephen P. Baker, Aaron Bensimon, and Nicholas Rhind. 2006. “DNA Replication Origins Fire Stochastically in Fission Yeast” *Molecular Biology of the Cell* 17: 308-16. doi:10.1091/mbc.E05–07–0657.

Patel, Smita S., and Ilker Donmez. 2006. “Mechanisms of Helicases.” *Journal of Biological Chemistry* 281 (27): 18265–68. doi:10.1074/jbc.R600008200.

Petersen, Janni, and Paul Russell. 2016. “Growth and the Environment of Schizosaccharomyces Pombe,” *Cold Spring Harbor Protocols* 2016 (3): 210–27. doi:10.1101/pdb.top079764.

Petojevic, Tatjana, James J. Pesavento, Alessandro Costa, Jingdan Liang, Zhijun Wang, James M. Berger, and Michael R. Botchan. 2015. “Cdc45 (Cell Division Cycle Protein 45) Guards the Gate of the Eukaryote Replisome Helicase Stabilizing Leading Strand Engagement.” *Proceedings of the National Academy of Sciences* 112 (3): E249–58. doi:10.1073/pnas.1422003112.

Petukhova, Galina, Sabrina A. Stratton, and Patrick Sung. 1999. “Single Strand DNA Binding and Annealing Activities in the Yeast Recombination Factor Rad59.” *Journal of Biological Chemistry* 274 (48): 33839–42. doi:10.1074/jbc.274.48.33839.

Petukhova, Galina, Sabrina Stratton, and Patrick Sung. 1998. “Catalysis of

Homologous DNA Pairing by Yeast Rad51 and Rad54 Proteins." *Nature* 393 (6680): 91–94. doi:10.1038/30037.

Petukhova, Galina, Stephen Van Komen, Sefton Vergano, Hannah Klein, and Patrick Sung. 1999. "Yeast Rad54 Promotes Rad51-Dependent Homologous DNA Pairing via ATP Hydrolysis-Driven Change in DNA Double Helix Conformation." *Journal of Biological Chemistry* 274 (41): 29453–62. doi:10.1074/jbc.274.41.29453.

Pfander, Boris, and Joao Matos. 2017. "Control of Mus81 Nuclease during the Cell Cycle." *FEBS Letters* 591 (14): 2048–56. doi:10.1002/1873-3468.12727.

Pfander, Boris, George-Lucian Moldovan, Meik Sacher, Carsten Hoege, and Stefan Jentsch. 2005. "SUMO-Modified PCNA Recruits Srs2 to Prevent Recombination during S Phase." *Nature* 436 (7049): 428–33. doi:10.1038/nature03665.

Piazza, Aure`le, William Douglass Wright, and Wolf-dietrich Heyer. 2017. "Multi-Invasions Are Recombination Byproducts That Induce Chromosomal Rearrangements Article Multi-Invasions Are Recombination Byproducts That Induce Chromosomal Rearrangements," 170: 760–73. doi:10.1016/j.cell.2017.06.052.

Piazza, Aurèle, and Wolf Dietrich Heyer. 2018. "Multi-Invasion-Induced Rearrangements as a Pathway for Physiological and Pathological Recombination." *BioEssays* 40: 1–11. doi:10.1002/bies.201700249.

Pike, Jason E., Peter M. J. Burgers, Judith L. Campbell, and Robert A. Bambara. 2009. "Pif1 Helicase Lengthens Some Okazaki Fragment Flaps Necessitating Dna2 Nuclease/Helicase Action in the Two-nuclease Processing Pathway." *Journal of Biological Chemistry* 284 (37): 25170-80. doi:10.1074/jbc.M109.023325.

Pittman, Douglas L, Leah Rosa Weinberg, and John C Schimenti. 1998. "Identification , Characterization , and Genetic Mapping of Rad51d , a New Mouse and Human RAD51 / RecA -Related Gene." *Genomics* 111 (49): 103–11.

Plosky, Brian S., Antonio E. Vidal, Antonio R.Fernández De Henestrosa, Mary P. McLenigan, John P. McDonald, Samantha Mead, and Roger Woodgate. 2006. "Controlling the Subcellular Localization of DNA Polymerases ι and η via Interactions with Ubiquitin." *EMBO Journal* 25 (12): 2847–55. doi:10.1038/sj.emboj.7601178.

Porro, Antonio, Matteo Berti, Julia Pizzolato, Serena Bologna, Svenja Kaden, Anja

Saxer, Yue Ma, Kazuo Nagasawa, Alessandro A. Sartori, and Josef Jiricny. 2017. “FAN1 Interaction with Ubiquitylated PCNA Alleviates Replication Stress and Preserves Genomic Integrity Independently of BRCA2.” *Nature Communications* 8 (1): 1–14. doi:10.1038/s41467-017-01074-6.

Postow, Lisa, Chris Ullsperger, Rebecca W. Keller, Carlos Bustamante, Alexander V. Vologodskii, and Nicholas R. Cozzarelli. 2001. “Positive Torsional Strain Causes the Formation of a Four-Way Junction at Replication Forks.” *Journal of Biological Chemistry* 276 (4): 2790–96. doi:10.1074/jbc.M006736200.

Prakash, Rohit, Dominik Satory, Elo??se Dray, Almas Papusha, J??rgen Scheller, Wilfried Kramer, Lumir Krejci, et al. 2009. “Yeast Mphl Helicase Dissociates Rad51-Made D-Loops: Implications for Crossover Control in Mitotic Recombination.” *Genes and Development* 23 (1): 67–79. doi:10.1101/gad.1737809.

Priego Moreno, Sara, Rachael Bailey, Nicholas Campion, Suzanne Herron, and Agnieszka Gambus. 2014. “Polyubiquitylation Drives Replisome Disassembly at the Termination of DNA Replication.” *Science* 346 (October): 477-81. doi:10.1126/science.1253585.

Puddu, Fabio, Gabriele Piergiovanni, Paolo Plevani, and Marco Muzi-Falconi. 2011. “Sensing of Replication Stress and Mec1 Activation Act through Two Independent Pathways Involving the 9-1-1 Complex and DNA Polymerase ε.” *PLoS Genetics* 7 (3). doi:10.1371/journal.pgen.1002022.

Pursell Isoz, Zachary F. 2007. “In Leading-Strand DNA Replication.” *Science* 317 (July): 127–30. http://science.sciencemag.org/content/sci/317/5834/127.full.pdf.

Pursell, Zachary F, Isabelle Isoz, Else-britt Lundström, Erik Johansson, and A Thomas. 2007. “Yeast DNA Polymerase ξ Participates in Leading-Strand DNA Replication” 317 (5834): 127–30. doi: 10.1126/science.1144067.

Qiu, Yupeng, Edwin Antony, Sultan Doganay, Hye Ran Koh, Timothy M. Lohman, and Sua Myong. 2013. “Srs2 Prevents Rad51 Filament Formation by Repetitive Motion on DNA.” *Nature Communications* 4: 1–10. doi:10.1038/ncomms3281.

Ragunathan, Kaushik, Cheng Liu, and Taekjip Ha. 2012. “RecA Filament Sliding on DNA Facilitates Homology Search.” *ELife* 2012 (1): 1–14. doi:10.7554/eLife.00067.

Ralf, Christine, Ian D. Hickson, and Leonard Wu. 2006. “The Bloom’s Syndrome

Helicase Can Promote the Regression of a Model Replication Fork." *Journal of Biological Chemistry* 281 (32): 22839–46. doi:10.1074/jbc.M604268200.

Rass, Ulrich, Sarah A. Compton, Joao Matos, Martin R. Singleton, Stephen C.Y. Ip, Miguel G. Blanco, Jack D. Griffith, and Stephen C. West. 2010. "Mechanism of Holliday Junction Resolution by the Human GEN1 Protein." *Genes and Development* 24 (14): 1559–69. doi:10.1101/gad.585310.

Raveendranathan, Miruthubashini, Sharbani Chattopadhyay, Yung-Tsi Bolon, Justin Haworth, Duncan J Clarke, and Anja-Katrin Bielinsky. 2006. "Genome-Wide Replication Profiles of S-Phase Checkpoint Mutants Reveal Fragile Sites in Yeast." *The EMBO Journal* 25 (15): 3627–39. doi:10.1038/sj.emboj.7601251.

Reddy, Gurucharan, Efim I. Golub, and Charles M. Radding. 1997. "Human Rad52 Protein Promotes Single-Strand DNA Annealing Followed by Branch Migration." *Mutation Research - Fundamental and Molecular Mechanisms of Mutagenesis* 377 (1): 53–59. doi:10.1016/S0027-5107(97)00057-2.

Reijns, Martin A.M., Harriet Kemp, James Ding, Sophie Marion De Procé, Andrew P. Jackson, and Martin S. Taylor. 2015. "Lagging-Strand Replication Shapes the Mutational Landscape of the Genome." *Nature* 518 (7540): 502–6. doi:10.1038/nature14183.

Remus, Dirk, Fabienne Beuron, Gökhan Tolun, Jack D. Griffith, Edward P. Morris, and John F.X. Diffley. 2009. "Concerted Loading of Mcm2-7 Double Hexamers around DNA during DNA Replication Origin Licensing." *Cell* 139 (4): 719–30. doi:10.1016/j.cell.2009.10.015.

Remus, Dirk, and John FX Diffley. 2009. "Eukaryotic DNA Replication Control: Lock and Load, Then Fire." *Current Opinion in Cell Biology* 21 (6): 771–77. doi:10.1016/j.ceb.2009.08.002.

Resnick, Michael A. 1976. "The Repair of Double-Strand Breaks in DNA: A Model Involving Recombination." *Journal of Theoretical Biology* 59 (1): 97–106. doi:10.1016/S0022-5193(76)80025-2.

Rhind, Nicholas, and David M Gilbert. 2013. "DNA Replication Timing" *Cold Spring Harbor Perspectives in Biology* 5 (8): a010132. doi:10.1101/cshperspect.a010132.

Robert, Thomas, Delphine Dervins, Francis Fabre, and Serge Gangloff. 2006. "Mrc1 and Srs2 Are Major Actors in the Regulation of Spontaneous Crossover." *EMBO*

Journal 25 (12): 2837–46. doi:10.1038/sj.emboj.7601158.

Roberts & Gordenin. 2014. “Hypermutation in Human Cancer Genomes: Footprints and Mechanisms Steven” 14 (12): 786–800. doi:10.2217/nnm.12.167.Gene.

Rohleder, Florian, Jing Huang, Yutong Xue, Jochen Kuper, Adam Round, Michael Seidman, Weidong Wang, and Caroline Kisker. 2016. “FANCM Interacts with PCNA to Promote Replication Traverse of DNA Interstrand Crosslinks.” *Nucleic Acids Research* 44 (7): 3219–32. doi:10.1093/nar/gkw037.

Roseaulin, Laura C., Chiaki Noguchi, Esteban Martinez, Melissa a. Ziegler, Takashi Toda, and Eishi Noguchi. 2013. “Coordinated Degradation of Replisome Components Ensures Genome Stability upon Replication Stress in the Absence of the Replication Fork Protection Complex.” *PLoS Genetics* 9 (1): 21–28. doi:10.1371/journal.pgen.1003213.

Ruff et al. 2016. “RPA Stabilization of Single-Stranded DNA Is Critical for Break-Induced Replication.” *Cell Reports* 17 (12). ElsevierCompany.: 3359–68. doi:10.1016/j.celrep.2016.12.003.

Sabatinos, Sarah A., and Susan L. Forsburg. 2010. "*Molecular Genetics of Schizosaccharomyces Pombe*." *Methods in Enzymology* 470 (C): 759-95. doi:10.1016/S0076-6879(10)70032-X.

Saini, Natalie, Sreejith Ramakrishnan, Rajula Elango, Sandeep Ayyar, Yu Zhang, Angela Deem, Grzegorz Ira, James E Haber, Kirill S Lobachev, and Anna Malkova. 2013. “Migrating Bubble during Break-Induced Replication Drives Conservative DNA Synthesis.” *Nature* 502 (7471): 389–92. doi:10.1038/nature12584.

Saito, Takamune T., Jillian L. Youds, Simon J. Boulton, and Monica P. Colaiácovo. 2009. “Caenorhabditis Elegans HIM-18/SLX-4 Interacts with SLX-1 and XPF-1 and Maintains Genomic Integrity in the Germline by Processing Recombination Intermediates.” *PLoS Genetics* 5 (11). doi:10.1371/journal.pgen.1000735.

Sakofsky, Cynthia J., Sandeep Ayyar, Angela K. Deem, Woo Hyun Chung, Grzegorz Ira, and Anna Malkova. 2015. “Translesion Polymerases Drive Microhomology-Mediated Break-Induced Replication Leading to Complex Chromosomal Rearrangements.” *Molecular Cell* 60 (6): 860–72. doi:10.1016/j.molcel.2015.10.041.

Sakofsky, Cynthia J., Sandeep Ayyar, and Anna Malkova. 2012. “Break-Induced

Replication and Genome Stability." *Biomolecules* 2 (4): 483–504. doi:10.3390/biom2040483.

Sakofsky, Cynthia J., and Anna Malkova. 2017. "Break Induced Replication in Eukaryotes: Mechanisms, Functions, and Consequences." *Critical Reviews in Biochemistry and Molecular Biology* 52 (4): 395–413. doi:10.1080/10409238.2017.1314444.

Sakofsky, Cynthia J., Steven A. Roberts, Ewa Malc, Piotr A. Mieczkowski, Michael A. Resnick, Dmitry A. Gordenin, and Anna Malkova. 2014. "Break-Induced Replication Is a Source of Mutation Clusters Underlying Kataegis." *Cell Reports* 7 (5): 1640–48. doi:10.1016/j.celrep.2014.04.053.

Saleh-Gohari, Nasrollah, Helen E. Bryant, Niklas Schultz, Kayan M. Parker, Tobias N. Cassel, and Thomas Helleda. 2005. *"*Spontaneous Homologous Recombination Is Induced by Collapsed Replication Forks That Are Caused by Endogenous DNA Single-Strand Breaks." *Molecular and Cell Biology* 25 (16): 7158-69. doi:10.1128/MCB.25.16.7158-7169.

Sambrook, Joseph, and DW Russell. 2001. *Molecular Cloning : A Laboratory Manual*. Third edition. Cold Spring Harbor, N.Y. 2001. https://search.library.wisc.edu/catalog/999897924602121.

Samel, Stefan A., Alejandra Fernández-Cid, Jingchuan Sun, Alberto Riera, Silvia Tognetti, M. Carmen Herrera, Huilin Li, and Christian Speck. 2014. "A Unique DNA Entry Gate Serves for Regulated Loading of the Eukaryotic Replicative Helicase MCM2-7 onto DNA." *Genes and Development* 28 (15): 1653–66. doi:10.1101/gad.242404.114.

Sánchez-Gorostiaga, A, C López-Estraño, D B Krimer, J B Schvartzman, and P Hernández. 2004. "Transcription Termination Factor Reb1p Causes Two Replication Fork Barriers at Its Cognate Sites in Fission Yeast Ribosomal DNA in Vivo." *Mol. Cell. Biol.* 24 (1): 398–406. doi:10.1128/MCB.24.1.398.

Sarbajna, Shriparna, and Stephen C. West. 2014. "Holliday Junction Processing Enzymes as Guardians of Genome Stability." *Trends in Biochemical Sciences* 39 (9): 409–19. doi:10.1016/j.tibs.2014.07.003.

Schär, P, and J Kohli. 1994. "Preferential Strand Transfer and Hybrid DNA Formation at the Recombination Hotspot Ade6-M26 of Schizosaccharomyces Pombe." *The EMBO Journal* 13 (21): 5212–19.

Schindelin, Johannes, Ignacio Arganda-Carreras, Erwin Frise, Verena Kaynig, Mark Longair, Tobias Pietzsch, Stephan Preibisch, Curtis Rueden, Stephan Saalfeld, Benjamin Schmid, Jean-Yves Tinevez, Daniel James White, Volker Hartenstein, Kevin Eliceiri, Pavel Tomancak, and Albert Cardona. 2012. “Fiji: an Open-Source Platform for Biological-Image Analysis.” *Nature Methods* 9 (7): 676-82. doi:10.1038/nmeth.2019.

Semlow, Daniel R., Jieqiong Zhang, Magda Budzowska, Alexander C. Drohat, and Johannes C. Walter. 2016. “Replication-Dependent Unhooking of DNA Interstrand Cross-Links by the NEIL3 Glycosylase.” *Cell* 167 (2): 498–511.e14. doi:10.1016/j.cell.2016.09.008.

Sengupta, sugopa, Frederick van Deursen, Giacomo de Piccoli, and Karim Labib. 2013. “Dpb2 Integrates the Leading-Strand DNA Polymerase into the Eukaryotic Replisome.” *Current Biology* 23 (7): 543-52. doi:10.1016/j.cub.2013.02.011.

Sharma, Sudha, Joshua A. Sommers, Saba Choudhary, Jinnifer Korin Faulkner, Sheng Cui, Lucia Andreoli, Laura Muzzolini, Alessandro Vindigni, and Robert M. Brosh. 2005. “Biochemical Analysis of the DNA Unwinding and Strand Annealing Activities Catalyzed by Human RECQ1.” *Journal of Biological Chemistry* 280 (30): 28072–84. doi:10.1074/jbc.M500264200.

Shechter, David F., Carol Y. Ying, and Jean Gautier. 2000. “The Intrinsic DNA Helicase Activity of Methanobacterium Thermoautotrophicum ??H Minichromosome Maintenance Protein.” *Journal of Biological Chemistry* 275 (20): 15049–59. doi:10.1074/jbc.M000398200.

Shibahara, Kei Ichi, and Bruce Stillman. 1999. “Replication-Dependent Marking of DNA by PCNA Facilitates CAF-1-Coupled Inheritance of Chromatin.” *Cell* 96 (4): 575–85. doi:10.1016/S0092-8674(00)80661-3.

Shinohara, Akira, Miki Shinohara, Tsutomu Ohta, Shimako Matsuda, and Tomoko Ogawa. 1998. “Rad52 Forms Ring Structures and Co-Operates with RPA in Single-Strand DNA Annealing.” *Genes to Cells* 3 (3): 145–56. doi:10.1046/j.1365-2443.1998.00176.x.

Shiomi, Yasushi, Ayako Shinozaki, Katsunori Sugimoto, Jiro Usukura, Chikashi Obuse, and Toshiki Tsurimoto. 2004. “The Reconstituted Human Chl12-RFC Complex Functions as a Second PCNA Loader.” *Genes to Cells* 9 (4): 279–90. doi:10.1111/j.1356-9597.2004.00724.x.

Signon, Laurence, Anna Malkova, Maria L Naylor, James E. Haber, and Hannah Klein. 2001. “Genetic Requirements for RAD51 - and Replication Repair of a Chromosomal Double-Strand Break Genetic Requirements for RAD51 - and RAD54 -Independent Break-Induced Replication Repair of a Chromosomal Double-Strand Break.” *Molecular and Cellular Biology* 21 (6): 2048–56. doi:10.1128/MCB.21.6.2048.

Sigurdsson, Stefan, Stephen Van Komen, Galina Petukhova, and Patrick Sung. 2002. “Homologous DNA Pairing by Human Recombination Factors Rad51 and Rad54.” *Journal of Biological Chemistry* 277 (45): 42790–94. doi:10.1074/jbc.M208004200.

Simon, Aline C., Jin C. Zhou, Rajika L. Perera, Frederick Van Deursen, Cecile Evrin, Marina E. Ivanova, Mairi L. Kilkenny, et al. 2014. “A Ctf4 Trimer Couples the CMG Helicase to DNA Polymerase Î± in the Eukaryotic Replisome.” *Nature* 510 (7504): 293–97. doi:10.1038/nature13234.

Singh, Shivani, Keren Shemesh, Batia Liefshitz, and Martin Kupiec. 2013. “Genetic and Physical Interactions between the Yeast ELG1 Gene and Orthologs of the Fanconi Anemia Pathway.” *Cell Cycle* 12 (10): 1625–36. doi:10.4161/cc.24756.

Sivakumar, Sasirekha, Mary Porter-Goff, Prasanta K Patel, Kristen Benoit, and Nicholas Rhind. 2004. “In Vivo Labeling of Fission Yeast DNA with Thymidine and Thymidine Analogs.” *Methods* 33 (3): 213–19. doi:10.1016/j.ymeth.2003.11.016.

Smith, C. E., A. F. Lam, and L. S. Symington. 2009. “Aberrant Double-Strand Break Repair Resulting in Half Crossovers in Mutants Defective for Rad51 or the DNA Polymerase Complex.” *Molecular and Cellular Biology* 29 (6): 1432–41. doi:10.1128/MCB.01469-08.

Smith, Catherine E., Bertrand Llorente, and Lorraine S. Symington. 2007. “Template Switching during Break-Induced Replication.” *Nature* 447 (7140): 102–5. doi:10.1038/nature05723.

Smith, Gerald R., Michael N. Boddy, Paul Shanahan, and Paul Russell. 2003. “Fission Yeast Mus81·Eme1 Holliday Junction Resolvase Is Required for Meiotic Crossing over but Not for Gene Conversion.” *Genetics* 165 (4): 2289–93.

Sogo, José M., Massimo Lopes, and Marco Foiani. 2002. “Fork Reversal and SsDNA Accumulation at Stalled Replication Forks Owing to Checkpoint Defects.” *Science* 297 (5581): 599–602. doi:10.1126/science.1074023.

Solinger, Jachen A., Konstantin Kiianitsa, and Wolf Dietrich Heyer. 2002. “Rad54, a Swi2/Snf2-like Recombinational Repair Protein, Disassembles Rad51:DsDNA Filaments.” *Molecular Cell* 10 (5): 1175–88. doi:10.1016/S1097-2765(02)00743-8.

Sonneville, Remi, Sara Priego Moreno, Axel Knebel, Clare Johnson, C. James Hastie, Anton Gartner, Agnieszka Gambus, and Karim Labib. 2017. “CUL-2LRR-1and UBXN-3 Drive Replisome Disassembly during DNA Replication Termination and Mitosis.” *Nature Cell Biology* 19 (5): 468–79. doi:10.1038/ncb3500.

Sotiriou, Sotirios K., Irene Kamileri, Natalia Lugli, Konstantinos Evangelou, Caterina Da-Ré, Florian Huber, Laura Padayachy, et al. 2016. “Mammalian RAD52 Functions in Break-Induced Replication Repair of Collapsed DNA Replication Forks.” *Molecular Cell* 64 (6): 1127–34. doi:10.1016/j.molcel.2016.10.038.

Stasiak, Alicja Z., Eric Larquet, Andrzej Stasiak, Shirley Müller, Andreas Engel, Eric Van Dyck, Stephen C. West, and Edward H. Egelman. 2000. “The Human Rad52 Protein Exists as a Heptameric Ring.” *Current Biology* 10 (6): 337–40. doi:10.1016/S0960-9822(00)00385-7.

Stillman, Bruce. 2015. “Reconsidering DNA Polymerases at the Replication Fork in Eukaryotes.” *Molecular Cell* 59 (2): 139–41. doi:10.1016/j.molcel.2015.07.004.

Stodola, Joseph L., and Peter M. Burgers. 2016. “Resolving Individual Steps of Okazaki-Fragment Maturation at a Millisecond Timescale.” *Nature Structural and Molecular Biology* 23 (5): 402–8. doi:10.1038/nsmb.3207.

Su, Guan Chin, Chan I. Chung, Chia Yu Liao, Sheng Wei Lin, Cheng Ting Tsai, Tao Huang, Hung Wen Li, and Peter Chi. 2014. “Enhancement of ADP Release from the RAD51 Presynaptic Filament by the SWI5-SFR1 Complex.” *Nucleic Acids Research* 42 (1): 349–58. doi:10.1093/nar/gkt879.

Su, Guan Chin, Hsin Yi Yeh, Sheng Wei Lin, Chan I. Chung, Yu Shan Huang, Yi Chung Liu, Ping Chiang Lyu, and Peter Chi. 2016. “Role of the RAD51-SWI5-SFR1 Ensemble in Homologous Recombination.” *Nucleic Acids Research* 44 (13): 6242–51. doi:10.1093/nar/gkw375.

Sugawara, N, G Ira, and J E Haber. 2000. “DNA Length Dependence of the Single-Strand Annealing Pathway and the Role of Saccharomyces Cerevisiae RAD59 in Double-Strand Break Repair.” *Molecular and Cellular Biology* 20 (14): 5300–5309. doi:10.1128/MCB.20.14.5300-5309.2000.

Sugiyama, T., J. H. New, and S. C. Kowalczykowski. 1998. “DNA Annealing by Rad52 Protein Is Stimulated by Specific Interaction with the Complex of Replication Protein A and Single-Stranded DNA.” *Proceedings of the National Academy of Sciences* 95 (11): 6049–54. doi:10.1073/pnas.95.11.6049.

Sun, Jingchuan, Yi Shi, Roxana E. Georgescu, Zuanning Yuan, Brian T. Chait, Huilin Li, and Michael E. O’Donnell. 2015. “The Architecture of a Eukaryotic Replisome.” *Nature Structural and Molecular Biology* 22 (12): 976–82. doi:10.1038/nsmb.3113.

Sun, Weili, Saikat Nandi, Fekret Osman, Jong Sook Ahn, Jovana Jakovleska, Alexander Lorenz, and Matthew C. Whitby. 2008. “The FANCM Ortholog Fml1 Promotes Recombination at Stalled Replication Forks and Limits Crossing Over during DNA Double-Strand Break Repair.” *Molecular Cell* 32 (1): 118–28. doi:10.1016/j.molcel.2008.08.024.

Sung, Patrick. 1997. “Yeast Rad55 and Rad57 Proteins Form a Heterodimer That Functions with Replication Protein A to Promote DNA Strand Exchange by Rad51 Recombinase.” *Genes and Development* 11 (9): 1111–21. doi:10.1101/gad.11.9.1111.

Svendsen, Jennifer M., Agata Smogorzewska, Mathew E. Sowa, Brenda C. O’Connell, Steven P. Gygi, Stephen J. Elledge, and J. Wade Harper. 2009. “Mammalian BTBD12/SLX4 Assembles A Holliday Junction Resolvase and Is Required for DNA Repair.” *Cell* 138 (1): 63–77. doi:10.1016/j.cell.2009.06.030.

Symington, Lorraine S. 2016. “Mechanism and Regulation of DNA End Resection in Eukaryotes.” *Critical Reviews in Biochemistry and Molecular Biology* 51 (3): 195–212. doi:10.3109/10409238.2016.1172552.

Symington, Lorraine S. 2002. “Role of RAD52 Epistasis Group Genes in Homologous Recombination and Double-Strand Break Repair.” *Microbiology and Molecular Biology Reviews : MMBR* 66 (4): 630–70. doi:10.1128/MMBR.66.4.630.

Szankasi, Philippe, and Gerald R Smith. 1995. “A Role for Exonuclease I from S . Pombe in Mutation Avoidance and Mismatch Correction Author" *Science* 267 (5201), 1166-1169. doi: 10.1126/science.7855597

Tahirov, Tahir H., Kira S. Makarova, Igor B. Rogozin, Youri I. Pavlov, and Eugene V. Koonin. 2009. “Evolution of DNA Polymerases: An Inactivated Polymerase-

Exonuclease Module in Pol ε and a Chimeric Origin of Eukaryotic Polymerases from Two Classes of Archaeal Ancestors." *Biology Direct* 4: 1–11. doi:10.1186/1745-6150-4-11.

Teixeira-Silva, Ana, Anissia Ait Saada, Julien Hardy, Ismail Iraqui, Marina Charlotte Nocente, Karine Fréon, and Sarah A.E. Lambert. 2017. "The End-Joining Factor Ku Acts in the End-Resection of Double Strand Break-Free Arrested Replication Forks." *Nature Communications* 8 (1). doi:10.1038/s41467-017-02144-5.

Terret, Marie-Emilie, Rebecca Sherwood, Sadia Rahman, Jun Qin, and Prasad V. Jallepalli. 2009. "Cohesin Acetylation Speeds the Replication Fork." *Nature* 462 (7270): 231–34. doi:10.1038/nature08550.

Thacker, John. 2005. "The RAD51 Gene Family, Genetic Instability and Cancer." *Cancer Letters* 219 (2): 125–35. doi:10.1016/j.canlet.2004.08.018.

Tong, Kevin, and Robert V. Skibbens. 2015. "Pds5 Regulators Segregate Cohesion and Condensation Pathways in *Saccharomyces Cerevisiae*." *Proceedings of the National Academy of Sciences* 112 (22): 7021–26. doi:10.1073/pnas.1501369112.

Tóth, Attila, Rafal Ciosk, Frank Uhlmann, Marta Galova, Alexander Schleiffer, and Kim Nasmyth. 1999. "Yeast Cohesin Complex Requires a Conserved Protein, Eco1p(Ctf7), to Establish Cohesion between Sister Chromatids during DNA Replication." *Genes and Development* 13 (3): 320–33. doi:10.1101/gad.13.3.320.

Tsai, Shang Pu, Guan Chin Su, Sheng Wei Lin, Chan I. Chung, Xiaoyu Xue, Myun Hwa Dunlop, Yufuko Akamatsu, Maria Jasin, Patrick Sung, and Peter Chi. 2012. "Rad51 Presynaptic Filament Stabilization Function of the Mouse Swi5-Sfr1 Heterodimeric Complex." *Nucleic Acids Research* 40 (14): 6558–69. doi:10.1093/nar/gks305.

Tsang, E., I. Miyabe, I. Iraqui, J. Zheng, S. A. E. Lambert, and A. M. Carr. 2014. "The Extent of Error-Prone Replication Restart by Homologous Recombination Is Controlled by Exo1 and Checkpoint Proteins." *Journal of Cell Science* 127 (13): 2983–94. doi:10.1242/jcs.152678.

Tsutsui, Yasuhiro, Takashi Morishita, Hiroshi Iwasaki, Hiroyuki Toh, and Hideo Shinagawa. 2000. "A Recombination Repair Gene of Schizosaccharomyces Pombe, Rhp57, Is a Functional Homolog of the Saccharomyces Cerevisiae RAD57 Gene and Is Phylogenetically Related to the Human XRCC3 Gene."

Genetics 154 (4): 1451–61.

Tsuzuki, T, Y Fujii, K Sakumi, Y Tominaga, K Nakao, M Sekiguchi, a Matsushiro, Y Yoshimura, and MoritaT. 1996. “Targeted Disruption of the Rad51 Gene Leads to Lethality in Embryonic Mice.” *Proceedings of the National Academy of Sciences of the United States of America* 93 (June): 6236–40. doi:10.1073/pnas.93.13.6236.

Tuduri, Sandie, Laure Crabbé, Chiara Conti, Hélène Tourrière, Heidi Holtgreve-Grez, Anna Jauch, Véronique Pantesco, et al. 2009. “Topoisomerase I Suppresses Genomic Instability by Preventing Interference between Replication and Transcription.” *Nature Cell Biology* 11 (11): 1315–24. doi:10.1038/ncb1984.

Ulrich, Helle D., Sabina Vogel, and Adelina A. Davies. 2005. “SUMO Keeps a Check on Recombination during DNA Replication.” *Cell Cycle* 4 (12): 1699–1702. doi:10.4161/cc.4.12.2194.

Unk, Ildiko, Ildikó Hajdú, Károly Fátyol, Barnabás Szakál, András Blastyák, Vladimir Bermudez, Jerard Hurwitz, Louise Prakash, Satya Prakash, and Lajos Haracska. 2006. “Human SHPRH Is a Ubiquitin Ligase for Mms2-Ubc13-Dependent Polyubiquitylation of Proliferating Cell Nuclear Antigen.” *Proceedings of the National Academy of Sciences of the United States of America* 103 (48): 18107–12. doi:10.1073/pnas.0608595103.

Urulangodi, Madhusoodanan, Marek Sebesta, Demis Menolfi, Barnabas Szakal, Julie Sollier, Alexandra Sisakova, Lumir Krejci, and Dana Branzei. 2015. “Local Regulation of the Srs2 Helicase by the SUMO-like Domain Protein Esc2 Promotes Recombination at Sites of Stalled Replication.” *Genes and Development* 29: 2067–80. doi:10.1101/gad.265629.115.

Vainio, Olli, and Beat A. Imhof. 1995. “The Immunology and Developmental Biology of the Chicken.” *Immunology Today* 16 (8): 365–70. doi:10.1016/0167-5699(95)80002-6.

Vaisman, Alexandra, and Roger Woodgate. 2017. “Translesion DNA Polymerases in Eukaryotes: What Makes Them Tick?” *Critical Reviews in Biochemistry and Molecular Biology* 52 (3): 274–303. doi:10.1080/10409238.2017.1291576.

Vasan, Soumini, Angela Deem, Sreejith Ramakrishnan, Juan Lucas Argueso, and Anna Malkova. 2014. “Cascades of Genetic Instability Resulting from Compromised Break-Induced Replication.” *PLoS Genetics* 10 (2).

doi:10.1371/journal.pgen.1004119.

Veaute, Xavier, Josette Jeusset, Christine Soustelle, Stephen C. Kowalczykowski, Eric Le Cam, and Francis Fahre. 2003. “The Srs2 Helicase Prevents Recombination by Disrupting Rad51 Nucleoprotein Filaments.” *Nature* 423 (6937): 309–12. doi:10.1038/nature01585.

Villa, Fabrizio, Aline C. Simon, Maria Angeles Ortiz Bazan, Mairi L. Kilkenny, David Wirthensohn, Mel Wightman, Dijana Matak-Vinkovíc, Luca Pellegrini, and Karim Labib. 2016. “Ctf4 Is a Hub in the Eukaryotic Replisome That Links Multiple CIP-Box Proteins to the CMG Helicase.” *Molecular Cell* 63 (3): 385–96. doi:10.1016/j.molcel.2016.06.009.

Vo, Tommy V., Jishnu Das, Michael J. Meyer, Nicolas A. Cordero, Nurten Akturk, Xiaomu Wei, Benjamin J. Fair, et al. 2016. “A Proteome-Wide Fission Yeast Interactome Reveals Network Evolution Principles from Yeasts to Human.” *Cell* 164 (1–2): 310–23. doi:10.1016/j.cell.2015.11.037.

Vujanovic, Marko, Jana Krietsch, Maria Chiara Raso, Nastassja Terraneo, Ralph Zellweger, Jonas A. Schmid, Angelo Taglialatela, et al. 2017. “Replication Fork Slowing and Reversal upon DNA Damage Require PCNA Polyubiquitination and ZRANB3 DNA Translocase Activity.” *Molecular Cell* 67 (5): 882–890.e5. doi:10.1016/j.molcel.2017.08.010.

Wade, Benjamin O, Hon Wing Liu, Catarina P Samora, Frank Uhlmann, and Martin R Singleton. 2017. “Structural Studies of RFC ^{Ctf18} Reveal a Novel Chromatin Recruitment Role for Dcc1.” *EMBO Reports* 18: 558-68. doi:10.15252/embr.201642825.

Wang, Y, M Vujcic, and D Kowalski. 2001. “DNA Replication Forks Pause at Silent Origins near the HML Locus in Budding Yeast.” *Molecular and Cellular Biology* 21 (15): 4938–48. doi:10.1128/MCB.21.15.4938-4948.2001.

Warbrick, Emma. 2000. “The Puzzle of PCNA's Many Partners” *Bioessays* 22 (11): 997-1006. doi:10.1002/1521-1878(200011)22:11<997::AID-BIES6>3.0.

Warbrick, Emma, David P. Lanet, David M. Glover, and Lynne S. Cox. 1995. “A Small Peptide Inhibitor of DNA Replication Defines the Site of Interaction Between the Cyclin-Dependent Kinase Inhibitor P21^{WAF1} and Proliferating Cell Nuclear Antigen.” *Current Biology* 5 (3): 275-82. doi:10.1016/S0960-9822(95)00058-3.

Warbrick, Emma, David P. Lanet, David M. Glover, and Lynne S. Cox. 1997.

"Homologous Regions of Fen1 and p21^{Cip1} Compete for Binding to the Same Site on PCNA: A Potential Mechanism to Co-Ordinate DNA Replication and Repair." *Oncogene* 14 (19): 2313-21. doi:10.1038/sj.onc.1201072.

Watts, Felicity Z. 2006. "Sumoylation of PCNA: Wrestling with Recombination at Stalled Replication Forks." *DNA Repair* 5 (3): 399–403. doi:10.1016/j.dnarep.2005.11.002.

Wechsler, Thomas, Scott Newman, and Stephen C. West. 2011. "Aberrant Chromosome Morphology in Human Cells Defective for Holliday Junction Resolution." *Nature* 471 (7340): 642–46. doi:10.1038/nature09790.

West, Stephen C. 2003. "Molecular Views of Recombination Proteins and Their Control." *Nature Reviews Molecular Cell Biology* 4 (6): 435–45. doi:10.1038/nrm1127.

Whitby, Matthew C. 2010. "The FANCM Family of DNA Helicases/Translocases." *DNA Repair* 9 (3): 224–36. doi:10.1016/j.dnarep.2009.12.012.

Williams, Dewight R, and J Richard Mcintosh. 2002. "Important for Chromosome Replication , Cohesion , and Segregation" 1 (5): 758–73. doi:10.1128/EC.1.5.758.

Wilson, Marenda A., Youngho Kwon, Yuanyuan Xu, Woo Hyun Chung, Peter Chi, Hengyao Niu, Ryan Mayle, et al. 2013. "Pif1 Helicase and Polδ Promote Recombination-Coupled DNA Synthesis via Bubble Migration." *Nature* 502 (7471) : 393–96. doi:10.1038/nature12585.

Wold, M.S. 1997. "Replication protein A: a heterotrimeric, single-stranded DNA-binding protein required for eukaryotic DNA metabolism." *Annual Review of Biochemistry* 66 (1): 61-92. doi:10.1146/annurev.biochem.66.1.61.

Wolner, Branden, and Craig L. Peterson. 2005. "ATP-Dependent and ATP-Independent Roles for the Rad54 Chromatin Remodeling Enzyme during Recombinational Repair of a DNA Double Strand Break." *Journal of Biological Chemistry* 280 (11): 10855–60. doi:10.1074/jbc.M414388200.

Wright, William Douglass, and Wolf Dietrich Heyer. 2014. "Rad54 Functions as a Heteroduplex DNA Pump Modulated by Its DNA Substrates and Rad51 during D Loop Formation." *Molecular Cell* 53 (3): 420–32. doi:10.1016/j.molcel.2013.12.027.

Wu, Leonard, and Ian O. Hickson. 2003. "The Bloom's Syndrome Helicase Suppresses Crossing over during Homologous Recombination." *Nature* 426

(6968): 870–74. doi:10.1038/nature02253.

Wu, Yun, Noriko Kantake, Tomohiko Sugiyama, and Stephen C. Kowalczykowski. 2008. “Rad51 Protein Controls Rad52-Mediated DNA Annealing.” *Journal of Biological Chemistry* 283 (21): 14883–92. doi:10.1074/jbc.M801097200.

Xu, Jingfei, Lingyun Zhao, Yuanyuan Xu, Weixing Zhao, Patrick Sung, and Hong Wei Wang. 2017. “Cryo-EM Structures of Human RAD51 Recombinase Filaments during Catalysis of DNA-Strand Exchange.” *Nature Structural and Molecular Biology* 24 (1): 40–46. doi:10.1038/nsmb.3336.

Xu, Xin, Lindsay Ball, Wangyang Chen, Xuelei Tian, Amanda Lambrecht, Michelle Hanna, and Wei Xiao. 2013. “The Yeast Shu Complex Utilizes Homologous Recombination Machinery for Error-Free Lesion Bypass via Physical Interaction with a Rad51 Paralogue.” *PLoS ONE* 8 (12): 1–9. doi:10.1371/journal.pone.0081371.

Yang, Kailin, George Lucian Moldovan, and Alan D. D’Andrea. 2010. “RAD18-Dependent Recruitment of SNM1A to DNA Repair Complexes by a Ubiquitin-Binding Zinc Finger.” *Journal of Biological Chemistry* 285 (25): 19085–91. doi:10.1074/jbc.M109.100032.

Yao, Nina, Jennifer Turner, Zvi Kelman, P. Todd Stukenberg, Frank Dean, David Shechter, Zhen Qiang Pan, Jerard Hurwitz, and Mike O’Donnell. 1996. “Clamp Loading, Unloading and Intrinsic Stability of the PCNA, β and Gp45 Sliding Clamps of Human, E. Coli and T4 Replicases.” *Genes to Cells* 1 (1): 101–13. doi:10.1046/j.1365-2443.1996.07007.x.

Yao, Nina Y., Aaron Johnson, Greg D. Bowman, John Kuriyan, and Mike O'Donnell. 2006. “Mechanism of Proliferating Cell Nuclear Antigen Clamp Opening by Replication Factor C.” *Journal of Biological Chemistry* 281 (25): 17528–39. doi:10.1074/jbc.M601273200.

Yao, Nina Y, and Mike O Donnell. 2012. “The Eukaryotic Replisome: A Guide to Protein Structure and Function” 62: 259–79. doi:10.1007/978-94-007-4572-8.

Yardimci, Hasan, Anna B. Loveland, Satoshi Habuchi, Antoine M. Van Oijen, and Johannes C. Walter. 2010. “Uncoupling of Sister Replisomes during Eukaryotic DNA Replication.” *Molecular Cell* 40 (5): 834–40. doi:10.1016/j.molcel.2010.11.027.

Yeeles, Joseph T.P., Tom D. Deegan, Agnieszka Janska, Anne Early, and John F.X.

Diffley. 2015. “Regulated Eukaryotic DNA Replication Origin Firing with Purified Proteins.” *Nature* 519 (7544): 431–35. doi:10.1038/nature14285.

Ying, Songmin, Sheroy Minocherhomji, Kok Lung Chan, Timea Palmai-Pallag, Wai Kit Chu, Theresa Wass, Hocine W. Mankouri, Ying Liu, and Ian D. Hickson. 2013. “MUS81 Promotes Common Fragile Site Expression.” *Nature Cell Biology* 15 (8): 1001–7. doi:10.1038/ncb2773.

Yu, Chang-en, Junko Oshima, Ying-hui Fu, Ellen M Wijsman, Fuki Hisama, Shellie Matthews, Jun Nakura, et al. 2016. “Positional Cloning of the Werner ’ s Syndrome Gene.” *American Association for the Advancement of Science* 272 (5259): 258–62. http://www.jstor.org/stable/2889636.

Yu, Chuanhe, Haiyun Gan, Junhong Han, Zhi-Xiong Zhou, Shaodong Jia, Andrei Chabes, Gianrico Farrugia, Tamas Ordog, and Zhiguo Zhang. 2014a. “Strand-Specific Analysis Shows Protein Binding at Replication Forks and PCNA Unloading from Lagging Strands When Forks Stall.” *Molecular Cell* 56 (4): 551–63. doi:10.1016/j.molcel.2014.09.017.

Yuan, Zuanning, Lin Bai, Jingchuan Sun, Roxana Georgescu, Jun Liu, Michael E. O’Donnell, and Huilin Li. 2016. “Structure of the Eukaryotic Replicative CMG Helicase and Pumpjack Motion.” *Nat Struct Mol Biol.* 23 (3): 217–24. doi:10.1158/1541-7786.MCR-15-0224.

Zaher, Manal S., Fahad Rashid, Bo Song, Luay I. Joudeh, Mohamed A. Sobhy, Muhammad Tehseen, Manju M. Hingorani, and Samir M. Hamdan. 2018. “Missed Cleavage Opportunities by FEN1 Lead to Okazaki Fragment Maturation Via the Long-Flap Pathway.” *Nucleic Acids Research* 46 (6): 2956-74. doi:10.1093/nar/gky082.

Zhang, G, E Gibbs, Z Kelman, M O’Donnell, and J Hurwitz. 1999. “Studies on the Interactions between Human Replication Factor C and Human Proliferating Cell Nuclear Antigen.” *Proceedings of the National Academy of Sciences of the United States of America* 96 (5): 1869–74.

Zhang, Yuqing, Sandra J. Shin, Debra Liu, Elena Ivanova, Friedrich Foerster, Haoqiang Ying, Hongwu Zheng, Yonghong Xiao, Zhengming Chen, Alexei Protopopov, Ronald A. DePinho, and Ji-Hye Paik. 2013. “ZNF365 Promotes Stability of Fragile Sites and Telomeres.” *Cancer Discovery* 3 (7): 798-811. doi:10.1158/2159-8290.CD-12-0536.

Zhao, Linlin, and M. Todd Washington. 2017. “Translesion Synthesis: Insights into the Selection and Switching of DNA Polymerases.” *Genes* 8 (1): 1–25. doi:10.3390/genes8010024.

Zhao, Weixing, Sivaraja Vaithiyalingam, Joseph San Filippo, David G. Maranon, Judit Jimenez-Sainz, Gerald V. Fontenay, Youngho Kwon, et al. 2015. “Promotion of BRCA2-Dependent Homologous Recombination by DSS1 via RPA Targeting and DNA Mimicry.” *Molecular Cell* 59 (2): 176–87. doi:10.1016/j.molcel.2015.05.032.

Zheng, Xiao Feng, Rohit Prakash, Dorina Saro, Simonne Longerich, Hengyao Niu, and Patrick Sung. 2011. “Processing of DNA Structures via DNA Unwinding and Branch Migration by the S. Cerevisiae Mph1 Protein.” *DNA Repair* 10 (10): 1034–43. doi:10.1016/j.dnarep.2011.08.002.

Zhu, Zhu, Woo Hyun Chung, Eun Yong Shim, Sang Eun Lee, and Grzegorz Ira. 2008. “Sgs1 Helicase and Two Nucleases Dna2 and Exo1 Resect DNA Double-Strand Break Ends.” *Cell* 134 (6): 981–94. doi:10.1016/j.cell.2008.08.037.